

**OFFICIAL JOURNAL OF THE SCIENTIFIC SOCIETY OF
ANATOMISTS, HISTOLOGISTS, EMBRYOLOGISTS AND
TOPOGRAPHIC ANATOMISTS OF UKRAINE**

**DOI: 10.31393
ISSN 1818-1295
eISSN 2616-6194**

ВІСНИК МОРФОЛОГІЇ REPORTS OF MORPHOLOGY

Vol. 25, №2, 2019

Scientific peer-reviewed journal in the fields of normal and pathological anatomy, histology, cytology and embryology, topographical anatomy and operative surgery, biomedical anthropology, ecology, molecular biology, biology of development

**Published since 1993
Periodicity: 4 times a year**

Vinnytsya • 2019

ВІСНИК МОРФОЛОГІЇ - REPORTS OF MORPHOLOGY

Founded by the "Scientific Society of Anatomists, Histologists, Embryologists, and Topographic Anatomists of Ukraine" and National Pyrogov Memorial Medical University, Vinnytsya in 1993

Certificate of state registration KB №9310 from 02.11.2004

Professional scientific publication of Ukraine in the field of medical sciences (approved by the order of the Ministry of Education and Science of Ukraine No. 528 dated 12.05.2015, annex 10); professional scientific publication of Ukraine in the field of biological sciences by specialty groups 14.01.00-14.03.00 (approved by the order of the Ministry of Education and Science of Ukraine No. 747 dated 13.07.2015, annex 17)

Chairman of the editorial board - Cherkasov V.G. (Kyiv)

Vice-chairman of editorial board: Chaikovsky Yu.B. (Kyiv), Pivtorak V.I. (Vinnytsya)

Responsible editor - Gunas I.V. (Vinnytsya)

Secretary - Kaminska N.A. (Vinnytsya)

Editorial Board Members:

Berenshtein E.L. (Jerusalem), Byard R. (Adelaida), Volkov K.S. (Ternopil), Gulmen M.K. (Adana), Guminskyi Yu.Y. (Vinnytsya), Dgebuadze M.A. (Tbilisi), Juenemann A.G.M. (Rostock), Graeb C. (Hof), Kryvko Yu.Ya. (Lviv), Rej dak R. (Lublin), Sarafinyuk L.A. (Vinnytsya), Stechenko L.O. (Kyiv), Shepitko V.I. (Poltava)

Editorial council:

Appelhans O.L. (Odessa), Bulyk R.Ye. (Chernivtsi), Gavrylyuk A.O. (Vinnytsya), Gerasymyuk I.Ye. (Ternopil), Gerashchenko S.B. (Ivano-Frankivsk), Golovatskyk A.S. (Uzhgorod), Yeroshenko G.A. (Poltava), Kovalchuk O.I. (Kyiv), Kostylenko Yu.P. (Poltava), Kostyuk G.Ya. (Vinnytsya), Lutsyk O.D. (Lviv), Maievskiy O.Ye. (Kyiv), Makar B.G. (Chernivtsi), Mishalov V.D. (Kyiv), Olkhovskyy V.O. (Kharkiv), Piskun R.P. (Vinnytsya), Rudyk S.K. (Kyiv), Sikora V.Z. (Sumy), Skybo G.G. (Kyiv), Sokurenko L.M. (Kyiv), Tverdokhlib I.V. (Dnipro), Tereshchenko V.P. (Kyiv), Topka E.G. (Dnipro), Fedonyuk L.Ya. (Ternopil), Fomina L.V. (Vinnytsya), Furman Yu.M. (Vinnytsya), Sherstyuk O.O. (Poltava), Yatsenko V.P. (Kyiv)

Approved by the Academic Council of National Pyrogov Memorial Medical University, Vinnytsya, protocol №11 from 26.06.2019

Indexation: CrossRef, elibrary.ru, Google Scholar Metrics, National Library of Ukraine Vernadsky

Address editors and publisher:

Pyrogov Str. 56,
Vinnytsya, Ukraine - 21018
Tel.: +38 (0432) 553959
E-mail: nila@vnmnu.edu.ua

Computer page-proofs - Klopotovska L.O.

Translator - Gunas V.I.

Technical support - Levenchuk S.S., Parashuk O.I.

Scientific editing - editorship

The site of the magazine - <https://morphology-journal.com>

CONTENT

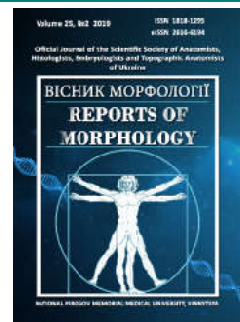
Moroz V.M., Yoltukhivskyy M.V., Vlasenko O.V., Moskovko G.S., Bogomaz O.V., Rokunets I.L., Tyshchenko I.V., Kostyuk L.V., Suprunov K.V. Sex-related features of walking with cognitive tasks	5
Cherkasov V.G., Lachtadyr T.V., Fedoniuk L.Ya., Shypitsyna O.V. Comparative analysis of the effects of various detoxification solutions on the structure of the kidneys in experimental burn disease in rats	16
Tymoshenko I.O. Structural changes of the intestinal epithelial barrier of the duodenum of rats in burn injury of skin under experimental streptozotocin-induced diabetes mellitus	28
Harapko T.V. Structural changes of the spleen in experimental obesity	36
Lysenko D.A., Lukianovych O.I., Sergyeyev S.V., Bobrowska O.A., Gurova O.O. Pharmacological correction of various morphological forms of oral mucositis in patients with leukemia	42
Fik V.B., Paltov Ye.V., Kryvko Yu.Ya. Ultrastructural condition of rats periodontal tissue in opioid influence during two weeks and after its four-week withdrawal on correction	49
Cherkasov V.G., Matkivska R.M., Cherkasov E.V., Kaminskyi R.F., Yaremenko L.M. Reactive and destructive changes of Peyer's patches in rats with experimental burn disease under infusion of detoxification solutions	56
Proniaiev D.V., Bulyk R.Ye. Characteristics of the uterine tubes in the fetal period: topographic and morphometric parallels	64
Sydorenko M.I. Structural organization of the ileum of laboratory animals in normal and in a comparative view aspect	72
Bobyry V.V., Stechenko L.O., Shyrobokov V.P., Cryvosheyeva O.I., Nazarchuk O.A., Ponyatovskiy V.A., Chuhrai S.M. Modeling of viral-bacterial infections against antibiotic-induced intestinal dysbiosis	78



REPORTS OF MORPHOLOGY

*Official Journal of the Scientific Society of Anatomists,
Histologists, Embryologists and Topographic Anatomists
of Ukraine*

journal homepage: <https://morphology-journal.com>



Sex-related features of walking with cognitive tasks

Moroz V.M., Yoltukhivskyy M.V., Vlasenko O.V., Moskovko G.S., Bogomaz O.V., Rokunets I.L., Tyshchenko I.V., Kostyuk L.V., Suprunov K.V.

National Pirogov Memorial Medical University, Vinnytsya, Ukraine

ARTICLE INFO

Received: 18 February, 2019

Accepted: 15 March, 2019

UDC: 612.766:612.01+612.661

CORRESPONDING AUTHOR

e-mail: admission@vnmu.edu.ua

Moroz V. M.

The organization of walking and its disorders remain one of the most difficult sections of the physiology of the nervous system and neurology. The purpose of the work is to analyze the sexual features of the spatio-temporal parameters of the person walking and the directions of their changes in the conditions of performing additional cognitive tasks. Sex-related features of human walking with cognitive tasks are investigated. 608 individuals of both sexes aged 12-43 years were examined by GAITRite®. Consistent naming of animals and consistent subtraction of 7 starting at 100 were used as cognitive tasks. Statistical processing of the obtained results was performed in the license package "STATISTICA 5.5" using parametric estimation methods. At performing the first (simpler) cognitive task in all age groups of men step length, stride length, step extremity ratio, support base, toe-in-out were increased. Temporal parameters in adolescents of both genders did not differ. Girls have longer step time, cycle time, single support, swing time and a slower velocity. The integral index of walking quality (FAP) tended to decrease in all examined groups: in adolescent males by 13.3±3.9%; in young men by 14.6±2.2%; in adolescent women by 15.3±1.8%; in young women by 14.4±1.1%; in middle-aged women 7.3±4.8%. Boys and girls performed more complex cognitive tasks with reduced spatial and temporal parameters (primarily by increasing the double support and swing time), the support base and toe-in-out were stable. The step cycle was rebuilt. The support base and toe-in-out remained unchanged both in boys and girls. The boys were moving at a faster velocity, taking more steps per minute. The step time right, cycle time for each leg, single support time and double support time in girls lasted much longer. FAP declined sharply by 30.4% in boys and by 33.4% in girls, indicating a major reorganization of basic mechanisms for regulating walking stability. Such a decrease in FAP leads to a decrease in the level of the balance maintaining and a decrease in body stability during movement, which means that it increases the risk of falls. A complex cognitive task led to a decrease in walking performance and a more critical decrease in the quality of walking in favor of moving forward and maintaining the balance. Thus, walking is not an automated process, but requires the use of a variety of additional CNS resources, primarily attention and cognitive resources.

Keywords: *spatial parameters of walking, temporal parameters of walking, different gender groups, gait with an additional cognitive task.*

Introduction

Free walking in everyday life is a prerequisite for independent and safe performance of multifaceted daily tasks, take care of yourself, maintaining social relationships and ensuring life quality. Therefore, the study of walking is of great importance for both physiologists and clinicians. There are daily situations with dual motor or cognitive tasks, such as a phone conversation while crossing a street. Walking is a complex motor and cognitive process that, when performed, integrates significant CNS resources [2, 9, 11,

12]. Elderly people [5, 9] and neurological patients [4, 28] have impaired walking while performing additional tasks. There are some studies of walking while performing additional tasks in young healthy people. In the most studies some gait indicators were studied without regard to age and gender [10].

The organization of walking and its disorders remain one of the most difficult section of nervous system physiology and neurology, not only because of the complexity and

insufficient study of intimate mechanisms, but also methodological problems of study of walking act. The advent of modern electronic equipment allows to obtain the parameters of a person's free walking in real time and to study its changes within different experimental paradigms, created a new opportunity for comparative analysis of this motor act and opened the prospects for clinical and instrumental comparisons [1].

After analyzing 62 publications on the results of study of the cognitive tasks impact on walking parameters in 2300 people [2], the team of authors concluded that the use of the dual task methodology (walking and cognitive task) has become a leading topic for research. However, despite the growing body of research on walking and its disorders, there are a lot of unknown issues.

The purpose of the work is to analyze gender features of human walking spatio-temporal parameters and directions of their changes while performing additional cognitive tasks.

Materials and methods

608 clinically healthy individuals of both sexes were examined to study the function of normal walking and to determine the organization features of its spatio-temporal parameters and trend of changes. At the time of the study the examined individuals should not have any injuries and diseases of different systems, which could lead to changes in gait parameters. Also, the examined volunteers were not required to consume alcohol, sedatives, drugs in the last 72 hours before the study.

Distribution of the examined individuals for age groups was as follows: 69 teenagers - 36 girls (12-15 years) and 33

boys (13-16 years); 502 young people - 241 young men (17-21 years) and 261 young women (16-20 years); 37 middle-aged women (21-43 years).

In our studies, spatio-temporal gait parameters were studied with the use of an automated GAITRite® system, produced in the USA (CIR Systems Inc., Clifton, NJ), which is a 4.2-meter-long and 1.5-meter-wide polymer track with 22,000 integrated sensor elements that respond to pressure. When walk along the track, the system scans sensors with 80 Hz frequency, processes them, saves and calculates walking' integral spatio - temporal parameters of the examined. In total, two trials were considered for each person. The data were combined and thus walking at a distance of 7-8 meters in each series was estimated. Spatio-temporal gait parameters were determined separately for the right and left legs. Walking studies were performed without shoes, as more accurate changes in spatio-temporal parameters were obtained [23]. We determined the following parameters: walking speed, steps number in passage of track, steps number per minute, step length, double step length, ratio of step length to the length of lower extremity, reliance (support) width, step time, step cycle time, foot transfer time, time of support, time of reliance on both feet, stepping cycle structure, integral indicator of quality, "normality" of walking - FAP.

Figure 1-4 shows graphical representation of footprints and methods for some parameters measuring, using GAITRite®.

The following walking parameters while performing additional cognitive tasks were analyzed: 1) consistent, without repeating pronounce of name of any known animals;

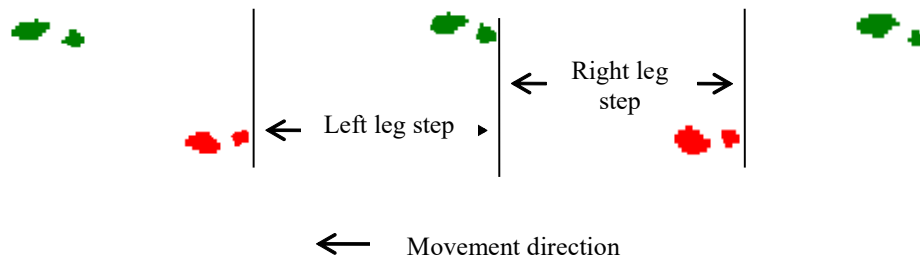


Fig. 1. Principle of step length determination (distance in cm from heel point of the previous step of one foot to the heel point of the current step of the other foot).

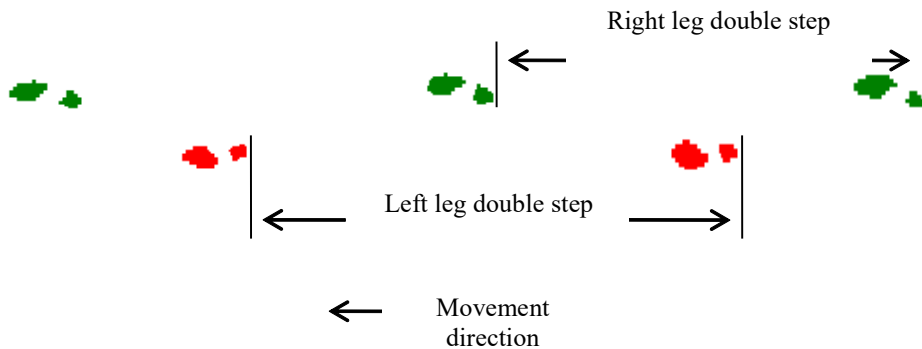


Fig. 2. Principle of double step length determination (distance in cm between heel points of two consecutive steps of one foot).

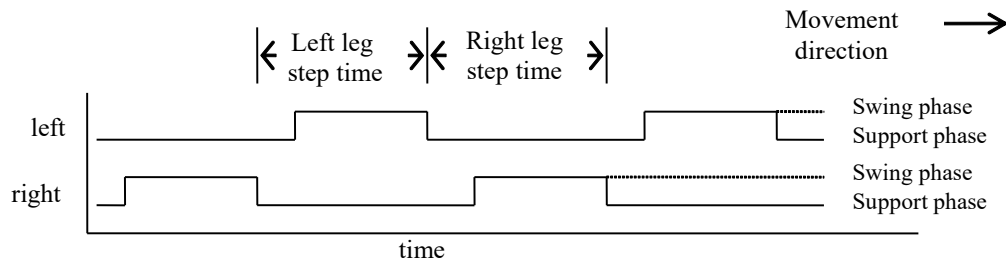


Fig. 3. Principle of step time determination (time period from the first contact of one foot to the first contact of the opposite foot).

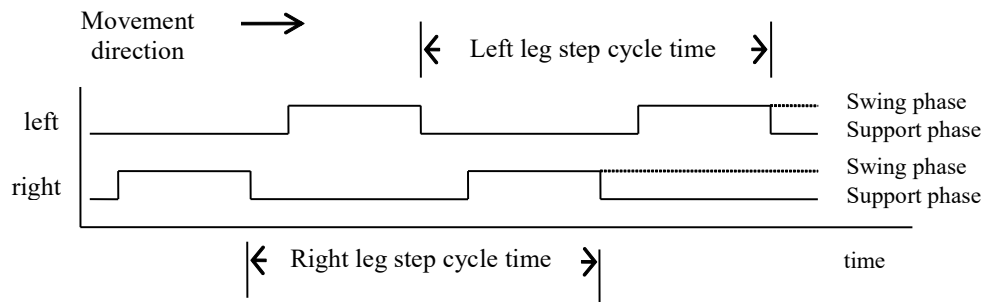


Fig. 4. Principle of step cycle time determination (time between the first contacts of two consecutive steps of one foot).

2) sequential subtraction 7, starting at 100. The quality of walking and the quality of cognitive task performance were assessed.

Statistical processing of the obtained results was carried out in the package "STATISTICA 5.5" (№AXXR910A374605FA) using parametric estimation methods.

Results

The spatio-temporal parameters of walking while simultaneously name known animals in male teenagers were as follows: average speed 118.6 ± 3.5 cm/s; number of steps per minute 101.8 ± 2.0 ; step length of the right leg 69.41 ± 1.46 cm, left - 70.03 ± 1.42 cm; ratio of step length to leg length was 0.771 ± 0.021 on the right and 0.781 ± 0.021 on the left; double step length of the right leg was 139.34 ± 2.83 cm, of the left one was 139.38 ± 2.81 cm; width of support base for the right leg 10.62 ± 0.59 cm, for the left - 10.25 ± 0.58 cm; right foot turning angle is $9.231 \pm 1.041^\circ$, for the left one is $7.401 \pm 1.082^\circ$. Duration of the right and left foot steps was equal to 0.602 ± 0.011 s; duration of stepping cycle for the right leg was 1.191 ± 0.032 s, for the left leg - 1.192 ± 0.021 s; duration of transfer of the right and left legs was the same and amounted to 0.502 ± 0.011 s; support (reliance) time for the right and left legs was the same and lasted 0.701 ± 0.022 s; duration of the single support was 0.502 ± 0.010 s on both sides; reliance on both legs when performing a step, both by right and left leg lasted the same time - 0.210 ± 0.010 s. FAP was 83.15 ± 3.88 %, which indicates a decrease in walking quality under these conditions.

In young men, the average velocity was 124.11 ± 3.29 cm/s; steps number per minute was 102.09 ± 1.68 ; step length for the right leg was 72.17 ± 1.21 cm, for the left one

was 72.98 ± 1.18 cm; ratio of stride length to leg length was the same on both sides and was 0.792 ± 0.011 ; double step length of the right leg was 145.57 ± 2.32 cm, of left one was 144.97 ± 2.20 cm; width of support base for the right leg was 10.48 ± 0.48 cm, for the left - 10.51 ± 0.46 cm; right foot rotation angle was $10.36 \pm 0.85^\circ$, for the left - $7.976 \pm 0.759^\circ$. Duration of the right leg steps was 0.587 ± 0.012 s, for the left one - 0.596 ± 0.010 s; duration of the stepping cycle for the right leg was 1.192 ± 0.031 s, for the left leg - 1.188 ± 0.019 s; duration of right and left foot movements was the same and amounted to 0.502 ± 0.009 s; support time for the right leg lasted 0.701 ± 0.010 s, for the left - 0.693 ± 0.008 s; duration of the single support was 0.502 ± 0.011 s on both sides; reliance on both feet when performing a step, both right and left leg lasted the same time - 0.210 ± 0.010 s. FAP was 82.1 ± 2.2 %, which indicates a decrease in walking quality under these conditions.

The spatio-temporal parameters of walking while naming known animals in teenager girls were as follows: mean speed 103.26 ± 4.51 cm/s; number of steps per minute 95.53 ± 2.71 ; stride length of the right leg 64.01 ± 1.37 cm, of the left leg 64.09 ± 1.32 cm; ratio of stride length to leg length was 0.761 ± 0.019 on the right and 0.761 ± 0.009 on the left; double step length of the right leg was 128.33 ± 2.62 cm, of the left one was 128.16 ± 2.67 cm; width of support base for the right leg was 7.101 ± 0.592 cm, for the left - 7.03 ± 0.591 cm; rotation angle for the right foot was $2.511 \pm 0.892^\circ$, for the left - $0.402 \pm 0.841^\circ$. Length of the right and left legs steps were the same and amounted to 0.654 ± 0.021 s; duration of stepping cycle for the right and left legs was the same and was 1.302 ± 0.041 s; duration of the right leg transfer was 0.543 ± 0.019 s, of the left - 0.536 ± 0.020 s; support time for the right leg was 0.768 ± 0.029 s, for the left

- 0.764 ± 0.031 s; duration of the single support was 0.502 ± 0.011 s on both sides; reliance on both feet when performing a step, both right and left leg lasted the same time - 0.310 ± 0.010 s. The FAP was 81.8 ± 1.8 %.

In the study of *spatio-temporal parameters of walking with simultaneous naming of known animals in juvenile girls* we found that the average speed was equal to 98.974 ± 3.32 cm/s; number of steps per minute was 93.56 ± 2.27 ; step length of the right leg was 62.53 ± 0.87 cm, of the left leg 62.98 ± 0.93 cm; ratio of stride length to leg length was 0.733 ± 0.009 on the right and 0.741 ± 0.011 on the left; double step length of the right leg was 125.7 ± 1.8 cm, of the left one was 125.6 ± 1.8 cm; width of support base for the right leg was 6.619 ± 0.494 cm, for the left - 6.553 ± 0.484 cm; rotation angle of the right foot was $2.952 \pm 0.658^\circ$, of the left - $0.501 \pm 0.687^\circ$. Duration of the right leg steps was 0.658 ± 0.017 s, of the left one was 0.681 ± 0.020 s; duration of the stepping cycle for the right leg was 1.341 ± 0.039 s, for the left - 1.337 ± 0.041 s; duration of the right leg transfer was 0.543 ± 0.021 s, of the left - 0.562 ± 0.020 s; support time for the right leg was 0.788 ± 0.031 s, for the left one - 0.769 ± 0.018 s; duration of the single support was 0.568 ± 0.021 on the right and 0.538 ± 0.019 on the left; reliance on both feet when performing a step, both right and left leg lasted the same time - 0.262 ± 0.011 s. FAP was 82.3 ± 1.1 %.

In the study of *spatio-temporal parameters of walking with simultaneous naming of known animals in middle-aged women*, it was found that the average speed was 101.32 ± 4.48 cm/s; number of steps per minute was 94.24 ± 3.11 ; right leg step length was 63.68 ± 1.12 cm, for the left leg 63.78 ± 1.07 cm; ratio of stride length to leg length was 0.738 ± 0.018 on the right and 0.751 ± 0.009 on the left; double step length of the right leg was 127.5 ± 2.1 cm, for the left one was 127.9 ± 2.2 cm; width of the support base for the right leg was 6.452 ± 0.576 cm, for the left - 6.482 ± 0.568 cm; rotation angle of the right foot was $2.281 \pm 0.802^\circ$, for the left - $4.148 \pm 0.942^\circ$. Duration of the right and left foot steps was the same - 0.669 ± 0.028 s; duration of stepping cycle for the right leg was 1.342 ± 0.051 s, for the left - 1.323 ± 0.048 s; duration of the right and left legs transfer was 0.542 ± 0.021 s; reliance time for the right leg lasted 0.803 ± 0.038 s, for the left one - 0.792 ± 0.032 s; duration of single reliance was 0.538 ± 0.019 s on both sides; reliance on both feet when performing a step, both right and left leg lasted the same time - 0.279 ± 0.018 s. FAP was 79.48 ± 4.71 %.

There were no significant differences in cognitive task performance quality in intergender comparisons in the study groups ($p > 0.05$).

In the study of *spatio-temporal parameters of walking with simultaneous performance of more complicated cognitive task (the examined person during normal walking had to subtract consistently 7 starting from the 100 and tell the result without giving priority to any of the tasks) in adolescent boys it was found*, that the average walking speed was 61.68 ± 2.77 cm/s; steps number per minute was 61.41 ± 2.43 . Step length of the right leg was $60.23 \pm$

1.042 cm, of the left leg 60.09 ± 1.09 cm; ratio of stride length to leg length was the same for the right and left legs and was 0.653 ± 0.012 ; the difference between step length of the right and left legs was 2.682 ± 0.248 cm; double step length of the right leg was 120.36 ± 2.11 cm, of the left one was 120.17 ± 2.14 cm; width of the support base for the right leg was 10.06 ± 0.49 cm, for the left - 10.01 ± 0.49 cm; rotation angle of the right foot was $8.232 \pm 0.691^\circ$, of the left - $5.518 \pm 0.672^\circ$. The average length of steps for the right leg was 1.187 ± 0.079 s, for the left one - 1.173 ± 0.068 s; duration of stepping cycle for the right leg was 2.35 ± 0.136 s, the left - 2.368 ± 0.136 s. Duration of the right leg transfer was 0.931 ± 0.062 s, of the left - 0.918 ± 0.057 s; reliance time for the right leg lasted 1.413 ± 0.078 s, for the left one 1.449 ± 0.087 s; duration of single reliance of the right leg was 0.921 ± 0.058 s, of the left one 0.928 ± 0.059 s; time of double reliance while performing a step by the right leg lasted 0.513 ± 0.041 s, by the left - 0.519 ± 0.039 s. The difference in step duration between the right and the left leg was 0.209 ± 0.038 s, and the difference in step cycles duration for both legs was 0.091 ± 0.019 s. In the structure of walking cycle with simultaneous performance of cognitive task in boys, the following ratios were obtained: the duration of foot transfer from the total duration of the walking cycle was 38.9 ± 0.5 % for the right leg, 38.8 ± 0.6 % for the left leg; reliance duration for the right leg was 61.1 ± 0.5 % of the total duration of stepping cycle, for the left leg - 61.2 ± 0.6 %; single reliance duration of the right leg in examined boys was 39.2 ± 0.6 %, of the left - 38.8 ± 0.7 % of the total duration of the respective step cycle; reliance on both feet for the stepping cycle for the right leg was 22.3 ± 0.8 %, for the left leg - 22.6 ± 0.8 %.

FAP of walking with simultaneous performance of cognitive task in adolescent boys was 67.6 ± 1.7 %, which indicates a significant decrease in quality of walking under the given physiological paradigm.

The spatio-temporal parameters when *walking with simultaneous performance of the same cognitive task in girls were as follows*: average speed of movement 47.16 ± 2.38 cm/s; per minute the girls performed 54.38 ± 2.18 steps; the right leg step length was 51.19 ± 0.91 cm, for the left leg 50.58 ± 0.88 cm; ratio of stride length to leg length was the same for the right and left legs and was 0.602 ± 0.009 ; difference between step length of the right and left legs was 2.602 ± 0.201 cm; double step length of the right leg was 101.7 ± 1.8 cm, of the left one was 102.0 ± 1.8 cm; width of the support base for the right leg was 6.209 ± 0.428 cm, for the left leg - 6.138 ± 0.418 cm; the right foot rotation angle was $4.019 \pm 0.621^\circ$, for the left - $0.501 \pm 0.658^\circ$. Right leg steps duration was 1.348 ± 0.068 s, for the left one - 1.279 ± 0.057 s. Stepping cycle duration for the right leg was 2.62 ± 0.127 s, for the left 2.581 ± 0.117 s; duration of the right leg transfer was 1.009 ± 0.058 s, of the left one - 0.948 ± 0.048 s; reliance duration for the right leg was 1.608 ± 0.082 s, for the left one - 1.638 ± 0.079 s; single reliance duration of the right foot was 0.947 ± 0.049 s, of the left one was 1.012 ± 0.058 s; reliance on both feet when

performing a step with the right leg lasted 0.662 ± 0.043 s, left - 0.668 ± 0.044 s; difference in step duration between the right and left legs was 0.212 ± 0.031 s, and the difference in step cycles duration for both legs was 0.139 ± 0.017 s; foot transfer duration from the total duration of stepping cycle was 37.9 ± 0.6 % for the right leg, 36.6 ± 0.6 % for the left leg; reliance duration for the right leg was 62.2 ± 0.6 % of the total duration of stepping cycle, for the left leg it was 63.4 ± 0.6 %; duration of a single reliance for the right leg was 36.5 ± 0.6 % of the total duration of stepping cycle, with the left - 38.1 ± 0.7 %; both feet reliance for stepping cycle for the right leg was 25.7 ± 0.8 %, for the left leg - 26.3 ± 0.9 %. FAP when walking with simultaneous cognitive task in girls was 63.4 ± 1.5 %.

In inter-gender comparison of spatio-temporal parameters of walking with simultaneous performance of more simple cognitive task (naming known animals) in teenager groups found that stride length in girls is shorter than in boys (left 9.4 ± 1.3 %, right 8.5 ± 1.2 %) ($p < 0.05$), double step length in girls is shorter than in boys (on the left by 8.9 ± 2.8 %, on the right by 8.7 ± 2.2 %) ($p < 0.05$), support base width on both sides is smaller for girls than for boys (left 45.8 ± 8.4 %, right 49.9 ± 8.3 %) ($p < 0.05$), rotation angles of both feet in girls were significantly smaller (in boys they were left $7.401 \pm 1.082^\circ$, right $9.231 \pm 1.041^\circ$, in girls on the left $0.402 \pm 0.841^\circ$, right $2.511 \pm 0.892^\circ$, $p < 0.001$). Unlike spatial, all temporal indicators in male and female teenager groups had no statistically significant differences ($p > 0.05$).

In adolescent groups, girls had a shorter step length (by 16.0 ± 1.8 % left, by 15.5 ± 1.7 % right), double step length (by 15.5 ± 1.7 % on the left, by 15.9 ± 1.7 % on the right), support base width (left by 60.4 ± 7.2 %, right by 58.6 ± 7.4 %), rotation angles of both feet (in women left $0.501 \pm 0.687^\circ$, right $2.952 \pm 0.658^\circ$, men left $7.976 \pm 0.759^\circ$, right $10.36 \pm 0.85^\circ$, $p < 0.001$), ratio of stride length to leg length (by 6.8 ± 1.4 % on both sides, $p < 0.001$).

Considerable part of temporal indicators was higher in female group: step duration was longer on the left by 11.8 ± 2.2 %, on the right by 10.6 ± 2.3 %, step cycle duration on the left by 10.6 ± 1.2 %, on the right by 11.3 ± 1.2 %, time of single reliance on the left by 7.4 ± 2.8 %, on the right by 10.7 ± 2.7 %, time of transfer on the left by 10.8 ± 2.8 %, on the right by 7.5 ± 2.9 %, reliance duration on the left by 10.4 ± 1.9 %, on the right by 11.4 ± 2.5 % ($p < 0.05$), passage time by 27.6 ± 4.0 %. Speed in women is less by 25.4 ± 3.3 % ($p < 0.001$).

Therefore, the study of spatio-temporal parameters of walking with simultaneous performance of simpler cognitive task (naming known animals) found an increase in step time duration, step cycle, time of foot transfer, support time and double support, decrease in walking speed and number of steps per minute. Inter-gender differences in the study groups had similar characteristics: in men, greater stride and double stride length, ratio of stride length to limb length, width of support base, significantly different feet rotation angles. There were no differences in temporal parameters while comparing teenager groups of boys and girls. However,

in inter-gender comparison of temporal parameters of walking with additional cognitive task in adolescent groups, differences were found in most of the parameters: women had longer stride time, stepping cycle, single support, transfer time, support time, passage time, and lower speed.

When comparing spatio-temporal parameters of walking in young men and young women with simultaneous performance of a cognitive task, which consisted of sequential subtraction 7, starting from the number 100, such differences were established. The average movements speed of young men was statistically significantly higher ($p < 0.001$). Number of steps, taken by young men to overcome the track length was statistically significantly smaller ($p < 0.001$), and the number of steps per minute in boys was statistically significantly greater ($p < 0.05$). Among the spatial parameters in young men statistically significantly greater were the usual steps length, double steps length, ratio of steps length to the corresponding leg length, as well as the width of support base for both right and left feet and feet rotation angle ($p < 0.001$ in all cases). In boys and girls, the asymmetry of stride length for the right and left leg was not significantly different ($p > 0.05$).

Among temporal indicators statistically significantly were smaller in boys: right foot step time, step cycles time for each extremity, support time for both the right and the left leg ($p < 0.05$ in all cases) and double support time (on both feet) when performing steps by each leg ($p < 0.01$). Left foot step time, right and left foot swing time, support time only for the right or left foot, as well as the difference in the right and left foot stride time, difference in step cycles time for both legs were not significantly different ($p > 0.05$ in all cases).

In young men, in the structure of step cycle when walking with additional cognitive task the proportion of the left leg swing time and single support time for the right leg was statistically significantly greater in comparison with the total step cycle time ($p < 0.01$). The percentage of the right foot swing time, the left leg single support time, and the right leg support time did not differ significantly ($p > 0.05$). The percentage of the left leg support time ($p < 0.01$) and the percentage of double support time for each leg were significantly lower in comparison with the total step cycle time of the corresponding lower limb ($p < 0.001$).

Thus, in adolescent boys and girls while walking with simultaneous performance of cognitive task did not differ much such indicators as: asymmetry of the right and left foot steps length (among the spatial parameters); left foot step time, the right and left foot swing time, support time on the right or left foot only, as well as the difference in the right and left foot step time and step cycles time for both feet (among temporal parameters). The average walking velocity, steps number per minute, all the spatial parameters, except for the abovementioned, were statistically significantly higher in boys than in girls under the same conditions. The number of steps performed by the boys to overcome the track length and the right foot step time, step cycles time for each leg, right and left legs support time, support time on both feet

when performing steps with each leg were less in boys. In step cycle structure when walking with a cognitive task in boys, statistically significantly higher were the proportions of the left leg swing time and right leg single support time from the total time of step cycle of the corresponding leg, and the share of the left leg support time and the share of double support time for both legs were smaller. The proportion of right foot swing time, left leg single support time, and right leg support time did not differ in stepping cycles of boys and girls while walking with simultaneous performance of a cognitive task.

In detailed analysis of *actual cognitive task quality*, it was found that standing in the general group of adolescents, out of 14 possible numbers to calculate, the average number of errors for them was 1.1 ± 1.4 , which is equal to 7.9 ± 9.8 %. When performing a cognitive task while walking on a track in adolescents group, the average total number of calculated numbers was 8.3 ± 3.2 , and the average number of errors in calculations - 1.3 ± 1.5 , which is equal to 17.4 ± 18.3 %.

Discussion

Contrary to the traditional notions of anatomical and functional separation of motor systems from cognitive ones, modern research can reasonably claim that these systems are interconnected [7, 9]. The basis for motion-building is the coordinated activity of different brain systems, both for those that directly control the implementation of motor act and those related to the processes of perception, attention, and memory [17].

It should be noted that the direction of changes in walking indicators while performing the cognitive task in our studies only in some cases coincided with those, reported in scientific literature.

When analyzing the effect of more simple cognitive task (sequential without repeating naming any known animal) on spatio-temporal walking parameters, it was found that gender differences of walking parameters with performance of additional cognitive task had similar directions in all studied age groups: in men longer stride and double stride length, stride length to limb length ratio, support base width, larger foot rotation angles, what probably related to anthropometric differences. Differences in temporal parameters of walking with additional cognitive task were not detected when comparing teenager groups (boys and girls). And in inter-gender comparison of walking temporal parameters with performance of additional cognitive task in adolescent groups we revealed differences in most parameters, namely: in women longer stride time, stepping cycle time, single support time, swing time, support time, longer passage time and less speed in relation to young men groups. Such changes in adolescence are likely to be associated with not only significant anthropometric gender differences (as in adolescents) but also significant neuro-humoral changes.

It should be noted that there are conflicting results of studies of cognitive tasks effect on human walking

parameters. There are reports of cognitive tasks no influence on walking of young healthy people as well as on healthy elderly people [22, 24]. The authors used easy cognitive tasks as additional ones (verbal response to auditory stimulus, verbal response to visual stimulus, etc.) that required little cognitive effort, or perhaps gave priority exclusively to walking, which was studied less accurately, mostly using electronic footswitch systems or kinematic body data estimation using video cameras [18, 21]. The study of walking using miniature gyroscopes found [4] in healthy young people performing verbal speed task caused significant changes in walking, but not in cognitive task performance: walking speed decreased and step time increased, stride length parameters did not change significantly.

In our case, the cognitive component (animal naming), apparently, was such by influence force that led to changes not in all walking parameters, but changed only some temporal parameters. Thus, it can be reasonably assumed that walking temporal parameters with additional cognitive task begin to change as soon as the simplest cognitive tasks are performed, and therefore they are more labile than spatial parameters, which change as the cognitive task complexity increases. It is important that walking speed decrease in dual tasks indicates to involvement of high-order cognitive systems in speed control [2]. The authors suggest that walking speed control zones are associated with networks of high-level cognitive functions, in particular prefrontal cortex.

When walking with more complex arithmetic cognitive task, speed decreased by 52.5 % in adolescent boys and 61.5 % in girls. The same effect of cognitive task performance on walking speed, but less significant, was also observed in other studies [8-10, 13, 27]. Thus, reducing walking speed with simultaneous additional task is likely to be a defensive reaction to maintain movement stability. On the other hand, there are data that slow walking speed, which is often accompanied by step cycle time variability increase, contributes to gait instability [17]. Therefore, in our case, in the context of simultaneous arithmetic counting walking, decrease in speed may indicate that such walking becomes less stable than normal walking. Instability may be associated with less effective walking control in speed decrease. In our studies, it was revealed that not only usual step and double step length decreases (right foot in boys by 14.9 %, in girls by 19.6 %; left foot in boys by 15.2 %, in girls by 20.8 %), but also steps length, performed by each leg to corresponding leg length ratio (in boys by 14.5 %, in girls by 20 %).

Invariability of support base width and feet rotation angles in both boys and girls may indicate that functional support base dimensions in normal walking is sufficient to maintain posture and balance even in walking with simultaneous performance of cognitive task, as well as on more rigid mechanisms of these two parameters regulation.

We have determined that both in boys and in girls'

decrease in walking speed with simultaneous calculus occurs due to increase of all without exception temporal parameters and first of all, due to increase of support time and foot swing time. With the help of special shoes, in sole of which were mounted touch sensors, we also found increase in mean step cycle time in group of healthy elderly people in walking with simultaneous counting. Although, researchers team, led by J.M. Hausdorff, in study of walking with cognitive load in healthy elderly people, found decrease in foot swing time [9].

The stepping cycle was adjusted in the direction of reducing percentage of each leg swing time and single support time for each lower extremity from their stepping cycles time (in boys by 3.9 % and 3.7 %, respectively; in girls in average by 7.6 % and 7.4 %, respectively), and increase in percentage of each leg support time and both legs support time in stepping cycles of corresponding lower extremities (in boys by 2.7 % and 18.5 %, respectively, in girls by 5.2 % and 34.7 % respectively). Therefore, to maintain equilibrium when walking with simultaneous arithmetic task helps longer support period in the stepping cycle of such walking. Moreover, the increased instability of walking with simultaneous calculation in comparison with normal walking is indicated by the increase of asymmetries of step time (from 0.010 ± 0.001 to 0.210 ± 0.040 s), step cycle time (from 0.010 ± 0.001 to 0.100 ± 0.020 s), and girls also have an asymmetry of stride length (from 1.620 ± 0.120 to 2.600 ± 0.200 cm).

The overall quality ("normality") of walking index with simultaneous cognitive task is critically reduced by 30.4 % in boys and 33.4 % in girls, indicating significant reorganization of basic mechanisms of walking stability regulation with participation of spinal and super-segmental structures under the influence of powerful commands from the highest cortex centers.

It should be noted that there are conflicting results of studies of cognitive tasks effect on human walking parameters. There are reports that cognitive tasks have no influence on walking of young healthy people as well as on healthy elderly people [19, 22]. The authors used easy cognitive tasks as additional ones that required little cognitive effort, or perhaps gave priority exclusively to walking.

Differences in spatio-temporal parameters of walking with simultaneous more complex, arithmetic cognitive task between boys and girls indicate that boys moved faster, performing more steps per minute. Right leg step time, step cycles time for each leg, support time for both right and left legs, and support time for two legs in girls was much longer than in boys. Probably, in girls the mechanisms of walking stabilization are more aimed at increasing contact time with support surface. When walking with simultaneous cognitive task, we found a certain sexual dimorphism of step cycle structure, which is not observed in ordinary walking. In boys stepping cycle, unlike girls, the percentage of double support time for each leg, as well as the percentage of left leg support time, are smaller, and the percentage of left leg swing time

and right leg single support time are greater. Perhaps, in significant complications of walking conditions, young men to maintain balance prioritize a particular leg, namely the right one in our research.

When assessing changes in walking parameters, which were caused by additional task performance, it is important to keep in mind that according to spatial and temporal parameters of walking we can indirectly assess the state of CNS structures, responsible for forming walking parameters.

Dynamic walking control includes a number of critical interaction criteria: external environmental data, goals, biomechanical constraints, and sensor integration. Dynamic walking control is based on coordinated motor neurophysiological pattern, in which appropriate interaction of body segments with each other and the environment is made to ensure progress and stability while walking. State of activity of such coordinated motor pattern, step-by-step and at long intervals is also a key factor, as walking variability is a unique area that provides data on intellectual awareness of falls risk and future mobility impairment. Dynamic walking control of higher level requires adaptability in the context of additional proposed tasks. Assessment of walking data obtained is the key to a comprehensive assessment and study of dynamic walking control [6].

It is reasonably believed [15] that step length and speed are controlled by phase output from basal ganglia into additional motor area, whereas spinal cord structures and brain stem determine the rhythm.

Locomotor phase control function is performed by cerebellar loop, which includes spinal cord, cerebrospinal tract, cerebellum, and descending pathways from brain stem. Each of these descending tracts carries both tonic (non-paternal) and phase (paternal) signals into spinal cord. These signals regulate upper and lower extremities movements by stimulation and inhibition of spinal interneurons and motoneurons activity. Change of such walking spatial parameters as stride length and double stride length, can be a sign of cerebellum pathology [26].

Closed cerebellar spinal circuits act as a control system for locomotor phase. In this case, pontomedullary reticular formation cells affect not only rhythm, but also force and phase of moving locomotor movements, increasing the importance of ventromedial system, which fibers primarily separated from vestibular nuclei, tectum, bridge and medulla oblongata reticular formation for locomotion control [6]. Based on these data, it can be predicted that changes in certain walking parameters as well as phase disturbances in overall walking pattern may indicate a shift in ventromedial system of locomotion control.

The data of our study argue the possibility of using additional tasks as a tool of isolated influence on temporal (cognitive task similar to ours in type and complexity - animal naming) and spatial (motor task) walking parameters, which allows indirectly evaluate the functional state of different parts of nervous system.

It is important to establish the fact that support base is characterized by the highest stability and plays a key role in locomotor tasks performance in difficult walking conditions. Stability of support base is required to maintain medio-lateral and anterior-posterior stability of walking. Support base is the most stable parameter, which does not change with different walking paradigms. In our study, the above-mentioned parameter did not change while performing all the additional tasks.

Thus, maintaining balance and preventing falls, which is the primary walking task, while walking with simultaneous additional tasks can be ensured by constant support base width - one of the most important components in control mechanism of balance and stability of walking.

We did not find differences in performance quality of simple cognitive task (naming animals) between gender groups. Walking quality with additional cognitive task tended to decrease in all study groups, as indicated by the results of FAP comparison. Accordingly, FAP decreased in teenager males from $96.4 \pm 4.04\%$ to $83.14 \pm 3.9\%$, in adolescent males from $96.7 \pm 4.9\%$ to $82.1 \pm 2.2\%$, in teenager women from $97.1 \pm 3.9\%$ to $81.8 \pm 1.8\%$, in adolescent women from $96.7 \pm 4.0\%$ to $82.3 \pm 1.1\%$, in middle-aged women from $96.8 \pm 5.3\%$ to $89.5 \pm 4.8\%$. Obviously, such FAP decrease proves that performing a cognitive task while walking leads to a decrease in balance level and body stability during movement, and thus increases falls risk, so significant FAP decrease can be used as a diagnostic criterion in neurological practice.

Significantly, when walking with simultaneous complex, arithmetic cognitive task, three girls refused to participate in this physiological paradigm (to perform both walking and counting) although the performance of these tasks separately, of course, did not cause any problems to them.

Decline in quality of dual tasks performing (walking and cognitive tasks) can be explained by neuropsychological theory of "resource allocation", according to which, if both tasks performed simultaneously they require the use of resources that exceed the resource of central general ability, then performing a single task, or, even, both will worsen, regardless to the specific nature of the tasks. According to the modified version of the theory of "resource allocation", due to the ability of attention to be distributed, when it is dispersed to perform two tasks that need attention, it may deteriorate, even if the capacity of the resource is not exceeded [16, 25].

There is an opinion that articulation may affect late control in healthy people [3]. Since naming animals requires coordination between the processes of articulation, phonation and respiration, this additional task can also be considered as a complex motor task. Sequent subtraction 7 and result pronunciation also requires coordination between the processes of articulation, phonation and respiration, and this additional task can also be seen as a complex motor task. Naming animals while walking can be classified as a rhythmic activity. In the scientific literature there are some data that, while performing two rhythmic tasks of different

frequencies, their powerful interference can occur [14]. Obviously, in our study, the rhythmic nature of naming animals could interfere with walking rhythm and thus provoke significant changes in walking.

You can reasonably argue about the interference of walking and counting in our study. We found a significant decrease in walking quality (decrease in FAP indices) as well as in arithmetic counting (critical increase in the number of errors in calculations from $7.9 \pm 9.8\%$ in standing to $17.4 \pm 18.3\%$ while walking). This can be explained by the neuropsychological theory of "resource allocation", according to which, if both tasks performed simultaneously they require the use of resources that exceed the resource of central general ability, then performing a single task, or, even, both will worsen, regardless to the specific nature of the tasks. According to the modified version of the theory of "resource allocation", due to the ability of attention to be distributed, when it is dispersed to perform two tasks that need attention, it may deteriorate, even if the capacity of the resource is not exceeded [16].

And according to the theory of the "bottle neck", the performance of two similar tasks reduces their performance quality [9, 20]. But it is essential, that studies on cognitive tasks influence on walking process show that the latter change walking even when the cognitive task does not have a motor component [8].

Thus, in practically healthy boys and girls, walking regulation with simultaneous performance of such cognitive task (arithmetic counting) is carried out by reducing spatial and increasing temporal parameters of walking, constant width of support base and foot rotation angle, restructuring of step cycle towards reducing the percentage of swing time and single support time and increase in percentage of support time for each leg and support time on both legs. We have used one of the complex cognitive tasks that needs maximum attention and memory. As a result, the quality of both walking and cognitive performance decreased, but the quality of counting (more than twice) declined more critically, in favor of moving forward and maintaining balance. Thus, the examined individuals subconsciously gave priority to walking.

This is coordinated with the "first pose strategy" put forward by A. Shumway-Cook, according to which, in case of increasing threat of falling, the subject prefers late control or stability of walking over the performance of additional, secondary task in order to reduce risk of falling and injury [24].

It should be emphasized that changes in spatio-temporal pattern of walking with simultaneous performance of certain tasks depend not only on task nature, but also increase in accordance with its difficulty. The greater impact of complex cognitive task on walking can be related to the mechanisms of information processing in CNS. Probably, in case of arithmetic counting, they were activated to a greater extent. In addition, counting is dependent on operative brain memory and thus directly on executive function. Competition

for executive function resource of two simultaneously performed tasks in walking conditions with additional cognitive task turned out to be quite intense.

Of course, the influence of articulation component on walking as a part of our chosen cognitive task cannot be excluded.

Therefore, regulation of spatio-temporal parameters of walking depends on the work of all levels of nervous system. The basic spatio-temporal pattern is initiated by central generators of spinal cord rhythm, whose work is set up and modulated by supra-segmental structures, and layered commands from cerebral cortex can substantially change the basic pattern by creating an appropriate spatio-temporal model of walking.

References

- [1] Abbruzzese, L. D., Rao, A. K., Bellows, R., Figueroa, K., Levy, J., Lim, E., & Puccio, L. (2014). Effects of manual task complexity on gait parameters in school-aged children and adults. *Gait & posture*, 40(4), 658-663. doi: 10.1016/j.gaitpost.2014.07.017
- [2] Al-Yahya, E., Dawes, H., Smith, L., Dennis, A., Howells, K., & Cockburn, J. (2011). Cognitive motor interference while walking: a systematic review and meta-analysis. *Neuroscience & Biobehavioral Reviews*, 35(3), 715-728. doi: 10.1016/j.neubiorev.2010.08.008
- [3] Dault, M. C., Yardley, L., & Frank, J. S. (2003). Does articulation contribute to modifications of postural control during dual-task paradigms? *Cognitive Brain Research*, 16(3), 434-440. doi: 10.1016/s0926-6410(03)00058-2
- [4] Dubost, V., Annweiler, C., Aminian, K., Najafi, B., Herrmann, F. R., & Beauchet, O. (2008). Stride-to-stride variability while enumerating animal names among healthy young adults: result of stride velocity or effect of attention-demanding task? *Gait & posture*, 27(1), 138-143. doi: 10.1016/j.gaitpost.2007.03.011
- [5] Dubost, V., Kressig, R. W., Gonthier, R., Herrmann, F. R., Aminian, K., Najafi, B., & Beauchet, O. (2006). Relationships between dual-task related changes in stride velocity and stride time variability in healthy older adults. *Human movement science*, 25(3), 372-382. doi: 10.1016/j.humov.2006.03.004
- [6] Earhart, G. M. (2013). Dynamic control of posture across locomotor tasks. *Movement disorders*, 28(11), 1501-1508. doi: 10.1002/mds.25592
- [7] Gonzales, J. U., James, C. R., Yang, H. S., Jensen, D., Atkins, L., Thompson, B. J., ... & O'Boyle, M. (2016). Different cognitive functions discriminate gait performance in younger and older women: A pilot study. *Gait & posture*, 50, 89-95. doi: 10.1016/j.gaitpost.2016.08.021
- [8] Grabiner, M. D., & Troy, K. L. (2005). Attention demanding tasks during treadmill walking reduce step width variability in young adults. *Journal of neuroengineering and rehabilitation*, 2(1), 25. doi: 10.1186/1743-0003-2-25
- [9] Hausdorff, J. M., Schweiger, A., Herman, T., Yogev-Seligmann, G., & Giladi, N. (2008). Dual-task decrements in gait: contributing factors among healthy older adults. *The Journals of Gerontology Series A: Biological Sciences and Medical Sciences*, 63(12), 1335-1343. doi: https://doi.org/10.1093/geron/63.12.1335
- [10] Hollman, J. H., Kovash, F. M., Kubik, J. J., & Linbo, R. A. (2007). Age-related differences in spatiotemporal markers of gait stability during dual task walking. *Gait & posture*, 26(1), 113-119. doi: 10.1016/j.gaitpost.2006.08.005
- [11] Hung, Y. C., Gill, S. V., & Meredith, G. S. (2013). Influence of dual-task constraints on whole-body organization during walking in children who are overweight and obese. *American journal of physical medicine & rehabilitation*, 92(6), 461-471. doi: 10.1097/PHM.0b013e31828cd59d
- [12] Hung, Y. C., Meredith, G. S., & Gill, S. V. (2013). Influence of dual task constraints during walking for children. *Gait & posture*, 38(3), 450-454. doi: 10.1016/j.gaitpost.2013.01.009
- [13] Lajoie, Y., Teasdale, N., Bard, C., & Fleury, M. (1996). Upright stand- ing and gait: are there changes in attentional requirements related to normal aging? *Exp. ging. Res.*, 22(2), 185-198. doi: 10.1080/03610739608254006
- [14] Montero-Odasso, M., Verghese, J., Beauchet, O., & Hausdorff, J. M. (2012). Gait and cognition: a complementary approach to understanding brain function and the risk of falling. *Journal of the American Geriatrics Society*, 60(11), 2127-2136. doi: 10.1111/j.1532-5415.2012.04209.x
- [15] Parihar, R., Mahoney, J. R., & Verghese, J. (2013). Relationship of gait and cognition in the elderly. *Current translational geriatrics and experimental gerontology reports*, 2(3), 167-173. doi: 10.1007/s13670-013-0052-7
- [16] Posner, M. I., Sheese, B. E., Odludas, Y., & Tang, Y. (2006). Analyzing and shaping human attentional networks. *Neural networks*, 19(9), 1422-1429. doi: 10.1016/j.neunet.2006.08.004
- [17] Priest, A. W., Salamon, K. B., & Hollman, J. H. (2008). Age-related differences in dual task walking: a cross sectional study. *Journal of neuroengineering and rehabilitation*, 5(1), 29. doi: 10.1186/1743-0003-5-29
- [18] Qu, X. (2014). Age-related cognitive task effects on gait characteristics: do different working memory components make a difference? *Journal of neuroengineering and rehabilitation*, 11(1), 149. doi: 10.1186/1743-0003-11-149
- [19] Regnaud, J. P., Robertson, J., Smail, D. B., Daniel, O., & Bussel, B. (2006). Human treadmill walking needs attention. *Journal of neuroengineering and rehabilitation*, 3(1), 19. doi: 10.1186/1743-0003-3-19
- [20] Ruthruff, E., Pashler, H. E., & Klaassen, A. (2001). Processing bottlenecks in dual-task performance: Structural limitation or strategic postponement? *Psychonomic bulletin & review*, 8(1), 73-80. doi: 10.3758/bf03196141
- [21] Schaefer, S., Jagenow, D., Verrel, J., & Lindenberger, U. (2015). The influence of cognitive load and walking speed on gait regularity in children and young adults. *Gait & posture*, 41(1), 258-262. doi: 10.1016/j.gaitpost.2014.10.013

Conclusions

1. The regulation of space-time parameters of walking depends on the work of all levels of the nervous system. The basic spatio-temporal pattern is initiated by the central generators of the spinal rhythm, whose work is set and modulated by supra-segmental structures, and the layered commands from the cerebral cortex can significantly change the basic pattern by creating an appropriate spatiotemporal model of walking.

2. Given the changes in quantitative and qualitative indicators of walking in different physiological paradigms, we can confidently state that walking is not an automated process, but requires the use of a variety of additional CNS resources, especially attention and cognitive resources.

- [22] Schrodt, L. A., Mercer, V. S., Giuliani, C. A., & Hartman, M. (2004). Characteristics of stepping over an obstacle in community dwelling older adults under dual-task conditions. *Gait & posture*, 19(3), 279-287. doi: 10.1016/S0966-6362(03)00067-5
- [23] Schulze, C., Lindner, T., Woitge, S., Schulz, K., Finze, S., Mittelmeier, W., & Bader, R. (2014). Influence of footwear and equipment on stride length and range of motion of ankle, knee and hip joint. *Acta of bioengineering and biomechanics*, 16(4), 45-51. doi: 10.5277/ABB-00043-2014-02
- [24] Shumway-Cook, A., Woollacott, M., Kerns, K. A., & Baldwin, M. (1997). The effects of two types of cognitive tasks on postural stability in older adults with and without a history of falls. *The Journals of Gerontology Series A: Biological Sciences and Medical Sciences*, 52(4), M232-M240. doi: 10.1093/gerona/52A.4.M232
- [25] Sigman, M., & Dehaene, S. (2008). Brain mechanisms of serial and parallel processing during dual-task performance. *Journal of Neuroscience*, 28(30), 7585-7598. doi: 10.1523/JNEUROSCI.0948-08.2008
- [26] Takakusaki, K. (2013). Neurophysiology of gait: from the spinal cord to the frontal lobe. *Movement Disorders*, 28(11), 1483-1491. doi: 10.1002/mds.25669
- [27] van Iersel, M. B., Ribbers, H., Munneke, M., Borm, G. F., & Rikkert, M. G. O. (2007). The effect of cognitive dual tasks on balance during walking in physically fit elderly people. *Archives of physical medicine and rehabilitation*, 88(2), 187-191. doi: 10.1016/j.apmr.2006.10.031
- [28] Yogev, G., Giladi, N., Peretz, C., Springer, S., Simon, E. S., & Hausdorff, J. M. (2005). Dual tasking, gait rhythmicity, and Parkinson's disease: which aspects of gait are attention demanding? *European journal of neuroscience*, 22(5), 1248-1256. doi: 10.1111/j.1460-9568.2005.04298.x

СТАТЕВІ ОСОБЛИВОСТІ ХОДЬБИ ПРИ ОДНОЧАСНОМУ ВИКОНАННІ КОГНІТИВНИХ ЗАВДАНЬ

Мороз В.М., Йолтухієвський М.В., Власенко О.В., Московко Г.С., Богомаз О.В., Рокунець І.Л., Тищенко І.В., Костюк Л.В., Супрунов К.В.

Організація ходьби та її порушення залишаються одними із найскладніших розділів фізіології нервової системи та неврології. Метою роботи є аналіз статевих особливостей просторово-часових параметрів ходьби людини та напрямків їх змін в умовах виконання додаткових когнітивних завдань. Досліджені статеві особливості ходьби людини при виконанні когнітивних завдань. Обстежено 608 осіб обох статей віком 12-43 років за допомогою системи GAITRite®. В якості когнітивних завдань використано послідовне називання тварин та послідовне віднімання 7, починаючи зі 100. Статистичну обробку отриманих результатів проводили в ліцензійному пакеті "STATISTICA 5.5" з використанням параметричних методів оцінки. При виконанні першого (простішого) когнітивного завдання в усіх вікових групах у чоловіків були більшими довжина кроку та подвійного кроку, співвідношення довжини кроку до довжини кінцівки, ширина бази опори, кути розвороту стоп. Часові параметри у підлітків обох статей не відрізнялись. У дівчат були більшими показники тривалості кроку, крокового циклу, одиночної опори, переносу, проходу й меншою швидкість. Інтегральний показник якості, "нормальності" ходьби (FAP) мав тенденцію до зниження в усіх досліджуваних групах: у хлопчиків-підлітків на 13,3±3,9 %; у чоловіків юнаків на 14,6±2,2 %; у дівчаток-підлітків на 15,3±1,8 %; у дівчат юнацького віку на 14,4±1,1 %; у жінок середнього віку на 7,3±4,8 %. В юнаків та дівчат при виконанні складнішого когнітивного завдання зменшувалися просторові та збільшувалися часові параметри (у першу чергу, за рахунок збільшення тривалості опори на обидві ноги та тривалості переносу ноги), були стабільними ширина бази опори та кути розвороту стоп. Перебудовувався кроковий цикл. Незмінними залишалися ширина бази опори та кути розвороту стоп як у юнаків, так і у дівчат. Юнаки рухалися з більшою швидкістю, виконуючи більшу кількість кроків за хвилину. Час кроку правою ногою, час крокових циклів для кожної ноги, час опори для обох ніг та на дві ноги в дівчат тривали значно довше. Показник FAP критично знижувався на 30,4 % у юнаків і на 33,4 % у дівчат, що свідчить про значну реорганізацію базових механізмів регуляції стабільності ходьби. Таке зниження FAP призводить до зниження рівня підтримки рівноваги та зниження стабільності тіла під час руху, а значить - збільшує ризик падінь. Складне когнітивне завдання призвело до зниження якості виконання ходьби та більш критичного зниження якості руху вперед і збереження при цьому рівноваги. Таким чином, ходьба не є автоматизованим процесом, а потребує використання різноманітних додаткових ресурсів ЦНС, насамперед уваги та когнітивних ресурсів.

Ключові слова: просторові параметри ходьби, різні гендерні групи, ходьба з додатковим когнітивним завданням.

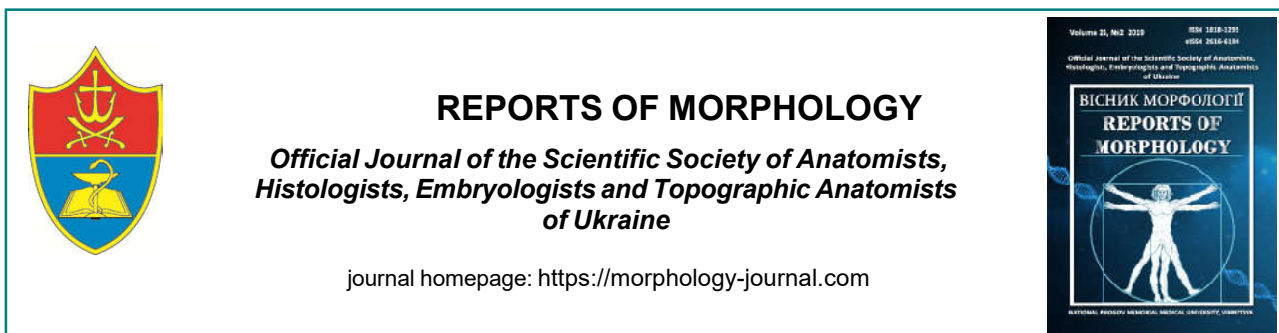
ПОЛОВЫЕ ОСОБЕННОСТИ ХОДЬБЫ ПРИ ОДНОВРЕМЕННОМ ИСПОЛНЕНИИ КОГНИТИВНЫХ ЗАДАНИЙ

Мороз В.М., Йолтуховский М.В., Власенко О.В., Московко Г.С., Богомаз О.В., Рокунець И.Л., Тищенко И.В., Костюк Л.В., Супрунов К.В.

Организация ходьбы и её нарушения остаются одними из наиболее сложных разделов физиологии нервной системы и неврологии. Целью работы есть анализ половых особенностей пространственно-временных параметров ходьбы человека и направлений их изменений в условиях выполнения дополнительных когнитивных задач. Исследованы половые особенности ходьбы человека при выполнении когнитивных заданий. Обследовано 608 лиц обоего пола возрастом 12-43 лет с помощью системы GAITRite®. В качестве когнитивных заданий использовано последовательное называние животных и последовательное вычитание 7, начиная со 100. Статистическую обработку полученных результатов проводили в лицензионном пакете "STATISTICA 5.5" с использованием параметрических методов оценки. При выполнении первого (более простого) когнитивного задания во всех возрастных группах у мужчин были больше длина шага и двойного шага, соотношения длины шага к длине конечности, ширина базы опоры, углы разворота стоп. Временные параметры у подростков обоего пола не отличались. У девушек больше показатели длительности шага, шагового цикла, одиночной опоры, переноса ноги, прохода и меньшая скорость. Интегральный показатель качества, "нормальности" ходьбы (FAP) имел тенденцию к снижению во всех исследуемых группах: у мальчиков-подростков на 13,3±3,9 %; у юношей на 14,6±2,2 %; у девочек-подростков на 15,3±1,8 %; у девушек на 14,4±1,1 %; у женщин среднего возраста на 7,3±4,8 %. У юношей и девушек при выполнении более сложного когнитивного задания уменьшались пространственные и увеличивались временные параметры (в первую очередь,

за счет увеличения длительности опоры на обе ноги и длительности переноса ноги), были стабильными ширина базы опоры и углы разворота стоп. Перестраивался шаговый цикл. Неизменными оставались ширина базы опоры и углы разворота стоп как у юношей, так и у девушек. Юноши двигались с большей скоростью, выполняя большее количество шагов за минуту. Время шага правой ногой, время шаговых циклов для каждой ноги, время опоры для обеих ног и на две ноги у девушек длились значительно дольше. Показатель FAP критически снижался на 30,4 % у юношей и на 33,4 % у девушек, что свидетельствует о значительной реорганизации базовых механизмов регуляции стабильности ходьбы. Такое снижение FAP приводит к снижению уровня поддержки равновесия и снижению стабильности тела во время движения, а значит - увеличивает риск падений. Сложное когнитивное задание привело к снижению качества выполнения ходьбы и более критическому снижению качества счета в пользу движения вперед и сохранение при этом равновесия. Таким образом, ходьба не является автоматизированным процессом, а требует использования разнообразных дополнительных ресурсов ЦНС, прежде всего внимания и когнитивных ресурсов.

Ключевые слова: пространственные параметры ходьбы, временные параметры ходьбы, разные гендерные группы, ходьба с дополнительным когнитивным заданием.



Comparative analysis of the effects of various detoxification solutions on the structure of the kidneys in experimental burn disease in rats

Cherkasov V.G.¹, Lachtadyr T.V.¹, Fedoniuk L.Ya.², Shypitsyna O.V.³

¹ O.O. Bogomolets National Medical University, Kiev, Ukraine

² Ivan Horbachevsky Ternopil State Medical University, Ternopil, Ukraine

³ National Pirogov Memorial Medical University, Vinnytsya, Ukraine

ARTICLE INFO

Received: 20 February, 2019

Accepted: 19 March, 2019

UDC: 611.611:57.012:57.08:616.5-001.17

CORRESPONDING AUTHOR

e-mail: anatomi@ukr.net
Cherkasov V.G.

The use of existing infusion solutions, as well as the development, scientific substantiation and implementation of the latest nephroprotective detoxification solutions, remain an urgent problem for combustiologists. The aim of this work is to compare the effects of various detoxification solutions (0.9 % NaCl solution and complex colloid-hyperosmolar solutions - lactoprotein with sorbitol and the newly developed HAES-LX-5 % solution) on the kidney structure in experimental burn disease in rats. The experimental rats were divided into seven groups (fifteen animals each): the first group was intact rats; the second, third and fourth groups were rats without reproduction of experimental burn disease, which had a separate intravenous infusion of 0.9 % NaCl solution, lactoprotein with sorbitol and HAES-LX-5 % at a dose of 10 ml/kg; the fifth, sixth and seventh groups were rats with experimental burn disease (by causing burn injury of the skin with an area of 21-23 % of the body surface), which under the same scheme had an intravenous infusion of the investigated solutions. All studies and the removal of rats from the experiment were performed under deep thiopental intraperitoneal anesthesia. Histological preparations of the renal cortex of the rat were stained with hematoxylin-eosin and examined on an Olympus BX51 microscope. Using ultramicrotome LKB-3 (Sweden) obtained semi-thin sections which were stained with toluidine blue and methylene blue - Azur II; and ultrathin sections were counterstained with uranyl acetate and lead citrate according to Reynolds and examined using a PEM-125K electron microscope. Morphometric measurements (estimation of the area of the vascular glomeruli, the area of the urinary lumen of the capsule of the renal corpuscles; the area of the renal tubules of the nephrons and the area of their lumens, the area of the renal corpuscles, the area of cytoplasm and nuclei of epithelial cells of tubules, and also their nuclear-cytoplasmic ratio) was carried out using the VideoTest-5.0, KAARA Image Base and Microsoft Excel on a personal computer. Statistical analysis of the obtained quantitative indicators was performed using the IBM SPSS v. 22.0. for Windows. Functionally different cells of nephrons have been found to die by necrosis, apoptosis and anoikis when infused with detoxification solutions during the development of burn disease; in epithelial cells of nephron tubules, mitophagy and mitoptosis occur. Mitoptosis in epithelial cells of rat tubules of nephrons with experimental burn skin injury is carried out in two ways related to: 1) destruction of the outer mitochondrial membrane; 2) preservation of the outer mitochondrial membrane and involvement of autophagic (mitophagic) mechanisms to release the cell from degraded mitochondrial material. In the first case, the mitochondria first condense, after which its matrix swells and the fragmentation of the cristae occurs due to the destruction of the junction of the cristae. Finally, the outer mitochondrial membrane breaks and the remnants of the cristae (in the form of vesicles) go into the cytoplasm. In the second case, the mitochondria condense, vesicular fragmentation of the cristae occurs, but the rupture of the outer mitochondrial membrane does not occur and the mitochondria are absorbed by the autophagosome (or transformed into the autophagosome). Next is the merger of autophagosomes with lysosomes and the formation of autophagolysosomes, which, under

the conditions of effective digestion of the contents, are transformed into vacuoles. The latter are emptied by exocytosis and ensure the release of cells from degraded material. Only lactoprotein with sorbitol has a membrane-plastic effect on the strengthening (enhancement of structuring) of the mitochondrial membrane in part of the mitochondria of epithelial cells of nephron tubules, which is ultrastructurally manifested by an increase in the electron density and thickness of all components of the mitochondria. The maximum membrane effect of lactoprotein with sorbitol against mitochondria manifests itself fourteen days after the experimental burn skin injury and gradually (after twenty-one and thirty days) disappears, which is correlated with an improvement in the overall clinical condition and an improvement in the structural changes in the kidney of animals with burn disease. There is every reason to believe that increased structuration of mitochondria is a preventer of the spread of mitoptosis and mitophagy, the excess of which can lead to cell death.

Keywords: burn disease, detoxification solutions, reactive and destructive changes of the kidneys.

Introduction

Severe and large skin burns cause structural and functional pathological changes in all organs and systems of burned persons, which initiates the development of burn disease [14], a disease that has become increasingly widespread in recent years [9, 26].

According to researchers [14], burn disease is a disease that involves a set of clinical, morphological and biochemical, metabolic and other related disorders in all organs and systems. One of the leading factors in these disorders is the direct burn of the local destruction of large tissue arrays, which becomes a source of endotoxins and a factor in the formation and distribution of various biologically active substances. A powerful source of endotoxins and other biologically active substances are also tissue components of organs that were not initially subjected to thermal alteration but were in a state of discirculating hypoxia and histotoxic ischemia for some time.

It should be noted that thermal damage and gradual endogenous intoxication cause imbalance of water-salt homeostasis, increased permeability and destruction of the hemocapillary wall. In the treatment of burn disease (caused by severe burn injuries), the main goal of intravenous infusion therapy is to ensure an adequate level of tissue perfusion at the initial stages of the burn disease; normalization of tissue metabolism; prevention of severe toxic, hypoxic and reperfusion damage of cells and tissues [21, 23, 25].

Therefore, for a long time, scientific justification for the use of existing infusion solutions for reducing the level of toxins in the body and for normalizing the function of the kidneys, aimed at maintaining water-salt metabolism, remains relevant for combustiologists [3, 5, 6, 8, 15, 17, 18, 25], as well as the development and implementation of the latest nephroprotective detoxification solutions.

The aim of this work is to compare the effects of various detoxification solutions (0.9 % NaCl solution and complex colloid-hyperosmolar solutions - lactoprotein with sorbitol and the newly developed HAES-LX-5 % solution) on the kidney structure in experimental burn disease in rats.

Materials and methods

Comparative analysis of structural changes in rat kidney after experimental skin burn under the conditions of

intravenous infusion, namely: isotonic sodium chloride solution (0.9 % NaCl solution) and colloid-hyperosmolar solutions (lactoprotein with sorbitol and HAES-LX-5 %) was performed on 105 white male rats weighing 155-160 grams.

Detention in the vivarium and all manipulations with rats were carried out in full compliance with the provisions of the "General Ethical Principles for Animal Experiments", approved by the First National Congress on Bioethics (Kyiv, 2001), with strict adherence to the recommendations of the "European Convention for the Protection of Vertebrate Animals Used for Experimental and Other Scientific Purposes" (Concil of Europe, Strasburg, 1986).

The experimental rats were divided into seven groups (fifteen animals each): the first group was intact rats; the second, third and fourth groups were rats without reproduction of experimental burn disease, which had a separate intravenous infusion of 0.9 % NaCl solution, lactoprotein with sorbitol and HAES-LX-5 % at a dose of 10 ml/kg; the fifth, sixth and seventh groups were rats with experimental burn disease, which under the same scheme was administered an intravenous infusion of the test solutions.

For the simulation of burn disease, an experimental skin burn was performed by pressing four heated copper plates (two plates on each side, an area of each 13.86 cm²) which were previously kept for six minutes in water at a constant temperature of 100°C. To determine the extent of damage in the experimental burn injury, the severity index was used, which considers the parameters of the area and depth of burns, as well as the total skin area of the burn. The calculation data show that the experimental burn injury covered 21-23 % of the animal's body surface, which is sufficient for the formation of grade II-III burns, the development of moderate-severity burn shock, and the initiation of burn disease.

The infusion of solutions at a dose of 10 ml/kg was carried out for five minutes in a caudal vena cava after its introduction of the catheter in aseptic conditions through the femoral vein. The course of infusion therapy lasted for seven days (the first intravenous infusion was performed one hour after the experimental burn injury, the subsequent injections were carried out once a day).

The experimental burn injury, catheterization of the main vessels was performed under anesthesia caused by

intraperitoneal injection of propofol at a dose of 60 mg/kg.

Material was removed from rats for morphological examination of the kidneys under deep thiopental intraperitoneal anesthesia fourteen, 21 and 30 days after the experimental burn skin injury. For histological examination, the obtained biopsies were treated according to the conventional procedure and stained with hematoxylin-eosin. Histological preparations of the rat renal cortex were examined on an Olympus BX51 microscope.

When receiving material for electron microscopic examination of rats under deep thiopental intraperitoneal anesthesia, the opening of the abdominal cavity was performed. The rat kidney biopsies were crushed into small blocks and fixed in glutaraldehyde solution. After standard wiring, the material was poured into an araldite mixture with epon.

Semi-thin and ultra-thin sections were made using an ultramicrotome LKB-3 (Sweden). The resulting semi-thin sections were stained with toluidine blue and methylene blue - azure II. Ultrathin sections were contrasted on copper support meshes with uranyl acetate and lead citrate according to Reynolds. Electron microscopic examination was performed using a PEM-125K electron microscope.

To objectify comparative analysis of the course of reactive and destructive processes in the renal cortex of burned rats, a morphometric study was performed. Evaluated: areas of vascular glomeruli, areas of urinary lumen of the capsule of the renal corpuscles; the renal tubule area of nephrons and the area of their lumen, the area of the renal corpuscles, the area of cytoplasm and nuclei of epithelial tubular cells, as well as their nuclear-cytoplasmic ratio.

Images from histological specimens stained with hematoxylin-eosin were taken to a computer monitor using a MICROMedSEOSCAN microscope and using a Vision CCD Camera. Morphometric measurements were performed using VideoTest-5.0, KAAPA Image Base, and Microsoft Excel on a personal computer.

Statistical analysis of the obtained quantitative indicators was performed using the IBM SPSS v. 22.0. for Windows. The values of the arithmetic mean (M), the error of the arithmetic mean (m) were calculated for all investigated parameters and the standard deviation (σ) was determined. The significance of the difference of values between the independent quantitative values was calculated under the conditions of normal distribution (the estimate of the type of distribution was verified by the χ^2 - Pearson criterion) by the Student's t-test (using the Bonferroni correction for more than two groups), and in other cases the Mann-Whitney U-test was used. Comparison of qualitative features was performed using criterion χ^2 . The differences at $p < 0.05$ were considered significant.

Results

Studies have shown the unconditional positive benefits of intravenous infusion of colloid-hyperosmolar solutions over infusion of 0.9 % NaCl solution, which is further

substantiated by statistical analysis of the data obtained from morphometric measurements. There are also differences in the influence on the structure of the renal cortex of burned rats of lactoprotein with sorbitol and HAES-LX-5%.

The study showed that experimental burn skin injury and the resulting burn disease lead to significant structural changes in the components of the kidney after fourteen, twenty-one and thirty days (in the stages of late toxemia and septicotoxemia of burn disease, manifestations of which were manifested by timely infusion therapy). In temporal terms, the process of destruction and structural restructuring in the renal cortex of experimental burned rats in the investigated time of the experiment does not fade, but is only modified.

Fourteen days (Fig. 1, 2) after experimental burn injury of the skin with the introduction of 0.9 % NaCl solution, the destruction of hemocapillaries, edema and hemorrhage in the interstitium of the renal cortex occurs (this process is mosaic and widespread). Twenty-one days and thirty days after, structural changes deepen and become focal, limited in nature: the necrosis and hemorrhage areas become larger, but their number decreases. A characteristic feature of these terms of burn disease is the involvement in the process of structural damage to the immune component, which is evidenced by the appearance of foci of lymphocytic and plasmacytic infiltrates in the renal cortex. The efficacy of recorded lymphocytic and plasmacytic infiltration of the renal cortex is questionable, because infiltrate plasmacytes are substantially structurally altered and subject to apoptotic transformation.

Summarizing the results of the study of the structural changes of the renal cortex of rats with skin burns, which were injected with 0.9 % NaCl solution, we can conclude that its infusion does not cause pronounced nephroprotective effects, and the structures of the renal cortex are characterized by the presence of morphological changes in the composition of the glomerular and tubular apparatus. Positive substantially compensatory-adaptive reactions include structural features of the presence of the functional potential of podocytes due to the preservation of podocytes and stabilization of the thickness of the basement membrane. The reactive manifestations can also be attributed to the process of eliminating damaged mitochondria by mitoptosis, but the dualism of this process should be emphasized. Mitoptosis is able to inhibit apoptosis, but its spread can lead to macroautophagy and necrotic cell death.

The use of infusion monotherapy alone with the effects of severe skin burns with 0.9 % NaCl solution has a certain positive effect on the body of burned rats (by reducing the level of endogenous intoxication, which is reflected in the mortality rate recorded in the study). At the same time, the results of the study indicate the benefits of using combined colloid-hyperosmolar infusion solutions, endowed with nephroprotective properties, which improves the regenerative capacity of kidney cells.

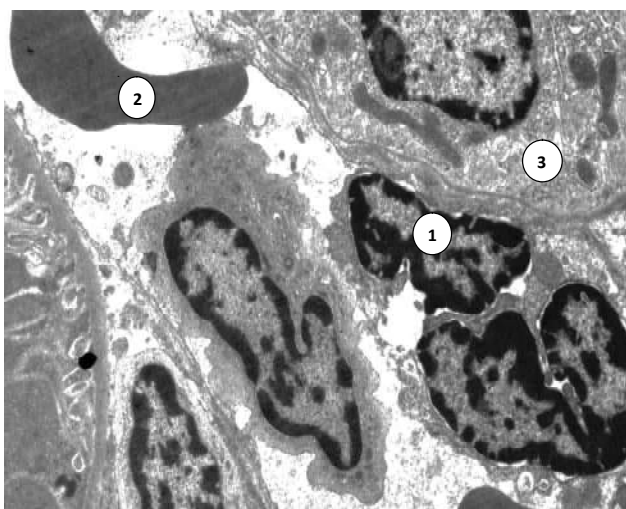


Fig. 1. Destruction of the wall of the peritubular hemocapillary, edema and hemorrhage in the interstitium of the renal cortex of the rat 14 days after the experimental burn injury with the introduction of 0.9 % NaCl solution. 1 - nucleus of destroyed endothelial cell; 2 - erythrocyte in swollen interstitial space; 3 - basal pole of the epithelial cell of the distal tubule of the nephron. Electronic micrograph. x10000.

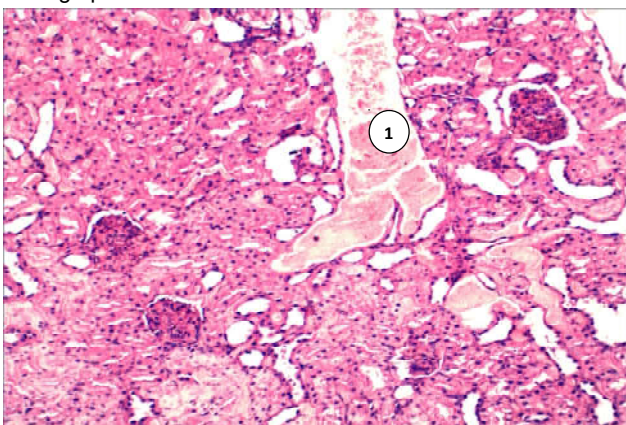


Fig. 2. Combination of sharp expansion of peritubular venules with the formation of sludge erythrocyte conglomerates (1) and with partial destruction of the vascular wall in the renal cortex of the rat 14 days after the experimental burn injury under the condition of 0.9 % NaCl solution. Photomicrograph. Hematoxylin-eosin staining. x100.

We have found that due to hyperosmolarity, lactoprotein with sorbitol and HAES-LX-5 % provide the transfer of excess fluid (resulting from the inflammatory response to burn injury) from the intracellular sector to the vascular bed. It optimizes the hemomicrocirculation and stabilizes the perfusion in the kidneys, which is morphologically determined and histophysiologicaly justified in the analysis of the results of this study.

Histological, electron microscopic and morphometric studies indicate that (unlike 0.9 % NaCl solution) lactoprotein with sorbitol and HAES-LX-5 % exert a cytoprotective effect on the structure of the rat kidney with experimental burn injury, thus revealing nephroprotective properties. The analysis of

morphometric data indicates statistically significant ($p < 0.001$) changes in different size of renal corpuscles, which can be divided into two groups: I - large (hypertrophied) renal corpuscles; II - small (atrophied) renal corpuscles. The size and structural organization of these renal corpuscles indicate the different degree of their functional load and the potential for the implementation of the filtration function. Fourteen days after the experimental burn skin injury, their average area under infusion of 0.9 % NaCl solution was $8453 \pm 203 \mu\text{m}^2$ and $4687 \pm 128 \mu\text{m}^2$, respectively. Comparison of the range of oscillations of the sizes of the average area of the large and small renal corpuscles at different periods of the experiment after the experimental burn skin injury (after fourteen, twenty-one and thirty days) shows a significant increase of the average area of the large renal corpuscles ($p < 0.001$), the size of the average area of the vascular glomerulus ($p < 0.01$) and mean area of the urinary space of the kidney capsule of renal corpuscles ($p < 0.01$) under the conditions of infusion of lactoprotein with sorbitol and HAES-LX-5 %, which indicate positive (compared to 0.9 % NaCl solution) positive effect of colloid-hyperosmolar solutions on the course of reactive processes in kidney cells of burned rats.

The influence of lactoprotein with sorbitol on the structural changes of the kidneys is reflected in the statistically significant difference of the majority of the investigated morphometric parameters characterizing the functional abilities of the filtration and reabsorption apparatus of the kidneys of burned rats of this experimental group, from the similar ones that characterize the state of the renal cortex of burned rats administered 0.9 % NaCl solution.

Only lactoprotein with sorbitol has a membrane-plastic effect on the strengthening (enhancement of structuring) of the mitochondrial membrane in part of the mitochondria of epithelial cells of nephron tubules, which is ultrastructurally manifested by an increase in the electron density and thickness of all components of the mitochondria. The maximum membranoplastic effect of lactoprotein with sorbitol on mitochondria manifests itself fourteen days after the experimental burn skin injury and gradually (twenty-one and thirty days later) disappears, which correlates with an improvement in overall clinical status and dynamics disease. There is every reason to believe that increased structuration of mitochondria is a preventer of the spread of mitoptosis and mitophagy, the excess of which can lead to cell death. This effect is not a consequence of the direct action of lactoprotein with sorbitol, but is a consequence of the action of lactoprotein with sorbitol under conditions of the development of burn disease (Fig. 3) and is absent under normal conditions (Fig. 4).

Summarizing the results of our study of structural changes in the renal cortex of the rat with experimental burn skin injury, which was administered lactoprotein with sorbitol, we can conclude that intravenous infusion of this solution leads to inhibition of nephrocyte alteration. The kidneys in rats of this experimental group have less pronounced

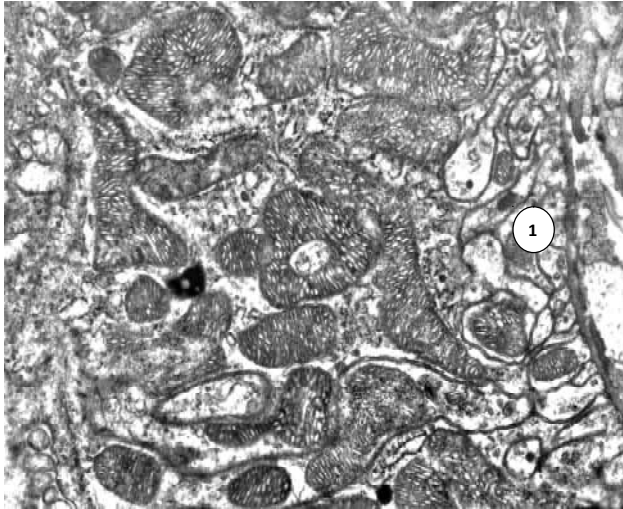


Fig. 3. The accumulation of over-structured mitochondria in the cytoplasm of the epithelial cell of the proximal tubule in the renal cortex of the rat 14 days after the experimental burn injury under the conditions of the introduction of lactoprotein with sorbitol. 1 - basal striations. Electronic micrograph. x40000.

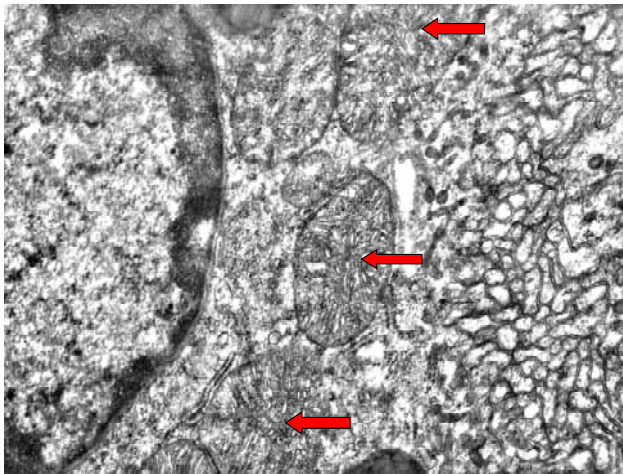


Fig. 4. Ultrastructural structure of mitochondria (marked by arrows) located in the cytoplasm of the epithelial cell of the proximal tubule in the renal cortex of the rat without experimental burn skin injury (normal). Electronic micrograph. x40000.

changes in the structure and, accordingly, more preserved functionality of the cells of nephrons, compared with those in the burned rats who were administered 0.9 % NaCl solution.

The intensification of the regenerative processes in the vascular component of the nephron tubules and renal corpuscles leads to an overall improvement in microcirculation and, consequently, a normalization of their functions. The protective effect covers not only the organelles of the epithelial cells of the tubules, but extends to the organelles of podocytes and endothelial cells of the hemocapillaries of the vascular glomerulus and to the common basement membrane, which inhibits the integrity of the filtration barrier.

Our studies indicate that a number of interrelated

pathological consequences of severe experimental burn skin injury are capable of producing renal damage at the cellular level, and the use of infusion of colloid-hyperosmolar combined solution of lactoprotein with sorbitol, which intentionally stimulates organelles protein-synthesizing apparatus and corrects the metabolic substrate of nephron cells, significantly limiting the gradient morphofunctional changes in the renal cortex in burned rats.

Like lactoprotein with sorbitol, the influence of HAES-LX-5 % under the development of burn disease manifests itself in nephroprotective action. Just as in the case of lactoprotein infusion with sorbitol, the structural features of HAES-LX-5 % influence are reflected in the statistically significant difference of the majority of the studied morphometric parameters characterizing the state of the filtration and reabsorption apparatus of rats with experimental burn skin trauma from similar, characterizing condition of the renal cortex of rats with experimental burn skin injury, which was administered 0.9 % NaCl solution.

Comparing the effects of the hyperosmolar solutions applied, it should be noted that the HAES-LX-5 % infusion provides a more harmonious effect on the renal cortex structure of the rat with experimental burn skin injury. The less pronounced manifestations of repair in this case are associated with a lower degree of destruction in the renal cortex of experimental animals, which is evidence of the nephroprotective properties of HAES-LX-5 % (Fig. 5, 6).

We found that mitochondria of epithelial cells are the most active organelles under normal conditions and the most vulnerable ones under experimental burn skin injury. Increased functional load leads to an acceleration of the aging of their mitochondria, and in worse conditions - to the destruction of not only old but also defective mature and young mitochondria. Infusion of HAES-LX-5 % promotes the ordering and normalization of mitoptosis in epithelial cells of nephron tubules (see Fig. 6).

In rats with experimental burn skin injury, we observed mitoptosis of mitochondria of epithelial cells of nephron tubules. These mitochondria undergo microautophagic changes, including fusion of lysosomes with small damaged mitochondria or with small isolated fragments of branched mitochondria. Autophagolysosomes thus formed undergo a step-by-step transformation that can be defined in spatial dimension as the "base apical transformation sequence". In this sequence, the transformation of the autophagolysosome occurs in the direction from the electron-dense autophagolysosome in the basal zone of the cytoplasm of the epithelial cell to the vacuole with electron-transparent content in the apical zone of the cytoplasm. Infusion of HAES-LX-5% leads to the stabilization of this sequence, which reflects the protective properties of the solution relative to mitochondria.

Summarizing the results of the study of the structural changes in the renal cortex of the rat with experimental burn skin injury, which was injected with HAES-LX-5 %, we can conclude that the use of infusion of HAES-LX-5 % does not

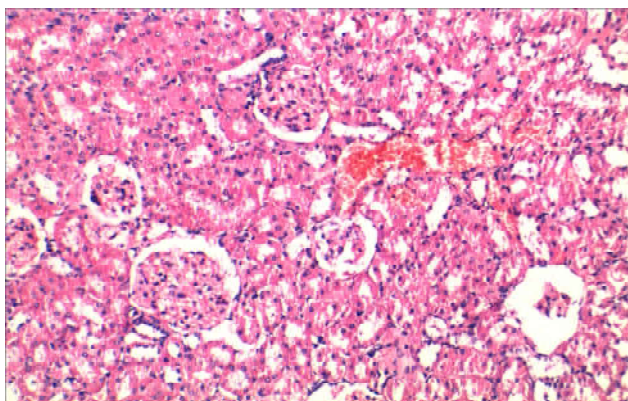


Fig. 5. The area of the renal cortex of the rat 14 days after the experimental burn injury with the introduction of HAES-LX-5 %. Photomicrograph. Hematoxylin-eosin staining. x100.

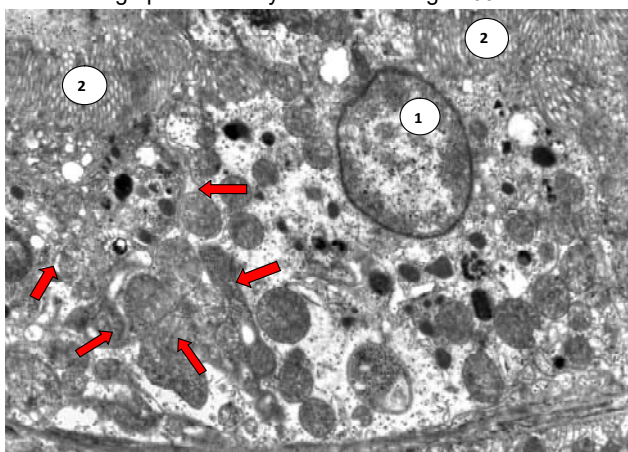


Fig. 6. Fusion of mitochondria, as well as their mitoptosis in the epithelial cell of the proximal tubule of nephron in the renal cortex of the rat 14 days after the experimental burn injury under the conditions of administration of HAES-LX-5 %. Arrowheads indicate zones of accumulation and confluence of mitochondria at different stages of their degradation. 1 - nucleus of epithelial cell; 2 - brush border. Electronic micrograph. x25000.

lead to a rapid complete restoration of the structural organization of the cells of the components of the nephron. However, the positive effect of such infusion therapy contributes to the activation of the organelles of the metabolic plan, improves hemomicrocirculation, and, accordingly, filtration and reabsorption functions. Such a normalizing effect makes it possible to recommend the use of a new colloidal-hyperosmolar HAES-LX-5 % solution to ensure timely prevention and optimization of complex treatment of the harmful effects of severe burn injuries to the skin.

Some dynamics and selectivity of cell death in the renal cortex of burned experimental rats were revealed. We have found that under the infusion of 0.9 % NaCl solution, part of all cells of the rat renal cortex perish by necrosis; part of the epithelial cells of nephron tubules, epithelial cells of the parietal layer of the glomerular capsule, and endothelial cells of the blood microvessels perish by anoikis; some mesangiocytes die by apoptosis; in the epithelial cells of

the tubules of the nephron there is a mitoptosis. The use of hyperosmolar colloidal solutions inhibits cell necrosis and modifies the remaining irreversible cell changes. It is worth noting that in all cases, the most resistant cells to the harmful effects of burn skin injury are podocytes. Podocytes maintain the structural integrity of the basement membrane and, as a result, stabilize the endothelial cells of the hemocapillaries of the vascular glomeruli, which exhibit a greater degree of resistance compared to the endothelial cells of the walls of the blood vessels of the peritubular mesh. The expression of reactive transformations of podocytes is the variability of the shape and size of cytotubules, cytopodia and soles of attachment of cytopodia. Their deformation modulations, together with changes in the basement membrane, are combined with an increase in the structure of the cytoskeleton elements (microfilaments and microtubules) located in the cytoplasm, which, in the aggregate, causes changes in the sizes and configurations of filtration slits and filtration diaphragms, thus changing.

We have noted that in some cells of the renal cortex of rat with experimental burn skin injury, structural changes of mitochondria occur by the mechanism of "out membrane mitoptosis". In this case, the mitochondria first condense, after which its matrix swells and the fragmentation of the cristae occurs due to the destruction of the junction of the cristae. Finally, the outer mitochondrial membrane breaks and the remnants of the cristae (in the form of vesicles) are released into the cytoplasm. As a rule, the mitochondria of the epithelial cells of the nephron tubules have an elongated rod-like shape, and when swollen, they fragment and become rounded (oval or spherical). However, in most epithelial cells of rat nephron tubules with experimental burn skin injury, a mixed type of mitoptosis has been reported. In this case, the mitochondria condense, there is a bubbling fragmentation of the cristae, but the rupture of the outer mitochondrial membrane does not occur and the mitochondria is absorbed by the autophagolysosome (or transformed into the autophagolysosome). Therefore, the final step in the transformation of the autophagolysosome is the formation of a vacuole with a transparent content (effective digestion of the content of the autophagolysosome), which by exocytosis releases its contents from the cell outside. Thus, mitoptosis can be accomplished both with and without the involvement of autophagic (mitophagic) mechanisms.

It is recognized that the mitophagy of damaged mitochondria of epithelial cells of nephron tubules inhibits the mitochondrial pathway of apoptosis activation. On the other hand, mitochondrial destruction and intense mitophagy contribute to cell death by accidental and unregulated or programmed necrosis involving lysosomal enzymes. Morphologically, both types of such cell death are accompanied by cell swelling, destruction of the plasmalemma, and release of cellular detritus into the extracellular space.

The stability of the mitochondrial shape in the basal

divisions of the epithelial cells of the proximal tubules of rat nephrons with experimental burn skin injury is lost, the basal streakiness is deformed. In this case, the mitochondria are snug against each other. This process can be interpreted as the fusion of mitochondria and the formation of giant branched or annular mitochondria. It is not excluded that, in fact, we observe as giant branched mitochondria fragment and their fragments merge into their ends, forming mitochondria of the annular shape. That is, "mitochondrial fission and fusion" and "membrane tethering" [30] occur, result in the formation of separate and united "mitochondrial complexes".

In rats with experimental skin trauma administered 0.9 % NaCl solution, significant changes in the basal membrane in all components of the renal cortex were noted: loosening and local destruction of the basement membrane; loss of its characteristic structure and electron density. These structural shifts occur in the basement membrane of the walls of the blood microvessels, the parietal and visceral layers of the glomerular capsule, tubules of the nephrons. The dynamics of these transformations are in accordance with the severity of the destructive changes of cells for which the basement membrane is a subordinate extracellular matrix. In our worst-case scenario, the damaged cells merge into the corresponding spaces and the basement membrane becomes exposed.

Against the background of the described changes, the membrane-plastic effect of the infusion of lactoprotein with sorbitol, the structural expression of which is to stabilize the normal structure of the basement membrane, and also to the hyperplastic repair of the damaged basement membrane, which has the character of excess and uneven, is most clearly manifested. The latter, in particular, concerns the basal membrane in the wall of the tubules of the proximal divisions (at separate loci, the thickness of the basal membrane increases 3-6 times). Producer components of the basement membrane are adjacent cells, which show the structural features of activation of the protein-synthesizing apparatus of cells (first of all - the expansion of the tubules of the granular mesh, which are completely filled with fine-grained content of average electron density).

The above-mentioned transformation of the basement membrane (the appearance of local defects and their inappropriate repair) reflects significant disorders of matrix-cytoplasmic relationships in the kidney of rats with experimental burn skin injury. Loss of typical adhesive ties in the areas of the distorted basement membrane leads to autophagic (in the worst case, necrotic) or apoptotic (anoikis) changes of epithelial and endothelial cells and their attachment to the lumen of the hollow.

Discussion

In accordance with the above, the data obtained by us about autophagic, necrotic and apoptotic cell changes in the rat kidney with experimental burn skin injury indicate that selectively stimulated microautophagy (and, in particular,

mitophagy) allows cells to survive when they have lost normal levels of extracellular matrix attachment for some time and then attach to it again. The latter is best manifested in the epithelial cells of the tubules of the proximal departments of the nephrons of rats with experimental burn skin injury, when the cytoplasmic processes (folds) of the basal striations are deformed, and the renewal of its typical architectonics (as a manifestation of the positive action of lactoprotein with sorbitol and HAES-LX-5 %) accompanied by the establishment of matrix-cytoplasmic contacts (establishment of a certain number of contacts and renewal or increase of the area of contact between the plasmalemma and the basement membrane).

Therefore, selective microautophagy in the form of mitophagy in the cells of the renal cortex of the rat with experimental burn skin injury is a manifestation of a compensatory-adaptive reaction whose balance has certain limits. If microautophagy is not adequately amplified, it leads to macroautophagy and may result in necrosis of the excessively vacuolated cell. If microautophagy is not adequately inhibited, it can lead to apoptotic changes in the cell. We found that the infusion solutions used lead to different variants of the destructive changes in the cells. Under the conditions of infusion of 0.9 % NaCl solution, mainly necrotic cell changes occur, which are accompanied by the development of interstitial edema, hemorrhage and lymphocytic infiltration. Under conditions of infusion of lactoprotein with sorbitol and HAES-LX-5 %, the spread of destructive changes in the renal cortex of burned rats is inhibited and substantially altered in both temporal and spatial dimensions. Intravenous infusion of applied colloid-hyperosmolar solutions provides inhibition of cell necrosis, thus suppressing the intensity of the inflammatory response, changing the way of realization of mechanisms of mitoptosis (the main is "out membrane mitoptosis" or mitoptosis with wide involvement of autophagic localized processes) and contributes to the limited, local nature of autophagic and apoptotic changes. The effects of the components of the combined colloid-hyperosmolar solutions on the mitochondria require further study, but there is no doubt that the regulation of mitoptosis is a "switch" to prevent irreversible changes in the cells of the kidney of rats that cause disorders of renal detoxification function and are a consequence of the effects of burn disease factors in experimental burn skin injury.

Mitochondria have a leading role in cell function, not only by providing them various metabolic responses and energy production, but also by being the main site of reactive oxygen species formation and a key player in initiating cell death [20, 30]. Therefore, mitochondrial dysfunction or damage can have serious consequences. Mitophagy (autophagic degradation of mitochondria) and mitoptosis (programmed destruction of mitochondria) are the processes by which cells are released from damaged mitochondria [2, 11, 13, 19, 22, 24, 27]. The effectiveness of these processes can be a factor that promotes or inhibits the development of various

pathological conditions [20, 28].

We have found a specific lactoprotein with sorbitol membrane-stimulating ultrastructural effect in the development of burn disease, which is to enhance the structuring of the mitochondria of epithelial cells of nephron tubules, which can be regarded as strengthening the mitochondrial membrane. It is known [24] that, under conditions of intense functioning, under the influence of pathogenic factors, mitochondria are particularly vulnerable to mutations of their own DNA and protein misfolding in the tubules of the granular endoplasmic reticulum. Under normal conditions it is in the tubular cavity of the granular endoplasmic reticulum that the linear chains of amino acids are subject to post-translational modification and collapse, acquiring the necessary three-dimensional configuration. The answer to misfolded proteins is endoplasmic reticulum stress (endoplasmaticum stress or ER-stress), which usually involves the involvement of autophagic mechanisms for the disposal of misfolded proteins. Given that mitochondria are constructed from proteins encoded by both the nuclear and mitochondrial genomes, this adds even more complexity to the coordination of protein synthesis and import to the mitochondria of proteins encoded by the nuclear genome. In the study by Tinari A. et al. [27], it has been proved that several protein molecules can cause such reconstruction of mitochondrial membranes, leading to rupture of the mitochondrial membrane and to complete destruction of mitochondria. In view of the foregoing, we have noted that the strengthening of the mitochondrial membrane of mitochondria of epithelial cells is a regulator and a potential inhibitor of the spread of mitoptosis degradation.

In view of the above literature, the membrane-plastic effect of lactoprotein with sorbitol, aimed at enhancing the structuralization of the outer and inner mitochondrial septum, is a preventer of the spread of mitoptosis and mitophagy.

We have investigated and compared the effects of the influence of different infusion solutions on the structure of the renal cortex of burned rats: 1) a typical crystalloid (0.9 % NaCl solution); 2) hyperosmolar colloidal solutions (lactoprotein with sorbitol and HAES-LX-5 %). Structural changes of the filtration and reabsorption apparatus of the kidneys under these conditions differed in the nature and temporal parameters of the compensatory-adaptive reactions, as well as the degree of expressiveness of destructive and reparative processes (which is a manifestation of the protective and therapeutic effect of the solutions). The success of the positive effects of infusion solutions is largely determined not only by their osmolarity, but also by the physicochemical characteristics of their components (which was planned when designing these drugs by the developers).

The studies have shown the unconditional positive benefits of intravenous infusion of colloidal-hyperosmolar solutions over infusion of isotonic solution, which is 0.9 % NaCl solution, which is confirmed and objectified by the data of the morphometric study. There are also differences in the

influence on the structure of renal cortex of burned rats of lactoprotein with sorbitol and HAES-LX-5 % groups.

It should be noted that the scientific literature continues to discuss the presence or absence of nephrotoxic effects of infusion colloid-electrolyte-hyperosmolar solutions based on hydroxyethyl starch of different generation [1, 4, 7, 10, 12, 16, 21, 23, 29]. The data obtained indicate the nephroprotective properties of a new (created on the basis of the hydroxyethyl starch of the third generation HES 130/0.4) balanced plasma substitute HAES-LX-5 %, which exerts a cytoprotective effect on the structure of the renal cortex of rats with experimental burn skin. These data are consistent with those of other researchers [3, 5, 6, 8, 15, 17, 18] regarding the positive effects of HAES-LX-5 %. All this gives reason to agree with the statement that colloid-hyperosmolar HAES-LX-5 % opens new opportunities in the treatment of burn disease. Prospects for further scientific research in this direction are to study the effects of different colloid-hyperosmolar infusion solutions on the structure of the kidneys in various pathological conditions.

Conclusions

1. Comparative analysis of the effects of intravenous infusion of 0.9 % NaCl solution and complex colloid-hyperosmolar solutions (lactoprotein with sorbitol and HAES-LX-5 %) on the structure of the kidneys under experimental simulation of burn disease in rats (by causing burn injury of 21-23 % skin area of the body surface) indicates that each solution is characterized by the peculiarities of the action on the course of reactive and destructive processes in cells. Functionally different cells of nephrons under conditions of infusion of detoxification solutions in the development of burn disease die by necrosis, apoptosis and anoikis; in epithelial cells of nephron tubules, mitophagy and mitoptosis occur.

2. With intravenous infusion of detoxification solutions applied, the most resistant cells to the harmful effects of experimental burn skin injury are podocytes. Podocytes maintain the structural integrity of the basement membrane and, as a result, stabilize the endothelial cells of the hemocapillaries of the vascular glomeruli, which exhibit a greater degree of resistance than the endothelial cells of the vessel wall of the peritubular mesh. The expression of reactive transformations of podocytes is the variability of the shape and size of cytotubules, cytopodia and soles of attachment of cytopodia. Their deformation modulations, together with changes in the basement membrane, are combined with an increase in the structure of the cytoskeleton elements (microfilaments and microtubules) located in the cytoplasm, which, in the aggregate, causes changes in the sizes and configurations of filtration slits and filtration diaphragms, thus changing.

3. Mitoptosis in rat epithelial tubule cells with experimental burn skin injury is carried out in two ways related to: 1) destruction of the outer mitochondrial membrane; 2) preservation of the outer mitochondrial membrane and

involvement of autophagic (mitophagic) mechanisms to release the cell from degraded mitochondrial material. In the first case, the mitochondria first condense, after which its matrix swells and the fragmentation of the cristae occurs due to the destruction of the junction of the cristae. Finally, the outer mitochondrial membrane breaks and the remnants of the cristae (in the form of vesicles) go into the cytoplasm. In the second case, the mitochondria condense, vesicular fragmentation of the cristae occurs, but the rupture of the outer mitochondrial membrane does not occur and the mitochondria are absorbed by the autophagosome (or transformed into the autophagosome). Next is the merger of autophagosomes with lysosomes and the formation of autophagolysosomes, which, under the conditions of effective digestion of the contents, are transformed into vacuoles. The latter are emptied by exocytosis and ensure the release of cells from degraded material.

4. Detoxification solutions used in the study give rise to different variants of reactive and destructive changes in the cells of renal cortex of rat with experimental burn skin injury. Under the conditions of intravenous infusion of 0.9 % NaCl solution, mainly necrotic changes of the cell occur, which are accompanied by the development of interstitial edema, hemorrhage and lymphocytic infiltration. Given the intravenous infusion of lactoprotein with sorbitol and HAES-LX-5 %, the spread of destructive changes in the renal cortex of rats with experimental burn skin injury is inhibited and substantially altered in both temporal and spatial dimensions. Intravenous infusion of applied colloid-hyperosmolar solutions provides inhibition of cell necrosis, thus suppressing the inflammatory response and contributing to the limited, local nature of mitoptosis and apoptotic changes. Limited selective microautophagy in the form of mitophagy in the cells of the renal cortex of rat with experimental burn skin injury is a manifestation of a compensatory-adaptive reaction whose balance has certain limits. If microautophagy is not adequately propagated, it leads to macroautophagy and may result in necrosis of the excessively vacuolated cell. If the spread of microautophagy is not adequately restricted, it can lead to apoptotic changes in the cell.

5. In rats without experimental burn skin injury, unstimulated mitoptosis of individual mitochondria of nephron epithelial cells occurs. Such mitoptosis can be considered as a manifestation of basic control of mitochondrial homeostasis whose effectiveness is

determined by the timely removal of defective mitochondria. Widespread mitoptosis in epithelial cells of nephron tubules in rats with experimental burn skin injury is a form of response to the factors of burn disease and associated degradation of distorted mitochondria. Such mitoptosis is characteristic of burn disease and can be defined as stimulated. Its morphological differences are: 1) the appearance of a large number of structurally degraded condensed mitochondria; 2) increasing the number of autophagosomes; 3) the association of vacuoles with a transparent content with a large number of diverse heteromorphic autophagolysosomes with the content of varying degrees of structured material resulting from inefficient hydrolytic digestion.

6. In the cytoplasm of epithelial cells of the tubules of rats nephrons with experimental burn skin injury there is impaired stability of the shape, size and distribution of mitochondria. Against the background of mitoptosis, the formation of the mitochondrial network occurs, the formation of new (small) mitochondria by budding and separation. This process has a dualistic meaning: on the one hand, it is a manifestation of physiological adaptation to stressful conditions, which contributes to the resilience of mitochondria integrated into the network; on the other hand, it leads to deformation and complete disappearance in the basal part of the epithelial cells of the tubules of the nephrons of the basal striations, which under normal conditions arises due to the placement of the rod-like mitochondria perpendicularly ordered with respect to the basement membrane (such changes, by definition, significantly affect the reabsorption state).

7. Only lactoprotein with sorbitol has a membrane-plastic effect on the strengthening (enhancement of structuring) of the mitochondrial membrane in part of the mitochondria of epithelial cells of nephron tubules, ultrastructurally manifested by an increase in the electron density and thickness of all components of the mitochondrial membrane. The maximum membrane-plastic effect of lactoprotein with sorbitol against mitochondria manifests itself fourteen days after the experimental burn skin injury and gradually (after twenty-one and thirty days) disappears, which correlates with the improvement of the general clinical condition of the animal. There is every reason to believe that increased structuration of mitochondria is a preventer of the spread of mitoptosis and mitophagy, the excess of which can lead to cell death.

References

- [1] Bunn, F., Alderson, P., & Hawkins, V. (2012). Colloid solutions for fluid resuscitation. *Cochrane Database of Systematic Reviews*, 7(6), 30-34. doi: 10.1002/14651858.CD001319.pub5
- [2] Bhatia-Kiššová, I., & Camougrand, N. (2010). Mitophagy in yeast: actors and physiological roles. *FEMS yeast research*, 10(8), 1023-1034. doi: 10.1111/j.1567-1364.2010.00659
- [3] Cherkasov, E. V., Gunas, I. V., Cheresnyuk, I. L., & Lysenko, D. A. (2012). Features of thymus cells cycle in rats after burn lesion of a skin. *Ukrainian morphological almanac*, 2(3), 109-113.
- [4] Davidson, I. J. (2006). Renal impact of fluid management with colloids: a comparative review. *European journal of anaesthesiology*, 23(9), 721-738. doi: 10.1017/S0265021506000639
- [5] Dzevujska, I. V., Cherkasov, E. V., Kovalchuk, O. I., Majewskyi, Y. G., Pastukhova, V. A., & Kyselova, T. M. (2018). Influence of lactoprotein solution with sorbitol on DNA content of cells of endocrine glands on the background of skin burn in

- rats. *World of Medicine and Biology*, 2(64), 33-39. doi: 10.26724/2079-8334-2018-2-64-33-39
- [6] Gavryluk, A. O., Galunko, G. M., Chereshniuk, I. L., Tikholaz, V. O., Cherkasov, E. V., Dzevulska, I. V., & Kovalchuk, O. I. (2018). Indicators cell cycle and DNA fragmentation in cells of small intestine mucosa 14, 21 and 30 days after skin burns on the background of preliminary infusion of solution lactoprotein with sorbitol or HAES-LX 5%. *World of Medicine and Biology*, 1(63), 104-108. doi: 10.26724/2079-8334-2017-4-62-104-108
- [7] Groeneveld, A. J., Navickis, R. J., & Wilkes, M. M. (2011). Update on the comparative safety of colloids: a systematic review of clinical studies. *Annals of surgery*, 253(3), 470-483. doi: 10.1097/SLA.0b013e318202ff00
- [8] Gunas, I. V., Guminskiy, Y. I., Ocheretna, N. P., Lysenko, D. A., Kovalchuk, O. I., Dzevulska, I. V., & Cherkasov, E. V. (2018). Indicators cell cycle and DNA fragmentation of spleen cells in early terms after thermal burns of skin at the background of introduction 0.9% NaCl solution. *World of Medicine and Biology*, 14(63), 116-120. doi: 10.26.724/2079-8334-2018-1-63-116-120
- [9] Haagsma, J. A., Graetz, N., Bolliger, I., Naghavi, M., Higashi, H., Mullany, E. C., ... & Ameh, E. A. (2016). The global burden of injury: incidence, mortality, disability-adjusted life years and time trends from the Global Burden of Disease study 2013. *Injury prevention*, 22(1), 3-18. doi: 10.1136/injuryprev-2015-041616
- [10] Hartog, C. S., Kohl, M., & Reinhart, K. (2011). A systematic review of third-generation hydroxyethyl starch (HES 130/0.4) in resuscitation: safety not adequately addressed. *Anesthesia & Analgesia*, 112(3), 635-645. doi: 10.1213/ANE.0b013e31820ad607
- [11] Jangamreddy, J. R., & Los, M. J. (2012). Mitoptosis, a novel mitochondrial death mechanism leading predominantly to activation of autophagy. *Hepatitis monthly*, 12(8), 6159-6163. doi: 10.5812/hepatmon.6159
- [12] Kancir, A. S. P., Johansen, J. K., Ekeloef, N. P., & Pedersen, E. B. (2015). The effect of 6% hydroxyethyl starch 130/0.4 on renal function, arterial blood pressure, and vasoactive hormones during radical prostatectomy: a randomized controlled trial. *Anesthesia & Analgesia*, 120(3), 608-618. doi: 10.1213/ANE.0000000000000596
- [13] Kaushal, G. P., & Shah, S. V. (2016). Autophagy in acute kidney injury. *Kidney international*, 89(4), 779-791. doi: 10.1016/j.kint.2015.11.021
- [14] Keck, M., Herndon, D. H., Kamolz, L. P., Frey, M., & Jeschke, M. G. (2009). Pathophysiology of burns. *Wiener Medizinische Wochenschrift*, 159(13-14), 327-336. doi: 10.1136/bmj.328.7453.1427
- [15] Kovalchuk, O., Cherkasov, E., Dzevulska, I., Kaminsky, R., Korsak, A., & Sokurenko, L. (2017). Dynamics of morphological changes of rats' adenohypophysis in burn disease. *Georgian medical news*, (270), 104-108. PMID:28972493
- [16] Kruer, R. M., & Ensor, C. R. (2012). Colloids in the intensive care unit. *American Journal of Health-System Pharmacy*, 69(19), 1635-1642.
- [17] Lachtadyr, T. V. (2019). Structural changes of the rat kidney cortical substance in the long-term period after burn injury of the skin under conditions of HAES-LX-5% infusion. *Emergency Medicine*, (5.100), 79-83. <https://doi.org/10.22141/2224-0586.5.100.2019.177023>
- [18] Lachtadyr, T. V. (2017). Structural changes of rats' renal cortex in late period of skin burn injury under the conditions of the infusion by lactoprotein with sorbitol. *Biomedical and Biosocial Anthropology*, 28, 81-87.
- [19] Lyamzaev, K. G., Nepryakhina, O. K., Saprunova, V. B., Bakeeva, L. E., Pletjushkina, O. Y., Chernyak, B. V., & Skulachev, V. P. (2008). Novel mechanism of elimination of malfunctioning mitochondria (mitoptosis): formation of mitoptotic bodies and extrusion of mitochondrial material from the cell. *Biochimica et biophysica acta (BBA)-Bioenergetics*, 1777(7-8), 817-825. doi: 10.1016/j.bbabi.2008.03.027
- [20] Mijaljica, D., Prescott, M., & Devenish, R. J. (2010). *Mitophagy and mitoptosis in disease processes. In Protein Misfolding and Cellular Stress in Disease and Aging* (pp. 93-106). Humana Press, Totowa, NJ. doi: 10.1007/978-1-60761-756-3_6
- [21] Mohanan, M., Rajan, S., Kesavan, R., Mohamed, Z. U., Ramaiyar, S. K., & Kumar, L. (2019). Evaluation of renal function with administration of 6% hydroxyethyl starch and 4% gelatin in major abdominal surgeries: A pilot study. *Anesthesia, essays and researches*, 13(2), 219-224. doi: 10.4103/aer.AER_25_
- [22] Muller, M., & Reichert, A. S. (2011). Mitophagy, mitochondrial dynamics and the general stress response in yeast. *Biochem Soc Trans*, 39(5), 1514-1519. doi: 10.1042/BST0391514
- [23] Mutter, T. C., Ruth, C. A., & Dart, A. B. (2013). Hydroxyethyl starch (HES) versus other fluid therapies: effects on kidney function. *Cochrane Database of Systematic Reviews*, (7), CD007594. doi: 10.1002/14651858.CD007594.pub3
- [24] Pickles, S., Vigié, P., & Youle, R. J. (2018). Mitophagy and quality control mechanisms in mitochondrial maintenance. *Current Biology*, 28(4), R170-R185. doi: 10.1016/j.cub.2018.01.004
- [25] Serghiou, M. A., Niszczak, J., Parry, I., Li-Tsang, C. W. P., Van den Kerckhove, E., Smailes, S., & Edgar, D. (2016). One world one burn rehabilitation standard. *Burns*, 42(5), 1047-1058. doi: 10.1016/j.burns.2016.04.002
- [26] Smolle, C., Cambiaso-Daniel, J., Forbes, A. A., Wurzer, P., Hundeshagen, G., Branski, L. K., ... & Kamolz, L. P. (2017). Recent trends in burn epidemiology worldwide: A systematic review. *Burns*, 43(2), 249-257. doi: 10.1016/j.burns.2016.08.013
- [27] Tinari, A., Garofalo, T., Sorice, M., Esposti, M. D., & Malorni, W. (2007). Mitoptosis: different pathways for mitochondrial execution. *Autophagy*, 3(3), 282-284. doi: 10.4161/auto.3924
- [28] Vigié, P., & Camougrand, N. (2017). Role of mitophagy in the mitochondrial quality control. *Medecine sciences: M/S*, 33(3), 231-237. doi: 10.1051/medsci/20173303008
- [29] Weiskopf, R. B. (2015). Lack of Nephrotoxicity of Hydroxyethyl Starch 130/0.4 When Used in Surgery. *The Journal of the American Society of Anesthesiologists*, 123(2), 482-483. doi: 10.1097/ALN.0000000000000719
- [30] Zemirli, N., Morel, E., & Molino, D. (2018). Mitochondrial dynamics in basal and stressful conditions. *International journal of molecular sciences*, 19(2), 564. doi: 10.3390/ijms19020564

ПОРІВНЯЛЬНИЙ АНАЛІЗ ВПЛИВІВ РІЗНИХ ДЕЗІНТОКСИКАЦІЙНИХ РОЗЧИНІВ НА СТРУКТУРУ НИРОК ПРИ ЕКСПЕРИМЕНТАЛЬНІЙ ОПІКОВІЙ ХВОРОБІ У ЩУРІВ

Черкасов В.Г., Лактадыр Т.В., Федонюк Л.Я., Шипицина О.В.

Застосування існуючих інфузійних розчинів, а також розробка, наукове обґрунтування і впровадження новітніх нефропротекторних дезінтоксикаційних розчинів залишається актуальною проблемою для комбустиологіє. Метою роботи є порівняльний аналіз впливів різних дезінтоксикаційних розчинів (0,9 % розчину NaCl та комплексних колоїдно-гіперосмолярних

розчинів - лактопротеїну із сорбітолом та нещодавно розробленого розчину HAES-LX-5 %) на структуру нирок при експериментальній опіковій хворобі у щурів. Піддослідні щури були розподілені на сім груп (по 15 тварин у кожній): перша група - інтактні щури; друга, третя й четверта групи - щури без відтворення експериментальної опікової хвороби, котрим було здійснено окремо внутрішньовенну інфузію 0,9 % розчину NaCl, лактопротеїну із сорбітолом та HAES-LX-5 % у дозі 10 мл/кг; п'ята, шоста та сьома групи - щури з експериментальною опіковою хворобою (шляхом нанесення опікової травми шкіри площею 21-23 % поверхні тіла), яким за аналогічною схемою було здійснено внутрішньовенну інфузію досліджуваних розчинів. Усі дослідження і виведення щурів із експерименту проводили під глибоким тіопенталовим внутрішньочеревним наркозом. Гістологічні препарати кіркової речовини нирок щурів забарвлювали гематоксиліном-еозином і вивчали на мікроскопі Олутрис ВХ51. Одержані за допомогою ультрамікротому LKB-3 (Швеція) напівтонкі зрізи забарвлювали толуїдиновим синім та метиленовим синім - азур II; а ультратонкі зрізи контрастували уранілацетатом і цитратом свинцю за Рейнольдсом і вивчали за допомогою електронного мікроскопа ПЕМ-125К. Морфометричні вимірювання (оцінка площі судинних клубочків, площі сечового просвіту капсули ниркових тілець; площі ниркових каналців нефронів та площі їхніх просвітів, площі ниркових тілець, площі цитоплазми та ядер епітеліальних клітин каналців, а також їх ядерно-цитоплазматичне співвідношення) здійснювали за допомогою програм ВидеоТест-5.0, КААРА Image Base та Microsoft Excel на персональному комп'ютері. Статистичний аналіз отриманих кількісних показників виконаний з використанням статистичного пакету IBM SPSS v. 22.0. for Windows. Встановлено, що функціонально різні клітини нефронів за умов інфузії дезінтоксикаційних розчинів при розвитку опікової хвороби гинуть шляхом некрозу, апоптозу та аноїкису; в епітеліальних клітинах каналців нефронів відбуваються мітофагія та мітоптоз. Мітоптоз в епітеліальних клітинах каналців нефронів щурів з експериментальною опіковою травмою шкіри здійснюється двома шляхами що пов'язані з: 1) руйнацією зовнішньої мітохондріальної мембрани; 2) збереженням зовнішньої мітохондріальної мембрани та залученням аутофагійних (мітофагійних) механізмів для звільнення клітини від деградованого мітохондріального матеріалу. У першому випадку мітохондрія спочатку конденсується, після чого відбувається набухання її матриксу і фрагментація крист за рахунок руйнації з'єднань крист. Нарешті, зовнішня мітохондріальна мембрана розривається і залишки крист (у вигляді везикул) виходять у цитоплазму. У другому випадку мітохондрія конденсується, відбувається везикулярна фрагментація крист, але розриву зовнішньої мітохондріальної мембрани не відбувається і мітохондрія поглинається аутофагосомою (або перетворюється на аутофагосому). Далі відбувається злиття аутофагосом з лізосомами і утворення аутофаголізосом, які, за умов ефективного перетравлення вмісту, трансформуються у вакуолі. Останні випорожнюються шляхом екзоцитозу і забезпечують вивільнення клітини від деградованого матеріалу. Притаманна тільки лактопротеїну з сорбітолом мембранопластична дія щодо укріплення (посилення структуралізації) мітохондріальної оболонки у частини мітохондрій епітеліальних клітин каналців нефронів ультраструктурно проявляється підвищенням електронної щільності та товщини усіх складових мітохондріальної оболонки. Максимально зазначений мембранопластичний ефект дії лактопротеїну із сорбітолом щодо мітохондрій проявляється через 14 діб після експериментальної опікової травми шкіри і поступово (через 21 та через 30 діб) зникає, що корелює з поліпшенням загального клінічного стану і покращенням показників структурних змін нирок тварин з опіковою хворобою. Є усі підстави вважати, що посилення структуралізації мітохондрій є запобіжником поширення мітоптозу та мітофагії, надлишковий характер яких може призвести до клітинної загибелі.

Ключові слова: опікова хвороба, дезінтоксикаційні розчини, реактивні та деструктивні зміни нирок.

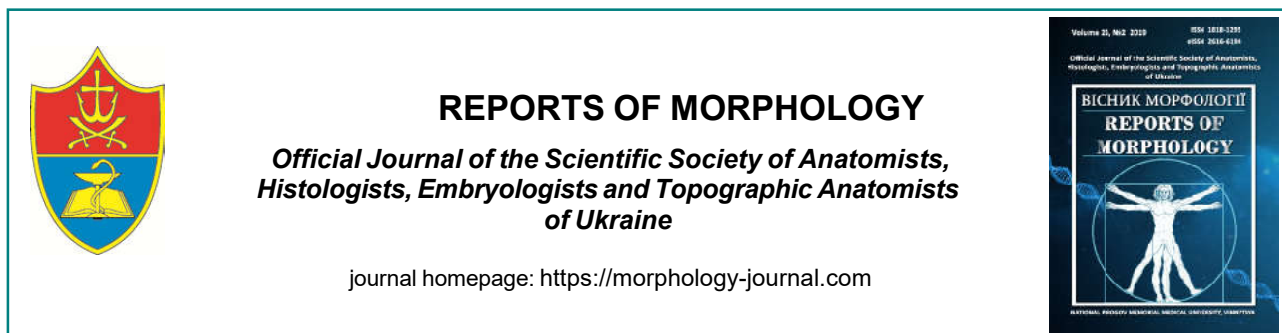
СРАВНИТЕЛЬНЫЙ АНАЛИЗ ВЛИЯНИЙ РАЗНЫХ ДЕЗИНТОКСИКАЦИОННЫХ РАСТВОРОВ НА СТРУКТУРУ ПОЧЕК ПРИ ЭКСПЕРИМЕНТАЛЬНОЙ ОЖОГОВОЙ БОЛЕЗНИ У КРЫС

Черкасов В.Г., Лахтадыр Т.В., Федонюк Л.Я., Шипицына А.В.

Применение существующих инфузионных растворов, а также разработка, научное обоснование и внедрение новейших нефропротекторных дезинтоксикационных растворов остается актуальной проблемой для комбустиологов. Целью работы является сравнительный анализ влияния различных дезинтоксикационных растворов (0,9 % раствора NaCl и комплексных коллоидно-гиперосмолярных растворов - лактопротеина с сорбитолом и недавно разработанного раствора HAES-LX-5 %) на структуру почек при экспериментальной ожоговой болезни у крыс. Испытуемые крысы были разделены на семь групп (по 15 животных в каждой): первая группа - интактные крысы; вторая, третья и четвертая группы - крысы без воспроизведения экспериментальной ожоговой болезни, которым была осуществлена отдельно инфузия 0,9 % раствора NaCl, лактопротеина с сорбитолом и HAES-LX-5 % в дозе 10 мл/кг пятая; шестая и седьмая группы - крысы с экспериментальной ожоговой болезнью (путем нанесения ожоговой травмы кожи площадью 21-23 % поверхности тела), которым по аналогичной схеме была осуществлена инфузия исследуемых растворов. Все исследования и вывод крыс из эксперимента проводили под глубоким тиопенталовым внутрибрюшным наркозом. Гистологические препараты коры почек крыс окрашивали гематоксилін-еозином и изучали на микроскопе Олутрис ВХ51. Полученные с помощью ультрамикротом LKB-3 (Швеция) полутонкие срезы окрашивали толуидиновым синим и метиленовым синим - азур II; а ультратонкие срезы - контрастировали уранілацетатом и цитратом свинца по Рейнольдсу и изучали с помощью электронного микроскопа ПЕМ-125К. Морфометрические измерения (оценка площади сосудистых клубочков, площади мочевого просвета капсулы почечных телец; площади почечных каналцев нефронов и размеры их просветов, площади почечных телец, площади цитоплазмы и ядер эпителиальных клеток каналцев, а также их ядерно-цитоплазматического соотношения) осуществляли с помощью программ ВидеоТест-5.0, КААРА Image Base и Microsoft Excel на персональном компьютере. Статистический анализ полученных количественных показателей выполнен с использованием статистического пакета IBM SPSS v. 22.0. for Windows. Установлено, что функционально разные клетки нефронов при инфузии дезинтоксикационных растворов в условиях развития ожоговой болезни погибают путем некроза, апоптоза и аноикиса; в эпителиальных клетках каналцев нефронов происходят митозы и митоптоз. Митоптоз в эпителиальных клетках каналцев нефронов крыс с экспериментальной ожоговой травмой кожи осуществляется двумя путями, которые связаны с: 1 - разрушением наружной митохондриальной

мембраны; II - сохранением наружной митохондриальной мембраны и присоединением аутофагических (митофагических) механизмов для освобождения клетки от деградированного митохондриального материала. В первом случае митохондрия сначала конденсируется, после чего происходит набухание ее матрикса и фрагментация крист за счет разрушения соединений крист. Наконец наружная митохондриальная мембрана разрывается и остатки крист (в виде везикул) выходят в цитоплазму. Во втором случае митохондрия конденсируется, происходит везикулярная фрагментация крист, но наружная митохондриальная мембрана сохраняет свою целостность и митохондрия поглощается аутофагосомой (или превращается в аутофагосому). Далее происходит слияние аутофагосом с лизосомами и образование аутофаголизосом, которые, при условии эффективной переработки содержимого, трансформируются в вакуоли. Последние опорожняются путем экзоцитоза и обеспечивают освобождение клетки от деградированного материала. Присуще только лактопротеину с сорбитолом мембранопластическое действие, направленное на укрепление (усиленная структурализация) митохондриальной оболочки у части митохондрий эпителиальных клеток канальцев нефрона ультраструктурно проявляется повышением электронной плотности и толщины всех составляющих митохондриальной оболочки. Максимально мембранопластический эффект действия лактопротеина с сорбитолом на митохондрии проявляется через 14 суток после экспериментальной ожоговой травмы кожи и постепенно (через 21 и через 30 суток) исчезает, что совпадает с улучшением общего клинического состояния и показателей структурных изменений в почках животных с ожоговой болезнью. Есть все основания считать, что усиление структурализации митохондрий является предохранителем распространения митоптоза и митофагии, чрезмерный характер которых может привести к клеточной гибели.

Ключевые слова: ожоговая болезнь, дезинтоксикационные растворы, реактивные и деструктивные изменения почек.



Structural changes of the intestinal epithelial barrier of the duodenum of rats in burn injury of skin under experimental streptozotocin-induced diabetes mellitus

Tymoshenko I.O.

O.O. Bogomolets National Medical University, Kyiv, Ukraine

ARTICLE INFO

Received: 21 February, 2019

Accepted: 20 March, 2019

UDC: 616.342:616-001.17:616.379-008.64:599.323.4:612.08

CORRESPONDING AUTHOR

e-mail: iryna.tymoshenko@i.ua
Tymoshenko I.O.

The aim of the study was to study the structural changes of the intestinal epithelial barrier in the duodenum in burn injury of skin in rat under experimental streptozotocin-induced diabetes mellitus. The study was carried out on laboratory white adult rats-males weighing 180-210 g. The control group consisted of 21 animals without somatic pathology, the first experimental group was 21 rats with burn skin injury, the second experimental group was 21 rats with burn skin and experimental streptozotocin-induced diabetes mellitus. The experimental diabetes model was reproduced by administering streptozotocin to the rats intraperitoneally at a single dose of 50 mg/kg. Thermal burn skin damage in rats corresponded to II - A-B degrees of dermal surface burn (according to the old classification III - A degree) with a total area of 21-23 % of the body surface with the development of burn shock. Duodenum was selected for morphological studies, fragments of which were processed by conventional methods of light and electron microscopy. The main criteria for assessing damage to the duodenal mucosa enterocytes were the results of a study comparing histological and ultrastructural data in dynamics at 7, 14, and 21 days after skin burns. The results of the studies showed that the base of damage to the intestinal epithelial barrier of the duodenum are deep destructive changes, which after 21 days (in the stage of septicotoxemia), as a rule, are not reverse and develop on the background of significant intoxication of the body. There was a decrease in the number of tight junctions in the intestinal epithelial barrier of the duodenum of rats of the first and second experimental groups and a loss of ordering (acquisition of some chaotic nature) of their localization as the time after burn injury increased. For the most part, the intestinal epithelial barrier loses the integrity of the cellular component with partial preservation of the basement membrane (the first occurs both due to necrosis of the enterocytes with a brush border and due to complete destruction of goblet cells). In all cases, defects exist in the intestinal epithelial barrier, which are potential pathways for paracellular translocation of the pathogenic contents of the duodenum. It is not inconceivable that part of this intestinal pathogenic content can be translocated also by partially damaged cells. Evidence of the latter is the presence of microbial bodies in the cytoplasm of cells with partially destroyed plasmalemma (but preserved organelles and nucleus). An adaptive mechanism for ensuring the repair of damaged enterocytes is selective autophagy, which acts as a factor in the recycling of destroyed organelles and the cytoplasmic matrix, aimed primarily at maintaining cell viability.

Keywords: burn injury, streptozotocin-induced diabetes mellitus, intestinal epithelial barrier.

Introduction

Nowadays, due to the acceleration of urbanization and the growth of industrial use of heat energy, severe thermal burn injury resulting in burn disease is becoming one of the most important problems of practical medicine [26].

Diabetes has also been recognized as a global health

and social challenge of the 21st century [21]. Diabetes mellitus and its related complications are becoming more common. The complex of gastrointestinal symptoms associated with diabetes is now known as diabetic enteropathy and can manifest as diarrhea, fecal

incontinence, constipation, dyspepsia, nausea and vomiting [11]. The ancient theory that autonomic neuropathy is a major contributor to diabetic enteropathy [17, 18, 25] has recently been supplemented by new theories of disease development [2]. In particular, it is now believed [11] that hyperglycemia and its associated oxidative stress in neural networks, including nitrergic neurons and interstitial cells of Cajal [2, 23], play a central role in the development of diabetic enteropathy. The authors of the latest (at the time of publication) scientific review article "Diabetes and the small intestine" [11] indicate that the latest scientific results are promising, but there is still a great need for further studies of the pathogenesis of diabetic enteropathy.

As of today, the leading role of intestinal dysfunction in the development of complications of diabetes has been demonstrated [2, 11, 17, 18, 25, 28] and caused by severe burns of burn disease [9, 10, 21]. However, until now, the study of structural changes in the intestinal epithelial barrier of the duodenum in burn skin injury under its association with diabetes has not been the subject of special studies.

The aim of this work was to study the structural changes of the intestinal epithelial barrier in the duodenum in burn injury of skin in rat under experimental streptozotocin-induced diabetes mellitus.

Materials and methods

This study was conducted on laboratory white adult rats-males weighing 180-210 g. The control group consisted of 21 animals without somatic pathology, the first experimental group was 21 rats with burn skin injury, the second experimental group was 21 rats with skin burn and experimental streptozotocin-induced diabetes. All studies and control of the animals were conducted in accordance with the rules for the use of the animals in the experiments, adopted by the "European Convention for the Protection of Vertebrate Animals Used for Experimental and other Scientific Purposes" (Strasbourg, 1986), "General Ethical Principles of Animal Experiments", adopted by the First National Congress On Bioethics (Kyiv, 2001), "Ethical Principles and Guidelines for Experiments on Animals: 3rd Edition" (Switzerland 2005) and the Law of Ukraine "On the Protection of Animals from Cruel Treatment" (2006).

The model of experimental diabetes mellitus [20] was reproduced by administering streptozotocin to rats intraperitoneally at a dose of 50 mg/kg, pre-dissolving it in 0.1 M citrate buffer solution (pH-4.5). The duration of the experiment was 1 month. The control of the development of hyperglycemia in the second experimental group was blood glucose level - 24.24 ± 0.79 mmol/L. In the control group 8.03 ± 0.4 mmol/L. In our study, burn injury of skin caused in accordance with the widespread model of researchers Regas F.C. and Ehrlich H.P. [24], which was slightly modified and optimized by Gunas I., Dovgan I. and Masur O. [12]. In the experimental simulation of skin burns, two copper plates in the form of an ellipse were kept in water at 100°C for 10 minutes and, under the conditions of ether anesthesia, were

applied simultaneously symmetrically to both exposed rats with an exposure of 10 seconds. Burning skin damage in rats was II -A-B degree of dermal surface burn (according to the old classification III - A degree) with a total area of 21-23 % of the body surface with the development of burn shock. Many researchers [4, 5, 7, 13, 14] have shown that under the conditions of using this model of experimental burn, the development of burn disease with such characteristic features as endogenous intoxication, generalized catabolic reaction, systemic inflammatory and apoptotic responses, polyorganic dysfunction is initiated. Duodenum was selected for morphological studies, fragments of which were processed by conventional methods of light and electron microscopy. Semi-thin and ultrathin sections from epoxy blocks were obtained on an LKB ultramicrotome (Sweden). Ultra-thin sections after appropriate contrast were examined under a PEM-125K electron microscope. Semi-thin sections were stained with methylene blue and toluidine blue. Sections of paraffin blocks were stained with hematoxylin-eosin. The main criteria for assessing damage to the duodenal mucosa enterocytes were the results of histological and ultrastructural data in dynamics 7, 14, and 21 days after skin burn. At that time, rats were given a single intraperitoneally high dose of sodium thiopental and were removed from the experiment by decapitation.

Results

In enterocytes of the mucous membrane of the duodenum of animals of the first experimental group 7 days after burns, the most characteristic feature of structural changes is the destruction of microvilli of the brush border of enterocytes, as well as changes of tight junctions. These contacts are clearly visualized on electron micrographs at the loci between the apicolateral surfaces of adjacent enterocytes with a brush border because the outer hydrophilic layers and the glycocalyx of adjacent plasmalemma seem to merge at one point into a public electron-dense layer with electron density (Fig. 1, 2). Note some chaotic arrangement of tight junctions

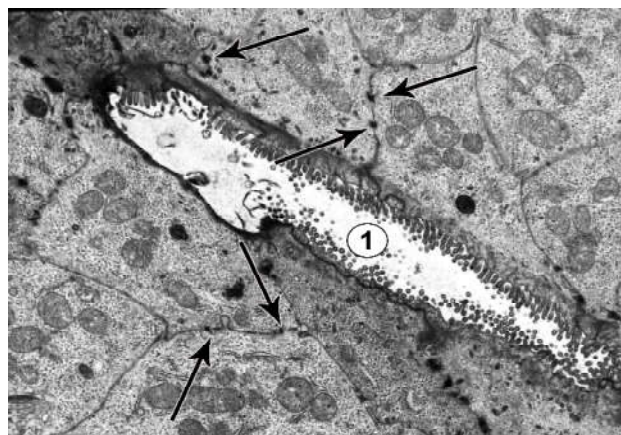


Fig. 1. Crypt of the mucous membrane of the duodenum of the rat of the first experimental group 7 days after burn. The arrows indicate dense contacts between the enterocytes with the brush border. 1 - crypt lumen. EM, x10000.

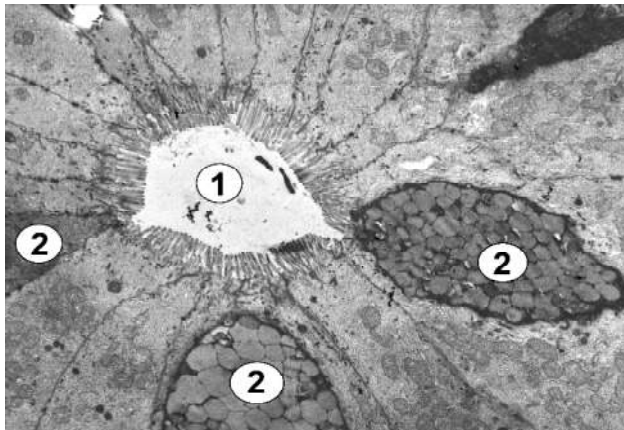


Fig. 2. Crypt of the duodenal mucosa of the rat under normal conditions (control group of animals). 1 - crypt lumen; 2 - cytoplasm of goblet cells. EM, x8000.

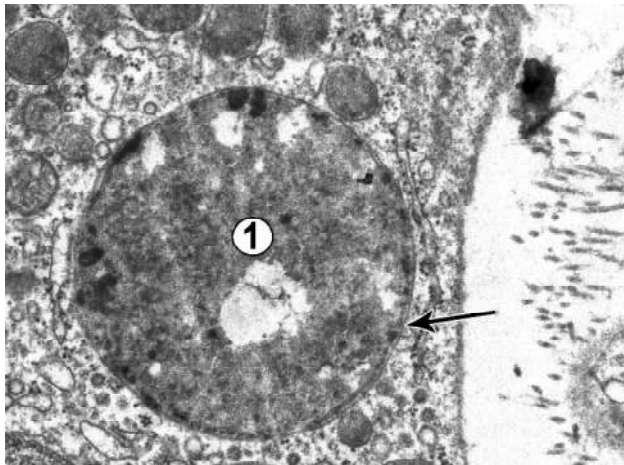


Fig. 3. Autophagolysosome (1) with heteromorphic electron-dense content in the cytoplasm of enterocyte with the remains of the brush border in the duodenal mucosa of the first experimental group 7 days after burn. The arrow marked the phagophore. EM, x25000.

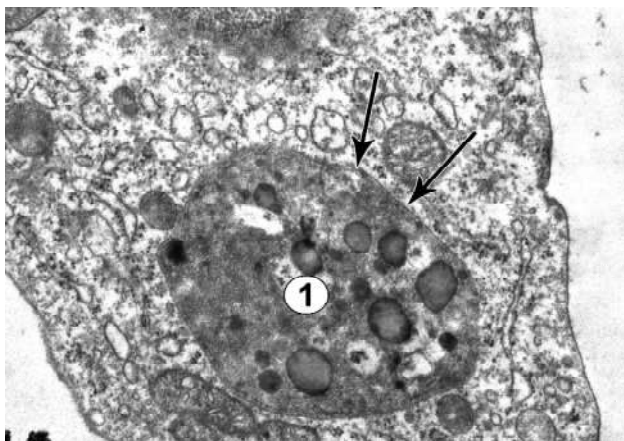


Fig. 4. Typical autophagolysosome (1) in the cytoplasm of the enterocyte with a brush border that has lost dense contact with adjacent enterocytes, in the mucous membrane of the duodenum of the rat of the first experimental group 21 days after burn. Arrows marked phagophore. EM, x25000.

in the epithelial monolayer (intestinal epithelial barrier) of the duodenum in rats of the first experimental group (see Fig. 1), which deepens with increasing time after burn.

The intestinal barrier of the duodenum also includes goblet cells (see Fig. 2), which, under normal conditions, have a holistic plasmalemma (which, however, does not form dense contacts with adjacent enterocytes with a brush border), and numerous secretory vesicles, medium electron density material.

Widespread phenomenon in this time interval is a variety of ultrastructural changes of enterocytes against the background of swelling of their cytoplasm (an indicator of which is the enlightenment of the cytoplasmic matrix): from the vacuolation of tubules of the endoplasmic reticulum and damage to the mitochondria (manifestation is their intense swelling, fragmentation of the cristae and inner membrane) to the complete destruction of organelles, the appearance of defects of plasmalemma and karyolemma.

In sections of cytoplasm of enterocytes with partially lost brush border are located rounded autophagosomes and autophagolysosomes of different size with heteromorphic electron-dense contents (Fig. 3).

Morphological evidence of the initial stage of autophagy is the grouping of damaged cell organelles in certain loci of the cytoplasmic matrix and their sequestration by concentric coverage of the characteristic autophagosome structure - phagophore (double insulating membrane). In the future, autophagosomes merge with lysosomes and form autophagolysosomes with different electron density and structure (which is an indicator of the stages and efficiency of digestion of the sequestered material).

Digestion of the content of autophagolysosomes is accompanied by destruction of the inner membrane of the phagophore (under these conditions, the products of digestion are likely to be absorbed and assimilated by the cytoplasm of the enterocyte). If part of the material remains undigested, then the autophagolysosome is transformed into an autophagic vacuole, which is directed to the plasmalemma of the apical region of the enterocyte and releases its contents outside.

In animals of the first experimental group, 14 days after burn in the duodenum, sections of the epithelial monolayer of enterocytes with preserved brush border alternated with areas free of brush border. The enterocytes of the epithelial monolayer were adjacent to desquamated cells of varying degrees of conservation. In the apical part of most enterocytes with partially lost brush border were located groups of rounded autophagosomes and autophagolysosomes of different size and content.

In the cytoplasm of many enterocytes with the presence of structural site defects of the plasmalemma and karyolemma in combination with local damage of the cytoplasmic matrix (which, given their variability, can probably be repaired) the signs of increase of functional activity of organelles are revealed (the evidence of which is a moderate expansion of the tubules of the granular endoplasmic

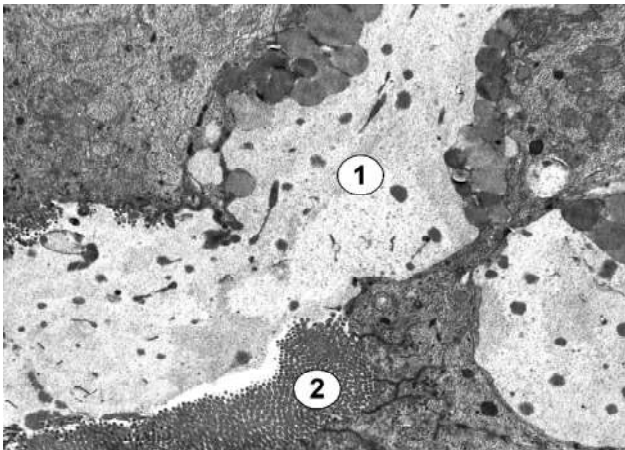


Fig. 5. Deformity of the lumen of the crypt of the mucous membrane of the duodenum of the rat of the second experimental group 7 days after burn. 1 - remnants of goblet cells in crypt lumen; 2 - the remnants of the brush border. EM, 25000.

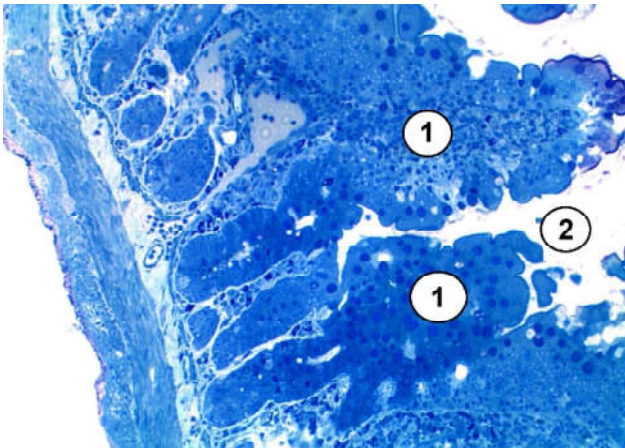


Fig. 6. Deformed villi and crypts of the mucous membrane of the duodenum of the rat of the second experimental group 21 days after burn. 1 - villi of the mucous membrane; 2 - intestinal lumen. Semi-thin section. Toluidine blue. x100.

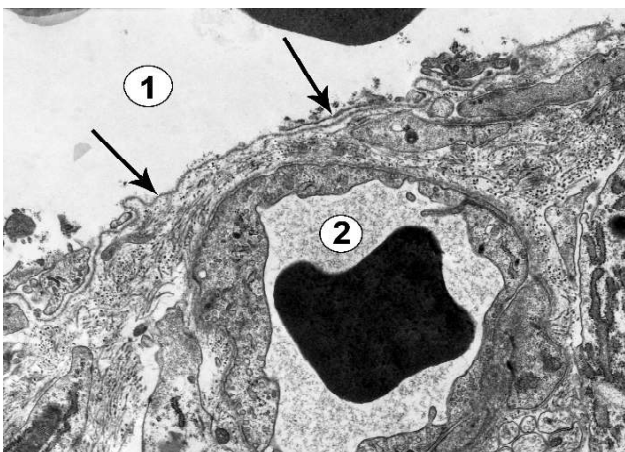


Fig. 7. Necrosis of the duodenal mucosa enterocyte of the duodenum of the rat of the second experimental group 21 days after burn. The arrows marked the "exposed" basement membrane of the epithelial monolayer. 1 - intestinal lumen; 2 - the lumen of the blood capillary. EM, x15000.

reticulum, an increase in the number of ribosomes, the presence of polysome, the aggregation of intact mitochondria, the integrity of the nucleus). In other enterocytes, at this time, the cytoplasm is vacuolated in the form of various enlargement of the tubules of the endoplasmic reticulum with enlightenment of their contents, vacuolar transformation of mitochondria, which is completed by complete necrotic destruction and cell fragmentation with the formation of cellular detritus.

In animals of the first experimental group after 21 days, after burns, morphologically focal atrophy of the mucous membrane was manifested by thickening and shortening of the villi; in some places they were completely absent. The erosions that have resulted from necrosis of enterocytes with a brush border and destruction of goblet cells were quite often found. In many areas of the intestinal epithelial barrier (due to loss of tight contacts) adjacent brush-bordered enterocytes were separated from each other, forming extended interepithelial spaces. Typical autophagolysosomes were detected in the cytoplasm of some of these enterocytes (Fig. 4).

The animals of the second experimental group after 7 days after the burn is common subtotal necrosis of enterocytes brush border, when the preservation of the cytoplasm of intact border area of necrotic cells subject to degeneration and cell detritus formed with microvilli border enters the intestinal area. Most goblet cells, which completely collapse after accumulation of secret, are destructive. If this occurs in crypts (Fig. 5), then the remains of goblet cells are included in the contents of the crypts and (along with enterocyte residues) deform their lumen.

14 days after burn in the mucous membrane of the duodenum of animals of the second experimental group, enterocytes in certain areas of the epithelial monolayer are subject to complete necrotic decay. In these areas, the basement membrane becomes "exposed". It is quite well preserved and even, it is somewhat thick compared to normal (in the control group of rats).

The structural changes described above are accompanied by deformation and destruction of the villi of the duodenal mucosa. The villi lose their typical leaf-like shape, often take on a "twisted" appearance, and filamentous villi appear, surrounded by groups of desquamated enterocytes and cellular detritus.

21 days after burns in animals of the second experimental group in some parts of the mucous membrane of the duodenum of the crypt and villi are clearly deformed. The villi lose their typical cytoarchitectonics and have the appearance of clustered (and sometimes mushroom) conglomerates of enterocytes of varying degrees of structural conservation (Fig. 6). To a greater extent, the intestinal epithelial barrier loses (Fig. 7) the integrity of the cellular component with partial preservation of the basement membrane (the first occurs both due to necrosis of the enterocytes with the brush border and due to complete destruction of the goblet cell). In all cases, defects exist in the intestinal epithelial barrier,

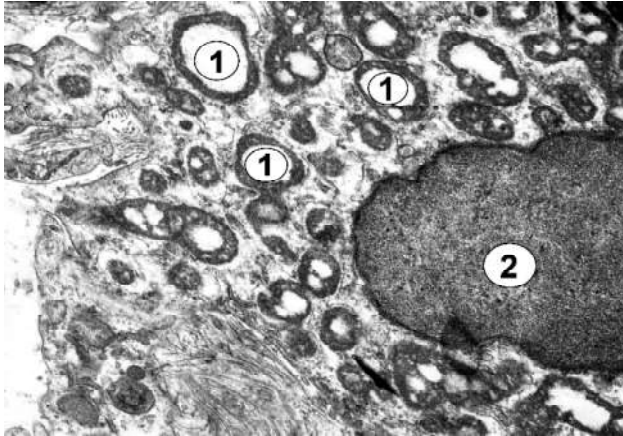


Fig. 8. Microbial bodies (1) in the cytoplasm of cells of the mucous membrane of the duodenum of the rat of the second experimental group 21 days after burn. 2 - the nucleus of the cell. EM, x20000.

which are potential pathways for paracellular translocation of the pathogenic contents of the duodenum. It is not inconceivable that part of this intestinal pathogenic content can be translocated and partially damaged by cells. Evidence of the latter is the presence of microbial bodies (Fig. 8) in the cytoplasm of cells with partially destroyed plasmalemma (but preserved organelles and nucleus).

Discussion

Many unresolved issues remain regarding the role of structural and functional changes in the small intestine in the pathogenesis of burn disease, and in particular, regarding dysfunction in the context of burns of the intestinal epithelial barrier [15].

The data obtained indicate the structural manifestations of a barrier violation (destruction of dense interepithelial contacts, disappearance of interdigitations of cytoplasmic processes of adjacent enterocytes) in burn skin injury under experimental streptozotocin-induced diabetes. In addition, we confirmed the Huang Ya. et al. data [16] regarding the involvement of autophagic processes in the development of gradual structural disorganization of the intestinal epithelial barrier, but unlike these authors, we consider their manifestation of an adaptive response.

It is worth noting that the role of autophagy in cell death is now widely regarded by researchers as quite controversial [16]. According to modern data [1], autophagy is the process of digestion of its own distorted organelles and sections of the cytoplasm by lysosomes (thus autophagy is both a type of programmed cell death and a strategy for cell survival by recycling cellular material). Thus, the adaptive response of the duodenal mucosa enterocytes to the destructive effects of burn disease factors involves the use as part of the plastic and energy resources of the degraded cellular material to repair the damaged enterocyte and to maintain its viability. Under the conditions of our experiment in rats of the first experimental group, the course of structural changes of enterocytes of the duodenal mucosa is slow enough to

include the adaptive mechanism of autophagy of distorted organelles. In the animals of the second experimental group, destruction of cytoplasmic and organelle enterocyte sites (due to the summation of the factors of burn disease and diabetes) is accelerated and cells die by necrosis.

It should be noted separately that Nighot P.K., Hu C.A., and Ma T.Y. [22] suggest that autophagy promotes restrictive tight junction function and enhances the intestinal epithelial barrier by targeting claudin-2 protein degradation. In the context of this view, Elshaer D. and Begun G. [8] emphasize the crucial role of the barrier function of intestinal epithelium, autophagy and cytokines in providing intestinal homeostasis.

It is now widely accepted that intact intestinal epithelial barrier is critical for maintaining homeostasis in human health and disease, and tight enterocyte contacts are an integral part of this barrier [27]. It is known [6, 16] that permeability proteins occludin and zonulin-1 are involved in ensuring the functioning of tight junctions in the intestinal epithelial barrier. Severe burns of the skin have been found to increase the permeability of the intestinal epithelial barrier, which is accompanied by decreased expression and localization of occludin and zonulin-1 [6, 16].

We obtained data on structural changes of the intestinal epithelial barrier of the duodenum of rats in burn skin injury under experimental streptozotocin-induced diabetes mellitus, indicating an increase in the paracellular permeability of the barrier. In animals of the second experimental group, intestinal microbes were found to penetrate the defective intestinal epithelial barrier of the duodenum, which is consistent with the data [3] on the role of intestinal microbiota translocation in the pathogenesis of diabetes.

With the development of burn disease, the translocation of pathogenic microflora from the lumen of the intestine to other organs leads to deepening of the systemic inflammatory response syndrome, hypermetabolism, multiple organ failure, sepsis. Such translocation is a factor in the worsening of diabetes mellitus [3, 19], which was once witnessed by Vaarala O. et al. [28], calling the intricate relationship between gut microbiota, permeability of the intestinal epithelial barrier and mucosal immunity a "perfect storm" for diabetes.

Summarizing, in the duodenal mucosa of rats of the second experimental group, the dynamics of morphological changes during different periods after burns (7 days - the stage of shock and early toxemia; 14 days - the stage of late toxemia; 21 days - the stage of septicotoxemia) differ from animals of the first experimental group. Comparison of the data obtained with those previously revealed suggests that the time intervals and the nature of the adaptive duodenal intestinal epithelial barrier are largely prolonged and impaired. Significant lesions of the intestinal epithelial barrier should lead to disruption of the processes of the digestive system, parietal digestion and absorption, as well as immunological protection (considering that the intestinal

epithelial barrier is the first zone of contact of the organism with environmental antigens and (and the leading element of the immune system), which undoubtedly affects the condition of the body with burns and, to a large extent, determines the development of burn disease, as well as the course of diabetes. The prospect of further research in this direction is related to the study of the effects on the duodenum of drugs that reduce the intoxication of the body and blood sugar level.

Conclusions

1. In the basis of damage to the enterocytes of the duodenal mucosa of rats with burn skin injury there are deep destructive changes, which after 21 days (in the stage of septicotoxemia), as a rule, are not reverse and develop

on the background of significant intoxication.

2. The revealed structural changes of the enterocytes are evidence of a violation of the structural integrity of the intestinal epithelial barrier. In animals of the first and second (mostly) experimental groups, the damaged epithelium of the duodenal mucosa critically weakens the adequacy of its function of the interface between the mucous membrane and the environment of the intestinal lumen, and is not capable of structurally providing a reliable barrier against toxins, pathogens and antigenic molecules.

3. The adaptive mechanism for ensuring the repair of damaged enterocytes is selective autophagy, which acts as a factor in the recycling of destroyed organelles and the cytoplasmic matrix, aimed primarily at maintaining cell viability.

References

- [1] Anding, A. L., & Baehrecke, E. H. (2015). Autophagy in cell life and cell death. *Current topics in developmental biology*, 114, 67-91. doi: 10.1016/bs.ctdb.2015.07.012
- [2] Azpiroz, F., & Malagelada, C. (2016). Diabetic neuropathy in the gut: pathogenesis and diagnosis. *Diabetologia*, 59(3), 404-408. <https://doi.org/10.1007/s00125-015-3831-1>
- [3] Blandino, G., Inturri, R., Lazzara, F., Di Rosa, M., & Malaguarnera, L. (2016). Impact of gut microbiota on diabetes mellitus. *Diabetes & metabolism*, 42(5), 303-315. doi: 10.1016/j.diabet.2016.04.004
- [4] Cherkasov, V. G., Kovalchuk, A. I., Dzevulska, I. V., Malikov, A. V., Lakhtadyr, T. V., & Matkivskaya, R. M. (2015). Structural transformations in the internal organs with infusion therapy for burn disease. *Medical science of Ukraine*, 11(3-4), 4-11.
- [5] Cherkasov, V. G., Kovalchuk, A. I., Dzevulska, I. V., & Cherkasov, E. V. (2015). Evaluation of the effect of infusion of composite hyperosmolar solutions on the structure of neuroimmunoendocrine system organs in burn diseases. *European International Journal of Science and Technology*, 4(9), 51-61.
- [6] Costantini, T. W., Loomis, W. H., Putnam, J. G., Drusinsky, D., Deree, J., Choi, S., ... & Coimbra, R. (2009). Burn-induced gut barrier injury is attenuated by phosphodiesterase inhibition: effects on tight junction structural proteins. *Shock* (Augusta, Ga.), 31(4), 416-422. doi: 10.1097/SHK.0bo13e3181863080
- [7] Dzevulska, I. V., Kovalchuk, O. I., Cherkasov, E. V., Majewskiy, O. Y., Shevchuk, Y. G., Pastukhova, V. A., & Kyselova, T. M. (2018). Influence of lactoprotein solution with sorbitol on dna content of cells of endocrine glands on the background of skin burn in rats. *World of medicine and biology*, 14(64), 033-039. doi: 10.26724/2079-8334-2018-2-64-33-39
- [8] Elshaer, D., & Begun, J. (2017). The role of barrier function, autophagy, and cytokines in maintaining intestinal homeostasis. *In Seminars in cell & developmental biology* (Vol. 61, pp. 51-59). Academic Press. doi: 10.1016/j.semcd.2016.08.018
- [9] Evers, L. H., Bhavsar, D., & Mailänder, P. (2010). The biology of burn injury. *Experimental dermatology*, 19(9), 777-783. doi: 10.1111/j.1600-0625.2010.01105.x
- [10] Galunko, G. M. (2017). Histological changes in the small intestine in the advanced stages of burn diseases. *World of Medicine and Biology*, 3(61), 90-96. doi: 10.26724/2079-8334-2017-3-61-90-96
- [11] Gotfried, J., Priest, S., & Schey, R. (2017). Diabetes and the small intestine. *Curr Treat Options Gastroenterol*, 15(4), 490-507. doi: 10.1007/s11938-017-0155-x
- [12] Gunas, I., Dovgan, I., & Masur, O. (1997). *Method of internal burn trauma correction by means of cryoinfluence*. Abstracts are presented in zusammen mit der Polish Anatomical Society with the participation of the Association des Anatomistes Verhandlungen der Anatomischen Gesellschaft, Olsztyn (p. 105). Jena-Munche: Der Urban & Fisher Verlag.
- [13] Gunas, I. V., Guminskiy, Y. I., Ocheretn, N. P., Lysenko, D. A., Kovalchuk, O. I., Dzevulska, I. V., & Cherkasov, E. V. (2018). Indicators cell cycle and dna fragmentation of spleen cells in early terms after thermal burns of skin at the background of introduction 0.9% NaCl solution. *World of Medicine and Biology*, 14(63), 116-120. doi: 10.26.724/2079-8334-2018-1-63-116-120
- [14] Gunas, I. V., Kovalchuk, O. I., Cherkasov, V. G., & Dzevulska, I. V. (2014). Structural aspects of the organs adaptive changes of the neuroimmunodocrine system in the treatment of burn disease with combined hyperosmolar solutions. *Galician Medical Herald*, 21(2), 21-26.
- [15] Hietbrink, F., Besselink, M. G., Renooij, W., de Smet, M. B., Draisma, A., van der Hoeven, H., & Pickkers, P. (2009). Systemic inflammation increases intestinal permeability during experimental human endotoxemia. *Shock*, 32(4), 374-378. doi: 10.1097/SHK.0bo13e318a2bcd6
- [16] Huang, Y., Feng, Y., Wang, Y., Wang, P., Wang, F., & Ren, H. (2018). Severe burn-induced intestinal epithelial barrier dysfunction is associated with endoplasmic reticulum stress and autophagy in mice. *Frontiers in physiology*, 9, 441. doi: 10.3389/fphys.2018.00441
- [17] Ihana-Sugiyama, N., Nagata, N., Yamamoto-Honda, R., Izawa, E., Kajio, H., Shimbo, T., ... & Noda, M. (2016). Constipation, hard stools, fecal urgency, and incomplete evacuation, but not diarrhea is associated with diabetes and its related factors. *World journal of gastroenterology*, 22(11), 3252-3260. doi: 10.3748/wjg.v22.i11.3252
- [18] Khoshbaten, M., Madad, L., Baladast, M., Mohammadi, M., & Aliasgarzadeh, A. (2011). Gastrointestinal signs and symptoms among persons with diabetes mellitus. *Gastroenterology and hepatology from bed to bench*, 4(4), 219-223. PMID: 24834186
- [19] Knip, M., & Siljander, H. (2016). The role of the intestinal microbiota in type 1 diabetes mellitus. *Nature Reviews Endocrinology*, 12(3), 154-167. doi: 10.1038/nrendo.2015.218.
- [20] Natrus, L. V., Ryzhko, I. N., Kozak, A. I., Kryvosheieva, O. I., & Stechenko, L. A. (2017). Ultrastructural base of the connective

- tissue skin'cells interactions at burn injury in the hyperglycemic white rats. *World of Medicine and Biology*, 13(62), 157-162. doi: 10.26724/2079-83342017-4-62-157-162
- [21] Netyukhailo, L. G., Kharchenko, S. V., & Kostenko, A. G. (2011). Pathogenesis of burn disease (in 2 parts). *World of Medicine and Biology*, (1), 127-135.
- [22] Nighot, P. K., Hu, C. A., & Ma, T. Y. (2015). Autophagy enhancement of intestinal epithelial tight junction barrier function by targeting claudin-2 degradation. *J. Biol. Chem.*, 290, 7234-7246. doi: 10.1074/jbc.M114.597492
- [23] Pasternak, A., Szura, M., Gil, K., & Matyja, A. (2016). Interstitial cells of Cajal - systematic review. *Folia Morphol.*, 75(3), 281-286. doi: 10.5603/FM.a2016.0002
- [24] Regas, F. C., & Ehrlich, H. P. (1992). Elucidating the vascular response to burns with a new rat model. *J. Trauma*, 32(5), 557-563. doi: 10.1097/00005373-199205000-00004
- [25] Rodrigues, M. L., & Motta, M. E. (2012). Mechanisms and factors associated with gastrointestinal symptoms in patients with diabetes mellitus. *J. Pediatr.*, 88(1), 17-24. doi: 10.2223/JPED.2153
- [26] Smolle, Ch., Cambiaso-Daniel, J., & Forbes, A. A. (2017). Recent trends in burn epidemiology worldwide: A systemic review. *Burns*, 43(2), 249-257. doi: 10.1016/j.burns.2016.08.013
- [27] Turner, J. R. (2009). Intestinal mucosal barrier function in health and disease. *Nat Rev. Immunol.*, 9(11), 799-809. doi: 10.1038/nri2653
- [28] Vaarala, O., Atkinson, M. A., & Neu, J. (2008). The "Perfect Storm" for Type 1 Diabetes: the complex interplay between intestinal microbiota, gut permeability, and mucosal immunity. *Diabetes*, 57(10), 2555-2562. <https://doi.org/10.2337/db08-0331>

СТРУКТУРНІ ЗМІНИ ІНТЕСТИНАЛЬНОГО ЕПІТЕЛІАЛЬНОГО БАР'ЄРА ДВАНДЦЯТИПАЛОЇ КИШКИ ЩУРІВ ПРИ ОПІКОВІЙ ТРАВМІ ШКИРИ ЗА УМОВ ЕКСПЕРИМЕНТАЛЬНОГО СТРЕПТОЗОТОЦИНІНДУКОВАНОГО ЦУКРОВОГО ДІАБЕТУ Тимошенко І.О.

Метою роботи було вивчення структурних змін інтестинального епітеліального бар'єра дванадцятипалої кишки при опіковій травмі шкіри щура за умов експериментального стрептозотоциніндукованого цукрового діабету. Дослідження здійснене на лабораторних білих статевозрілих щурах-самцях масою 180-210 г. Групу контролю склали 21 тварина без соматичної патології, першу експериментальну групу склали - 21 щур з опіковою травмою шкіри, другу експериментальну групу склали - 21 щур з опіком шкіри та експериментальним стрептозотоциніндукованим діабетом. Модель експериментального цукрового діабету відтворювали шляхом введення щурам стрептозотину внутрішньоочеревинно одноразово в дозі 50 мг/кг. Термічне опікове пошкодження шкіри у щурів відповідало II - А-Б ступеню дермального поверхневого опіку (за старою класифікацією III - А ступінь) загальною площею 21-23 % поверхні тіла з розвитком опікового шоку. Для морфологічних досліджень вилучали відділ дванадцятипалої кишки, фрагменти якого обробляли загальноприйнятими методами світлової та електронної мікроскопії. Основними критеріями оцінки пошкодження ентероцитів слизової оболонки дванадцятипалої кишки стали результати дослідження щодо порівняння гістологічних та ультраструктурних даних в динаміці через 7, 14, та 21 добу після опіку шкіри. Результати проведених досліджень показали, що в основі пошкодження інтестинального епітеліального бар'єра дванадцятипалої кишки лежать глибокі деструктивні зміни, які через 21 добу (в стадії септикотоксемії), як правило, мають незворотній характер і розвиваються на фоні значної інтоксикації організму. Відмічено зменшення кількості щільних контактів в інтестинальному епітеліальному бар'єрі дванадцятипалої кишки щурів першої та другої експериментальних груп та втрата упорядкованості (набуття певної хаотичності) їхньої локалізації у міру збільшення часу після опікової травми. На більшій своїй протяжності інтестинальний епітеліальний бар'єр втрачає цілісність клітинної складової при частковій збереженості базальної мембрани (перше відбувається як за рахунок некрозу ентероцитів з щіточковою облямівою, так і за рахунок повної деструкції келихоподібних клітин). У всіх випадках в інтестинальному епітеліальному бар'єрі з'являються дефекти, які є потенційними шляхами парацелюлярної транслокації патогенного вмісту дванадцятипалої кишки. Не виключно, що частина цього інтестинального патогенного вмісту може бути транслокована і через частково пошкоджені клітин. Свідченням останнього є виявлені мікробні тіла в цитоплазмі клітин з частково зруйнованою плазмолемою (але збереженими органелами та ядром). Адаптивним механізмом щодо забезпечення репарації ушкоджених ентероцитів є селективна автофагія, яка виступає чинником рециклізації матеріалу зруйнованих органел і цитоплазматичного матриксу, спрямованого, в першу чергу, на підтримку життєздатності клітин.

Ключові слова: опікова травма, стрептозотоциніндукований цукровий діабет, інтестинальний епітеліальний бар'єр.

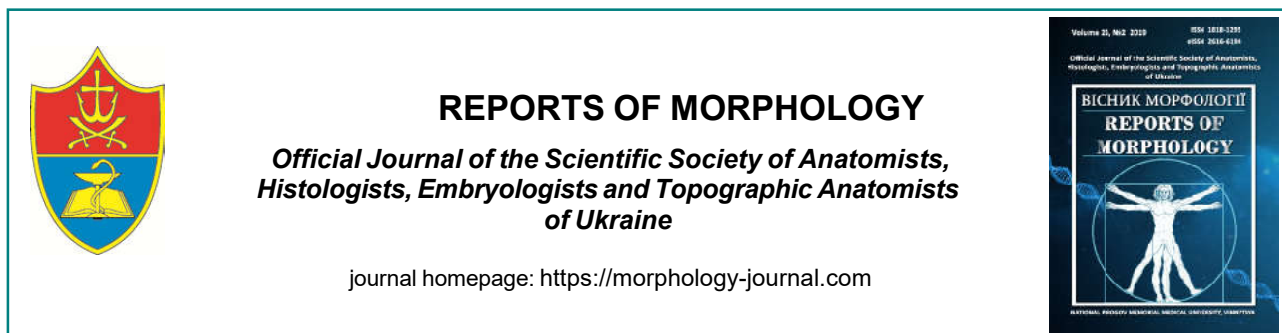
СТРУКТУРНЫЕ ИЗМЕНЕНИЯ ИНТЕСТИНАЛЬНОГО ЭПИТЕЛИАЛЬНОГО БАРЬЕРА ДВАНДЦАТИПЕРСТНОЙ КИШКИ КРЫС ПРИ ОЖГОВОЙ ТРАВМЕ КОЖИ В УСЛОВИЯХ ЭКСПЕРИМЕНТАЛЬНОГО СТРЕПТОЗОТОЦИНІНДУЦИРОВАННОГО САХАРНОГО ДИАБЕТА

Тимошенко И.А.

Целью работы было изучение структурных изменений интестинального эпителиального барьера дванадцатиперстной кишки при ожоговой травме кожи крысы в условиях экспериментального стрептозотоцининдуцированного сахарного диабета. Исследование осуществлено на лабораторных белых половозрелых крысах-самцах массой 180-210 г. Группу контроля составили 21 животное без соматической патологии, первую экспериментальную группу составили - 21 крыса с ожоговой травмой кожи, вторую экспериментальную группу составили - 21 крыса с ожогом кожи и экспериментальным стрептозотоцининдуцированным диабетом. Модель экспериментального сахарного диабета воспроизводили путем введения крысам стрептозотина внутривентрально однократно в дозе 50 мг/кг. Термическое ожоговое повреждение кожи у крыс соответствовало II - А-Б степени дермального поверхностного ожога (по старой классификации III - А степень) общей площадью 21-23 % поверхности тела с развитием ожогового шока. Для морфологических исследований изымали отдел дванадцатиперстной кишки, фрагменты которого обрабатывали общепринятыми методами световой и электронной микроскопии. Основными критериями оценки повреждения энтероцитов слизистой оболочки дванадцатиперстной кишки стали результаты сравнения гистологических и ультраструктурных данных в динамике через 7, 14 и 21 сутки после ожога кожи. Результаты проведенных исследований показали, что в основе поврежденного интестинального эпителиального барьера дванадцатиперстной кишки лежат глубокие деструктивные изменения, которые через 21 день (в стадии

септикотоксемии), как правило, имеют необратимый характер и развиваются на фоне значительной интоксикации организма. Отмечено уменьшение количества плотных контактов в интестинальном эпителиальном барьере двенадцатиперстной кишки крыс первой и второй экспериментальных групп и потеря упорядоченности (приобретение определенной хаотичности) их локализации по мере увеличения времени после ожоговой травмы. На большей части своей протяженности интестинальный эпителиальный барьер теряет целостность клеточной составляющей при частичной сохранности базальной мембраны (первое происходит как за счет некроза энтероцитов с щеточной каймой, так и за счет полной деструкции бокаловидных клеток). Во всех случаях в интестинальном эпителиальном барьере появляются дефекты, которые являются потенциальными путями парацеллюлярной транслокации патогенного содержимого двенадцатиперстной кишки. Часть этого интестинального патогенного содержания может быть транслоцирована и через частично поврежденные клетки. Свидетельством последнего является выявленное наличие микробных тел в цитоплазме клеток с частично разрушенной плазмолеммой (но сохранившимися органеллами и ядром). Адаптивным механизмом по обеспечению репарации поврежденных энтероцитов является селективная аутофагия, которая выступает фактором рециклизации материала разрушенных органелл и цитоплазматического матрикса, направленного, в первую очередь, на поддержание жизнеспособности клеток.

Ключевые слова: ожоговая травма, стрептозотоцининдуцированный сахарный диабет, интестинальный эпителиальный барьер.



REPORTS OF MORPHOLOGY

*Official Journal of the Scientific Society of Anatomists,
Histologists, Embryologists and Topographic Anatomists
of Ukraine*

journal homepage: <https://morphology-journal.com>

Structural changes of the spleen in experimental obesity

Harapko T.V.

Uzhhorod National University, Medical Faculty, Uzhhorod, Ukraine

ARTICLE INFO

Received: 19 February, 2019

Accepted: 20 March, 2019

UDC: 611.41.018:616-056.257-092.9

CORRESPONDING AUTHOR

e-mail: garapkotv@gmail.com

Harapko T.V.

The paper presents and analyzes data from an experimental study conducted on white rats in females and males of reproductive age. Obesity is one of the leading causes of premature death worldwide. The purpose of the research is to establish the morphometric and histological changes of the rat spleen parenchyma in experimental obesity and after the abolition of the high-calorie diet (HCD). We conducted a study on 70 white rats of reproductive age (2.5-6.5 months) weighing 120-280 g. High-calorie diet was achieved due to the fact that food was added sodium glutamate at a dose of 67 mg/kg of body weight of the rat. Controls were 10 white rats that received a standard vivarium diet instead of a high-calorie diet. Statistical processing of digital data was performed using Excel software and STATISTICA 6.0 using the parametric methods. Eight weeks after HCD, there was a significant decrease in the relative area of white pulp in the spleen parenchyma of white rats in males and females by 16.2% and 17.4%, respectively, and an increase in the relative area of red pulp by 5.6% and 6.2%, respectively. There is an immuno-inducing effect with enhanced proliferation of activated lymphocytes and their subsequent differentiation into plasma cells. Eight weeks after the abolition of HCD, the relative area of white pulp in the spleen parenchyma of white rats in males and females was 16.8% and 16.9% less than the parameters of the intact group of animals. Accordingly, the relative area of the red pulp by 5.8% and 6.1% exceeds the parameters of the intact group of animals. The area of the lymph nodes and the size of their reproductive centers decrease. The number of monocytes, macrophages and plasmacytes increases in the organ parenchyma. Hemosiderin residues occur both in the cytoplasm of macrophages and in intercellular spaces. Arteries with thickened wall, full-blooded, veins enlarged and full-blooded. The venous sinuses of the red pulp are dilated to contain hemosiderin residues. Thus, the depletion of lymphoid tissue with progression of mainly white pulp atrophy has been established. In the conditions of the eight-week abrogation of the HCD, no reverse changes in the structure of the parenchyma of the spleen were detected.

Keywords: obesity, rat, spleen, white pulp, red pulp.

Introduction

Obesity is one of the leading causes of premature death worldwide [5]. This is due to the fact that obesity increases the risk of cardiovascular disease (coronary heart disease, congestive heart failure, hypertension) [1, 11, 21], type II diabetes [10, 17], obstructive sleep apnea syndrome, neuropathy [6], osteoarthritis, dementia, splenomegaly [4, 8], fatty liver disease [19], and others [12, 16]. Obesity is also associated with a wide range of cancers (colon, breast, endometrium, kidney, esophagus, stomach, pancreas, and gall bladder), and along with insulin resistance (IR) is a risk factor for developing hepatocellular carcinoma [14, 17]. In chronic diseases, obesity as a concomitant pathology complicates the course of the underlying disease [5, 16, 22, 23].

In the current scientific literature there is not enough information about the effect of obesity on the immune (lymphoid) organs, which provide protection of the body against foreign antigens. Adipose tissue is a complex endocrine organ whose effect on organs and tissues is significant and diverse, increasing the likelihood of multiple diseases [9, 15, 18, 20]. Investigations into the dynamics of changes in the structural organization of organs and tissues, as well as possible methods for their correction, remain relevant and important for both theoretical and practical medicine.

Aim of the study: to study the morphometric and histological changes of the rat spleen parenchyma in experimental obesity and after abolition of the high-calorie

diet.

Materials and methods

This study is part of the complex theme "Structural organization, angioarchitectonics and anthropometric features of organs in the intra- and extracorporeal periods of development, under the influence of exogenous and endogenous factors" - state registration number 0115U000041.

The study was performed on 70 white rats of reproductive age (2.5-6.5 months) weighing 120-280 g.

Microanatomy of the structural components of the white rat's spleen under physiological norms was examined in 10 intact animals (first group). The experimental animals were divided into 5 groups: a second group of animals (10 rats) fed a high-calorie diet (HCD) for 8 weeks; a third group of animals (10 rats) fed HCD for 8 weeks, followed by 2 weeks of withdrawal (standard vivarium diet); a fourth group of animals (10 rats) fed HCD for 8 weeks followed by 4 weeks of withdrawal; 5 group of animals (10 rats) fed HCD for 8 weeks followed by 6 weeks of withdrawal; 6 group of animals (10 rats) that were fed HCD for 8 weeks, followed by 8 weeks of withdrawal. Each group had 5 male rats and 5 female rats. HCD was achieved due to the fact that glutamate sodium was added to food at a dose of 67 mg/kg of body weight of the rat. Controls were 10 white rats that received a standard vivarium diet instead of a high-calorie diet.

All experimental animals were kept in the vivarium of Danylo Halytsky Lviv National Medical University. The studies were conducted in accordance with the provisions of the "European Convention for the Protection of Vertebrate Animals Used for Experimental and Other Scientific Purposes" (Strasbourg, 1986), Council of Europe Directive 86/609/EEC (1986), Law of Ukraine No. 3447-IV "On the protection of animals against abuse", the general ethical principles of animal experimentation, approved by the First National Congress of Ukraine on Bioethics (2001).

Morphometric studies were performed using a system of visual analysis of histological preparations. The studies were performed at certain times of the experiment in samples stained with hematoxylin and eosin. Images from histological specimens of the spleen were taken to a computer monitor using a MICROmed SEO SSCAN by microscope and using a Vision CCD Camera. Morphometric studies were performed using VideoTest-5.0, KAAPA Image Base, Stepanizer and Microsoft Excel on a personal computer.

Statistical processing of digital data was performed using "Excel" and "STATISTICA 6.0" software using parametric methods. The numerical values of the parameters are represented by sample averages (M), standard deviation (σ), standard error of the mean (m), Student's t test (t). The results of the calculations were presented in graph form in histograms using Microsoft Office, with confidence intervals.

Results

The spleen belongs to the secondary lymphoid organs, in which there is antigen-dependent proliferation and differentiation of T and B lymphocytes. The histological structure of the spleen of intact animals corresponds to the species norm. Outside, the organ is surrounded by a capsule from which the lugs depart. The spleen is consisting of red and white pulp. The red pulp contains blood cells surrounded by reticular cells. The white pulp consists of splenic lymph nodes and surrounding arteriolar lymphoid vagina (Fig. 1).

After 8 weeks of HCD, a significant decrease in the relative area of white pulp in the spleen parenchyma of white rats of males and females was observed to $21.59 \pm 1.22\%$ and $21.78 \pm 1.31\%$, which is 16.2% and 17.4% less than the parameters of the intact group of animals (Table 1). Accordingly, the relative area of the red pulp increases to $78.41 \pm 1.45\%$ in male rats and to $78.22 \pm 1.54\%$ in female rats. These figures are 5.6% and 6.2% higher than the parameters of the intact group of animals (see Table 1).

After 8 weeks of high-calorie diet (second group of animals) in both male and female rats, the number of monocytes, macrophages and plasmocytes increased. Hemosiderin residues occur both in the cytoplasm of macrophages and in intercellular spaces (Fig. 2). The presence of iron-containing pigment is evidence of erythrocyte death. The proportion of reticular connective tissue in Billroth cords is increasing. The veins of the red pulp are full-blooded. There is an immuno-inducing effect with enhanced proliferation of activated lymphocytes and their subsequent differentiation into plasma cells. Around small vessels, eosinophilic aggregation and lipid accumulation in the enlarged sinuses are found.

At 2 weeks after the abolition of HCD (third group of animals), the relative area of white pulp in the spleen

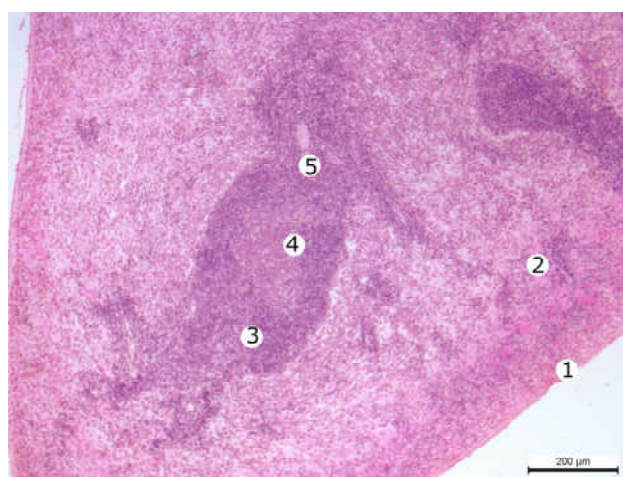


Fig. 1. A fragment of the spleen of an intact white male rat. Hematoxylin-eosin. Objective lens x10, eyepiece x10. 1 - capsule; 2 - red pulp; 3 - white pulp; 4 - center of reproduction of the lymph node; 5 - central artery.

Table 1. Dynamics of changes of relative areas (%) of red and white pulp of spleen of white rats of control and experimental groups (M±m).

Group of animals	Male rats		Female rats	
	S _{white pulp}	S _{red pulp}	S _{white pulp}	S _{red pulp}
Group 1 - intact animals	25.78±1.18	74.22±1.33	26.38±1.02	73.62±1.42
Group 2 - 8 weeks of HCD	21.59±1.22*	78.41±1.45*	21.78±1.31*	78.22±1.54*
Group 3 - 8 weeks of HCD, 2 weeks of discontinuation	21.65±1.43*	78.35±1.87*	21.53±1.21*	78.47±1.65*
Group 4 - 8 weeks of HCD, 4 weeks of discontinuation	21.51±1.09*	78.49±1.56*	21.19±0.69*	78.81±1.23*
Group 5 - 8 weeks of HCD, 6 weeks of discontinuation	21.53±1.03*	78.47±1.34*	21.88±0.98*	78.12±1.76*
Group 6 - 8 weeks of HCD, 8 weeks of discontinuation	21.46±1.05*	78.54±1.54*	21.91±1.23*	78.09±1.43*

Note: * - values that are statistically significantly different from those of the intact animal group (p<0.05).

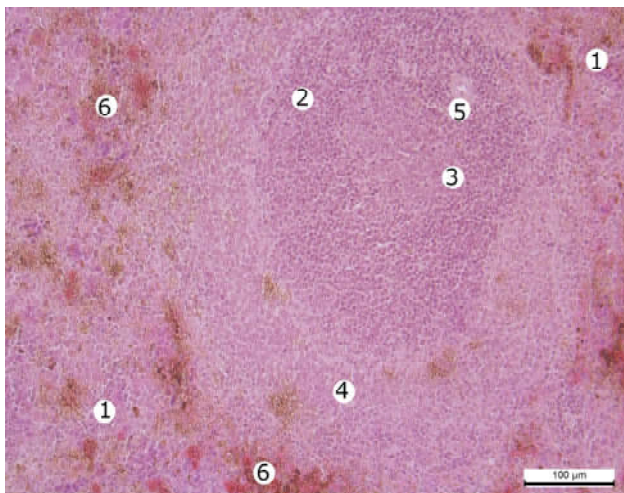


Fig. 2. A fragment of the white rat female spleen after eight weeks of HCD. Hematoxylin-eosin. Objective lens x20, eyepiece x10. 1 - red pulp; 2 - white pulp, secondary lymph node 3 - center of reproduction of the lymph node; 4 - boundary zone; 5 - central artery; 6 - accumulation of hemosiderin and lipids in the venous sinuses of the red pulp.

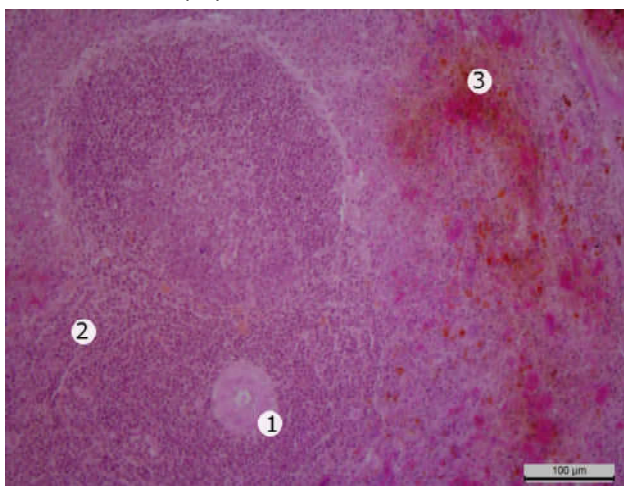


Fig. 3. A fragment of the spleen of a white rat female after two weeks of HCD cancellation. Hematoxylin-eosin. Objective lens x20, eyepiece x10. 1 - central artery with a swollen wall and a narrowed lumen; 2 - white pulp, unclear border of mantle zone, 3 - accumulation of hemosiderin and lipids in venous sinuses of red pulp.

parenchyma of white rats in males and females was almost unchanged from the previous group of animals and was 21.65±1.43% and 21.53±1.21%. These figures are 16.0% and 18.4% lower the parameters of the intact group of animals (see Table 1). Accordingly, the relative area of the red pulp is 78.35±1.87% in male rats and up to 78.47±1.65% in female rats. These figures are 5.6% and 6.6% higher than the parameters of the intact group of animals (see Table 1).

Histological specimens show thickening of the central artery wall and narrowing of the lumen, which may be associated with edema (Fig. 3). Vascular edema is observed. Venous sinuses of red pulp are enlarged, containing hemosiderin and accumulation of lipids. Macrophages are filled with drops of hemosiderin.

4 weeks after abolition of HCD (4 group of animals), the relative area of white pulp in the spleen parenchyma of white rats of males and females decreased by 0.7% and 1.6% compared with the previous group of animals and is 21.51±1.09% and 21.19±0.69%. These figures are 16.6% and 19.7% below the parameters of the intact group of animals (see Table 1). Accordingly, the relative area of the red pulp increases by 0.2% and 0.4% compared to the previous group of animals and is 78.49±1.56% in male rats and 78.81±1.23% in female rats. These figures are 5.8% and 7.0% higher than the parameters of the intact group of animals (see Table 1).

Six weeks after discontinuation of HCD (5 group of animals), the relative area of white pulp in the spleen parenchyma of white rats of males and females increased by 0.1% and 3.3% compared to the previous group of animals and is 21.53±1.03% and 21.88±0.98%. These figures are 16.5% and 17.1% less than the parameters of the intact group of animals (see Table 1). Accordingly, the relative area of the red pulp decreases by 0.04% and 0.9% compared to the previous group of animals and is 78.47±1.34% in male rats and up to 78.12±1.76% in female rats. These figures are 5.7% and 6.1% higher than the parameters of the intact group of animals (see Table 1).

Eight weeks after abolition of HCD (6 group of animals), the relative area of white pulp in the spleen parenchyma of white rats in males and females is almost unchanged from

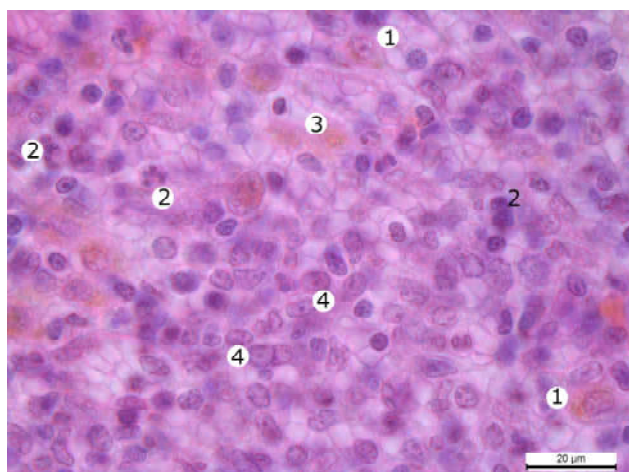


Fig. 4. A fragment of the spleen of a white rat female four weeks after abolition of HCD. Hematoxylin-eosin. Objective lens x100, eyepiece x10. 1 - macrophages with drops of hemosiderin in the cytoplasm; 2 - necrotic altered lymphocytes; 3 - drops of hemosiderin in the intercellular space of the red pulp; 4 - lymphocytes.

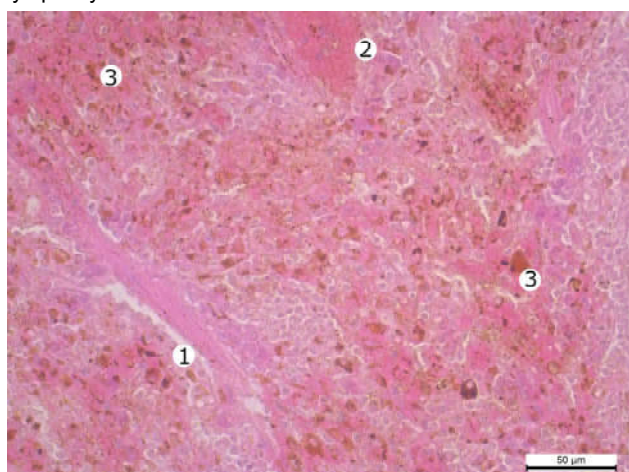


Fig. 5. A fragment of the red pulp of the white rat male spleen eight weeks after abolition of HCD. Hematoxylin-eosin. Objective lens x40, eyepiece x10. 1 - thickened and swollen Billroth cord; 2 - adhesion of erythrocytes and platelets in the enlarged and full-blooded venous sinuses; 3 - accumulation of hemosiderin and lipids in the red pulp.

the previous group of animals and is $21.46 \pm 1.05\%$ and $21.91 \pm 1.23\%$. These figures are 16.8% and 16.9% less than the parameters of the intact group of animals (see Table 1). Accordingly, the relative area of red pulp is $78.54 \pm 1.54\%$ in male rats and up to $78.09 \pm 1.43\%$ in female rats. These figures are 5.8% and 6.1% higher than the parameters of the intact group of animals (see Table 1).

The depletion of lymphoid tissue with progression of mainly white pulp atrophy has been established. The area of the lymphoid nodules and the size of their centers of reproduction decreases, the boundaries between the nodules become not clear, differentiation into zones is not followed everywhere (Fig. 3). Billroth cords of red pulp thicken, become more tortuous. In the nuclei of cells, the

phenomena of karyorrhexis and apoptosis are observed.

Therefore, no changes in the structure of the parenchyma of the spleen were detected in the 8-week abrogation of HCD.

Discussion

Similar structural changes, namely the enlargement and filling of the venous sinuses of the red pulp of the spleen were found in the spleen of rats with 30-day administration of Loratadine [7].

The authors describe that the administration to white rats of SiO_2 nanoparticles, together with lead acetate, leads to hypoplasia of the white pulp of the spleen with a decrease in the T-lymphocytic zone, causes karyorrhexis and apoptosis of red pulp cells. There was also a sharp increase in the amount of iron-containing pigment, reflecting the process of erythrocyte death. In addition, the formation of diffuse small-focal lymphocyte clusters among the red pulp along the course of the vessels was revealed [3].

Intraperitoneal administration of extracts of mountain arnica and tormentil at a dose of $30 \mu\text{l}$ per 20 g of mouse weight leads to a significant advantage of white pulp over red, lymphoid follicles have lost a distinct structure. Among the red pulp there are single megakaryocytes, and their number in the field of view of the microscope is higher, compared with the control samples [19].

The authors of studies showed that a high-nutrition diet reduced the expression of CD20, a surface molecule present on B-cells, which plays a large role in the immune response and produces IL-10 mainly in the spleen [13]. Moreover, splenocyte proliferation stimulated by T-cell and B-cell mitogens was significantly lower in obese individuals; thus, the functions of both T-cells and B-cells in the spleen can be impaired in obesity. The authors suggest that obesity-induced decrease in IL-10 synthesis in the spleen can lead to inflammatory reactions in the kidneys and metabolic disorders [13].

The authors describe that obesity reduces the size of inguinal lymph nodes, impairs lymphatic fluid transport and migration of dendritic cells to peripheral lymph nodes, and reduces the number of T-lymphocytes in lymph nodes. In general, obesity impairs the integrity of the immune system and leads to changes in the development of leukocytes, their migration and diversity [2].

Decreasing the population of "naive" T-cells (helpers) leads to a worsening of the immune system, which occurs with the onset of age. In animal model studies, obesity compromises the T-cell immune system due to increased adipogenesis in primary lymphoid organs and systemic inflammation. Due to the fact that obesity increases the risk of multiple age-related diseases, impaired immune competence is a possible mechanistic link between obesity and disease development in the elderly [24].

The prospects for further development are related to the further study of the morphometric and electron microscopic changes of the structural components of the

rat spleen through different terms of experimental obesity and its correction.

Conclusions

1. After 8 weeks of HCD there is a significant decrease in the relative area of white pulp in the parenchyma of the spleen of white rats-males and females by 16.2% and 17.4%, respectively, and an increase in the relative area of red pulp by 5.6% and 6.2%.

2. At 8 weeks after HCD withdrawal, the relative area of white pulp in the spleen parenchyma of white male rats and females was 16.8% and 16.9% less than that of the intact animal group. Accordingly, the relative area of the red

pulp is 5.8% and 6.1% higher than the parameters of the intact group of animals.

3. The depletion of lymphoid tissue with progression of mainly white pulp atrophy has been established. The area of the lymph nodes and the size of their reproductive centers decrease. Arteries with thickened wall, full-blooded, veins enlarged and full-blooded. Sinus red pulp dilated, hemosiderin and accumulation of lipids in the lumen of the venous sinuses. Macrophages are filled with drops of hemosiderin. In the conditions of 8-week cancellation of HCD, no reverse changes in the structure of the parenchyma of the spleen were detected.

References

- [1] Alpert, M.A., Omran, J., & Bostick, B.P. (2016). Effects of Obesity on Cardiovascular Hemodynamics, Cardiac Morphology, and Ventricular Function. *Curr. Obes. Rep.*, 15, 156-171. doi: 10.1007/s13679-016-0235-6
- [2] Andersen, C.J., Murphy, K.E., & Fernandez, M.L. (2016). Impact of Obesity and Metabolic Syndrome on Immunity. *Adv. Nutr.*, 7(1), 66-75. doi: 10.3945/an.115.010207
- [3] Bandas, I.A., Kulitska, M.I., & Korda, M.M. (2017). Structural changes of rat liver, kidney and spleen when exposed to silica nanoparticles and lead acetate. *Bulletin of problems of biology and medicine*, 1(135), 322-327.
- [4] Buchan, L., Chaheyla, R., Fisher, A., Hellings, A., Castro, M., Al-Nakkash, L. ... Plochocki, J.H. (2018). High-fat, high-sugar diet induces splenomegaly that is ameliorated with exercise and genistein treatment. *BMC Res Notes*, 11, 752. doi: 10.1186/s13104-018-3862-z
- [5] Chien, M.Y., Ku, Yu.H., Chang, J.M., Yang, C.M., & Chen, C.H. (2016). Effects of herbal mixture extracts on obesity in rats fed a high-fat diet. *Journal of Food and Drug Analysis*, 24(3), 594-601. doi: 10.1016/j.jfda.2016.01.012
- [6] Coppey, L., Shevalye, H., Obrosova, A., Davidson, E., & Yorek, M. (2018). Determination of peripheral neuropathy in high-fat diet fed low-dose streptozotocin-treated female C57Bl/6J mice and Sprague-Dawley rats. *J. Diabetes Investig.*, 9(5), 1033-1040. doi: 10.1111/jdi.12814
- [7] Dudok, O.V. (2015). The state of the microstructure of the spleen under the conditions of application of Loratadine. *World of medicine and biology*, 2, 96-99.
- [8] El-Aziza, R., Naguiba, M., & Rashedb, L. (2018). Spleen size in patients with metabolic syndrome and its relation to metabolic and inflammatory parameters. *The Egyptian Journal of Internal Medicine*, 30, 78-82. doi: 10.4103/ejim.ejim_86_17
- [9] Escobedo, N., & Oliver, G. (2017). The Lymphatic Vasculature: Its Role in Adipose Metabolism and Obesity. *Cell metabolism*, 26(4), 598-609. doi: 10.1016/j.cmet.2017.07.020
- [10] Esser, N., Legrand-Poels, S., Piette, J., Scheen, A.J., & Paquot N. (2014). Inflammation as a link between obesity, metabolic syndrome and type 2 diabetes. *Diabetes Research and Clinical Practice*, 105(2), 141-150. doi: 10.1016/j.diabres.2014.04.006
- [11] Fedecostante, M., Spannella, F., Giulietti, F., Espinosa, E., Dessi-Fulgheri, P., & Sarzani, R. (2015). Associations between body mass index, ambulatory blood pressure findings, and changes in cardiac structure: relevance of pulse and nighttime pressures. *J. Clin. Hypertens. (Greenwich)*, 17(2), 147-153. doi: 10.1111/jch.12463
- [12] Giles, E., Jackman, M., & MacLean, P. (2016). Modeling Diet-Induced Obesity with Obesity-Prone Rats: Implications for Studies in Females. *Front. Nutr.*, 3, 50-55. doi: 10.3389/fnut.2016.00050
- [13] Gotoh, K., Fujiwara, K., Anai, M., Okamoto, M., Masaki, T., Kakuma, T., & Shibata, H. (2017). Role of spleen-derived IL-10 in prevention of systemic low grade inflammation by obesity. *Endocr. J.*, 64, 375-378.
- [14] Holmes, A., Coppey, L., Davidson, E., & Yorek, M. (2015). Rat Models of Diet-Induced Obesity and High Fat/Low Dose Streptozotocin Type 2 Diabetes: Effect of Reversal of High Fat Diet Compared to Treatment with Enalapril or Menhaden Oil on Glucose Utilization and Neuropathic Endpoints. *Journal of Diabetes Research*, 2015, 60-68. doi: 10.1155/2015/307285.
- [15] Inoue, H., Kodani, E., Atarashi, H., Okumura K., Yamashita, T., & Origasa, H. (2016). Impact of Body Mass Index on the Prognosis of Japanese Patients with Non-Valvular Atrial Fibrillation. *Am. J. Cardiol.*, 118(2), 215-221. doi: 10.1016/j.amjcard.2016.04.036
- [16] Jin, W., Cui, B., Li, P., Hua, F., Lv, X., Zhou, J., & Zhang, X. (2018). 1,25-Dihydroxyvitamin D3 protects obese rats from metabolic syndrome via promoting regulatory T cell-mediated resolution of inflammation. *Acta Pharmaceutica Sinica B*, 8(2), 178-187. doi: 10.1016/j.apsb.2018.01.001
- [17] Kothari, V., Luo, Y., Tornabene, T., O'Neill, A.M., Greene, M.W., Geetha, T., & Babu, J.R. (2017). High fat diet induces brain insulin resistance and cognitive impairment in mice. *Biochim Biophys Acta.*, 1863(2), 499-508. doi: 10.1016/j.bbadis.2016.10.006
- [18] Oliveira, E., Castro, S., Ayupe, C.M., Ambrósio, G.E., Souza, P.V., Macedo, C.G., & Ferreira, A.P. (2019). Obesity affects peripheral lymphoid organs immune response in murine asthma model. *Immunology*, 157(3), 268-279. doi: 10.1111/imm.13081
- [19] Shemediuk, N.P., Zaitsev, O.O., & Butsiak, V.I. (2010). Histological changes of the spleen, liver, kidneys of animals due to the action of bioactive complexes. *Modern problems of toxicology*, 2-3, 54-57.
- [20] Song, Z., Xie, W., Chen, S., Strong, J.A., Print, M.S., Wang, J.I., ... Zhang, J.M. (2017). High-fat diet increases pain behaviors in rats with or without obesity. *Sci. Rep.*, 7(1), 1-14. doi: 10.1038/s41598-017-10458-z
- [21] Wang, H.J., Si, Q.J., Shan, Z.L., Guo, Y.T., Lin, K., Zhao, X.N., & Wang, Y.T. (2015). Effects of body mass index on risks for ischemic stroke, thromboembolism, and mortality in Chinese atrial fibrillation patients: a single-center experience. *PLoS*

- One, 10(4), 231-242. doi: 10.1371/journal.pone.0123516
- [22] Wan, H., Wu, S., Wang, J., Yang, Y., Zhu, J., Shao, X. ... Zhang, H. (2017). Body mass index and the risk of all-cause mortality among patients with nonvalvular atrial fibrillation: a multicenter prospective observational study in China. *Eur. J. Clin. Nutr.*, 71(4), 494-499. doi: 10.1038/ejcn.2016.183
- [23] Yanagisawa, S., Inden, Y., Yoshida, N., Kato, H., Miyoshi-Fujii, A., Mizutani, Y., ... Murohara, T. (2016). Body mass index is associated with prognosis in Japanese elderly patients with atrial fibrillation: an observational study from the outpatient clinic. *Heart Vessels*, 31(9), 1553-1561. doi: 10.1007/s00380-015-0765-y
- [24] Yoshida, K., Nakashima, E., Kubo, Y., Yamaoka, M., Kajimura, J., Kyoizumi, S., ... Kusunoki, Y. (2014). Inverse Associations between Obesity Indicators and Thymic T-Cell Production Levels in Aging Atomic-Bomb Survivors. *Survivors. PLoS One*, 9(6), 98-101. doi: 10.1371/journal.pone.0091985

СТРУКТУРНІ ЗМІНИ СЕЛЕЗІНКИ ПРИ ЕКСПЕРИМЕНТАЛЬНОМУ ОЖИРІННІ

Гарайко Т.В.

В статті наведені та проаналізовані дані експериментального дослідження, яке проводилося на білих щурах самках та самцях репродуктивного віку. Ожиріння є однією з головних причин передчасної смерті у всьому світі. Метою дослідження було вивчення морфометричних та гістологічних змін паренхіми селезінки щурів при експериментальному ожирінні та після відміни висококалорійної дієти (ВКД). Дослідження проведено на 70 білих щурах репродуктивного віку (2,5-6,5 місяців) масою 120-280 г. Висококалорійна дієта досягалася завдяки тому, що в їжу додавали глютамат натрію в дозі 67 мг/кг маси тіла щура. Контролем слугували 10 білих щурів, які замість висококалорійної дієти отримували стандартний харчовий раціон віварію. Статистичну обробку цифрових даних проводили за допомогою програмного забезпечення "Excel" та "STATISTICA 6.0" з використанням параметричних методів. Через 8 тижнів ВКД спостерігається достовірне зменшення відносної площі білої пульпи в паренхімі селезінки білих щурів самців та самок на 16,2% та 17,4%, та відповідно збільшення відносної площі червоної пульпи на 5,6% та 6,2%. Спостерігається імуноіндукуючий ефект з посиленою проліферацією активованих лімфоцитів та їх подальшим диференціюванням у плазматичні клітини. Через вісім тижнів після відміни ВКД відносна площа білої пульпи в паренхімі селезінки білих щурів самців та самок на 16,8% та 16,9% менше параметрів інтактної групи тварин. Відповідно відносна площа червоної пульпи на 5,8% та 6,1% перевищує параметри інтактної групи тварин. Площа лімфоїдних вузликів та розміри їх центрів розмноження зменшуються. В паренхімі органу зростає кількість моноцитів, макрофагів та плазмоцитів. Залишки гемосидерину трапляються як в цитоплазмі макрофагів, так і в міжклітинних просторах. Артерії з потовщеною стінкою, повнокровні, вени розширені та повнокровні. Венозні пазухи червоної пульпи розширені, містять залишки гемосидерину. Таким чином, встановлено виснаження лімфоїдної тканини з прогресуванням атрофії переважно білої пульпи. В умовах 8-тижневої відміни ВКД зворотних змін у структурі паренхіми селезінки не виявлено.

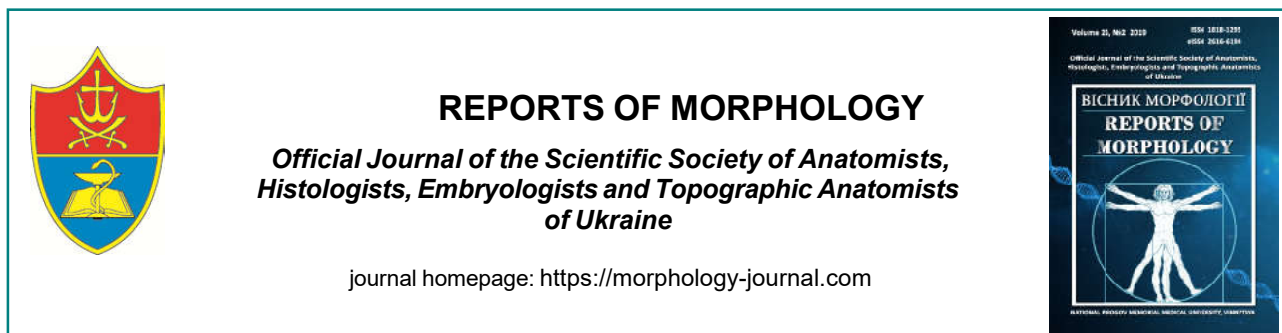
Ключові слова: ожиріння, щур, селезінка, біла пульпа, червона пульпа.

СТРУКТУРНЫЕ ИЗМЕНЕНИЯ СЕЛЕЗЕНКИ ПРИ ЭКСПЕРИМЕНТАЛЬНОМ ОЖИРЕНИИ

Гарайко Т.В.

В статье приведены и проанализированы данные экспериментального исследования, которое проводили на белых крысах самках и самцах репродуктивного возраста. Ожирение является одной из главных причин преждевременной смерти во всем мире. Целью исследования было изучение морфометрических и гистологических изменений паренхимы селезенки крыс при экспериментальном ожирении и после отмены высококалорийной диеты (ВКД). Исследование проведено на 70 белых крысах репродуктивного возраста (2,5-6,5 месяцев) массой 120-280 г. Высококалорийная диета достигалась благодаря тому, что в пищу добавляли глютамат натрия в дозе 67 мг/кг массы тела крысы. Контролем служили 10 белых крыс, которые вместо высококалорийной диеты получали стандартный пищевой рацион вивария. Статистическую обработку цифровых данных проводили с помощью программного обеспечения "Excel" и "STATISTICA 6.0" с использованием параметрических методов. Через 8 недель ВКД наблюдается достоверное уменьшение относительной площади белой пульпы в паренхиме селезенки белых крыс самцов и самок на 16,2% и 17,4%, и, соответственно, увеличение относительной площади красной пульпы на 5,6% и 6,2%. Наблюдается иммуноиндуцирующий эффект с усиленной пролиферацией активированных лимфоцитов и их последующим дифференцированием в плазматические клетки. Через 8 недель после отмены ВКД относительная площадь белой пульпы в паренхиме селезенки белых крыс самцов и самок на 16,8% и 16,9% меньше параметров интактной группы животных. Соответственно, относительная площадь красной пульпы на 5,8% и 6,1% превышает параметры интактной группы животных. Площадь лимфоидных узелков и размеры их центров размножения уменьшаются. В паренхиме органа растет количество моноцитов, макрофагов и плазмоцитов. Остатки гемосидерина случаются как в цитоплазме макрофагов, так и в межклеточных пространствах. Артерии с утолщенной стенкой, полнокровные, вены расширены и полнокровные. Венозные пазухи красной пульпы расширены, содержат остатки гемосидерина. Таким образом, установлено истощение лимфоидной ткани с прогрессированием атрофии преимущественно белой пульпы. В условиях 8-недельной отмены ВКД обратных изменений в структуре паренхимы селезенки не обнаружено.

Ключевые слова: ожирение, крыса, селезенка, белая пульпа, красная пульпа.



Pharmacological correction of various morphological forms of oral mucositis in patients with leukemia

Lysenko D.A.¹, Lukianovych O.I.², Sergyeyev S.V.¹, Bobrowska O.A.¹, Gurova O.O.³

¹National Pirogov Memorial Medical University, Vinnytsya, Vinnytsya, Ukraine;

²Vinnitsa Regional Pathoanatomical Bureau, Vinnytsya, Ukraine;

³Vinnytsya Regional Clinical Hospital n.a. M.I. Pirogov, Vinnytsya, Ukraine

ARTICLE INFO

Received: 20 February, 2019

Accepted: 22 March, 2019

UDC: 616.311-002.44-02-085.277.3-08-039.71

CORRESPONDING AUTHOR

e-mail: bastyl@bigmir.net
Lysenko D.A.

Oral mucositis (OM) is a common complication against the background of modern leukemia therapy, which significantly impairs patients' quality of life. The purpose of the study was to evaluate the effectiveness of the use of local Cyanocobalamin and Decamethoxine therapy for the prevention and treatment of OM. The study was conducted on the basis of the hematology department of Vinnytsya Regional Clinical Hospital n.a. M.I. Pirogov in 2013-2019 (58 patients were studied with standard combination chemotherapy with Cytarabine, Methotrexate and anthracycline antibiotics). In addition to the standard clinical and laboratory study, dental examination was performed before treatment, at 7 and 14 days of treatment with determination of the degree of mucositis according to the NCI-CTC criteria and determination of quality of life indicators. At the same time, a sample incisional biopsy of the oral mucosa was performed with photo-fixation of histopreparations. In a group of 28 patients, 7 days orally administered a combination of Septefril (Decamethoxine) 0.2 mg 4-6 times daily, and Cyanocobalamin 500 mg 3 times daily. Statistical processing of the obtained results was carried out in the license package "STATISTICA 6.1" using non-parametric methods of evaluation of the obtained results. Prior to the onset of cytostatic therapy, no signs of inflammatory lesions were reported. However, patients with pre-established signs of caries, periodontal disease and lack of teeth subsequently experienced OM, even with the use of Cyanocobalamin and Septefril. Thus, after 7 days in 8 patients on the background of medication correction I-II degree of OM according to NCI-CTC was recorded, and only in 2 - III degree, unlike the group without correction. In the group where this combination of drugs was used, OM was recorded after 7 days in 12 patients, in contrast to the indices where the correction was not performed and the development of OM had a more pronounced course and was present in all patients. According to the morphological study, several degrees of OM were observed in patients. Initially, catarrhal stomatitis with pronounced plethora and swelling of the mucous membrane was detected. During the transition to the second stage of mucositis, the aphthous stomatitis was morphologically observed, as well as dead epithelial cells and the cells undergoing parakeratotic transformation. After the application of the proposed therapy, erosion remained after the film rejection, which recovered without scarring. Thus, cytostatic therapy in patients with leukemia always causes manifestations of OM, which are more pronounced in patients with concomitant risk factors. The use of a combination of Cyanocobalamin and Septefril significantly reduces the manifestation of OM and improves the quality of life of patients against cytostatic therapy.

Keywords: cytostatic therapy, oral mucositis, Septefril, Cyanocobalamin, quality of life, morphological examination.

Introduction

Oral mucositis (OM) is a common complication that develops against the background of modern leukemia therapy, significantly impairing the quality of life of patients,

leading to the need to discontinue treatment of the underlying disease and the appointment of concomitant treatment [10]. Despite the emergence of new targeted therapies for

leukemia, OM remains a frequent complication and, while continuing to significantly affect the patient's condition, requires active therapeutic tactics [9, 16]. This problem is constantly in the focus of attention of pathomorphologists, in order to obtain new data on the pathogenetic features of the emergence and course of OM. This will provide an opportunity to offer new methods of treatment for hematologists, dentists, pharmacologists [11, 16]. According to many studies, with standard cytostatic treatment, the frequency of OM was 80-90 %, and in high-dose chemotherapy - up to 100 % of patients had manifestations of this complication [7, 10].

At the same time, inadequate oral hygiene, neutropenia, the elderly, progression of the underlying disease was among the aggravating factors contributing to exacerbation of OM [2, 8]. Accordingly, at the cellular level, factors of impaired OM development were damage to epithelial cells, development of local inflammation with induction of apoptosis of cells of different layers of the mucosa [1, 10]. As a consequence, additional infectious agents penetrate into the depths of the mucosa through the damaged epithelium, the rapid spread of which is due to cytostatic immunosuppression [3, 9]. Thus, the development of OM, as a phenomenon with complex pathogenetic character, requires complex therapy [20, 21].

To date, the recommendations and guidelines for cytostatic treatment observed the actual absence of a consistent algorithm for the prevention and treatment of OM [6, 20]. Among the remedies recommended for the prevention and treatment of OM include: caphosol, zinc sulfate, povidone iodide, palifermin as a topical cytoestimulatory factor, cryotherapy, other local anti-inflammatory drugs, vitamin complexes [5, 13, 14, 15, 19]. However, their use does not fully control the occurrence and course of OM. And this is the reason for the further search for both new pharmacological agents and the use of well-known medicines [10].

Based on our own previous research, the decision was made to combine topical use of cyanocobalamin and decamethoxine as a pathogenetic effect on infectious pathogens that triggered the development of OM in the event of damage to the oral mucosa. After all, vitamin B12 (cyanocobalamin), being a well-known factor in the stimulation of DNA synthesis, which is particularly vulnerable to the action of cytostatics, in combination with decamethoxine, a drug with proven antiseptic effect on the oral flora [11, 18].

A complicating factor for the development of effective OM therapy regimens is the lack of data on the clinical and morphological features of the course of this complication, as well as the lack of clear criteria for both diagnosis and treatment effectiveness [9, 10].

The aim of the study is to evaluate the clinical and morphological features and effectiveness of local cyanocobalamin and decamethoxine therapy for the prevention and treatment of OM.

Materials and methods

The study was conducted at the hematology department of Vinnitsa Regional Clinical Hospital in 2013-2019. The study monitored 58 patients receiving standard combination cytostatic chemotherapy using cytarabine, methotrexate and anthracycline antibiotics [17]. All patients were divided into the following observation groups: 23 of them had acute myeloid leukemia; 20 acute lymphoid leukemia; the remaining 15 are other oncohematological diseases. Treatment protocols for all patients included the use of combined cytostatic chemotherapy. Observed patients ranged in age from 18 to 60 years, including 30 women and 28 men. Patients were divided into 2 comparison groups, randomization was blind in nature to maintain compliance. In addition to the standard clinical and laboratory examination, a dental examination was performed to determine the degree of mucositis according to the NCI-CTC criteria and to examine the quality of life indices according to the methodology proposed by us earlier [12]. The production of histological preparations from the affected areas of the oral mucosa was performed according to the standard method, including incisional biopsy, fixation of small pieces of material in 10 % buffered formalin solution. The paraffin sections obtained on the dome microtome are processed in three steps: dehydration, deparaffinization and staining with hematoxylin-eosin followed by confinement in polystyrene. The results of the study were recorded using an Olympus B-41 light microscope with an Olympus E-410 digital camera.

Dental checkpoints were 0 days of therapy, 7 and 14 days of treatment. A group of 28 patients was prescribed a combination of 0.2 mg septefril (decamethoxine) 4-6 times a day and orally 500 mg cyanocobalamin 3 times a day for 7 days. In 30 patients, no specific local treatment was performed. All studies were performed with the informed consent of the patients.

Statistical processing of the obtained results was performed in the license package "STATISTICA 6.1" using non-parametric methods of estimation of the obtained results according to the recommendations of F. Bonnetain and others [4]. The correctness of the distribution of traits by each of the variations obtained, the mean values of each trait studied and the standard deviation were evaluated. The significance of the difference in values between the independent quantitative values was determined using the Mann-Whitney U test.

Results

The previous distribution of groups showed that by age, gender representation and administration of cytostatic drugs we maintained the representativeness and randomization of groups.

The age distribution of both groups from 18 to 60 years was due to recommendations for high-dose cytostatic therapy only in patients less than 60 years of age. In patients over 60 years of age, this mode of cytostatic therapy has no

benefits in terms of results and significantly increases the risk of side effects and even recorded an increase in mortality with prolonged use.

The mean age of patients in both groups was 45 and 48 years. The correction and non-medication group, therefore, did not have a significant age difference that could not be a risk factor for OM. During the dental examination, no signs of inflammatory lesion of the oral mucosa were detected prior to the initiation of cytostatic therapy in all patients examined. However, in 10 and 9 patients in the group with correction and without, respectively, pre-established signs of caries, periodontal disease and uncorrected absence of teeth, which are recognized [11] risk factors for OM were found. It should be noted that all of these patients subsequently experienced OM, even when using a combination of cyanocobalamin and septeftiril. However, when using this combination after 7 days in 8 patients on the background of correction I-II degree of OM according to NCI-CTC was recorded and only in 2 - III degree. Unlike in the group without correction, no cases of grade I stomatitis were detected in 9 patients without correction on the background of dental pathology. According to the NCI-CTC, all cases of OM in this group showed signs of grade II-III, which was confirmed by histological examination. This difference indicates that there is a protective effect of the proposed combination of drugs in the presence of the patient of this risk factor for OM.

All patients in both groups had moderate and severe neutropenia according to the NCCN Clinical Practice Guidelines in Oncology criteria [20], with no significant differences in leukocyte counts after 7 and 14 days, following standard cytostatic therapy. Given the nosological diversity and differences of cytostatic therapy of individual nosologies, we did not analyze the leukocyte formula in all patients studied. It should also be noted that granulocyte-macrophage colony-stimulating factors were standardized to achieve $1.5 \times 10^9/L$ leukocyte levels in all patients with neutropenia, as recommended by national and international protocols [6, 17, 20]. In the case of neutropenic fever, which was recorded in 27 out of 28 and 29 out of 30 patients of the respective groups, standardized antibacterial therapy was also prescribed [6, 20], which did not affect the development and course of OM. This can be explained by the appearance of neutropenic fever 10-12 days after the start of cytostatic therapy, and histological signs of OM were recorded from the 7 day of therapy. We will also note that patients have noted clinical manifestations of oral irritation at 4-5 days from the beginning of treatment.

That is, all the patients we examined had this risk factor for OM, and a further discrepancy in the frequency and course of this complication was only due to the use of a combination of cyanocobalamin and septeftiril. In general, OM in the group where the use of this combination was recorded after 7 days in 12 patients, in contrast to the group ($p < 0.05$), where no medical correction was performed and the development of OM had a more severe course and was found in all patients.

Also, according to our findings, quality of life indicators was reduced in the group that did not use a combination of cyanocobalamin and septeftiril. In particular, the overall quality of life score in the group using the above scheme after 7 days was 57 ± 12 points, and without the combination - 34 ± 7 points ($p < 0.05$). Among the components of quality of life, the indicators of role social functioning of 2.7 points in the group without correction were the lowest and 11 points with correction ($p < 0.05$). After 14 days, the quality of life indicators and their constituents did not differ significantly in the two groups.

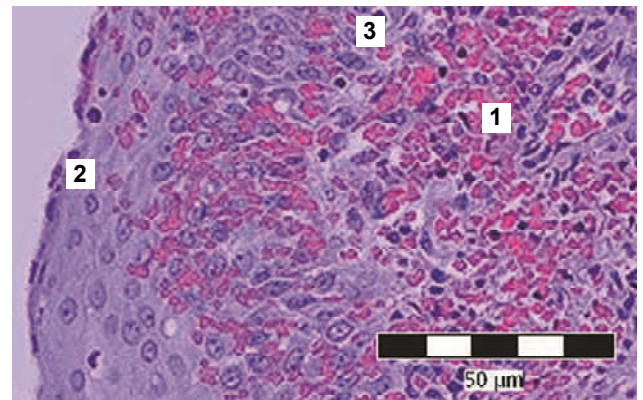


Fig. 1. Catarrhal mucositis. There is hemorrhage into the epithelial layer of the mucous membrane (1), dyskeratosis of the integumentary squamous epithelium (2), single segmented nucleotides (3). Hematoxylin-eosin. x400.

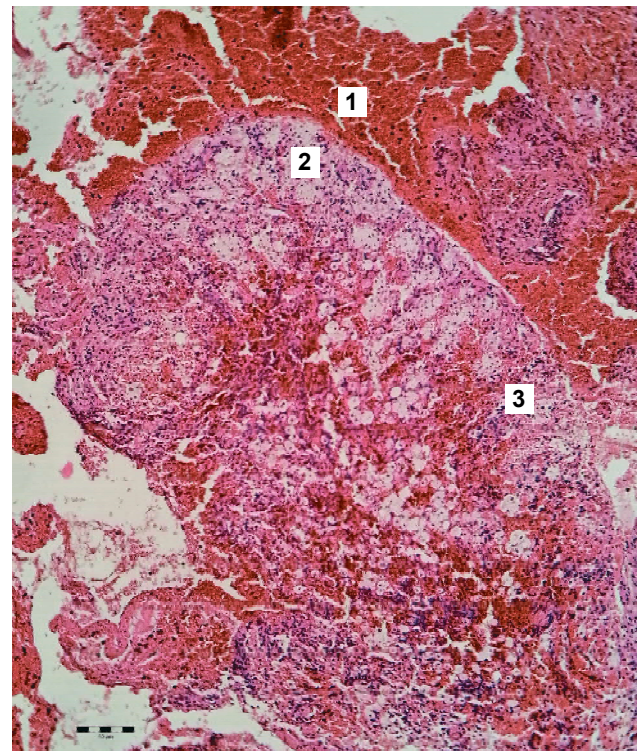


Fig. 2. The area of ulcerative stomatitis after demarcation. Massive hemorrhages (1), dystrophically altered cells, sharp swelling of the submucosal base (2), tissue detritus with cells of inflammatory infiltration (3). Hematoxylin-eosin. x200.

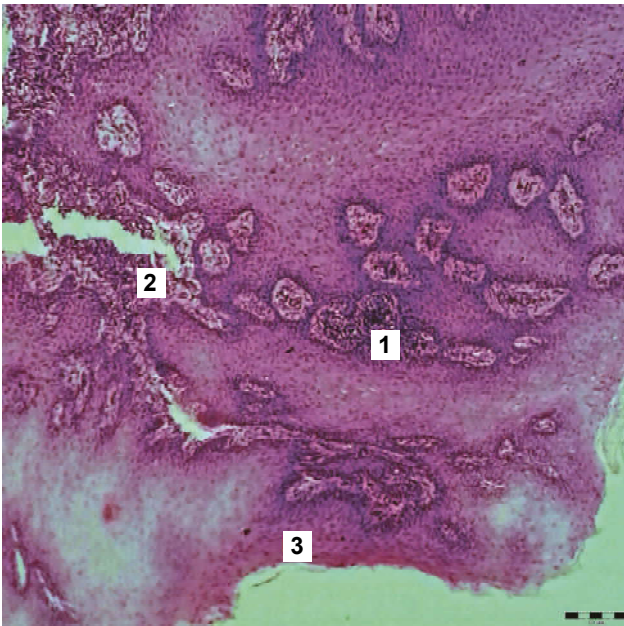


Fig. 3. Catarrhal mucositis with signs of reparation. Foci of inflammatory infiltration in the submucosa involving the squamous epithelium (1), tangles of thin-walled full-blood vessels forming granulation glomeruli (2), dyskeratotic changes of the superficial layers of the squamous epithelium (3). Hematoxylin-eosin. x200.

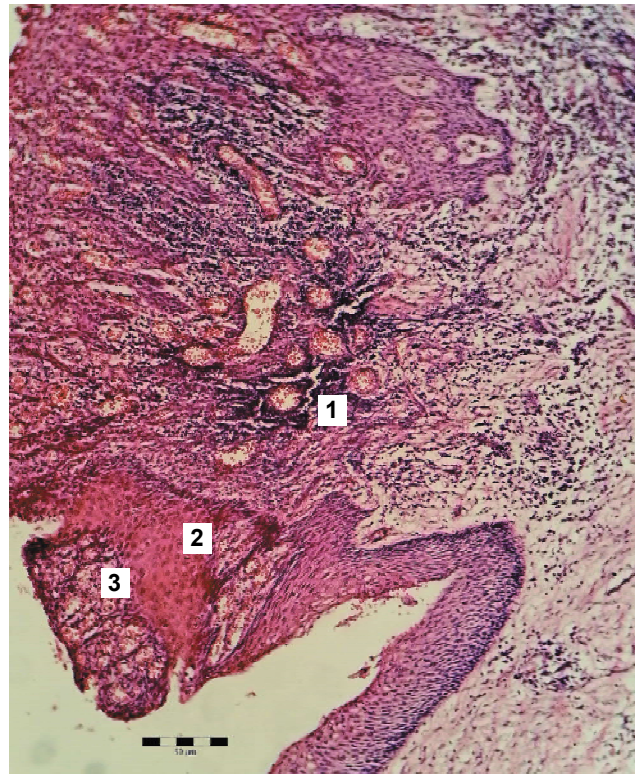


Fig. 5. Hyperplastic reaction in the area of uncorrected absence of tooth. Purulent-proliferative inflammatory reaction with the area of ulceration (1). Hyper- and parakeratosis of the squamous epithelium (2). Granulation tissue (3). Hematoxylin-eosin. x200.

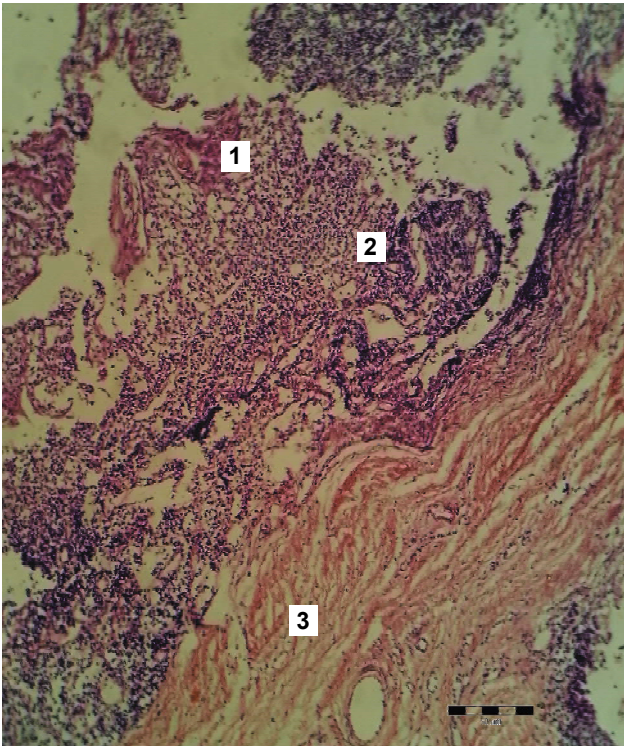


Fig. 4. Ulcerative mucositis. Active ulcer, perifocal inflammation with a large number of segmented neutrophils, tissue detritus (1), dyskeratotic phenomena in desquamated epithelium (2). Severe submucosal edema (3). Hematoxylin-eosin. x200.

Histological examination revealed that I-II degree of OM according to NCI-CTC corresponded to catarrhal

inflammation (Fig. 1).

Catarrhal mucositis in macroscopic examination was characterized by pronounced plethora and swelling of the mucous membrane. The desquamated epithelium accumulated on the lips and tongue in the form of a thick, dirty gray in color, layer. Microscopically, the surface of the mucous membrane was covered with serous exudate with impurities of segmented neutrophils. Also, a significant amount of mucus was determined, which was strongly secreted by the glandular cells of the mucous membrane. Desquamated cells of the superficial layers of the epithelium were present, both keratinized and alive, many of which with dystrophic changes, the phenomena of dyskeratosis and parakeratosis. Depending on the nature of the exudate and the prevalence of mucus, leukocytes, or fused cells, it could be referred to sero-mucoid, purulent or desquamative catarrh (Fig. 2).

With a large number of leukocytes that have passed through the epithelium, macroscopic opacification of the mucous membrane is observed, masking inflammatory redness. However, the majority of patients had a pattern of minor local inflammation due to neutropenia. The use of the proposed combination of cyanocobalamin and septefril alters the course of cytostatic mucositis at the morphological level (Fig. 3).

In the development of ulcerative mucositis, we found

the appearance of hyperemic, swollen mucous membrane, limited areas of necrosis of grayish-yellow color, which represent foci of necrotic or necrotic-fibrinous inflammation (Fig. 4). The rejection or melting of necrotic areas leads to the formation of ulcers. Ulcerative mucositis is particularly characteristic of the gangrenous disintegration of dead tissue sections, in which spirochetes and spindle-shaped sticks are observed. After demarcation and rejection of the dead tissue sections, the ulcers are filled with granulations, their scarring and recovery of the epithelial layer occurs (Fig. 5).

We also note that we observed a clear correspondence between the degree of clinical manifestations of OM, quality of life and histological examination data, in our opinion, the classification of NCI-CTC should be supplemented given the complex results we received, which will allow to differentiate more clearly the manifestations of this complication and to predict further therapeutic management.

Discussion

The small sample size of the study does not allow us to conclude on the expediency of standardized use of the proposed combination of drugs. Also, for the sake of proof, a comparison of this regimen with the previously proposed drugs should be made. Similar studies have already been conducted regarding the use of topical antiseptic agents, recombinant keratinocyte growth factor (palifermin), and other means of preventing and treating of OM [6, 7, 8, 9, 10].

There is no doubt about the importance of the prevention of mucositis. According to the data obtained by us and other researchers [5, 15, 19], the presence of risk factors requires careful dental examination and correction prior to cytostatic therapy. But even the absence of these factors or their correction does not reduce the percentage of manifestations of OM in this category of patients in the treatment of patients with leukemia with high doses of cytostatic drugs. In particular, as established in our study, it is consistent with the data obtained in similar works [5, 19], devoted to the study of clinical manifestations of OM against the use of cytostatic agents. In our opinion, this issue requires further study to identify possible latent risk factors for the development of OM in patients with oncohematologic pathology.

Also, the use of preventive agents has a significant positive effect on the quality of life of patients, which has been recorded, both in our study and in similar studies devoted to the prevention and treatment of OM [2, 3]. Given that this complication is frequent and significantly affects

patients, the prevention and treatment of OM is an important aspect of concomitant treatment of oncohematologic patients. For concomitant therapy, the primary goal is to improve quality of life, and quality of life indicators are important indicators of the effectiveness of this link in therapy [4].

Attention is drawn to the lack of common protocols, especially at the national level, on the conduct of OM. Stratification of risk factors, reasonable prevention and treatment measures will significantly improve the quality of life of patients, even with high dose cytostatic therapy and at risk groups. It is also necessary to analyze the morphological manifestations of OM and the clinical features of this complication, in order to clearly identify possible risk groups early and further develop recommendations for the prevention of this complication. At present, there are no detailed recommendations [8, 9, 11], considering histological manifestations and clinical features, since the existing ones do not consider the complexity of this lesion.

We also emphasize the urgent need for further study of the various groups of drugs that may prevent the development of oral mucositis and the development of optimal measures for the prevention and therapy of oral mucositis. This trend is relevant according to the current trends of scientific research on the study of OM [9, 10, 11].

Also, in our opinion, the existing classification of OM according to NCI-CTC, which does not consider the peculiarities of clinical manifestations of this complication and quality of life indicators, requires detail and further refinement. Histological examinations allow verifying the OM and its extent, but it is also necessary to clarify the prognostic value of these studies in order to improve prevention and therapy and rational choice of treatment regimen.

The prospect of further developments is to clarify the clinical and morphological manifestations of OM on the background of different modes of cytostatic therapy and to evaluate the effectiveness of treatment regimens and prevention of oral mucositis.

Conclusions

1. Cytostatic therapy in patients with leukemia always causes manifestations of grade I-II OM according to NCI-CTC.
2. More pronounced clinical and morphological manifestations of OM are observed in patients with risk factors.
3. The use of a combination of cyanocobalamin and septefril significantly reduces the manifestation of OM and improves the quality of life of patients against cytostatic therapy.

References

- [1] Ahmad, P., Akhtar, U., Chaudhry, A., Rashid, U., Saif, S., & Asif, J. A. (2019). Treatment and prevention of oral mucositis: A literature review. *European Journal of General Dentistry*, 8(2), 23. doi: 10.4103/ejgd.ejgd_30_19
- [2] Basile, D., Di Nardo, P., Corvaja, C., Garattini, S. K., Pelizzari, G., Lisanti, C., & Gerratana, L. (2019). Mucosal Injury during Anti-

- Cancer Treatment: From Pathobiology to Bedside. *Cancers*, 11(6), 857. <https://doi.org/10.3390/cancers11060857>
- [3] Blakaj, A., Bonomi, M., Gamez, M. E., & Blakaj, D. M. (2019). Oral mucositis in head and neck cancer: Evidence-based management and review of clinical trial data. *Oral oncology*, 95, 29-34. <https://doi.org/10.1016/j.oraloncology.2019.05.013>

- [4] Bonnetain, F., Fiteni, F., Efficace, F., & Anota, A. (2016). Statistical Challenges in the Analysis of Health-Related Quality of Life in Cancer Clinical Trials. *Journal of clinical oncology: official journal of the American Society of Clinical Oncology*, 34(16), 1953. <https://doi.org/10.1200/JCO.2014.56.7974>
- [5] Bradstock, K. F., Link, E., Collins, M., Di Iulio, J., Lewis, I. D., Schwarzer, A., & Cull, G. (2014). A randomized trial of prophylactic palifermin on gastrointestinal toxicity after intensive induction therapy for acute myeloid leukaemia. *British journal of haematology*, 167(5), 618-625. <https://doi.org/10.1111/bjh.13086>
- [6] Brown, P. A., Wieduwilt, M., Logan, A., DeAngelo, D. J., Wang, E. S., Fathi, A., & Bhatnagar, B. (2019). Guidelines Insights: Acute Lymphoblastic Leukemia, Version 1.2019: Featured Updates to the NCCN Guidelines. *Journal of the National Comprehensive Cancer Network*, 17(5), 414-423. <https://doi.org/10.6004/jnccn.2019.0024>
- [7] Carrozzo, M., Eriksen, J. G., Bensadoun, R. J., Boers-Doets, C. B., Lalla, R. V., & Peterson, D. E. (2019). Oral Mucosal Injury Caused by Targeted Cancer Therapies. *JNCI Monographs*, (53), lgz012. <https://doi.org/10.1093/jncimonographs/lgz012>
- [8] Chaveli-López, B., & Bagán-Sebastián, J. V. (2016). Treatment of oral mucositis due to chemotherapy. *Journal of clinical and experimental dentistry*, 8(2), e201-9. doi: 10.4317/jced.52917
- [9] Cidon, E. U. (2017). Chemotherapy induced oral mucositis: prevention is possible. *Chinese clinical oncology*, 7(1), 6. doi: 10.21037/cco.2017.10.01
- [10] Cinausero, M., Aprile, G., Ermacora, P., Basile, D., Vitale, M. G., Fanotto, V., ... & Sonis, S. T. (2017). New Frontiers in the Pathobiology and Treatment of Cancer Regimen-Related Mucosal Injury. *Frontiers in pharmacology*, 8, 354. doi: 10.3389/fphar.2017.00354
- [11] Daugėlaitė, G., Užkuraitytė, K., Jagelavičienė, E., & Filipauskas, A. (2019). Prevention and Treatment of Chemotherapy and Radiotherapy Induced Oral Mucositis. *Medicina*, 55(2), 25. doi: 10.3390/medicina55020025
- [12] Isakova, L. M., & Lysenko, D. A. (2006). Methodology of the quality of life estimation in oncohematology. *Ukrainian Medical Journal*, 3, 47-50.
- [13] Kanagalingam, J., Chopra, A., Hong, M. H., Ibrahim, W., Villalon, A., & Lin, J. C. (2017). Povidone-iodine for the management of oral mucositis during cancer therapy. *Oncology reviews*, 11(2), 341. doi: 10.4081/oncol.2017.341
- [14] Kim, J. W., Kim, M. G., Lee, H. J., Koh, Y., Kwon, J. H., Kim, I., ... & Yoon, S. S. (2017). Topical recombinant human epidermal growth factor for oral mucositis induced by intensive chemotherapy with hematopoietic stem cell transplantation: final analysis of a randomized, double-blind, placebo-controlled, phase 2 trial. *PLoS one*, 12(1), e0168854. doi: 10.1371/journal.pone.0168854
- [15] Mahendran, V. J., Stringer, A. M., Semple, S. J., Song, Y., & Garg, S. (2018). Advances in the Use of Anti-inflammatory Agents to Manage Chemotherapy-induced Oral and Gastrointestinal Mucositis. *Current pharmaceutical design*, 24(14), 1518-1532. doi: 10.2174/1381612824666180409093918
- [16] Mori, K., Horinouchi, M., Domitsu, A., Shimotahira, T., Soutome, S., Yamaguchi, T., & Oho, T. (2017). Proper oral hygiene protocols decreased inflammation of gingivitis in a patient during chemotherapy with bevacizumab: a case report. *Clinical case reports*, 5(8), 1352-1357. doi: 10.1002/ccr3.1034
- [17] Order of the Ministry of Health of Ukraine from 30.06.2010 №647. On approval of clinical protocols for the provision of medical care to patients in the specialty "Hematology". http://moz.gov.ua/ua/portal/dn_20100730_647.html
- [18] Paliy, G. K., Nazarchuk, O. A., Faustova, M. O., Pali, V. G., & Yatsula, O. V. (2016). Investigation of the effectiveness of antimicrobials in patients with inflammatory diseases of the oral cavity. *Bulletin of problems of biology and medicine*, 2(3), 220-225.
- [19] Rambod, M., Pasyar, N., & Ramzi, M. (2018). The effect of zinc sulfate on prevention, incidence, and severity of mucositis in leukemia patients undergoing chemotherapy. *European Journal of Oncology Nursing*, 33, 14-21. doi: 10.1016/j.ejon.2018.01.007
- [20] Tallman, M. S., Wang, E. S., Altman, J. K., Appelbaum, F. R., Bhatt, V. R., Bixby, D., ... & Foran, J. M. (2019). Acute Myeloid Leukemia, Version 3.2019, NCCN Clinical Practice Guidelines in Oncology. *Journal of the National Comprehensive Cancer Network*, 17(6), 721-749. <https://doi.org/10.6004/jnccn.2019.0028>
- [21] Villa, A., & Sonis, S. T. (2015). Mucositis: pathobiology and management. *Current opinion in oncology*, 27(3), 159-164. doi: 10.1097/CCO.0000000000000180

ФАРМАКОЛОГІЧНА КОРЕКЦІЯ РІЗНИХ МОРФОЛОГІЧНИХ ФОРМ ОРАЛЬНОГО МУКОЗИТУ У ХВОРИХ НА ЛЕЙКЕМІЮ

Лисенко Д.А., Лук'янович О.І., Сергєєв С.В., Бобровська О.А., Гурова О.О.

Оральний мукозит (ОМ) є частим ускладненням на фоні сучасної терапії лейкемії, що суттєво погіршує якість життя пацієнтів. Мета дослідження - оцінити ефективність використання місцевої терапії ціанкобаламіном та декаметоксином з метою профілактики та лікування ОМ. Дослідження було проведене на базі гематологічного відділення Вінницької обласної клінічної лікарні ім. М.І. Пирогова в 2013 - 2019 роках (вивчені 58 пацієнтів, зі стандартною комбінованою хіміотерапією цитарабіном, метотрексатом та антрацикліновими антибіотиками). Крім стандартного клініко-лабораторного дослідження, проводили стоматологічне обстеження до лікування, на 7 та 14 добу лікування із визначенням ступеня мукозиту за критеріями NCI-CTC та показників якості життя. Одночасно провели вибірку інцизійну біопсію слизової оболонки ротової порожнини з фотофіксацією гістопрепаратів. У групі із 28 пацієнтів 7 днів перорально призначали комбінацію септефрилу (декаметоксину) 0,2 мг 4-6 разів на добу, та ціанкобаламіну 500 мг 3 рази на добу. Статистичну обробку отриманих результатів провели в ліцензійному пакеті "STATISTICA 6.1" із застосуванням непараметричних методів оцінки отриманих результатів. До початку цитостатичної терапії ознак запального ураження слизової оболонки порожнини рота виявлено не було. Однак, у пацієнтів з попередньо встановленими ознаками карієсу, пародонтозу та відсутністю зубів у подальшому виник ОМ, навіть при використанні ціанкобаламіну та септефрилу. Так, у 8 пацієнтів через 7 днів на фоні медикаментозної корекції була зафіксована I-II ступінь ОМ за NCI-CTC, і лише у 2 - III ступінь, на відміну від групи без корекції. В групі, де була використана дана комбінація препаратів, ОМ зафіксовано через 7 днів у 12 пацієнтів, на відміну від показників групи, де корекцію не проводили і розвиток ОМ мав більш виразний перебіг і був наявний у всіх пацієнтів. За даними морфологічного дослідження у пацієнтів спостерігали декілька ступенів ОМ. На початковій стадії виявлений катаральний стоматит із вираженим повнокрів'ям та набряком слизової оболонки. При переході в другу стадію мукозиту

морфологічно спостерігали афтозний стоматит, а також відмерлі клітини епітелію та клітини, що підлягали паракератотичній трансформації. Після застосування запропонованої терапії та відторгнення плівки залишалася ерозія, яка відновлювалась без рубцювання. Таким чином, цитостатична терапія у хворих на лейкемію завжди викликає прояви ОМ, котрі більш виразно проявляються у пацієнтів зі супутніми факторами ризику. Застосування комбінації ціанокобаламіну та септефрилу суттєво зменшує прояви ОМ та покращує якість життя пацієнтів на фоні проведення цитостатичної терапії.
Ключові слова: цитостатична терапія, оральний мукозит, септефрил, ціанокобаламін, якість життя, морфологічне дослідження.

ФАРМАКОЛОГИЧЕСКАЯ КОРРЕКЦИЯ РАЗЛИЧНЫХ МОРФОЛОГИЧЕСКИХ ФОРМ ОРАЛЬНОГО МУКОЗИТА У БОЛЬНЫХ ЛЕЙКЕМИЕЙ

Лысенко Д.А., Лукьянович О.И., Сергеев С.В., Бобровская О.А., Гурова О.О.

Оральный мукозит (ОМ) является частым осложнением, которое развивается на фоне современной терапии лейкемии, что существенно ухудшает качество жизни пациентов. Цель работы - оценить эффективность использования местной терапии цианокобаламином и декаметоксином с целью профилактики и лечения различных морфологических форм ОМ. Исследование было проведено на базе гематологического отделения Винницкой областной клинической больницы имени Н.И. Пирогова в 2013 - 2019 годах (изучены 58 пациентов со стандартной комбинированной химиотерапией цитарабина, метотрексата и антрациклиновых антибиотиков). Кроме стандартного клинико-лабораторного обследования проводили стоматологическое обследование до лечения, на 7 и 14 сутки лечения с определением степени мукозита по критериям NCI-CTC и определением показателей качества жизни. Одновременно проведена избирательная инцизионная биопсия слизистой оболочки ротовой полости и последующая фотофиксация гистопрепаратов. В группе из 28 пациентов 7 дней перорально назначали комбинацию септефрила (декаметоксина) 0,2 мг 4-6 раз в сутки и цианокобаламина 500 мг 3 раза в сутки. Статистическая обработка полученных результатов проведена в лицензионном пакете "STATISTICA 6.1" с применением непараметрических методов оценки полученных результатов. До начала цитостатической терапии признаков воспалительного поражения слизистой оболочки ротовой полости не было обнаружено. Однако у пациентов с предварительно установленными признаками кариеса, пародонтоза и отсутствия зубов в дальнейшем возник ОМ, даже при использовании цианокобаламина и септефрила. Так, через 7 дней у 8 пациентов на фоне медикаментозной коррекции был зафиксирован ОМ I-II степени по NCI-CTC и только у 2 - III степени, в отличие от показателей группы без коррекции. В группе, где использовали вышеприведенную комбинацию препаратов, ОМ был зафиксирован у 12 пациентов через 7 суток, в отличие от показателей группы, где коррекцию не проводили и ОМ присутствовал у всех и протекал более тяжело. По данным морфологического исследования у пациентов наблюдали несколько степеней ОМ. На начальной стадии выявлен катаральный стоматит с выраженным полнокровием и отеком слизистой оболочки. При переходе во вторую стадию мукозита морфологически наблюдали афтозный стоматит, а также омертвевшие клетки эпителия и клетки, подвергшиеся паракератотической трансформации. После применения предложенной терапии и отторжения пленки оставалась эрозия, которая восстанавливалась без рубцевания. Таким образом, цитостатическая терапия у больных лейкемией всегда вызывает проявления ОМ, которые более выражены у пациентов с сопутствующими факторами риска. Применение комбинации цианокобаламина и септефрила существенно уменьшает проявления ОМ и улучшает качество жизни пациентов на фоне проведения цитостатической терапии.

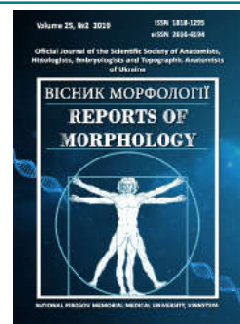
Ключевые слова: цитостатическая терапия, оральный мукозит, септефрил, цианокобаламин, качество жизни, морфологическое исследование.



REPORTS OF MORPHOLOGY

Official Journal of the Scientific Society of Anatomists,
Histologists, Embryologists and Topographic Anatomists
of Ukraine

journal homepage: <https://morphology-journal.com>



Ultrastructural condition of rats periodontal tissue in opioid influence during two weeks and after its four-week withdrawal on correction

Fik V.B.¹, Paltov Ye.V.¹, Kryvko Yu.Ya.²

¹Danylo Halytsky Lviv National Medical University, Lviv, Ukraine

²Andrey Krupinsky Lviv Medical Academy, Lviv, Ukraine

ARTICLE INFO

Received: 22 February, 2019

Accepted: 20 March, 2019

UDC: 611.311-

018.73:615.214.24:615.03:616-076.4

CORRESPONDING AUTHOR

e-mail: fikvolodymyr@ukr.net

Fik V.B.

Given that the dental status of drug addicts is burdened with numerous diseases of the tissues and organs of the oral cavity, the issues of developing an optimal scheme of therapeutic tactics for the purpose of restoring their trophic and balance of the oral microflora against opioid background remain relevant in modern periodontology. The aim of the study was to investigate the ultrastructure of periodontal tissues with experimental two-week opioid action and after its abolition for four weeks under conditions of complex medical corrective action. The study material was white male rats (22) of reproductive age (4.5-6 months), Wistar line, with an average body weight of 200 g. The animals were injected with nalbuphine for two weeks, the dose was 0.212 mg/kg and its subsequent withdrawal for four weeks. In order to correct pathological changes arising from the action of opioids in periodontal tissues, pentoxifylline and the antibiotic ceftriaxone were used. Pentoxifylline was administered intramuscularly daily for four weeks after opioid withdrawal (3-6 weeks) at a dose of 2.857 mg/kg. Ceftriaxone was administered once for 11 days at the end of the experiment (5-6 weeks) at a dose equivalent to rat (2.857 mg/kg). Periodontal tissue sampling was performed in the area of the papilla, followed by ultrastructural examination. Submicroscopically found that the structural components of the periodontium have minor changes, their organization is close to normal. The ultrastructure of all sections of the epithelial lining of the mucosa is characterized by a layered arrangement of cells. In epitheliocytes, part of the nuclei has invaginations of the nuclear membrane, indicating their functional activity, clear outlines of compact nucleolus and plasmalemma. In the cytoplasm, most organelles are virtually unchanged, in the mitochondria there are cristae, clearly identified tonofilaments, desmosomal contacts and the basement membrane. Plasmalemma contours are clear, the intercellular contacts are preserved, and the individual intercellular regions appear thickened. The periodontium is represented by well-ordered collagen fiber bundles, the cellular components are unchanged. The detected submicroscopic structure of fibroblasts indicates their synthetic activity aimed at updating the intercellular substance of connective tissue. Electron microscopic studies of the hemocapillaries of the mucous membrane of the gums of animals of this group showed that in their wide lumens there are formed blood elements, mainly erythrocytes. The nuclei of the endothelial cells have an ellipsoidal shape, small invaginations of nuclear membrane, clear nuclear membranes, organelles are few. Perivascular spaces without signs of edema. Venules are unaltered, have wide lumens, cytoplasmic portions of endothelial cells are not wide, their nuclear parts protrude into the lumen, the basement membrane is thickened in places. Thus, sub-microscopically established that when canceling opioid analgesic and drug correction at the end of the two-week action of opioid there are signs of positive dynamics in the structural components of periodontium, which is explained by the pathogenic reasonableness of pentoxifylline when disturbed by the opioid analgesia and by medication of the opioid analgesia and medication. effect on the ultrastructural and functional organization of periodontal tissues.

Keywords: electron microscopic studies, periodontal tissues, rats, opioid analgesic, correction.

Introduction

Uncontrolled or deliberate misuse of opioid medications in chronic pain is a determining risk of patient addiction, leading to the development of withdrawal syndrome and high overdose death rates [3, 10]. Diseases of the organs and tissues of the oral cavity are most commonly found in drug addicts, whose dental status is burdened with numerous diseases of the tissues of the tooth and mucous membrane of the oral cavity [18, 19, 23]. According to the professional scientific literature, the main features of the pathology of the oral cavity in drug addicts include the slow course of the disease, the inhibition of the blockade of acute phenomena and the progression of bone damage [22].

In the pathogenesis of periodontitis, which also takes place under the influence of narcotic substances, the leading role belongs to disorders of the microcirculation, lack of antioxidant protection and dysbiotic changes of the microbiota in the oral cavity [4, 5, 13, 14, 17, 18, 20, 21, 23]. The course of periodontitis in the chronic process develops against the background of inhibition of phagocytic protection, where the immune response does not depend on the severity of pathomorphological changes, and the function of macrophages when interacting with bacterial flora can cause excessive production of toxic substances that damage the periodontal tissues [18]. Therefore, there is a need to develop the optimal treatment tactics for opioid agents, with the aim of restoring tissues and organs, improving their trophism and restoring the balance of microflora [7, 11, 12, 18]. Since we cannot study periodontal tissues in patients in dynamics at different timing of opioid exposure, the experimental study allows us to simulate the pathological process in periodontal animals and to apply a complex medication correction of the destructive changes that occur during opioid exposure.

The aim of the study was to investigate periodontal tissue biopsy specimens under the experimental action of opioid for two weeks and after its four-week withdrawal under conditions of complex medical corrective action at the ultrastructural level.

Materials and methods

White rats of reproductive age of the Wistar line (n=22), with an average weight of 200 g, 4.5-6 months old, were used as the study material. The experimental animals were divided into 2 groups. The first group consisted of intact animals (n=10), the second group was rats injected with nalbuphine, the opiate receptor antagonist agonist group for the first two weeks at 0.212 mg/kg, and the subsequent withdrawal of the opioid drug over the four weeks. In order to correct pathological changes arising from the action of opioids in periodontal tissues, pentoxifylline and the antibiotic ceftriaxone were used. Pentoxifylline was administered intramuscularly daily for four weeks after opioid withdrawal (3-6 weeks) at a dose of 2.857 mg/kg. Ceftriaxone was administered once for 11 days at the end of the experiment (5-6 weeks) in a dose equivalent to rat - 2.857 mg/kg. As a

control, 3 male rats were injected with 0.9 % sodium chloride solution. Animals were kept under standard vivarium conditions and experiments were carried out in accordance with ethical principles in accordance with the provisions of the "European Convention for the Protection of Vertebrate Animals Used for Experimental and Other Scientific Purposes". For electron microscopic examination, fragments of periodontal soft tissue were used in the area of the gum margin. The tissue pieces were fixed in a 2.5 % solution of glutaraldehyde and in a 1 % solution of osmium tetroxide on phosphate buffer pH 7.2-7.4, dehydrated in alcohols and propylene oxide and poured into a mixture of epoxy resins with araldite [9]. UMPT3m ultramicrotome produced ultrathin sections that were counterstained with uranyl acetate and lead citrate and studied in an electron microscope PEM-100-01.

Results

Conducted electron microscopic studies have shown that in the rats of this subgroup structural components of the periodontium have minor changes, their organization is close to normal. The ultrastructure of all sections of the epithelial lining of the mucosa is characterized by a layered arrangement of cells. In the basal layer, the epithelial cells of the free part of the rat gums have an oval or rounded nucleus with clear outline of the nuclear membrane, a small perinuclear space. The cytoplasm includes numerous tonofilaments, small mitochondria, many ribosomes and a polysome. The basal membrane to which cells of the basal layer are attached by means of a hemidesmosome is clearly defined (Fig. 1).

The epitheliocytes of the spinous layer are smaller in

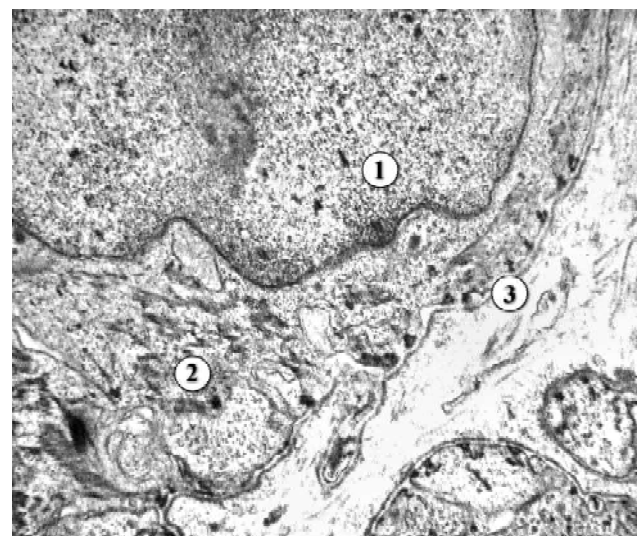


Fig. 1. Ultrastructure of the epitheliocyte of basal layer of the free epithelium of the rat gingiva after six weeks: two weeks of opioid administration, four weeks after its abolition and correction with pentoxifylline and ceftriaxone. 1 - rounded nucleus, 2 - cytoplasm of epitheliocytes, 3 - basement membrane. x14000.

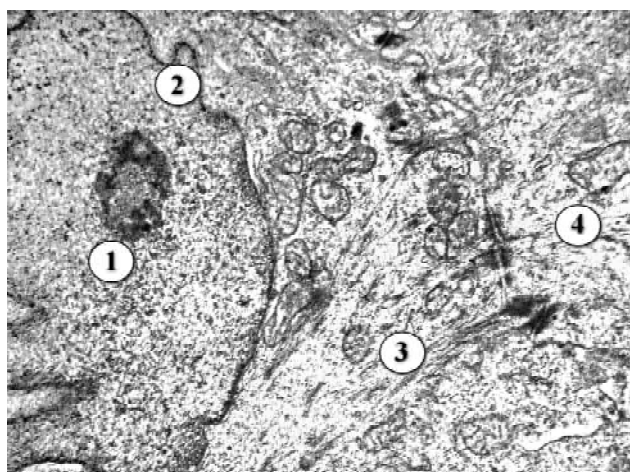


Fig. 2. Ultrastructure of the epitheliocyte spinous layer of the rat gingival epithelium after six weeks: two weeks of opioid administration, four weeks after its abolition, and correction with pentoxifylline and ceftriaxone. 1 - nucleolus, 2 - intussusception of nuclear membrane, 3 - mitochondria, tonofilaments, 4 - intercellular contacts. x14000.

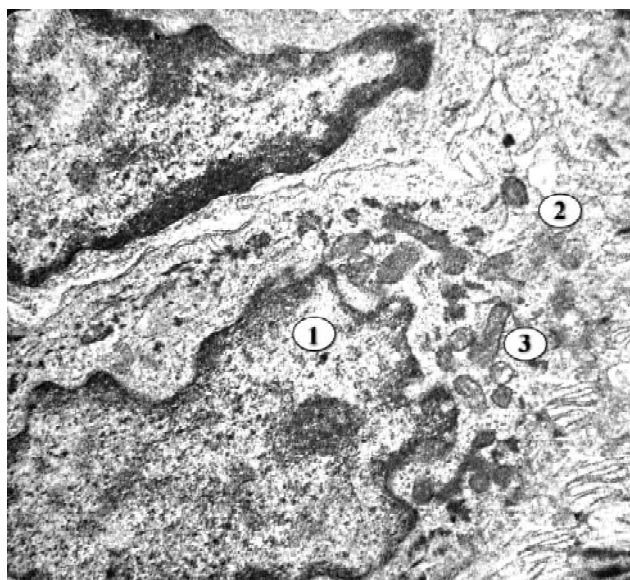


Fig. 3. Ultrastructure of the epitheliocyte spinous layer of the epithelium of the attached part of the rat gingiva after six weeks: two weeks of opioid administration, four weeks of its abolition, and correction with pentoxifylline and ceftriaxone. 1 - nucleus, 2 - cytoplasm of epitheliocyte, 3 - mitochondria. x12000.

size, separated from each other by narrow intercellular spaces, but tightly interconnected by desmosomal contacts. In their cytoplasm many thin tonofibrils. The density of organelles is low, there are separate tubules of granular endoplasmic reticulum, small mitochondria, primary lysosomes. Ultrastructural studies of the epithelial plate of the furrow of animals in this group showed that the cells in its layers are also unchanged. No cytoplasm swelling of the epitheliocytes of the basal and spinous layers is noted. However, part of the nuclei of the cells have invasions of nuclear membrane, which indicates their functional activity. Clear outlines of compact nucleolus and plasmalemma are

observed. In the cytoplasm, most organelles are virtually unchanged, with clear tonofilaments and desmosomal contacts (Fig. 2). In the granular layer, the epitheliocytes have small elongated, osmiophilic, with irregular contours of the nuclear membrane nucleus. Characteristic of the cytoplasm is the presence of electron-density keratohyalin granules. The stratum corneum is formed by rugose scales formed by degeneratively altered epitheliocytes. This layer is thick in the free part of the mucous membrane of the gums, thin in the area of the epithelium of the gums, and absent in the attached part of the gums.

At the ultrastructural level, it has been found that the epithelium of the attached part of the gums of animals has moderate changes and they reflect its functional activity. This applies to the nuclei of cells, which are predominantly elongated with shallow invasions of the nuclear membrane, and euchromatin is noted in the karyoplasm. In the cytoplasm, mitochondrial hyperplasia is observed, they are small, elongated or rounded, and cristae are present in their moderately osmiophilic matrix. Plasmalemma contours are clear, intercellular contacts are preserved, and individual intercellular areas appear thickened (Fig. 3).

Submicroscopic studies of the periodontal organization showed that it is represented by well-ordered collagen fibers, between which are layers of loose connective tissue. Cellular components of the periodontium - fibroblasts, fibrocytes, tissue basophils, lymphocytes, plasmocytes, macrophages are also unchanged. In fibroblasts the nuclei have a long or rounded shape, a developed cytoplasm and a small process. In their cytoplasm there are organelles of general purpose, granular endoplasmic reticulum, Golgi complex, mitochondria, ribosomes, as well as primary polyribosomes, rarely secondary lysosomes (Fig. 4).



Fig. 4. The ultrastructure of the rat periodontium after six weeks: two weeks of opioid administration, four weeks after withdrawal, and correction with pentoxifylline and ceftriaxone. 1 - nucleus and cytoplasm of fibroblast, 2 - collagen fibrils, 3 - amorphous component of intercellular substance. x17000.

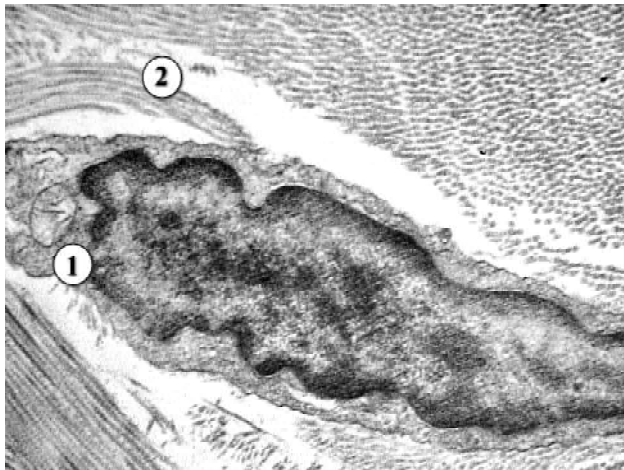


Fig. 5. The ultrastructure of the rat periodontium after six weeks: two weeks of opioid administration, four weeks after withdrawal, and correction with pentoxifylline and ceftriaxone. 1 - nucleus and cytoplasm of fibrocytes, 2 - collagen fiber. x17000.

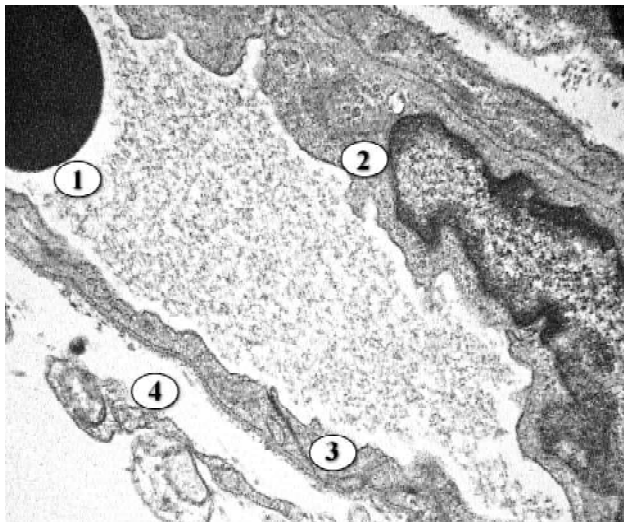


Fig. 6. The hemocapillary ultrastructure of the rat after six weeks: two weeks of opioid administration, four weeks after its abolition, and correction with pentoxifylline and ceftriaxone. 1 - a small lumen with erythrocyte, 2 - the nucleus and cytoplasm of endothelial cell, 3 - the basement membrane, 4 - perivascular space. x12000.

The detected submicroscopic structure of fibroblasts indicates their synthetic activity aimed at updating the intercellular substance of connective tissue. Between the tufts of collagen fibrils, fibrocytes with a much smaller volume of cytoplasm, few organelles, and an elongated nucleus are also found (Fig. 5).

Electron microscopic examination of the hemocapillaries of the mucous membrane of the gums of the animals of this group showed that in their wide lumens there are formed elements of blood, mainly erythrocytes. The wall of the blood capillary is formed by endothelial cells and the basement membrane. The nuclei of the endothelial cells have an ellipsoidal shape, small invaginations of the nuclear membrane, and clear nuclear membranes.

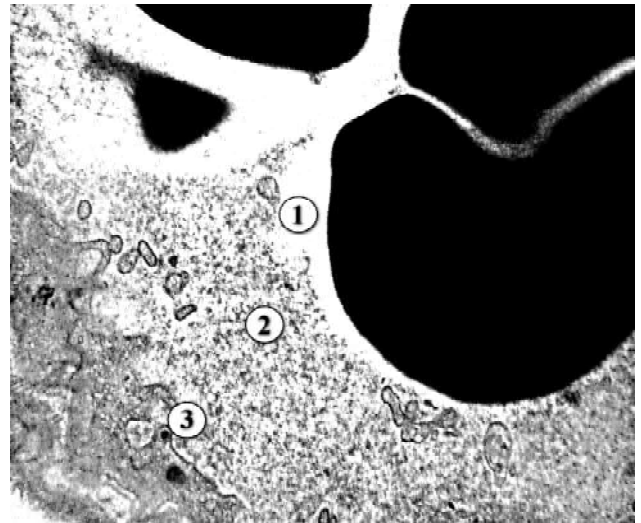


Fig. 7. The ultrastructure of the venous rat after six weeks: two weeks of opioid administration, four weeks after its abolition, and correction with pentoxifylline and ceftriaxone. 1 - a wide lumen with the formed elements of blood, 2 - cytoplasm of endothelial cell, 3 - basal membrane. x15000.

The organelles are few and they are located mainly in the paranuclear regions of the cytoplasm. The cytoplasmic areas are not wide, with foamy vesicles and caveolae. The luminal part of the endothelial cell plasmalemma forms cytoplasmic patches and microvilli. The basal membrane is narrow, in the form of a relatively uniform ribbon separating the endothelium from the loose connective tissue of its own lamina. Perivascular spaces without signs of edema (Fig. 6).

Submicroscopically during this term, the venules are unchanged. They have a wide lumen, available red blood cells, platelets, rarely neutrophils, lymphocytes. The cytoplasmic regions of the endothelial cells are not wide, their nuclear parts protruding into the lumen. There are few organelles in the cytoplasm, separate non-elastic tubules of the endoplasmic reticulum, small mitochondria, different sizes of vacuoles and vesicles. The basal membrane is thickened in some places, the perivascular spaces are small (Fig. 7).

Discussion

Given that narcotic substances cause intoxication of many systems and organs, pronounced pathomorphological changes are also observed in periodontal tissues, with further progression of inflammatory process and development of generalized periodontitis [18, 23]. The morpho-functional condition of the periodontium, in particular, the mucous membrane of the gums, as a universal nonspecific criterion for periodontitis, determines the tactics of therapeutic measures that are required for disorders of peripheral microcirculation that cause the development of tissue hypoxia and their energy deficiency [1, 15]. According to the medical literature, the drug pentoxifylline has a

pathogenetic validity not only in dysfunction of peripheral circulation, but also it is characterized by anti-inflammatory and antioxidant effects, which was confirmed during experimental and clinical studies [2, 8, 16]. In the pathogenesis of diseases of the mucous membrane of the gums under the action of narcotic drugs is also important dysbiosis and pathogenic microflora of the oral cavity on the background of caries and its complications, which necessitates the need for antibacterial therapy with determination of sensitivity to antibiotics [6, 11, 12, 18].

Thus, despite the long-term withdrawal of opioid after two weeks of its action in animals, we considered it necessary to apply in the experiment a complex corrective action to accelerate reparative processes and normalize the ultrastructural organization of periodontal tissues. At the ultrastructural level, the organization of the gum components is close to the structure of intact animals. Reactive changes in the nuclei and organelles of the cytoplasm of cells of the epithelium of the mucous membrane of the gums are noted. The submicroscopic organization of the periodontal animals of this group is also not significantly different from the norm. The ultrastructure of fibroblasts and macrophages indicates their active state. The positive effect of the complex application of drugs causes a significant normalization of the ultrastructure of the links of the hemomicrocirculatory bed. Moderately blood-filled hemocapillaries and venules are

observed. The endothelial cells, the basement membrane and the perivascular space have a specific structure. The analysis of the peculiarities of the submicroscopic organization of the structural components of the periodontium in the short-term effect of the opioid and its abolition under the correction of pentoxifylline and ceftriaxone was not possible due to the lack of such data in the domestic and foreign professional literature.

Prospects for further research are to study the ultrastructural organization of periodontal tissues under the action of opioids at a later date and the features of drug correction under such conditions.

Conclusions

1. Submicroscopically found that with the abolition of opioid analgesic and complex corrective effects of drugs after two weeks of opioid exposure, there is a positive dynamic of ultrastructural reorganization in the components of rats' periodontal constituent components.

2. The use of pentoxifylline is explained by its pathogenetic validity in disorders of microcirculation and anti-inflammatory and antioxidant effect, which in combination with the antibacterial agent ceftriaxone provide therapeutic effect on the ultrastructural and functional organization of periodontal cells under the action of opioids.

References

- [1] Babai, O. M. (2016). Condition of periodontal tissues and evaluation of clinical efficacy of essential phospholipids: results of long-term monitoring of patients with generalized periodontitis. *Bulletin of problems of biology and medicine*, 2(1), 159-163.
- [2] Brie, D., Sahebkar, A., Penson, P.E., Dinca, M., Ursoniu, S., Serban, M.C., ... Banach, M. (2016). Effects of pentoxifylline on inflammatory markers and blood pressure: a systematic review and meta-analysis of randomized controlled trials. *J. Hypertens.*, 34(12), 2318-2329. doi: 10.1097 / HJH.0000000000001086
- [3] Chou, R., Turner, J. A., Devine, E. B., Hansen, R. N., Sullivan, S. D. ... Deyo, R. A. (2015). The effectiveness and risks of long-term opioid therapy for chronic pain: a systematic review for a National Institutes of Health Pathways to Prevention Workshop. *Ann. Intern. Med.*, 162, 276-286. doi: 10.7326/ M14-2559
- [4] Cvintama, I. E., & Misula, I. R. (2014). The state of lipid peroxidation in periodontal animals in experimental periodontitis with altered body reactivity. *Bulletin of scientific research*, (4), 127-129. <https://doi.org/10.11603/2415-8798.2014.4.4654>
- [5] Demkovich, A. E. (2015). Violation of immunological reactivity of the organism in the pathogenesis of inflammatory periodontal diseases. *Clinical Dentistry*, 2, 30-37.
- [6] Fik, V. B. (2015). Influence of opioid analgesic on the content and antibiotic sensitivity of the oral microflora of rats. *Bulletin of Dentistry*, 1(90), 27-32.
- [7] Fik, V. B., Paltov, E. V., & Kryvko, Y. Y. (2018). Morphofunctional peculiarities of the periodontal tissue under conditions of simulated eight-week opioid effect. *Deutscher Wissenschaftsberod German Science Herald*, 1, 14-17. doi: 10.19221/201814
- [8] Genovés, P., Garcia, D., Cejalvo, D., Martin, A., Zaragoza, C., Toledo, A. H., ... Lloris-Carsi, J. M. (2014). Pentoxifylline in liver ischemia and reperfusion. *J. Invest. Surg.*, 27, 114-124. doi: 10.3109/08941939.2013.835454
- [9] Glauert, A. M. (1975). *Fixation, Dehydration and Embedding of Biological Specimens*. In: Practical methods in electron microscopy. North-Holland: American Elsevier.
- [10] Guy, G. P. Jr., Zhang, K., Bohm, M. K., Losby, J., Lewis, B., Young, R., ... Dowell, D. (2017). Vital signs: changes in opioid prescribing in the United States, 2006-2015. *MMWR Morb Mortal Wkly Rep.*, 66(26), 697-704. doi: 10.15585/ mmwr.mm6626a4
- [11] Jain, Y. (2013). Local Drug Delivery. *International Journal of Pharmaceutical Science Invention.*, 2(1), 33-36.
- [12] Joshi, D., Garg, T., Goyal, A. K., & Rath, G. (2016). Advanced drug delivery approaches against periodontitis. *Drug delivery*, 23(2), 363-377. <http://doi.org/10.3109/10717544.2014.935531>
- [13] Kholodniak, O. V. (2017). *Treatment, prevention and prognosis of localized inflammatory diseases of periodontal tissues* (Candidate dissertation).
- [14] Kimak, G. B., & Melnychuk G. M. (2018). Changes in indicators of lipid peroxidation and peroxidation of proteins in the oral fluid of patients with generalized periodontitis of young persons due to complex treatment. *Innovations in Dentistry*, 1, 17-21.
- [15] Matviyukiv, T. I., & Gerelyuk, V. I. (2012). Clinical condition of periodontal tissues in patients with chronic generalized periodontitis on the background of systemic antibiotic concomitant pathology. *Halych Medicinal Bulletin*, 4(19), 49-52.
- [16] McCarty, M. F., O'Keefe, J. H., & DiNicolantonio, J. J. (2016). Pentoxifylline for vascular health: a brief review of the literature. *Open Heart*, 3(1), e000365. doi: 10.1136/openhrt-2015-000365

- [17] Mira, A., Simon-Soro, A., & Curtis, M. A. (2017). Role of microbial communities in the pathogenesis of periodontal diseases and caries. *Journal of clinical periodontology*, 44(18), 23-38. doi: 10.1111/jcpe.12671
- [18] Patalakha, O. V. (2019). *Features of the immune response and optimization of treatment of generalized periodontitis in patients with toxic opioid hepatitis* (Candidate dissertation).
- [19] Schroeder, A. R., Dehghan, M., Newman, T. B., Bentley, J. P., & Park, K. T. (2019). Association of Opioid Prescriptions from Dental Clinicians for US Adolescents and Young Adults With Subsequent Opioid Use and Abuse. *JAMA Intern Med.*, 179(2), 145-152. doi: 10.1001/jamainternmed.2018.5419
- [20] Semenyuk, G. D., Melnychuk, G. M., & Makarenko, O. A. (2014). Dynamics of oral dysbiosis in patients with generalized periodontitis on the background of complex treatment. *Bulletin of Dentistry*, 4, 26-30.
- [21] Silva, N., Abusleme, L., Bravo, D., Dutzan, N., Garcia-Sesnich, J., Vernal, R., ... & Gamonal, J. (2015). Host response mechanisms in periodontal diseases. *J. Applied Oral Sci.*, 23(3), 329-355. <http://doi.org/10.1590/1678-775720140259>
- [22] Tokmakova, S. I., & Lunitsyna, Yu. V. (2014). Features of dental status of patients with opium addiction. *Far Eastern Medical Journal*, 1, 130-135.
- [23] Zubachik, V. M., & Fedun, I. R. (2017). Biochemical parameters of oral fluid in drug-addicted patients with chronic generalized periodontitis. *Clinical Dentistry*, 2, 9-14. doi: 10.11603/2311-9624.2017.2.7741

УЛЬТРАСТРУКТУРНИЙ СТАН ТКАНИН ПАРОДОНТУ ЩУРІВ ПРИ ОПІОЇДНОМУ ВПЛИВІ УПРОДОВЖ ДВОХ ТИЖНІВ ТА ПІСЛЯ ЙОГО ЧОТИРИТИЖНЕВОЇ ВІДМІНИ ЗА УМОВ КОРЕКЦІЇ
Фік В.Б., Пальтов Є.В., Кривко Ю.Я.

Враховуючи, що стоматологічний статус наркозалежних осіб обтяжений численними захворюваннями тканин і органів порожнини рота, у сучасній пародонтології залишаються актуальними питання розробки оптимальної схеми лікувальної тактики з метою відновлення їх трофіки та балансу мікрофлори ротової порожнини на фоні опіоїдного впливу. Метою роботи було дослідити ультраструктуру тканин пародонту при експериментальній двотижневій дії опіоїду та після його відміни упродовж чотирьох тижнів за умов комплексного медикаментозного коригуючого впливу. Матеріалом дослідження слугували білі щури-самці (22) репродуктивного віку (4,5 - 6 місяців), лінії Wistar, середньою вагою тіла 200 г. Тваринам проводили ін'єкції препарату налбуфін у дозі 0,212 мг/кг впродовж двох тижнів з подальшою його відміною протягом чотирьох тижнів. З метою корекції патологічних змін, що виникають при дії опіоїду в тканинах пародонту, застосовано лікарські засоби пентоксифілін та антибіотик цефтріаксон. Пентоксифілін вводили щоденно внутрішньом'язово протягом чотирьох тижнів після відміни опіоїду (3 - 6 тижнів) у дозі 2,857 мг/кг. Цефтріаксон вводили одноразово, внутрішньом'язово упродовж 11 діб наприкінці експерименту (5 - 6 тижні) в дозі, еквівалентній для щура (2,857 мг/кг). Збір тканин пародонту здійснювали в ділянці ясенного сосочка з подальшим проведенням електронно-мікроскопічного дослідження. Субмікроскопічно встановлено, що структурні компоненти пародонту мають незначні зміни, їх організація наближена до норми. Для ультраструктури всіх ділянок епітеліальної пластинки слизової оболонки ясен характерно поширене розташування клітин. В епітеліоцитах частина ядер мають інвагінації каріолеми, що свідчить про їх функціональну активність. Чіткі контури компактних ядерць і плазмолем. У цитоплазмі більшість органел практично не змінені, у мітохондріях наявні кристи, чітко визначаються тонофіламенти, десмосомальні контакти та базальна мембрана. Контури плазмолем чіткі, міжклітинні контакти збережені, окремі міжклітинні ділянки виглядають потовщеними. Пародонт представлений добре упорядкованими пучками колагенових волокон, клітинні компоненти незмінні. Виявлена субмікроскопічна будова фібробластів свідчить про їх синтетичну активність, направлену на оновлення міжклітинної речовини сполучної тканини. Електронно-мікроскопічні дослідження гемокapілярів слизової оболонки ясен тварин даної групи показали, що у нешироких їх просвітах наявні формені елементи крові, переважно еритроцити. Ядра ендотеліоцитів мали еліпсоподібну форму, невеликі інвагінації каріолеми, чіткі ядерні мембрани, органел було небагато. Периваскулярні простори без ознак набряку. Вени малозмінні, мають широкі просвіти, цитоплазматичні ділянки ендотеліоцитів неширокі, їх ядерні частини випинають у просвіт, базальна мембрана місцями потовщена. Таким чином, субмікроскопічно встановлено, що при відміні опіоїду та застосуванні медикаментозної корекції через 2 тижні опіоїдного впливу, наявні ознаки позитивної динаміки в структурних компонентах пародонту, що пояснюється патогенетичною обґрунтованістю призначення пентоксифіліну при розладах мікроциркуляції, його протизапальною і антиоксидантною дією та у поєднанні з антибактеріальним засобом цефтріаксон забезпечують лікувальну дію на ультраструктуру та функціональну організацію тканин пародонту.

Ключові слова: електронно-мікроскопічні дослідження, тканини пародонту, щури, опіоїдний анагетик, корекція.

УЛЬТРАСТРУКТУРНОЕ СОСТОЯНИЕ ТКАНЕЙ ПАРОДОНТА КРЫС ПРИ ДЕЙСТВИИ ОПИОИДА НА ПРОТЯЖЕНИИ ДВУХ НЕДЕЛЬ И ПОСЛЕ ЕГО ЧЕТЫРЕХНЕДЕЛЬНОЙ ОТМЕНЫ В УСЛОВИЯХ КОРРЕКЦИИ
Фик В.Б., Пальтов Е.В., Кривко Ю.Я.

Учитывая, что стоматологический статус наркозависимых обременен многочисленными заболеваниями тканей и органов полости рта, в современной пародонтологии остаются актуальными вопросы разработки оптимальной схемы лечебной тактики с целью восстановления их трофики и баланса микрофлоры ротовой полости на фоне опиоидного воздействия. Целью работы было исследовать ультраструктуру тканей пародонта в эксперименте при двухнедельном воздействии опиоида и после его отмены в течение четырех недель с использованием комплексной медикаментозной коррекции. Материалом исследования послужили белые крысы-самцы (22) репродуктивного возраста (4,5 - 6 месяцев), линии Wistar, средней массой тела 200 г. Проводили животным инъекции препарата налбуфин в течение двух недель, доза составляла 0,212 мг/кг, с последующей его отменой в течение четырех недель. С целью коррекции патологических изменений, возникающих при воздействии опиоида в тканях пародонта, применены лекарственные средства пентоксифиллин и антибиотик цефтриаксон. Пентоксифиллин вводили ежедневно внутримышечно в течение четырех недель после отмены опиоида (3 - 6 недель) в дозе 2,857 мг/кг. Цефтриаксон вводили однократно в течение 11 суток в конце эксперимента (5 - 6 недель) в дозе, эквивалентной для крысы (2,857 мг/кг). Забор тканей пародонта осуществляли в области десневого

сосочка с последующим проведением электронно-микроскопического исследования. Субмикроскопически установлено, что структурные компоненты пародонта имеют незначительные изменения, их организация близка к норме. Для ультраструктуры всех участков эпителиальной пластинки слизистой оболочки десны характерно послойное расположение клеток. В эпителиоцитах часть ядер имеют инвагинации кариолемы, что свидетельствует об их функциональной активности. Четкие контуры компактных ядрышек и плазмолемм. В цитоплазме большинство органелл практически не изменена, в митохондриях имеются кристы, четко определяются тонофиламенты, десмосомальные контакты и базальная мембрана. Контуры плазмолемм отчетливые, межклеточные контакты сохранены, отдельные межклеточные участки выглядят утолщенными. Периодонт представлен хорошо структурированными пучками коллагеновых волокон, клеточные компоненты изменены. Субмикроскопическое строение фибробластов свидетельствует об их синтетической активности, направленной на обновление межклеточного вещества соединительной ткани. Электронно-микроскопические исследования гемакапилляров слизистой оболочки десны животных данной группы показали, что в нешироких их просветах имеются форменные элементы крови, преимущественно эритроциты. Ядра эндотелиоцитов имеют эллипсообразную форму, небольшие инвагинации кариолемы, четкие ядерные мембраны, немного органелл. Периваскулярные пространства без признаков отека. Вены малоизмененные, имеют широкие просветы, цитоплазматические участки эндотелиоцитов неширокие, их ядерные части выпячивают в просвет, базальная мембрана местами утолщена. Таким образом, субмикроскопически установлено, что при отмене опиоидного анальгетика и применении медикаментозной коррекции через 2 недели опиоидного воздействия, имеется положительная динамика в структурных компонентах пародонта, что объясняется патогенетической обоснованностью назначения пентоксифиллина при расстройствах микроциркуляции, его противовоспалительным и антиоксидантным эффектом и в сочетании с антибактериальным средством цефтриаксон обеспечивают лечебное воздействие на ультраструктурную и функциональную организацию тканей пародонта.

Ключевые слова: электронно-микроскопические исследования, ткани пародонта, крысы, опиоидный анальгетик, коррекция.



Reactive and destructive changes of Peyer's patches in rats with experimental burn disease under infusion of detoxification solutions

Cherkasov V.G., Matkivska R.M., Cherkasov E.V., Kaminskyi R.F., Yaremenko L.M.

O.O. Bogomolets National Medical University, Kyiv, Ukraine

ARTICLE INFO

Received: 25 February, 2019

Accepted: 21 March, 2019

UDC: 611.428:57.012.4:611.344:
616.5-001.17:57.085

CORRESPONDING AUTHOR

e-mail: rujena011279@gmail.com
Matkivska R.M.

The pathogenesis of burn immune dysfunction and burn enteropathy needs further clarification given that the cellular lesions of lymphoid tissue associated with mucous membranes are the least studied. The purpose of the study was to establish reactive and destructive changes in Peyer's patches of rats after burn injury of the skin with the use of intravenous infusion of isotonic sodium chloride solution and combined colloid-hyperosmolar solutions. White male rats weighing 160-200 g at 6 months of age were divided into 4 groups (18 animals in each group): I, II, III - rats with burn skin injury (grade II-III burn with an area of 23% of body surface area and the development of moderate-severity shock state) which was administered a separate intravenous infusion once a day for the first 7 days of the experiment with isotonic sodium chloride, lactoprotein with sorbitol and HAES-LX-5%, in each case at a dose of 10 ml/kg; IV - intact animals. The material was collected from rats under deep thiopental intraperitoneal anesthesia after 1, 3, 7, 14, 21 and 30 days after burn injury. Biopsies from Peyer's patches for histological and electron microscopic examination were processed using conventional methods. Investigation of histological preparations stained with hematoxylin-eosin was performed on an Olympus BX51 microscope. Ultrathin sections were contrasted on copper support meshes with uranyl acetate and lead citrate according to Reynolds and studied using a PEM-125K electron microscope. Electron and light microscopy data indicate that intravenous infusion of colloidal-hyperosmolar solutions (lactoprotein with sorbitol and HAES-LX-5%) promotes suppression of inflammatory response, inhibits necrosis, and optimizes lymphoid apoptosis at Peyer's patches of rats with experimental burn disease caused by burn injury to the skin of 21-23% of the body surface. Apoptotic lymphocytes and their apoptotic bodies are effectively phagocytosed by macrophages and are digestible in heterophagolysosomes. The apoptotic altered dendritic cells in Peyer's patches are characterized by osmiophilic cytoplasm and a nucleus with high electron density amorphous nucleoplasm. In the cytoplasm are located mitochondria with enlightened matrix and destroyed cristae, irregularly expanded tubules of variable configuration of a granular endoplasmic reticulum with electronically transparent content and numerous derivatives of their vacuole transformation, which are sharply darkened. The fusion of vacuoles leads to the formation of large electron-luminous cavities filled with various residues of compacted degraded cellular structures. Vacuolization promotes site segmentation of condensed cytoplasm of apoptotic dendritic cells and formation of apoptotic blebs, which are subject to entrapment and subsequent sequential degradation with the participation of neighboring macrophages. The structural changes of the organelles of the protein-synthesizing apparatus found in Peyer's plaque cells in rats with experimental burn disease can be regarded as a manifestation caused by functional overload of the granular endoplasmic reticulum (ER-stress). The consequence of optimal development of ER-stress and subsequent unfolded protein response is the apoptotic degradation of the corresponding cell, the course of which is modified by the use of colloid-hyperosmolar solutions.

Keywords: Peyer's patches, structural changes, burn disease, detoxification solutions.

Introduction

It is generally accepted [16] that severe thermal skin burns cause the development of burn disease, the main factor of which is endogenous intoxication. That is why infusion of detoxification solutions is considered to be a mandatory component of the treatment of burn disease, which makes it possible to correct its course or, even, to prevent the development of some of its stages and complications [5, 24].

Considering the stage of burn disease and the different orientation of the individual parts of its pathogenesis, infusion therapy raises not only the question of restoration of water-electrolyte balance and detoxification of the organism, but also a number of tasks for the protection of intact and repair of damaged cells, normalization and stabilization of vital (including immune) functions of the body. It stimulates the development of new infusion drugs and studies the differences of their effect on different organs, tissues and cells [4, 6, 7, 9, 11, 12, 17, 20, 21].

The benefits of widespread introduction of colloidal solutions have, until recently, seemed convincing and valid [4, 10, 18, 23]. However, in recent times the discussion regarding the feasibility and benefits of using colloidal and crystalloid drugs in infusion therapy has become more acute [13, 14, 22, 29].

One of the components of burn disease is immune system dysfunction [16] and burn enteropathy [7, 9]. However, the pathogenesis of burn immune dysfunction and burn enteropathy needs further clarification given that the cellular damage of the lymphoid tissue associated with the mucous membranes (quantitatively the largest part of the immune system) is the least studied. In turn, it does not allow adequately developing and effectively improving the means of correcting the immune status of burns and the treatment of burn enteropathy. This actualizes the study of the structural changes of Peyer's patches in burn disease, which by modern definition [15] are immune sensors of the small intestine, which provide the induction of immune tolerance to commensal bacteria and dietary antigens, as well as provide protection against pathogenic intestinal content [3, 8, 19].

The aim of this study is to establish reactive and destructive changes in Peyer's patches (clusters of lymph nodes of the ileum) of rats at the stages of development of burn disease caused by experimental thermal burn injury of the skin under the conditions of intravenous infusion of isotonic tonic solution and combined colloid-hyperosmolar solutions (lactoprotein with sorbitol and HAES-LX-5%).

Materials and methods

Reactive and destructive changes in Peyer's patches in rats with experimental burn disease under infusion of detoxification solutions (isotonic sodium chloride solution and colloid-hyperosmolar solutions) were studied in 72 white male rats weighing 200-200 g in age 6 month.

Animal retention, as well as experimentation with

thermal burn injury of the skin, infusion of detoxification solutions and other related manipulations were carried out in full compliance with the requirements of the "General Ethical Principles of Animal Experiments", approved by the First National Congress on Bioethics (Kyiv, 2001), in compliance with all the recommendations of the "European Convention for the Protection of Vertebrate Animals Used for Experimental and Other Scientific Purposes", and the provisions of the Methodological Recommendations for the "Preclinical study of medicines".

The experimental animals, the material of which was subjected to histological and electron microscopic examination, were divided into 4 groups (18 animals in each group): I, II, III - rats with burn injury to the skin, which were subjected to a separate infusion of isotonic sodium chloride solution, lactoprotein with sorbitol and HAES-LX-5%, in each case at a dose of 10 ml/kg; IV - intact animals (control group).

Simulation of burn disease was performed by applying to the side surfaces of the trunk of animals four copper plates (two plates on each side, the surface area of each plate was 13.86 cm²), which was previously kept for 6 minutes in water at a constant temperature of 100°C. The severity of injury in burn injury was assessed by the severity index of the injury, which takes into account the parameters of the area and depth of burns. The results of the calculation showed that the total area of skin burn in rats was 21-23% of the body surface, the exposure was 10 s, which is sufficient for the formation of burns II-III degree and the development of a shock state of moderate severity.

Intravenous infusion of detoxification solutions at a dose of 10 ml/kg was performed for 5 minutes in a caudal vena cava after its catheterization in aseptic conditions through the femoral vein. The first infusion was performed 1 hour after burn, subsequent injections were performed once a day for the first 7 days of the experiment.

Material extraction from rats was performed under conditions of deep thiopental intraperitoneal anesthesia after 1, 3, 7, 14, 21 and 30 days after the experimental burn injury of the skin.

The material for histological and electron microscopic examination (biopsies from Peyer's patches) was processed using conventional methods. Investigation of histological preparations stained with hematoxylin-eosin was performed on an Olympus BX51 microscope. Ultrathin sections were contrasted on copper support meshes with uranyl acetate and lead citrate according to Reynolds and studied using a PEM-125K electron microscope.

Results

In rats with burn disease that underwent intravenous infusion of isotonic sodium chloride in Peyer's patches cells, destructive changes outweigh the reactive ones. A common manifestation of destructive changes is necrosis and apoptosis of functionally different cells, which occur

on the background of expressive changes in blood vessels of the hemo- and lymphomicrocirculatory bed. Crucial in this process is the change in cell death types of lymphocytes and dendritic cells - the main immunocompetent cells of Peyer's patches. It should be noted that under normal conditions, only single dendritic cells and individual lymphocytes are asynchronously killed by apoptosis; it is characterized by all classical structural manifestations and is terminated by a macrophage reaction that provides phagocytosis of apoptotic bodies and cells.

Under conditions of burn disease, apoptosis and the necrotic changes of lymphocyte and dendritic cell groups occur, to which necrosis of initially apoptotic altered dendritic cells and lymphocytes is involved. Under these conditions, the macrophages of Peyer's patches shift to a state of phagocytic over-voltage, which often ends in their necrotic death.

In phagocytic macrophages, the concentration of dilated and electron-dense contents of tubules of granular endoplasmic reticulum is associated with an increase in the number of lysosomes in the cytoplasm. Lysosomes coalesce with phagosomes and ultimately form different sizes of heterophagolysosomes with varying degrees of structure. The cytoplasm of these macrophages looks swollen, sometimes vacuolated; some mitochondria contain an enlightened matrix, partially destroyed cristae, and a locally defective inner mitochondrial membrane (Fig. 1). The expression of the combination of necrotic and apoptotic changes in lymphocytes and dendritic cells of Peyer's patches is the presence in the focal necrotic cell detritus of apoptotic cells and apoptotic bodies (Fig. 2).

In Peyer's patches of rats with burn disease under conditions of infusion of isotonic sodium chloride solution in dendritic cells, vacuolation of the cytoplasm was observed, which was combined with an increase in cyto- and nucleoplasmic osmiophilia. Such dendritic cells are characterized by destruction of the mitochondria (most often in the form of destruction of the inner membrane and cristae, the remains of which are well contoured against the background of the enlightened mitochondrial matrix). Fragmentation of the tubules of the granular endoplasmic reticulum occurs, which leads to disruption of the ordering of the tubules and their transformation into a vacuole-like formation. The formation of different vacuoles in the cytoplasm of dendritic cells indicates the depletion of the reparative capacity of the cell and the beginning of its death.

Vacuoles originating from tubules of the granular endoplasmic reticulum have an irregular (sometimes wavy) shape, often turning into cavities with uneven edges, but single ribosomes are attached to their surrounding membranes. Transformation of the tubules of the granular endoplasmic reticulum in the vacuole is a transitional stage to the ultimate disintegration of these organelles and is identified, most often, in hyperchromic shrunken dendritic cells. A large number of light vacuoles (Fig. 3, 4) compressing the cytoplasm to the level of transitions

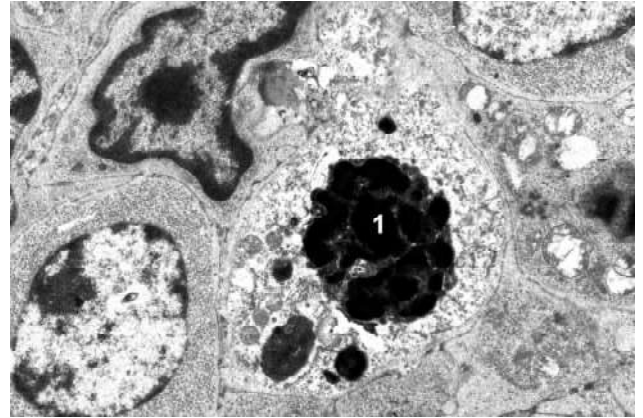


Fig. 1. Macrophage phagocytosed (and partially digested in phagolysosomes) apoptotic body and its fragments in a Peyer's patch 14 days after experimental burn injury under conditions of Isotonic Sodium Chloride infusion. 1 - large phagolysosome. Electronic micrograph. x20000.

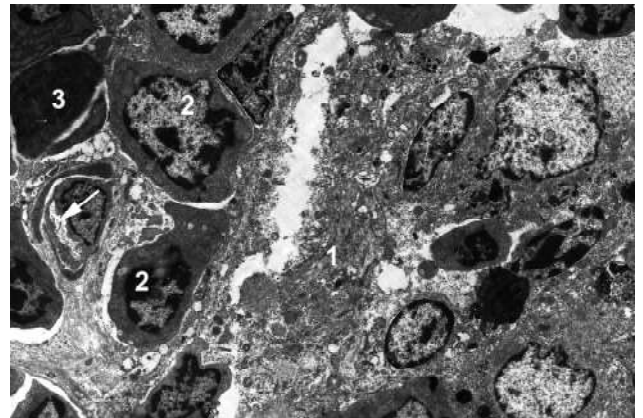


Fig. 2. Focal ultrastructural changes of cells in the Peyer's patches of the rat with experimental burn injury under the conditions of infusion of Isotonic Sodium Chloride Solution. The combination of apoptotic and necrotic signs of cell death. The arrow indicates the lumen of the blood capillary. 1 - dendritic cell necrosis; 2 - nucleus of apoptotic lymphocyte; 3 - erythrocyte. Electronic micrograph. x4000.

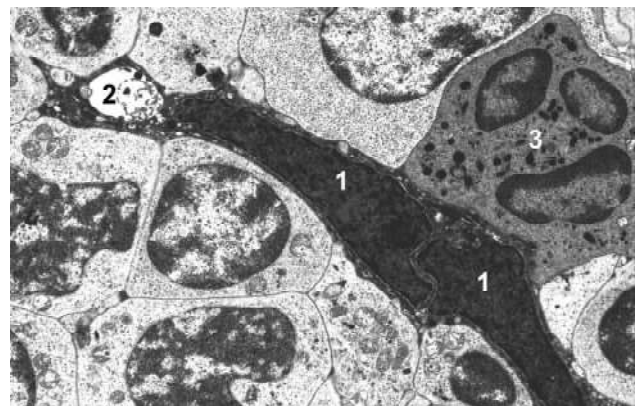


Fig. 3. Blebbing in the cytoplasm of apoptotic dendritic cells of Peyer's patches of rat 21 days after the experimental burn injury under the conditions of infusion of Isotonic Sodium Chloride Solution. 1 - nucleus of apoptotic dendritic cell; 2 - a bubble (surrounded by small vesicles and vacuoles) in the cytoplasm of an apoptotic dendritic cell; 3 - neutrophil leukocyte cytoplasm; 4 - lymphocytes. Electronic micrograph. x7000.

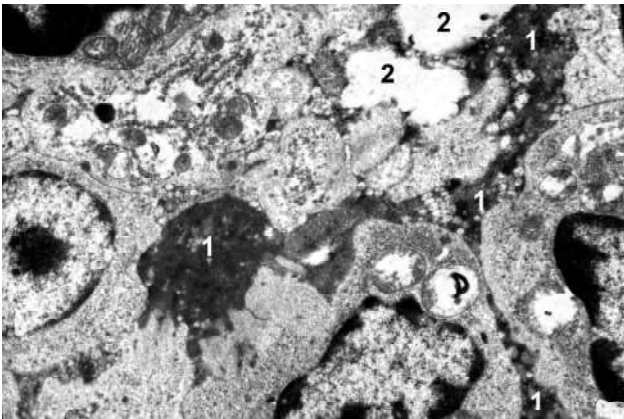


Fig. 4. Intense blebbing in the cytoplasm of the apoptotic dendritic cell of a Peyer's patches of rat 30 days after the experimental burn injury under the conditions of infusion of Isotonic Sodium Chloride Solution. Dystrophic cytopathological changes of cells, swelling and destruction of cristae mitochondria. 1 - shrunken cytoplasm of apoptotic dendritic cell; 2 - a bubble (surrounded by small vesicles and vacuoles) in the cytoplasm of an apoptotic dendritic cell; ← damaged mitochondria. Electronic micrograph. x10000.

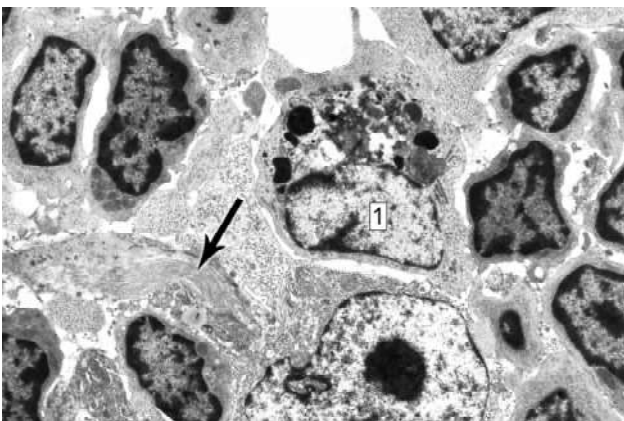


Fig. 5. Phagocytosis by macrophage of apoptotic bodies in a Peyer's patches of the rat 3 days after the experimental burn injury under infusion of Lactoprotein with Sorbitol. 1 - macrophage nucleus. Electronic micrograph. x15000.

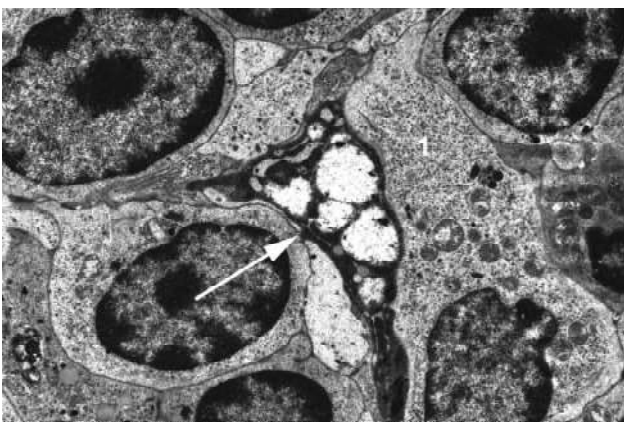


Fig. 6. Blebbing in the process of supercondensed dendritic cell in a Peyer's patches of the rat 14 days after the experimental burn injury under infusion of HAES-LX-5%. 1 - cytoplasm of a "dark" dendritic cell of normal structure; ← blebbing. Electronic micrograph. x15000.

between transparent vacuoles, creates a common enlightened honeycomb background, contrasting with a homogeneous dark osmiophilic nucleus framed by a narrow electron-light band around the nucleus. The described destructive changes are a classic morphological manifestation of apoptotic "bubble formation" or "blebbing". Subsequently, the long, narrow, branched branches of apoptotic dendritic cells are fragmented into apoptotic blebs, and the separated nucleated dendritic cell section is transformed into a larger apoptotic body.

Our findings indicate that intravenous infusion of colloidal-hyperosmolar solutions (lactoprotein with sorbitol and HAES-LX-5%) promotes suppression of inflammatory response, inhibits necrosis, and optimizes apoptosis of lymphocytes and dendritic cells in Peyer's patches of rats with experimental burn disease. Apoptotic lymphocytes and their apoptotic little bodies (Fig. 5) are effectively phagocytosed by macrophages and are digestible in heterophagolysosomes.

Dendritic cells with osmiophilic cytoplasm in Peyer's patches are characterized by a nucleus with high electron density amorphous nucleoplasm. In the cytoplasm are located mitochondria with enlightened matrix and destroyed cristae, irregularly expanded tubules of variable configuration of a granular endoplasmic reticulum with electronically transparent content and numerous derivatives of their vacuole transformation, which are sharply darkened. The fusion of vacuoles leads to the formation of large electron-luminous cavities filled with various residues of compacted degraded cellular structures (Fig. 6). Vacuolization promotes segmental segmentation of condensed cytoplasm of apoptotic dendritic cells, fragments of which are subject to entrapment and subsequent sequential degradation with the participation of neighboring macrophages.

Discussion

We have established significant reactive and destructive transformations of Peyer's patches lymphocytes and dendritic cells in rats with experimental burn disease under the conditions of intravenous infusion of various detoxification solutions.

According to modern concepts [15], dendritic cells are the major antigen-presenting cells in the immune system (and, in particular, in Peyer's patches). The presentation of antigens to lymphocytes is a finely coordinated and multicomponent process that includes: 1 - capture of native (unchanged) antigenic material by phagocytosis, pinocytosis or receptor-mediated endocytosis; 2 - partial proteolysis (processing) of antigenic material in endosomes (or lysosomes) with the release of epitopes of antigens (antigenic determinants); 3 - under these conditions, the synthesis of Major Histocompatibility Complex (MHC) molecules and the binding of the synthesized MHC molecules to the antigen epitopes; 4 - transport of complexes of MHC molecule antigen epitope

to the surface of the dendritic cell, where they are represented by their recognizing lymphocytes. 5 - secretion of soluble mediators (preferably IL-1) that cause lymphocyte activation. To determine the critical threshold of reactive and destructive changes of dendritic cells and lymphocytes of Peyer's patches revealed by us in the conditions of burn disease is difficult, but the ordering of the course of this complex process of presentation of antigenic material from the lumen of the small intestine is, at least, impaired and impaired hyperosmolar solutions.

We found structural changes of organelles of protein-synthesizing apparatus in cells of Peyer's patches in rats with experimental burn disease, which coincides with the scientific literature [16] about the characteristic of burn disease syndrome of hypermetabolism and its component - hypercatabolism. Our study found that the most sensitive organelle of Peyer's patches cells is a granular endoplasmic reticulum, structural changes of which can be regarded as a manifestation caused by functional overload of the granular endoplasmic reticulum (ER-stress) [25, 26, 30], which results in a response to unfolded protein response. Under the norm [25], protein folding occurs in the tubules of the granular endoplasmic reticulum, in which the synthesized proteins undergo post-translational modification, acquiring a characteristic three-dimensional configuration. Unfolded protein response occurs due to the accumulation in the lumen of the tubules of the granular endoplasmic reticulum of uncoiled or misfolded proteins [27, 28].

The sequence of structural and molecular manifestations of unfolded protein response [2] indicates: an adaptive attempt to restore normal cell function by arresting protein translation and subsequent degradation of misfolded proteins, as well as activation of signaling pathways leading to increased production of molecular chaperones, proteins. Thus, unfolded protein response, under normal conditions, is a stress pathway to homeostatic regulation [27]. If the constant overvoltage of unfolded protein response is not eliminated within a certain period of time, apoptotic degradation of the corresponding cell occurs, leading to the development of various pathological conditions [26, 28, 30].

Manifestations of the typical crystalline solution, which is an isotonic solution of sodium chloride, lactoprotein with sorbitol (protein-saline colloidal-hyperosmolar solution) and HAES-LX-5% (infusion colloid-hyperosmolar plasma replacement of the new generation, created on the basis of third generation hydroxyethyl starch HES 130/0.4) have been the subject of our previous research [20, 21], as well as of other scientists [6, 9, 11, 12, 17], and have proved their differences in influencing the course of experimental burn disease. The study of reactive and destructive changes in Peyer's patches of rats with experimental burn disease, as well as the impact of ER-stress on the dynamics of necrotic and apoptotic cell changes, was updated by a new wave of controversy regarding the official assessment of possible limitations on the use of colloidal solutions based

on hydroxyethyl starch. The divergent opinions of pharmacology scientists and experts found their symbolic reflection in a name published [1] in the 2019 scientific review "Starch Wars - New Episodes of the Saga. Changes in Regulation on Hydroxyethyl Starch in the European Union". At the same time, it should be noted that, for the first time in the 1960s, various infusion solutions based on synthetic hydroxyethyl starch became widely known in intensive care units and veterinary medicine worldwide (for example, over 60 drugs were registered in 2010 in Europe and 4 in the United States). The flow of "crystalloid-colloidal debate" and "starch wars" in the scientific literature does not stop until this time, it has a wavy chain character (when one article causes the appearance of several articles with opposite conclusions, which, in turn, stimulates the publications of the authors-opponents).

Conclusions

The question about the benefits and feasibility of "use - not use" infusion solutions based on hydroxyethyl starch of different generation is still open, but there is no doubt reliable experimental evidence that demonstrates the ability of colloidal infusion vessels improve intravascular osmotic pressure improve hemomicrocirculation, limit swelling of tissues of primary intact organs in burn disease [5, 14]. We agree with the opinion of many researchers that the answer to this question should be further experimental and clinical studies of the action of specific crystalloid and colloidal infusion solutions, judiciously applied on the principle of "What? Where? When? What dose?" The results of our study indicate that timely administration of colloid-hyperosmolar solutions such as lactoprotein with sorbitol and HAES-LX-5%, in a timely manner, positive effects on the manifestations of reactive and destructive changes in Peyer's patches in burn disease caused by severe skin burns.

Conclusions

1. Intravenous infusion of colloidal-hyperosmolar solutions (lactoprotein with sorbitol and HAES-LX-5%) promotes suppression of inflammatory response, inhibits necrosis, and optimizes apoptosis of lymphocytes and dendritic cells in Peyer's patches of rats with experimental burn disease. Apoptotic lymphocytes and their apoptotic bodies are effectively phagocytosed by macrophages and are digestible in heterophagolysosomes.

2. Osmophilic cytoplasm and a nucleus with high electron density amorphous nucleoplasm are characteristic of apoptotic altered dendritic cells in Peyer's patches. In the cytoplasm are located mitochondria with enlightened matrix and destroyed cristae, irregularly expanded tubules of variable configuration of a granular endoplasmic reticulum with electronically transparent content and numerous derivatives of their vacuole transformation, which are sharply darkened. The fusion of vacuoles leads to the formation of large electron-luminous

cavities filled with various residues of compacted degraded cellular structures. Vacuolization promotes segmental segmentation of condensed cytoplasm of apoptotic dendritic cells, and the formation of apoptotic blebs, which are subject to entrapment and subsequent sequential degradation with the participation of neighboring macrophages.

3. Structural changes of organelles of protein-

synthesizing apparatus found in Peyer's patches cells in rats with experimental burn disease can be regarded as a manifestation of functional overload of the granular endoplasmic reticulum (ER-stress). The consequence of optimal development of ER-stress and subsequent unfolded protein response is the apoptotic degradation of the corresponding cell, the course of which is modified by the use of colloid-hyperosmolar solutions.

References

- [1] Adamik, K. N., & Yozova, I. D. (2018). Starch Wars-new episodes of the saga Changes in regulations on hydroxyethyl starch in the European Union. *Frontiers in veterinary science*, 5, 336. <https://doi.org/10.3389/fvets.2018.00336>
- [2] Adams, C. J., Kopp, M. C., Larburu, N., Nowak, P. R., & Ali, M. M. (2019). Structure and molecular mechanism of ER stress signaling by the unfolded protein response signal activator IRE1. *Frontiers in Molecular Biosciences*, 6, 11. doi: 10.1111/fmmb.2019.00011
- [3] Ahluwalia, B., Magnusson, M. K., & Öhman, L. (2017). Mucosal immune system of the gastrointestinal tract: maintaining balance between the good and the bad. *Scandinavian Journal of Gastroenterology*, 52(11), 1185-1193. <https://doi.org/10.1080/00365521.2017.1349173>
- [4] Bunn, F., & Trivedi, D. (2012). Colloid solutions for fluid resuscitation. *Cochrane database of systematic reviews*, 6, 30-34. doi: 10.3389/14651858.CD001319.pub5
- [5] Cartotto, R., & Greenhalgh, D. (2016). Colloids in acute burn resuscitation. *Critical care clinics*, 32(4), 507-523. doi: 10.1016/j.ccc.2016.06.002
- [6] Cherkasov, E. V., Gunas, I. V., Cheresnyuk, I. L., & Lysenko, D. A. (2012). Features of thymus cells cycle in rats after burn lesion of a skin. *Ukrainian morphological almanac*, 2(3), 109-113. URL: <https://dspace.vnu.edu.ua/123456789/580>
- [7] Cherkasov, V. H., & Tymoshenko, I. O. (2019). Structural changes of duodenal mucosa enterocytes of rats in burn skin injury under experimental streptozotocin-induced diabetes mellitus. *Reports of Morphology*, 25(1), 55-56. [https://doi.org/https://doi.org/10.31393/morphology-journal-2019-25\(1\)-08](https://doi.org/https://doi.org/10.31393/morphology-journal-2019-25(1)-08)
- [8] Dicks, L. M. T., Geldenhuys, J., Mikkelsen, L. S., Brandsborg, E., & Marcotte, H. (2018). Our gut microbiota: a long walk to homeostasis. *Beneficial microbes*, 9(1), 3-20. <https://doi.org/10.3920/BM2017.0066>
- [9] Gavryluk, A. O., Galunko, G. M., Cheresnyuk, I. I., Tikholaz, V. O., Cherkasov, E. V., Dzevulska, I. V., & Kovalchuk, O. I. (2018). Indicators cell cycle and DNA fragmentation in cells of small intestine mucosa 14, 21 and 30 days after skin burns on the background of preliminary infusion of solution lactoprotein with sorbitol or HAES-LX5%. *World of Medicine and Biology*, 63(1), 104-108. doi: 10.26724/2079-8334-2017-4-62-104-108
- [10] Groeneveld, A. J., Navickis, R. J., & Wilkes, M. M. (2011). Update on the comparative safety of colloids: a systematic review of clinical studies. *Annals of surgery*, 253(3), 470-483. doi: 10.1097/SLA.0b013e318202ff00
- [11] Gunas, I. V., Dzevulska, I. V., Kovalchuk, O. I., Cherkasov, E. V., Majewski, A. Ye., Shevchuk, Yu. G. ... Kyselova, T. M. (2018). Influence of lactoprotein solution with sorbitol on DNA content of cells of endocrine glands on the background of skin burn in rats. *World of Medicine and Biology*, 64(2), 33-39. doi: 10.26724/2079-8334-2018-2-64-33-39
- [12] Gunas, I. V., Ocheretna, N. P., Lysenko, D. A., Kovalchuk, O. I., & Cherkasov, E. V. (2018). Indicators cell cycle and dna fragmentation of spleen cells in early terms after thermal burns of skin at the background of introduction 0.9% NaCl solution. *World of Medicine and Biology*, 63(1), 116-120. doi: 10.26.724/2079-8334-2018-1-63-116-120
- [13] Hartog, C. S., Kohl, M., & Reinhard, K. (2011). A systematic review of third-generation hydroxyethyl starch (HES 130/0.4) in resuscitation: safety not adequately addressed. *Anesthesia & Analgesia*, 112(3), 635-645. doi: 10.1213/ANE.0b013e31820ad607
- [14] He, H., Liu, D., & Ince, C. (2017). Colloids and the Microcirculation. *Anesthesia & Analgesia*, 126(5), 1747-1754. doi: 10.1213/ANE.0000000000002620
- [15] Jung, C., Hugot, J. P., & Barreau, F. (2010). Peyer's patches: the immune sensors of the intestine. *International Journal of Inflammation*, 2010, 1-12. doi: 10.4061/2010/823710
- [16] Keck, M., Herndon, D. H., Kamolz, L. P., Frey, M., & Jeschke, M. G. (2009). Pathophysiology of burns. *Wiener Medizinische Wochenschrift*, 159(13-14), 327-336. doi: 10.1136/bmj.328.7453.1427
- [17] Kovalchuk, O., Cherkasov, E., Dzevulska, I., Kaminsky, R., Korsak, A., & Sokurenko, L. (2017). Dynamics of morphological changes of rats'adenohypophysis in burn disease. *Georgian medical news*, (270), 104-108. PMID: 28972493
- [18] Kruer, R. M., & Ensor, C. R. (2012). Colloids in the intensive care unit. *American Journal of Health-System Pharmacy*, 69(19), 1635-1642. <https://www.ncbi.nlm.nih.gov/pubmed/22997116>
- [19] Million, M., Tomas, J., Wagner, C., Lelouard, H., Raoult, D., & Gorvel, J. P. (2018). New insights in gut microbiota and mucosal immunity of the small intestine. *Human Microbiome Journal*, 7, 23-32. <https://doi.org/10.1016/j.humic.2018.01.004>
- [20] Matkivska, R. M. (2017). Structural changes of rats' aggregated lymphoid nodules of ileum in an experimental skin burn injury under the conditions of infusion by gekoton. *Biomedical and Biosocial Anthropology*, 29, 20-26.
- [21] Matkivska, R. M. (2017). Structural changes of rats' aggregated lymphoid nodules of ileum in an experimental skin burn injury under the conditions of infusion by 0.9% NaCl solution. *Reports of morphology*, 23(2), 231-240.
- [22] Mohanan, M., Rajan, S., Kesavan, R., Mohamed, Z. U., Ramaiyar, S. K., & Kumar, L. (2019). Evaluation of renal function with administration of 6% hydroxyethyl starch and 4% gelatin in major abdominal surgeries: A pilot study. *Anesthesia, essays and researches*, 13(2), 219. doi: 10.4103/aer.AER_25_
- [23] Mutter, T. C., Ruth, C. A., & Dart, A. B. (2013). Hydroxyethyl starch (HES) versus other fluid therapies: effects on kidney function. *Cochrane Database of Systematic Reviews*, 7, PMID:23881659. doi: 10.1002/14651858.CD007594.pub3
- [24] Serghiou, M. A., Niszcak, J., Parry, I., Li-Tsang, C. W. P., Van den Kerckhove, E., Smailes, S., & Edgar, D. (2016). One world one burn rehabilitation standard. *Burns*, 42(5), 1047-1058. doi: 10.1016/j.burns.2016.04.002
- [25] Schwarz, D. S., & Blower M. D. (2016). The endoplasmic

- reticulum: structure, function and response to cellular signaling. *Cell Mol. Life Sci.*, 73(1), 79-94. doi: 10.1007/s00018-015-2052-6
- [26] Taniguchi, M., & Yoshida, H. (2015). Endoplasmic reticulum stress in kidney function and disease. *Current opinion in nephrology and hypertension*, 24(4), 345-350. doi: 10.1097/MNH.000000000000141
- [27] Walter, P., & Ron, D. (2011). The unfolded protein response: from stress pathway to homeostatic regulation. *Science*, 334(6059), 1081-1086. doi: 10.1126/science.1209038
- [28] Wang, M., & Kaufman, R. J. (2016). Protein misfolding in the endoplasmic reticulum as a conduit to human disease. *Nature*, 529(7586), 326-335. doi: 10.1038/nature17041
- [29] Wong, C., & Koenig, A. (2017). The Colloid Controversy: Are Colloids Bad and What Are the Options? *Veterinary Clinics: Small Animal Practice*, 47(2), 411-421. doi: 10.2016/j.cvsm.2016.09.008
- [30] Yan, M., Shu, S., Guo, C., Tang, C., & Dong, Z. (2018). Endoplasmic reticulum stress in ischemic and nephrotoxic acute kidney injury. *Annals of medicine*, 50(5), 381-390. doi: 10.1080/07853890.2018.1489142

РЕАКТИВНІ ТА ДЕСТРУКТИВНІ ЗМІНИ БЛЯШОК ПЕЙЄРА У ЩУРІВ З ЕКСПЕРИМЕНТАЛЬНОЮ ОПІКОВОЮ ХВОРОБОЮ ЗА УМОВ ІНФУЗІЇ ДЕЗІНТОКСИКАЦІЙНИХ РОЗЧИНІВ

Черкасов В.Г., Матківська Р.М., Черкасов Е.В., Камінський Р.Ф., Яременко Л.М.

Патогенез опікової імунної дисфункції та опікової ентеропатії потребує подальшого уточнення з огляду на те, що клітинні пошкодження лімфоїдної тканини, асоційованої зі слизовими оболонками, є найменш вивченими. Мета дослідження - встановити можливі реактивні та деструктивні зміни в бляшках Пейєра щурів після опікової травми шкіри за умов застосування внутрішньовенної інфузії ізотонічного розчину хлориду натрію та комбінованих колоїдно-гіперосмолярних розчинів. Білі щурі-самці масою 160-200 г віком 6 місяців були розділені на 4 групи (по 18 тварин у кожній групі): I, II, III - щури з опіковою травмою шкіри (опік II-III ступеня площею 23% поверхні тіла та розв'язком шокowego стану середнього ступеня важкості), котрим проводили окрему внутрішньовенну інфузію 1 раз на добу протягом перших 7 діб експерименту ізотонічного розчину натрію хлориду, лактопротеїну із сорбітолом та HAES-LX-5%, у кожному випадку у дозі 10 мл/кг; IV - інтактні тварини. Забір матеріалу від щурів проводили за умов глибокого тіопенталового внутрішньоочеревинного наркозу через 1, 3, 7, 14, 21 та через 30 діб після нанесення опікової травми шкіри. Біоптати із бляшок Пейєра для гістологічного та електронно-мікроскопічного дослідження обробляли за допомогою загальноприйнятих методів. Дослідження гістологічних препаратів, забарвлених гематоксилином та еозином, виконували на мікроскопі Оlymrus VX51. Ультратонкі зрізи контрастували на мідних опорних сіточках ураніацетатом і цитратом свинцю за Рейнольдсом та вивчали на електронному мікроскопі ПЕМ-125К. Одержані методами електронної та світлової мікроскопії дані свідчили, що внутрішньовенна інфузія колоїдно-гіперосмолярних розчинів (лактопротеїну із сорбітолом та HAES-LX-5%) сприяє пригніченню запальної реакції, гальмує некроз та оптимізує апоптоз лімфоцитів та дендритних клітин в бляшках Пейєра щурів з експериментальною опіковою хворобою, викликану опіковою травмою шкіри площею 21-23% поверхні тіла. Апоптозні лімфоцити та їхні апоптозні тільки ефективно фагоцитуються макрофагами та підлягають перетравленню в гетерофаголізосомах. Для апоптозно змінених дендритних клітин в бляшках Пейєра характерною є осміофільна цитоплазма і ядро з аморфною нуклеоплазмою високої електронної щільності. В цитоплазмі локалізовані мітохондрії з просвітленим матриксом і зруйнованими кристами, нерівномірно розширені каналці варіабельної за конфігурацією гранулярної ендоплазматичної сітки з електронно прозорим вмістом та численні похідні їхньої вакуольної трансформації, які різко виділяються у виляді світлих плям на темному фоні цитоплазми. Злиття вакуолей призводить до формування великих електронно світлих порожнин, заповненими різноманітними залишками ущільнених деградованих клітинних структур. Вакуолізація сприяє ділянковій сегментації конденсованої цитоплазми апоптозних дендритних клітин і утворенню апоптозних блебів (apoptotic blebs), які підлягають захопленню і наступній послідовній деградації за участі сусідніх макрофагів. Виявлені структурні зміни органел білок-синтезуючого апарату в клітинах бляшок Пейєра у щурів з експериментальною опіковою хворобою, можуть бути розцінені як прояв, викликаний функціональним перенавантаженням гранулярної ендоплазматичної сітки, стресу ендоплазматичного ретикулу (ER-стресу). Наслідком оптимального розвитку ER-стресу і подальшої відповіді на незгорнуті білки (unfolded protein response) є апоптозна деградація відповідної клітини, перебіг котрої модифікується за умов використання застосованих колоїдно-гіперосмолярних розчинів.

Ключові слова: бляшки Пейєра, структурні зміни, опікова хвороба, дезінтоксикаційні розчини.

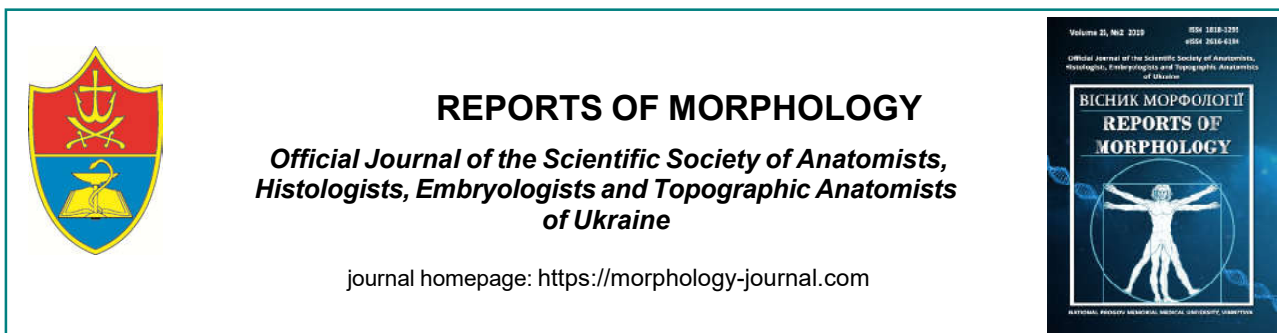
РЕАКТИВНЫЕ И ДЕСТРУКТИВНЫЕ ИЗМЕНЕНИЯ БЛЯШЕК ПЕЙЕРА У КРЫС С ЭКСПЕРИМЕНТАЛЬНОЙ ОЖГОВОЙ БОЛЕЗНЬЮ В УСЛОВИЯХ ИНФУЗИИ ДЕЗИНТОКСИКАЦИОННЫХ РАСТВОРОВ

Черкасов В.Г., Маткиевская Р.М., Черкасов Э.В., Каминский Р.Ф., Яременко Л.М.

Патогенез ожоговой иммунной дисфункции и ожоговой энтеропатии требует дальнейшего уточнения с учетом того, что клеточные повреждения лимфоидной ткани, ассоциированной со слизистыми оболочками, наименее изучены. Цель исследования - установить возможные реактивные и деструктивные изменения в Пейеровых бляшках крыс после ожоговой травмы кожи в условиях применения внутривенной инфузии изотонического раствора хлорида натрия и комбинированных коллоидно-гиперосмолярных растворов. Белые крысы-самцы массой 160-200 г в возрасте 6 месяцев были разделены на 4 группы (по 18 животных в каждой группе): I, II, III - крысы с ожоговой травмой кожи (ожог II-III степени площадью 23% поверхности тела и развитием шокowego состояния средней степени тяжести), которым проводили отдельную инфузию 1 раз в сутки в течение первых 7 дней эксперимента изотонического раствора натрия хлорида, лактопротеина с сорбитолом и HAES-LX-5%, в каждом случае в дозе 10 мл/кг; IV группа - интактные животные. Забор материала от крыс проводили в условиях глубокого тиопенталового внутрибрюшинного наркоза через 1, 3, 7, 14, 21 и через 30 суток после нанесения ожоговой травмы кожи. Биоптаты из Пейеровых бляшек для гистологического и электронно-микроскопического исследования обрабатывали с помощью общепринятых методов. Исследование гистологических препаратов, окрашенных гематоксилином и еозином, проводили на микроскопе Оlymrus VX51. Ультратонкие срезы контрастировали на медных

опорных сеточках уранилацетатом и цитратом свинца по Рейнольдсу и изучали на электронном микроскопе ПЭМ-125К. Полученные методами электронной и световой микроскопии данные свидетельствуют о том, что внутривенная инфузия коллоидно-гиперосмолярных растворов (лактопротеина с сорбитолом и HAES-LX-5%) способствует угнетению воспалительной реакции, тормозит некроз и оптимизирует апоптоз лимфоцитов и дендритных клеток в бляшках Пейера крыс с экспериментальной ожоговой болезнью, которая вызвана ожоговой травмой кожи площадью 21-23% поверхности тела. Апоптозные лимфоциты и их апоптозные тельца эффективно фагоцитируются макрофагами и подлежат перевариванию в гетерофаголизосомах. Для апоптозно измененных дендритных клеток бляшек Пейера характерной является осмиофильная цитоплазма и ядро с аморфной нуклеоплазмой высокой электронной плотности. В цитоплазме локализуются митохондрии с просветленным матриксом и разрушенными кристами, неравномерно расширенные канальцы переменной по конфигурации гранулярной эндоплазматической сетки с электронно прозрачным содержимым и многочисленные производные их вакуольной трансформации, которые резко выделяются в виде светлых пятен на темном фоне цитоплазмы. Слияние вакуолей приводит к формированию больших электронно светлых полостей, которые заполнены разными остатками уплотненных деградированных клеточных структур. Вакуолизация способствует участковой сегментации конденсированной цитоплазмы апоптозных дендритных клеток и образованию апоптозных бляшек (apoptotic blebs), которые подлежат захвату и последующей деградации при участии соседних макрофагов. Обнаруженные структурные изменения органелл белоксинтезирующего аппарата в клетках бляшек Пейера у крыс с экспериментальной ожоговой болезнью могут быть оценены как проявление, вызванное функциональным перенапряжением гранулярной эндоплазматической сетки, стресса эндоплазматического ретикулума (ER-стресса). Следствием оптимального развития ER-стресса и последующего ответа на несвернутые белки (unfolded protein response) является апоптозная деградация соответствующей клетки, ход которой модифицируется в условиях использования примененных коллоидно-гиперосмолярных растворов.

Ключевые слова: бляшки Пейера, структурные изменения, ожоговая болезнь, дезинтоксикационные растворы.



Characteristics of the uterine tubes in the fetal period: topographic and morphometric parallels

Proniaiev D.V., Bulyk R.Ye

Higher State Educational Establishment of Ukraine "Bukovinian State Medical University", Chernivtsi, Ukraine

ARTICLE INFO

Received: 25 February, 2019

Accepted: 26 March, 2019

UDC: 611.651.013.018-022.5-053.15

CORRESPONDING AUTHOR

e-mail: proniaiev@bsmu.edu.ua
Proniaiev D.V.

Topicality of the study is stipulated by the importance of objective data for medicine concerning formation of the structure and topographic-anatomical interrelations of the uterine tubes with adjacent organs and structures during the prenatal period of human ontogenesis. Objective: to find and compare tendencies of changes of the uterine tube morphologic parameters in the two groups of fetuses remote in time, and determine age peculiarities of their topography during perinatal period of development. The experimental material (specimens of fetuses) was divided into two groups: I group - 35 specimens of fetuses deceased during 2017-2019; II group - 105 specimens of fetuses taken from the Museum of the Departments of Anatomy, Clinical Anatomy and Operative Surgery at Higher State Educational Establishment of Ukraine "Bukovinian State Medical University", collected during 1970-1990. Every group was subdivided into 7 subgroups according to 10 months of the fetal period of development (from the 4th to the 10th months). The results obtained were statistically processed in the licensed statistical package "Statistica 6.0" using nonparametric methods to evaluate the results. Regular changes in the topography of the right and left uterine tubes, changes in their shape and histological structure are observed. Both uterine tubes were found to occupy an ascending position in thirty cases out of sixty examined specimens of early fetuses (4-6 months of age). In twenty cases one uterine tube was found to be in an ascending position, and in ten cases both uterine tubes were placed practically horizontally. The study of uterine tube morphogenesis in 7-month fetuses found that the structure and topography of the uterine tubes in different age periods differ. In two 7-month fetuses the uterine tubes were found to be in an ascending position, in eight cases one uterine tube (the left one - in six cases out of eight) was in a horizontal position, and in ten cases two uterine tubes were directed practically horizontally. During the 8th month of the antenatal development one uterine tube was found to be in an ascending position out of eight cases; in ten cases both uterine tubes were in the position close to a horizontal one; and in two cases the left uterine tube was in a descending position. In 9-month fetuses both uterine tubes were found to be in a horizontal position in twelve cases, in eight cases one of the uterine tubes was in the position close to a descending one. In fourteen fetuses 10 months of development one uterine tube was in a descending position, and only in six cases both uterine tubes were located horizontally. The length of the uterine tubes of 4-7-month fetuses deceased during 2017-2019 was not found to differ reliably. Similar regularity was found in the group of fetuses aged from 9 to 10 months. The length of the uterine tubes of the archival specimens increases reliably every two months. In this group of fetuses the parameters of the uterine tube length aged from 9 to 10 months were found to differ reliably contrary to the length of the uterine tubes in the group of modern specimens of a similar age. Comparison of dynamics in changes of the uterine tube length in the two groups of fetuses remote in time showed that within the frame of one group differences in the morphometric parameters between the right and left uterine tubes are not considerable. Therefore, the study of peculiarities in the structure of the uterine tubes at every stage of the perinatal period found certain peculiarities and regularities of their development.

Keywords: uterine tubes, fetus, anatomy, human.

Introduction

The importance of studies dealing with spatial-temporal dynamics of transformations of the human organ systems during antenatal period of development is difficult to be overestimated for modern morphological science. A number of scientific works published in modern scientific periodical editions deal with investigation of these processes. The priority and importance of investigations of different organs and/or systems is not possible to determine. Undoubtedly, the study of embryotopography and perinatal morphology of the female reproductive system will contribute greatly in understanding of interrelations and interaction on shape-generating processes and spatial-temporal organization of anatomical structures, detection of time and morphological preconditions of a possible development of variants in their structure and congenital defects [4]. Though even now literature contains disputable, fragmentary and non-systematize information concerning age morphological peculiarities of the organ systems of fetuses on the whole and uterine tubes in particular. Certain data [2] determine that close shape-generating interrelations are established between the mesenchymal membrane of the paramesonephral ducts and caudal ligament of mesonephros (Wolffian body/inguinal fold) on the eighth week of development. Some other data determined [3] that the mucous membrane of the uterine tubes during early reproductive age is covered with simple columnar epithelium with a small amount of ciliated and secretory cells available. Single lymphocytes are found in the submucous layer. The serous layer is presented by the mesothelium. At the same time, the muscular layer of the uterine tube wall is found [4] to consist of the external layer (spiral), intermediate layer (circular) and internal one (longitudinal). Moreover, certain differences are found in the scientific literature in definition of terms denoting the origin of the embryo and formation of the paramesonephral ducts, the terms and mechanisms of occurrence of congenital defects of the uterine tubes; different data are contained concerning development of derivatives of the paramesonephral ducts. Little attention is paid to the investigation of the shape, length and diameter of the uterine tubes, histotopography of their walls in the dynamics of the fetal period of ontogenesis. Peculiarities of the structure and structural transformation of the uterine tubes remain a topical issue of morphologists and clinicians [5, 25].

A thorough examination of the perinatal processes of morphogenesis will help to isolate trigger components promoting development of congenital pathology. Defects of the urogenital system are third by their occurrence, including 5.4% of developmental defects of the uterine tubes.

Determination of accurate and complete information concerning regularities of topographic-anatomical interrelations of the uterine tubes between themselves and adjacent structures during the antenatal period of human ontogenesis, specification of time and morphological preconditions of possible occurrence of their variants of structure and congenital defects is one of the important areas

of anatomical science [27].

An active introduction of ante- and perinatal prevention of congenital defects of the internal organs requires modern approaches and methods of investigation of the antenatal period of human ontogenesis. Antenatal diagnostics, therapy, surgical correction and prevention of fetal pathology are the most considerable components of reproductive strategy and perinatology. At the present stage of development of perinatal medicine the main principle should be realized - attitude to the fetus as a patient [26].

A wide introduction of computed tomography, magnetic-resonance imaging, ultrasound diagnostics into clinical practical work promotes timely detection and prediction of development of perinatal pathology. Considering present requirements, the relations between morphology and clinical studies should be advanced.

Fragmentary and non-systematized character of the scientific studies concerning typical and variant anatomy of the uterine tubes promotes topicality of the study and requirement of its solution. Therefore, topicality of the study is caused by a medical importance of objective data concerning the formation of structure and topographic-anatomical interrelations of the uterine tubes with adjacent organs and structures during the prenatal period of human ontogenesis [21-24].

Objective: to find and compare tendencies of changes of the uterine tube morphologic parameters in the two groups of fetuses remote in time, and determine age peculiarities of their topography during perinatal period of development.

Materials and methods

The scientific study was conducted at the Department of Anatomy, Clinical Anatomy and Operative Surgery, M.G. Turkevych Department of Human Anatomy, at Higher State Educational Establishment of Ukraine "Bukovinian State Medical University" (BSMU), and it is a fragment of their planned scientific-research work "Peculiarities of Morphogenesis and Topography of the Systems and Organs during Pre- and Postnatal Periods of Human Ontogenesis" (state registration № 0115U002769). The materials of the scientific research have been considered by the BSMU Biomedical Ethics Board. The Board approved that the study was performed according to the European Convention for the Protection of Vertebrate Animals Used for Experimental and other Scientific Purposes (18.03.1986), "Ethical Principles for Conducting Research with Human Participants", approved by Helsinki Declaration (1964-2013), ICH GCP (1996), EU Directives № 609 (24.11.1986), the Orders of the Ministry of Health of Ukraine № 690 (23.09.2009), № 944 (14.12.2009), № 616 (03.08.2012). The experimental material (specimens of fetuses) was divided into two groups: I group - 35 specimens of fetuses deceased during 2017-2019; II group - 105 specimens of fetuses taken from the Museum of the Departments of Anatomy, Clinical Anatomy and Operative

Table 1. Correspondence of fetal length to the term of the fetal development.

Modern specimens								
Months	4	5	6	7	8	9	10	
Parietal-calcanal length (mm)	165.0	210.0	260.0	310.0	355.0	405.0	455.0	
	170.0	220.0	260.0	310.0	360.0	420.0	455.0	
	170.0	220.0	270.0	325.0	360.0	430.0	460.0	
	180.0	230.0	280.0	340.0	370.0	430.0	465.0	
	180.0	240.0	300.0	340.0	380.0	445.0	470.0	
	Archive specimens							
	170.0	210.0	260.0	310.0	355.0	410.0	455.0	
	170.0	210.0	260.0	310.0	355.0	410.0	455.0	
	170.0	210.0	260.0	310.0	355.0	410.0	455.0	
	170.0	220.0	265.0	320.0	360.0	420.0	460.0	
	170.0	220.0	265.0	320.0	360.0	420.0	460.0	
	170.0	220.0	270.0	320.0	360.0	425.0	460.0	
	170.0	225.0	270.0	330.0	360.0	430.0	460.0	
	170.0	230.0	275.0	335.0	365.0	430.0	465.0	
	180.0	230.0	275.0	340.0	365.0	430.0	465.0	
	180.0	235.0	290.0	340.0	370.0	440.0	465.0	
	180.0	240.0	290.0	340.0	370.0	440.0	465.0	
	180.0	240.0	300.0	340.0	370.0	440.0	470.0	
	180.0	245.0	300.0	345.0	380.0	445.0	470.0	
	180.0	250.0	300.0	345.0	380.0	445.0	470.0	
185.0	250.0	300.0	350.0	380.0	445.0	470.0		

Surgery at Higher State Educational Establishment of Ukraine "Bukovinian State Medical University", collected during 1970-1990. Every group was subdivided into 7 subgroups according to 10 months of the fetal period of development (from the 4th to the 10th months) [1].

The age of fetuses and neonates was determined immediately after obtaining them before preservation by means of measuring the parietal-coccygeal length and parietal-calcanal length according to A.A. Zavarzin, A.G. Knorre, B.M. Petten tables; recommendations by B.P. Khvatov and Yu.N. Shapovalov, A.I. Brusylovsky and G.G. Avtandilov. Correspondence of fetal length to the term of the fetal development is presented in Table 1. The choice of the preserving solution was caused by the fact that it is this neutral formaldehyde solution according to V.I. Proniayev et al. [20] that least changes the colour of the specimen. The specimens of fetuses were first measured, preserved in 5-7% formaldehyde solution during 2-3 weeks, and after that kept in 3-5% formaldehyde solution. The specimens of fetuses from the first group were examined directly in the prosectorium of Chernivtsi Regional Municipal Medical Institution "Pathologic-Anatomical Bureau" during planned dissections.

The results obtained were statistically processed in the licensed statistical package "Statistica 6.0" using nonparametric methods to evaluate the results. The character

of distribution for every variation series obtained, mean values for every sign examined, standard quadratic deviation, and percentile scale of parameters were evaluated. Difference reliability of parameters between independent quantitative values was determined by means of Mann-Whitney U-criterion [8, 18, 23].

Results

While examining peculiarities of the uterine tube structure at every stage of the perinatal period we have found certain peculiarities and regularities of their development. Particularly, regular topographic changes of the right and left uterine tubes, changes of their shape and histological structure were observed. Peculiarities of the uterine tube topography found by us should be characterized by a certain compliance with the ovarian topography, since regular interrelations in the development of these organs are found in the fetal period of human ontogenesis. Numerous studies dealing with investigation of the uterine tube topography of fetuses conducted by scientists [26, 27] and published on the pages of periodical scientific editions are indicative of certain unconformity of results. Specifically it is indicated [7, 25] that at the beginning of the fetal period the uterine tubes passing parallel to the dorsal-lateral abdominal wall in a free upper margin of the broad uterine ligament till the end of the fetal period descend synchronously into the pelvic cavity and in all the cases they are located on the level with the uterine fundus. At the same time, their skeletopia changes from the level of the 5th lumbar vertebra at the beginning of the fetal period to the 2nd sacral vertebra in neonates. We can agree with a thesis concerning a skeletopic change of the uterine tube position, but we cannot agree with the thesis about synchronous descending of the right and left uterine tubes to the level of the uterine fundus. We have determined that in 30 out of 60 examined specimens of the early fetuses (4-6 months of age) both uterine tubes were found to be in an ascending position, in 20 cases one uterine tube was in an ascending position and in 10 cases both uterine tubes were located practically horizontally.

We have found successive stages of the uterine tube shapes: conditionally straight, curved, zigzag, and spiral (Fig. 1).

At the beginning of the fetal period (4-5 month fetuses) a zigzag shape of the uterine tubes prevails over the rest of variants of their shape practically twice as much (50%). Cases with a spiral shape were found in 30%, and conditionally straight uterine tubes were found in 20% cases (Fig. 2).

Spiral and zigzag uterine tubes were found in 30 and 70% of cases respectively in fetuses of 6 months of age.

Examination of the uterine tube morphogenesis of 7-month fetuses found that the structure and topography of the uterine tubes at different terms differ. In two fetuses both uterine tubes were in an ascending position, in 8 cases one of the uterine tubes (the left one - in 6 cases out of 8) was in

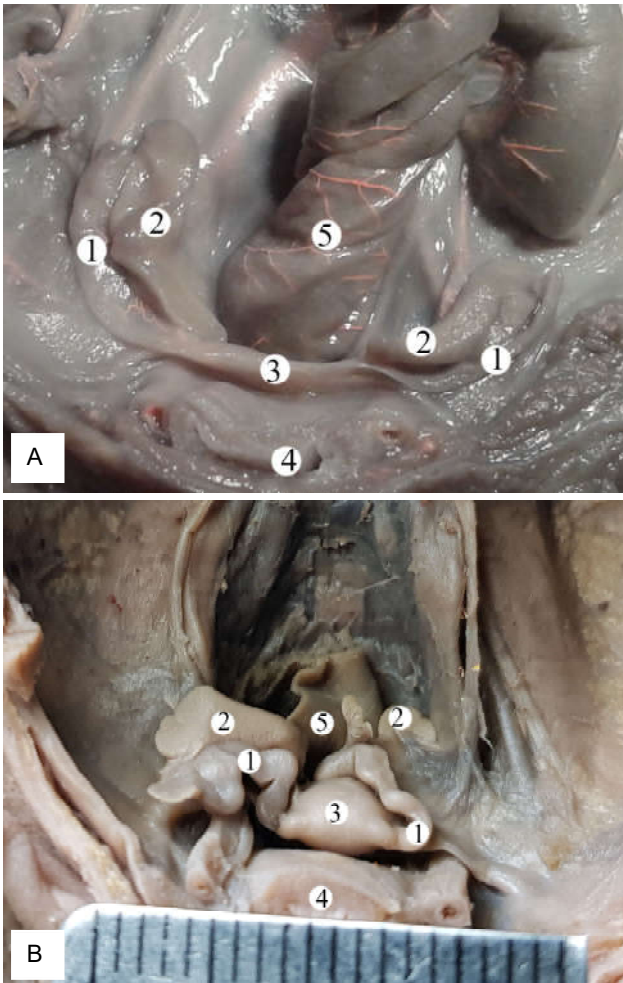


Fig. 1. Internal female reproductive organs of fetuses 210,0 (A) and 300,0 (B) mm of the parietal-calcaneal length. Specimen. 1 - uterine tubes; 2 - ovaries; 3 - uterus; 4 - urinary bladder; 5 - rectum; A - conditionally straight or curve uterine tubes, B - spiral or zigzag uterine tubes.

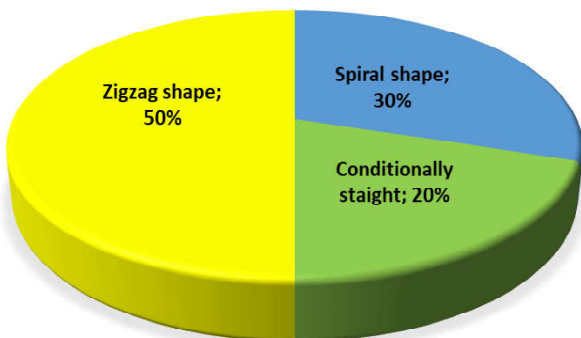


Fig. 2. Variability of shapes of the uterine tubes in 4-5-month fetuses.

a horizontal position, and in 10 cases two uterine tubes were directed practically horizontally.

During the 8th month of the prenatal development one uterine tube was found to be in an ascending position out of

eight cases; in ten cases both uterine tubes were in the position close to a horizontal one; and in two cases the left uterine tube was in a descending position (Fig. 3).

In 9-month fetuses both uterine tubes were found to be in a horizontal position in twelve cases, in eight cases one of the uterine tubes was in the position close to a descending one.

In fourteen fetuses 10 months of development one uterine tube was in a descending position, and only in six cases both uterine tubes were located horizontally (Fig. 4).

Analyzing the dynamics of changes of the right uterine tube length in 4-10-month fetuses from the first group (Fig. 5 A), it should be noted that its length in 4, 5, 6 and 7 month

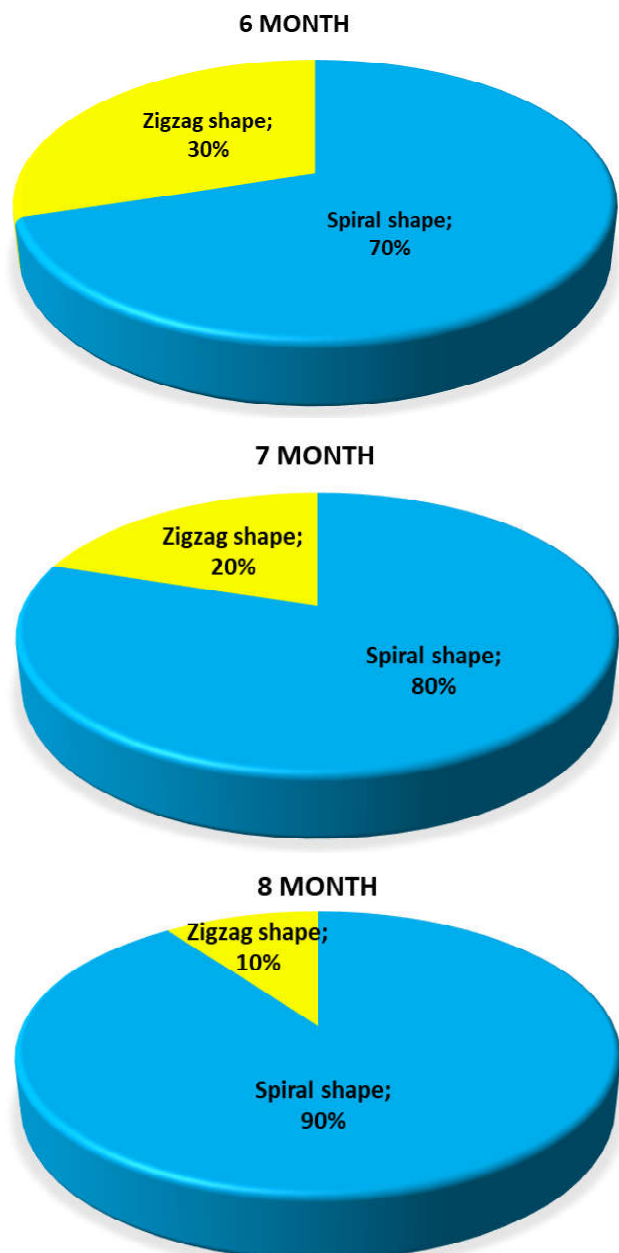


Fig. 3. Variants of uterine tubes in 6-8-month fetuses.

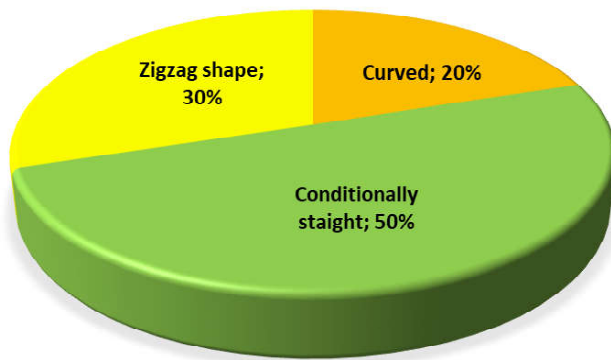


Fig. 4. Variability of the uterine tube shape at the end of the fetal period.

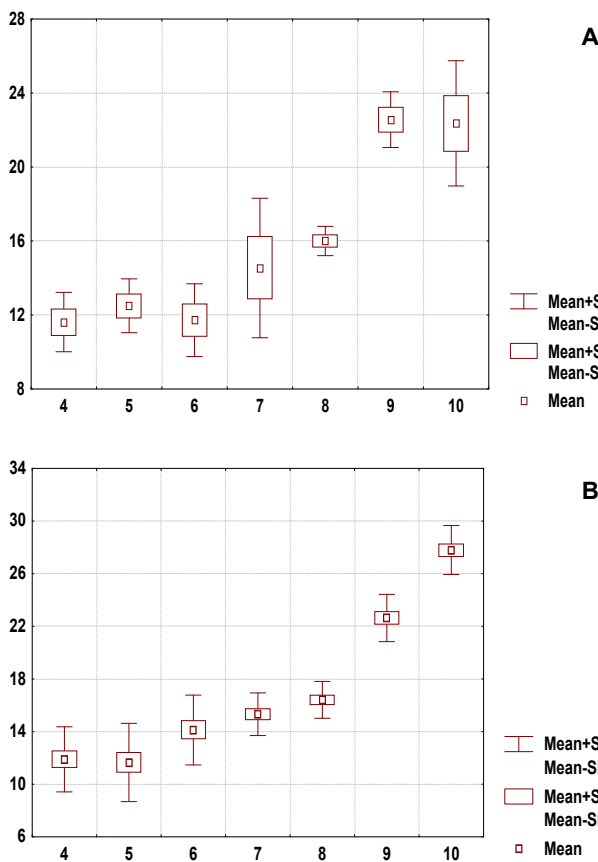


Fig. 5. Length of the right uterine tube of fetuses from different age groups. Here and further: A - first group, the studies of 2017-2019; B - seconds group, specimens of 1970-1990.

fetuses does not differ reliably similar to that of 7 and 8, 9 and 10 month fetuses ($p > 0.05$). Though, in 4-7 month fetuses its length is reliably shorter than in the rest of terms ($p < 0.05-0.01$).

In fetuses from the second group (Fig. 5 B) the length of the right uterine tube in 4-month fetuses does not differ reliably from that of 5-month fetuses ($p > 0.05$), though it is reliably shorter than that of fetuses of the rest age groups. In 5-month fetuses the length of the right uterine tube is

reliably shorter than in 6-10-month fetuses. This parameter of 6 and 7-month fetuses does not differ reliably ($p > 0.05$). In the rest of cases the length of the right uterine tube in 8-month fetuses is reliably shorter than that of 9 and 10-month fetuses. In 9-month fetuses this parameter is shorter than that of 10-month fetuses ($p < 0.05-0.01$).

The dynamics of length of the left uterine tube in fetuses from the first group (Fig. 6 A) is similar to that of the right uterine tube. This parameter in 4-7-month fetuses does not differ reliably ($p > 0.05$), though it is reliably shorter than the length of the left uterine tube in 8-10-month fetuses ($p < 0.05-0.01$). There is no reliable difference found in 7 and 8-month fetuses except comparison with the length of the left uterine tube in the first group. There is no reliable difference found between the length of the left uterine tube in the first group of 9 and 10-month fetuses. The length of the left uterine tube in this group of 8-month fetuses is reliably shorter than that of 9 and 10-month fetuses ($p < 0.01$).

The length of the left uterine tube in the second group has certain considerable peculiarities (Fig. 6 B), both in comparison with the length of the right uterine tube in both groups, and in comparison with the same parameter in the first group. That is, there is no reliable difference found between specimens of 4 and 5-month fetuses from the second group in the length of the left uterine tube ($p > 0.05$),

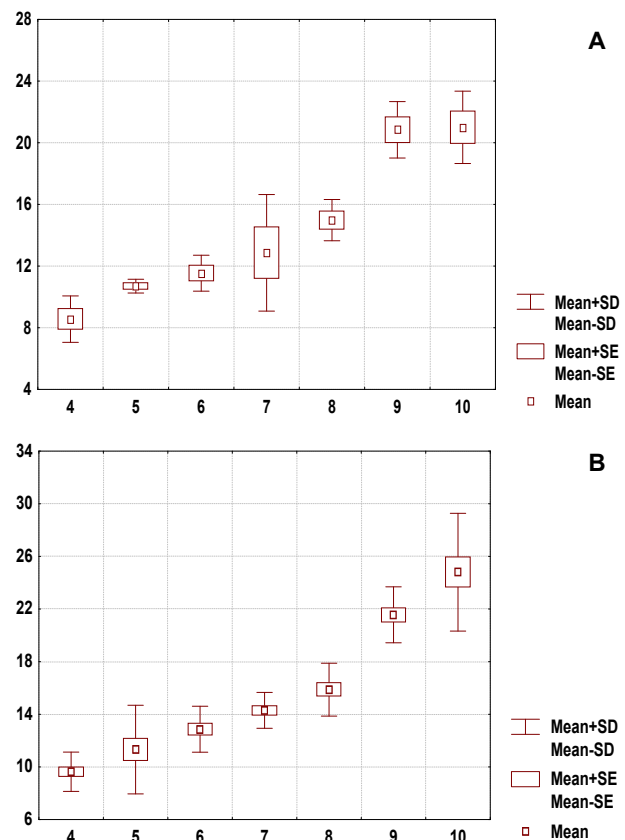


Fig. 6. Length of the left uterine tube of fetuses from different age groups.

similar to that of 5 and 6-month, 6 and 7-month fetuses. Though, the length of the left uterine tube in 4-month fetuses from the second group is reliably shorter than that of 6-10-month fetuses. Similar situation is observed in 5 and 6-month fetuses. The length of the left uterine tube in 5-month fetuses is reliably shorter than that of 7-10-month fetuses. The length of the left uterine tube from the second group in 6-month fetuses is reliably shorter than that of 8-10-month fetuses, though it is longer than that in 4-month fetuses ($p < 0.05-0.01$). In this case the length of the left uterine tube in 9 and 10-month fetuses does not differ reliably ($p < 0.001$). During 7 month of development the length of the left uterine tube in fetuses from the second group is reliably shorter than that in 8-10-month fetuses. Though, it is longer than that in 4 and 5-month fetuses and does not differ from that of 6-month fetuses ($p > 0.05$). The left uterine tube in 8-month fetuses is reliably shorter than in 9-10-month fetuses and longer than in 4-7-month fetuses.

Discussion

Summing up the above a conclusion can be drawn concerning nonsynchronous descending of the uterine tubes into the pelvic cavity. Immersion of the uterine tubes into the uterine-rectal depression was often observed in late fetuses, which differs considerably from the results of studies conducted by the majority of authors [16-19].

During perinatal period certain transformations are found in the shape of the uterine tubes. Numerous researchers [6, 15, 11] do not have agreed points of view concerning the shape of uterine tubes and dynamics of its changes. Authors differentiate straight uterine tubes in early fetuses, serpentine uterine tubes - in 6-10-month fetuses. Moreover, they differentiate curved uterine tubes, in the form of "corrugated tube", L-like, C-like, in the form of a hook, etc. Though, the results of our investigations do not allow complete agreement with such definitions, since detection of the uterine tube shape should be based on understanding of regularities of a comprehensive morphological transformations occurring in their walls. The authors have certain reasons to consider that topography and location of the uterine tubes depend on the degree of development and position of the ovaries, that is: the longer ovarian length the more inclined position of the uterine tube is.

The importance of the suspensory ligament of the ovary concerning its topography and topography of the uterine tube is a well-known fact [7-9, 24]. Of course, there are no grounds to refuse it, but we think that the processes of morphogenesis having a leading value during the embryonic period produce less effect on morphological transformations during the perinatal period. Since the 5th month of the antenatal

development leading morphological transformations occur at the expense of plastic processes both in the wall of the uterine tube and ovarian parenchyma. And it is these processes produce a crucial value on the formation of topography and morphology of the fetal uterine tube. That is, in our studies we indicate that with the beginning of the perinatal period a leading role concerning detection of anatomical characteristics changes between the uterine tube and ovary. During the embryonic and pre-fetal periods the ovaries with their suspensory apparatus determine topography of the uterine tubes [10-11], but during the fetal period ovarian topography depends on the topography of the uterine tubes.

Analysis of the statistical investigation conducted is indicative of certain peculiarities of age dynamics in transformation of morphometric parameters of the uterine tubes during the fetal period. The length of the uterine tubes of 4-7-month fetuses deceased during 2017-2019 was not found to differ reliably. Similar regularity was found in the group of fetuses aged from 9 to 10 months. The length of the uterine tubes of the archival specimens increases reliably every two months ($p > 0.05$). In this group of fetuses the parameters of the uterine tube length aged from 9 to 10 months were found to differ reliably contrary to the length of the uterine tubes in the group of modern specimens of a similar age.

Comparison of dynamics in changes of the uterine tube length in the two groups of fetuses remote in time showed that within the frame of one group differences in the morphometric parameters between the right and left uterine tubes are not considerable. Though, a tendency can be observed concerning a relative enlargement of length of both uterine tubes among the specimens of fetuses from the second group.

Conclusions

1. In 4-8-month fetuses the uterine tubes descend gradually: from the ascending position near the rectum to the iliac fossa or the uterine-rectal depression.

2. Dynamics of both uterine tubes demonstrates a tendency to a relative enlargement of length of both uterine tubes among museum (archive) specimens of 10-month fetuses. The length of the uterine tubes of 4-7-month fetuses deceased during 2017-2019 was not found to differ reliably. Similar regularity was found in the group of fetuses aged from 9 to 10 months. The length of the uterine tubes of the archival specimens increases reliably every two months. In this group of fetuses the parameters of the uterine tube length aged from 9 to 10 months were found to differ reliably contrary to the length of the uterine tubes in the group of modern specimens of a similar age.

References

- [1] About the introduction of Instructions about the recognition of criteria for live births, dead births and the perinatal period. The order of the Ministry of Health of Ukraine № 179 (z0427-06) 29.03.2006. <https://zakon.rada.gov.ua/laws/show/z0160-96>
- [2] Acién, P., & Acién, M. (2016). Diagnostic imaging and cataloguing

of female genital malformations. *Insights into Imaging*, 7(5), 713-726. doi: 10.1007/s13244-016-0515-4

- [3] Ando, H., Watanabe, Y., Ogawa, M., Tamura, H., Deguchi, T., Ikeda, K., ... Adachi, S. (2017). Mesonephric adenocarcinoma of the uterine corpus with intracystic growth completely

- confined to the myometrium: a case report and literature review. *Diagnostic Pathology*, 12(1), 63. doi: 10.1186/s13000-017-0655-y
- [4] Akhtemiichuk, Yu. T., & Piatnytska, T. V. (2010). Histotopography of the uterine tubes in human fetuses. *Clinical Anatomy and Operative Surgery*, 9(4), 50-54.
- [5] Akhtemiichuk, Yu. T., Piatnytska, T. V., & Manchulenko, D. G. (2012). *Morphogenesis of the uterine tubes during prenatal period of human ontogenesis*. Theses published in the Materials of the 3rd Scientific Symposium "Anatomical-Surgical Aspects of Pediatric Gastroenterology", Chernivtsi. Chernivtsi: BSMU.
- [6] Akhtemiichuk, Yu. T., Piatnytska, T. V., & Marchuk, V. F. (2011). *Microstructure of the uterine tubes during the prenatal period of ontogenesis*. Theses published in the Materials of the Scientific-Practical Conference: "Morphological Aspects of Microcirculation in the Norm and Pathology". Ternopil: Ukrmedknyha.
- [7] Banul, B. Yu., & Marchuk, F. D. (2013). Development of the uterine tubes at the end of the fetal period of human ontogenesis. *Bukovinian Medical Herald*, 18(2), 206-208.
- [8] Banul, B. Yu., Marchuk, F. D., & Liutyk, M. D. (2013). *Development of the uterine tubes at the end of the pre-fetal and early fetal periods of human ontogenesis*. Theses published in the Materials of the 94th Final Scientific Conference of the Professional and Teaching Staff of Bukovinian State Medical University, Chernivtsi. Chernivtsi: BSMU.
- [9] Caliskan, S. (2017). Bilateral ureteral duplication of complete left and incomplete right side with lower pole kidney stone. *Journal of the College of Physicians and Surgeons*, 27(3), 65-66. PMID: 28302252
- [10] Chapel, D. B., Joseph, N. M., Krausz, T., & Lastra, R. R. (2018). An Ovarian Adenocarcinoma With Combined Low-grade Serous and Mesonephric Morphologies Suggests a Müllerian Origin for Some Mesonephric Carcinomas. *International Journal of Gynecological Pathology*, 37(5), 448-459. doi: 10.1097/PGP.0000000000000444
- [11] Darcy, D. G., Yao-Cohen, M., Olson, T. R., & Downie, S. A. (2017). Unilateral complete agenesis of mesonephric duct derivatives in an 82-year-old male cadaver: embryology, anatomy and clinical considerations. *Urology Case Reports*, 15, 20-22. doi: 10.1016/j.eucr.2017.06.003
- [12] Davidson, E. R. W., & Barber, M. D. (2017). A gartner duct cyst masquerading as anterior vaginal prolapse. *Obstetrics & Gynecology*, 130(5), 1039-1041. doi: 10.1097/AOG.0000000000002315
- [13] George, C., & Berge, L. R. (2002). *Hypothesis Testing, Statistical Inference*. Second Edition. Pacific Grove, CA: Duxbury.
- [14] Jin, Z. W., Abe, H., Hinata, N., Li, X. W., Murakami, G., & Rodriguez-Vázquez, J. F. (2016). Descent of mesonephric duct to the final position of the vas deferens in human embryo and fetus. *Anatomy & Cell Biology*, 49(4), 231-240. doi: 10.5115/acb.2016.49.4.231
- [15] Khmara, T. V., & Voitenko, S. G. (1994). *To the issue of development of the human uterine tubes*. Theses published in the Materials of the Conference "Scientists of Bukovyna - to the Public Health Care", Chernivtsi: [w.p.].
- [16] Ludwig, K. S. (1993). The development of the caudal ligaments of the mesonephros and of the gonads: a contribution to the development of the human gubernaculum (Hunteri). *Anatomy and Embryology*, 88, 571-577. doi: 10.1007/bf00187012
- [17] Mirkovic, J., McFarland, M., Garcia, E., Sholl, L. M., Lindeman, N., MacConaill, L., ... & Howitt, B. E. (2018). Targeted genomic profiling reveals recurrent kras mutations in mesonephric-like adenocarcinomas of the female genital tract. *The American Journal of Surgical Pathology*, 42(2), 227-233. doi: 10.1097/PAS.0000000000000958
- [18] Moisiuk, D. V., Syniuk, O. S., & Zayats, V. V. (2006). *Peculiarities of the uterine tube structure*. Theses published in the Materials of the IV International Scientific-Practical Conference of Students and Young Scientists, Uzhgorod. Uzhgorod: Grazhda.
- [19] Piantnytska, T. V. (2010). *Formation of the uterine tubes during the pre-fetal period of ontogenesis*. Theses published in the Materials of the Scientific-Practical Conference devoted to the 70th anniversary of the Honoured Scientist and Technician of Ukraine, Professor Ya.I. Fedoniuk "Topical Issues of Morphology", Ternopil. Ternopil: Ukrmedknyha.
- [20] Pronyayev, V. I., Svistonyuk, I. U., & Akhtemiichuk, Yu. T. (1995). *Changes in the length of embryos depending on their age, type and concentration of fixatives*. Thesis in materials of "International Congress on Integrative Anthropology". Ternopil: [w.p.].
- [21] Puljiz, M., Danolić, D., Kostić, L., Alvir, I., Tomica, D., Mamić, I., & Balja, M. P. (2016). Mesonephric adenocarcinoma of endocervix with lobular mesonephric hyperplasia: case report. *Acta Clinica Croatica*, 55(2), 326-330. doi: 10.20471/acc.2016.55.02.22
- [22] Roder, D., Davy, M., Selva-Nayagam, S., Paramasivam, S., Adams, J., Keefe, D., ... Oehler, M. K. (2018). Exploring the added value of hospital-registry data for showing local service outcomes: cancers of the ovary, fallopian tube and peritoneum. *BMJ Open*, 9(2), e024036. doi: 10.1136/bmjopen-2018-024036
- [23] Shelamova, M. A., Insarova, N. I., & Leshchenko, V. H. (2010). *Statistical analysis of medical-biological data using Excel program*. Teaching-Methodical Manual. Minsk: BSMU.
- [24] Singh, K., Sung, C. J., Lawrence, W. D., & Quddus, M. R. (2017). Testosterone-induced "virilization" of mesonephric duct remnants and cervical squamous epithelium in female-to-male transgenders: a report of 3 cases. *The International Journal of Gynecological Pathology*, 36(4), 328-333. doi: 10.1097/PGP.0000000000000333
- [25] Tiwari, C., Shah, H., Desale, J., & Waghmare, M. (2017). Neonatal gartner duct cyst: two case reports and literature review. *Developmental Period Medicine*, 21(1), 35-37. PMID: 28551690
- [26] Voitenko, S. G. (1996). *Topography of the uterine tubes during the fetal period of human ontogenesis*. Theses published in the Materials of the Scientific Conference "Topical Issues of Morphogenesis", Chernivtsi. Chernivtsi: [w.p.].
- [27] Yeo, M. K., Choi, S. Y., Kim, M., Kim, K. H., & Suh, K. S. (2016). Malignant mesonephric tumor of the cervix with an initial manifestation as pulmonary metastasis: case report and review of the literature. *European journal of gynaecological oncology*, 37(2), 270-277. PMID: 27172762

ХАРАКТЕРИСТИКА МАТКОВИХ ТРУБ У ПЛОДОВОМУ ПЕРІОДІ: ТОПОГРАФІЧНІ ТА МОРФОМЕТРИЧНІ ПАРАЛЕЛІ
Проняєв Д.В., Булик Р.Є.

Актуальність даного дослідження зумовлена важливістю для медицини об'єктивних даних про становлення будови і топографоанатомічних взаємовідношень маткових труб зі суміжними органами та структурами в пренатальному періоді онтогенезу людини. Мета роботи - встановити та порівняти тенденції змін морфологічних параметрів маткових труб двох віддалених у часі груп плодів та з'ясувати вікові особливості їх топографії у перинатальному періоді розвитку.

Дослідний матеріал (препарати плодів) було розподілено на дві групи: I група - 35 препаратів плодів, котрі померли впродовж 2017-2019 рр.; II група - 105 препаратів плодів із музею кафедри анатомії, клінічної анатомії та оперативної хірургії Вищого державного навчального закладу України "Буковинський державний медичний університет", що були зібрані впродовж 1970-1990 рр. Кожну із груп було розподілено на 7 підгруп відповідно 10-ти місяцям плодового періоду розвитку (з 4-го по 10-й). Статистичний аналіз отриманих результатів проведений у ліцензійному статистичному пакеті "Statistica 6.0" з використанням непараметричних методів оцінки результатів. Встановлені закономірні зміни топографії правої та лівої маткових труб, зміна їх форми та гістологічної будови. Виявлено, що із 60 досліджених препаратів ранніх плодів (віком 4-6 місяців) у 30 випадках обидві маткові труби займали висхідне положення, у 20 випадках одна маткова труба займала висхідне положення і в 10 випадках дві маткові труби розташовувались майже горизонтально. При дослідженні морфогенезу маткових труб плодів 7 місяців внутрішньоутробного розвитку виявлено, що будова і топографія маткових труб у різні вікові періоди має свої відмінності. У двох плодів віком 7 місяців дві маткові труби займали висхідне положення, у 8 випадках одна з маткових труб (ліва - у 6 випадках із 8) займала горизонтальне положення і в 10 випадках дві маткові труби спрямовувалися майже горизонтально. На восьмому місяці внутрішньоутробного розвитку у 8 випадках, одна з маткових труб займала висхідне положення, у 10 випадках обидві маткові труби займали положення, наближене до горизонтального, і в 2 випадках ліва маткова труба займала низхідне положення. У плодів 9 місяців у 12 випадках обидві маткові труби займали горизонтальне положення, а у 8 випадках - одна з маткових труб займала положення, наближене до низхідного. У 14 плодів віком 10 місяців одна маткова труба займала низхідне положення і лише в 6 випадках обидві маткові труби розташовувались горизонтально. Встановлено, що довжина маткових труб плодів віком 4-7 місяців, що померли впродовж 2017-2019 рр., достовірно не відрізнялась. Аналогічну закономірність встановлено для груп плодів віком 9 та 10 місяців. Довжина маткових труб архівних препаратів кожні 2 місяці достовірно збільшується. В даній групі також достовірно відрізняються параметри довжини маткових труб плодів віком 9 та 10 місяців на відміну від довжини маткових труб плодів групи сучасних препаратів аналогічного віку. Порівняння динаміки зміни довжини маткових труб двох розведених у часі груп плодів показало, що в межах однієї групи відмінності в морфометричних параметрах між правою та лівою матковою трубою є незначними. Таким чином, при дослідженні особливостей будови маткових труб на кожному з етапів перинатального періоду виявлені певні особливості та закономірності їх розвитку.

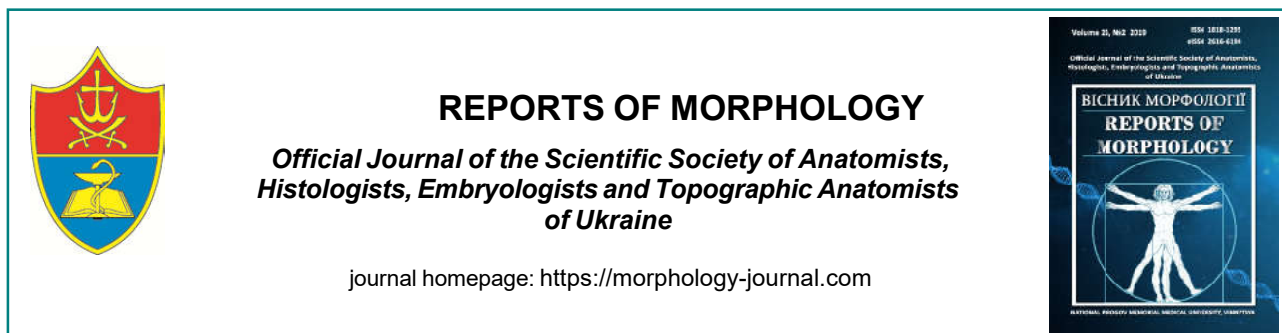
Ключові слова: маткові труби, плід, анатомія, людина.

ХАРАКТЕРИСТИКА МАТОЧНЫХ ТРУБ В ПЛОДОВОМ ПЕРИОДЕ: ТОПОГРАФИЧЕСКИЕ И МОРФОМЕТРИЧЕСКИЕ ПАРАЛЛЕЛИ

Проняев Д.В., Булык Р.Е.

Актуальность данного исследования обусловлена важностью для медицины объективных данных о становлении строения и топографо-анатомическом взаимоотношении маточных труб со смежными органами и структурами в пренатальном периоде онтогенеза человека. Цель работы - определить и сравнить тенденции изменений морфологических параметров маточных труб двух отдаленных во времени групп плодов и выяснить возрастные особенности их топографии в перинатальном периоде развития. Исследуемый материал (препараты плодов) был разделен на две группы: I группа - 35 препаратов плодов, умерших в течение 2017-2019 гг.; II группа - 105 препаратов плодов из музея кафедры анатомии, клинической анатомии и оперативной хирургии Высшего государственного учебного заведения "Буковинский государственный медицинский университет", собранные в течение 1970-1990 гг. Каждую из групп распределили на 7 подгрупп соответственно 10-ти месяцам плодного периода развития (с 4-го по 10-й). Статистический анализ полученных результатов выполнен в лицензионном статистическом пакете "Statistica 6.0" с использованием непараметрических методов оценки результатов. Установлены закономерные изменения топографии правой и левой маточных труб, изменение их формы и гистологического строения. Вывявлено, что из 60 исследованных препаратов ранних плодов (в возрасте 4-6 месяцев) в 30 случаях обе маточные трубы занимали восходящее положение, в 20 случаях одна маточная труба занимала восходящее положение и в 10 случаях две маточные трубы располагались почти горизонтально. При исследовании морфогенеза маточных труб плодов 7 месяцев внутриутробного развития, выявлено что строение и топография маточных труб в разные возрастные периоды имеют свои отличия. У двух плодов в возрасте 7 месяцев две маточные трубы занимали восходящее положение, в 8 случаях одна из маточных труб (левая - в 6 случаях из 8) занимала горизонтальное положение и в 10 случаях две маточные трубы направлены почти горизонтально. На 8 месяце внутриутробного развития в 8 случаях, одна из маточных труб занимала восходящее положение, в 10 случаях обе маточные трубы занимали положение, близкое к горизонтальному, и в 2 случаях левая маточная труба занимала нисходящее положение. У плодов 9 месяцев в 12 случаях обе маточные трубы занимали горизонтальное положение, а в 8 случаях - одна из маточных труб занимала положение, близкое к нисходящему. У 14 плодов в возрасте 10 месяцев одна маточная труба занимала нисходящее положение и только в 6 случаях обе маточные трубы размещались горизонтально. Установлено, что длина маточных труб плодов в возрасте 4-7 месяцев, умерших на протяжении 2017-2019 гг., достоверно не отличается. Аналогичную закономерность установлено для групп плодов возрастом 9 и 10 месяцев. Длина маточных труб архивных препаратов каждые 2 месяца достоверно увеличивается. В данной группе также достоверно отличаются параметры длины маточных труб плодов возрастом 9 и 10 месяцев в отличии от длины маточных труб плодов группы современных препаратов соответствующего возраста. Сравнение динамики изменений длины маточных труб в двух разведенных во времени групп плодов показало, что в границах одной группы различия в морфометрических параметрах между правой и левой маточной трубой являются незначительными. Таким образом, при исследовании особенностей строения маточных труб на каждом из этапов перинатального периода выявлены определенные особенности и закономерности их развития.

Ключевые слова: маточные трубы, плод, анатомия, человек.



Structural organization of the ileum of laboratory animals in normal and in a comparative view aspect

Sydorenko M.I.

Ukrainian Medical Dental Academy, Department of Clinical Anatomy and Operativ Surgery, Poltava, Ukraine

ARTICLE INFO

Received: 26 February, 2019

Accepted: 26 March, 2019

UDC: 611.344-092.9

CORRESPONDING AUTHOR

e-mail: sidorenko999@ukr.net
Sydorenko M.I.

In recent decades, diseases of the digestive system that require immediate, both therapeutic and surgical treatment, have become widespread, and it is therefore a natural task to find new and optimize existing technologies and methods for correcting the above-mentioned nosologies. Preclinical studies of such developments are conducted exclusively on laboratory animals and knowledge of the morphological features of their structure for further comparison with the morphology of similar human organs is an urgent task of modern medical and biological science. The purpose of the study was to study the structural organization of the ileum of rabbits in comparative species and to obtain control data on its morphological features. Adequate research methods were used in the work according to the set goal, namely: histological, histochemical, electron microscopic, morphometric and statistical and biopsies of the ileum of 10 rabbits were studied. The correctness of the distribution of traits by each of the variations obtained, the average values for each trait studied, standard errors and standard deviations were evaluated. The significance of the difference of values between independent micrometric values in the normal distribution of features was determined by Student's criterion. The paper describes the main structural components of the ileum of rabbits and compared with similar structures of the human ileum. The ileum of rabbits, as in humans, has been determined to have four membranes: mucous, submucosal, muscular and serous. The mucous membrane is constructed from the epithelial layer, which is located on the basement membrane and the muscular plate and contains cellular elements (exocrinocytes, enterocytes of various kinds, elements of the diffuse endocrine system associated with the mucous membrane, intraepithelial lymphocytes), blood and lymphatic vessels and nerve endings. The submucosa is composed of loose fibrous connective tissue, which contains collagen and reticular fibers, elements of diffuse lymphoid tissue, blood vessels, and nerve endings. The muscular and serous membranes are constructed in the same way as in the human ileum. Thus, after the study, it was determined that the morphological organization of the ileum of rabbits at the optical and electron microscopic levels has general patterns of structure similar to those in the ileum of the human.

Keywords: ileum, exocrinocytes, endocrinocytes, lymphocytes, arterioles, capillaries, venules.

Introduction

Digestive diseases are one of the most widespread not only in the territory of our country, but in the whole world. Mortality from digestive diseases is a significant proportion of all diseases [12, 13, 15]. In recent years, there has been a steady increase in the incidence of malignant tumors of the small intestine, including malignant non-epithelial tumors, most often stromal tumors accounting for 4-10 % [9, 14]. Despite the fact that the therapeutic options for conservative therapy of small bowel disease have expanded

significantly over the last decade, about 20-60 % of patients with inflammatory bowel disease may need surgical treatment over the course of their lives [2, 17, 18].

In the available literature, data are available on the morphological features of the structure of both the middle section of the digestive tube as a whole and its individual parts [3, 4, 5, 6, 7, 8]. However, these studies relate to the morphology of the rat digestive tube, and the structural features of the rabbit ileum have not been studied. The

urgency of studying this issue is due to the fact that rabbits are used as laboratory animals in the development of tactics for surgical treatment of diseases of the small intestine, which is related to the linear dimensions of the latter. Based on the above study of morphology of the ileum of rabbits is a normal medical and biological task, and the data obtained will serve as reference indicators in the course of a series of experimental developments.

The purpose of the study was to study the structural organization of the ileum of rabbits in comparative species and to obtain control data on its morphological features.

Materials and methods

This study used rabbits of the "Chinchilla" breed (n=10). Animals were kept and all manipulations were carried out in accordance with the "Rules for the Use of Laboratory Experimental Animals" (2006, Annex 4) and the Declaration of Helsinki on Animal Welfare, Law of Ukraine "On the Protection of Animals against Cruelty" (No. 3447-IV of 21.02.2006) in compliance with the requirements of the Bioethics Commission of the Ukrainian Medical Dental Academy, in accordance with the provisions of the "European Convention for the Protection of Vertebrate Animals Used for Experimental and Other Scientific Purposes" (Strasbourg, 1986).

Histological, ultramicroscopic, morphometric and statistical methods of investigation were used in the work. For this purpose, in the operating department of clinical anatomy and surgery, surgery was performed on the small intestine in the ileum. To determine the main morphological parameters of the ileum biopsy was removed and compacted into paraffin and epoxy resin according to conventional methods. From paraffin blocks, semi-thin sections of 4-5 μm thick were made, which were then stained with hematoxylin and eosin, followed by Van Gizon with Harte refinement. Thin sections 1-2 μm thick were made of epoxy blocks and stained with methylene blue and toluidine blue. Further histological sections were examined using an Olympus C 3040-ADU digital microscope with programs adapted for this study (Olympus DP - Soft, license no. VJ285302, VT310403, 1AV4U13B26802) and Biorex 3 (serial number 5604). Morphometric studies were performed using a system of visual analysis of histological preparations. Images of histological specimens on a computer monitor were taken from a microscope and using a Visiion CCD Camera. Morphometric studies were performed using VideoTest-5.0, KAAPA Image Baseeta Microsoft Excel software on a personal computer. Ultramicroscopic investigations were performed on the basis of the electron microscopy laboratory of the Ternopil National Medical University named after I. Gorbachevsky in accordance with the concluded agreement on scientific cooperation.

The average size of the intestinal wall was determined morphometrically, namely: the average total thickness of the intestinal wall; the average thickness of the mucous

membrane; the average thickness of the submucosa; the average thickness of the muscle; the average thickness of the serous membrane. The morphometric characteristics of the elements of the hemomicrocirculatory bed were determined in accordance with the guidelines [11, 12, 18] and the index of their capacity (Wogenworth index) was determined. We measured the average height of the villi, the average apical width of the villi, the average basal width of the villi, the average diameter of the lumen of the lymphatic vessel of the villi, the average depth of the crypts, the average diameter of the crypts. In parallel, the average number of structural elements of the ileum of the ileum in the villi was calculated: the average number of columnar epitheliocytes with a border; the average number of goblet cells; average number of endocrinocytes; average number of intraepithelial lymphocytes; in crypts: average number of columnar epitheliocytes; the average number of goblet cells; average Paneth cell count; average number of endocrinocytes.

The statistical methods of the study evaluated the correctness of the distribution of traits by each of the variations obtained, the average values for each trait studied, standard errors and standard deviations. The significance of the difference between independent micrometric values in the normal distribution of features was determined by the Student's test.

Results

The study found that the ileum of rabbits is a tubular organ which is made of mucous, submucosal, muscular and serous membranes. The total wall thickness averaged $401.3 \pm 12.4 \mu\text{m}$.

The average thickness of the mucous membrane was $288.6 \pm 8.3 \mu\text{m}$. The mean thickness of the submucosa was $17.12 \pm 2.25 \mu\text{m}$. The average thickness of the muscle was determined in the range $97.47 \pm 1.35 \mu\text{m}$, and the mean thickness of the serous membrane was $8.161 \pm 1.871 \mu\text{m}$. As part of the mucous membrane of the ileum was determined epithelial plate, which was represented by a single-layer columnar epithelium. Below it was a lining of the mucous membrane, which in turn consisted of loose fibrous connective tissue, and even more deeply visualized a muscular lining of the mucous membrane, which was built of several layers of smooth myocytes (Fig. 1).

On histological preparations the mucous membrane of the ileum of the rabbits formed a kind of relief pattern in the form of villi and crypts. The villi of the ileum of the ileum had a finger-like shape, and their average height was $179.2 \pm 3.6 \mu\text{m}$. The average thickness of the villi varied depending on its topography. Thus, the mean apical width of the villi was $33.97 \pm 0.54 \mu\text{m}$ and the mean basal width was $39.22 \pm 0.55 \mu\text{m}$. In the middle of the villus was a lymphatic duct that was closely linked to the muscular plate of the ileum of the ileum. Its average lumen diameter was $12.16 \pm 1.81 \mu\text{m}$. Reticular fibers and a large number of hemomicrocirculatory bed elements were visualized

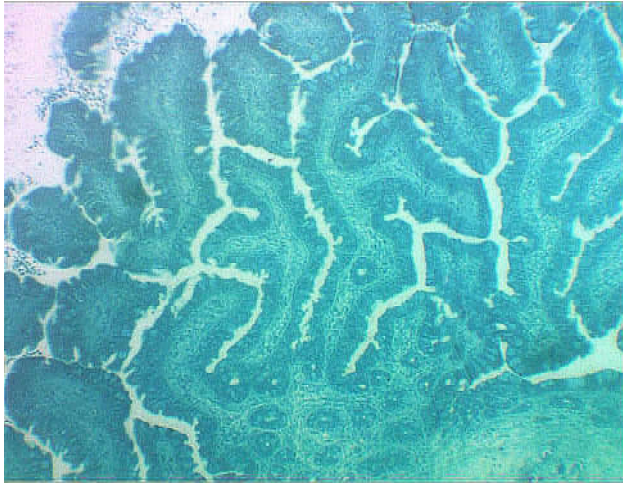


Fig. 1. General plan for the structure of the mucous membrane of the ileum. Thin section. Methylene blue. x100.

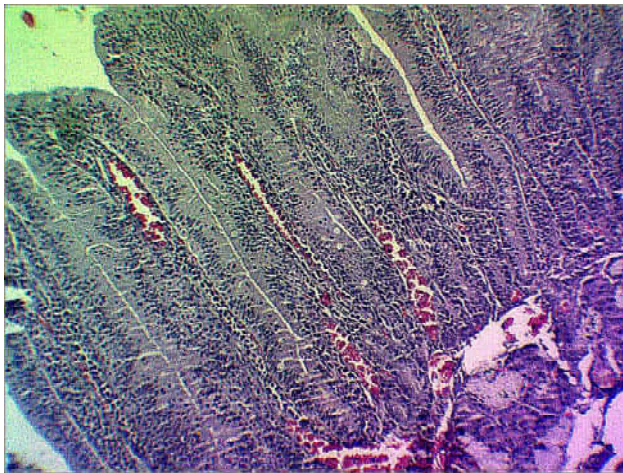


Fig. 2. Microenvironment of the villi of the ileum. Semi-thin section. Hematoxylin and eosin. x400.

around it, but capillaries prevailed among the latter (Fig. 2).

The cellular composition of the ileum of the ileum was represented by different types of epitheliocytes. On histological preparations their varieties were clearly visualized: enterocytes with banded edges, goblet exocrinocytes, microfold cells. At the same time, prismatic cells with oxyphilic cytoplasm and a well-developed nuclear apparatus were visualized among the above-mentioned epitheliocytes. In our opinion, these are stem cells, which in humans are localized only in the crypts and in a small number in the basal departments of the villi, and in rabbits they are also available in the lateral departments.

Cells with a striped border were located mainly in the apical departments of the villi and had a cylindrical shape, an oval nucleus. A well-developed granular endoplasmic reticulum and lysosome complexes were visualized in their cytoplasm. The average number of columnar enterocytes with a border in the composition of the ileum of rabbits was 92.35 ± 1.84 in 10 fields of view. The goblet exocrinocytes were located predominantly in the middle departments of

the villi. Their mean number was 10.98 ± 2.14 in 10 fields of view. They had an elongated shape that, in our opinion, depended on the secretory cycle phase of these exocrinocytes. At the ultramicroscopic level, they had a variable shape: with the accumulation of secretions, the apical part expanded and the basal part narrowed and contained a nucleus and an endoplasmic reticulum. Above the nucleus, a well-developed Golgi complex was visualized (Fig. 3).

At the same time, elements of the diffuse endocrine system were visualized among the cellular composition of the epithelial layer of the ileum of the ileum. At the optical level, endocrinocytes had a triangular or polygonal shape with a sharply basophilic cytoplasm and, as a rule, capillaries were visualized next to them. The average number of endocrinocytes was 0.741 ± 0.081 in 10 fields of view. At the ultramicroscopic level, endocrinocytes had a rounded nucleus with a large amount of heterochromatin. The moderately developed granular endoplasmic reticulum and the Golgi complex were determined in the nucleolar zone. In the cytoplasm of these cells, a large number of secretory granules with signs of polymorphism were determined. It was noted that the cells of the diffuse endocrine system had no direct contact with the lumps of the villi and were separated from them by a group of little differentiated cells. Also, intraepithelial lymphocytes with classical structure were visualized among the cellular composition of the epithelial layer of the ileum of the ileum, and their average number was 0.382 ± 0.041 in 10 fields of view.

Also among the cellular composition of the epithelial layer of the mucous membrane of the villi in its basal divisions were found micro-folding cells, which on their apical surface formed the invagination of the nuclear membrane. Histotopographically, these cells were usually located near the clusters of lymphoid tissue. When visualizing the electronograms, it is noteworthy that under the micro-folding cells there is no basement membrane, that is, the

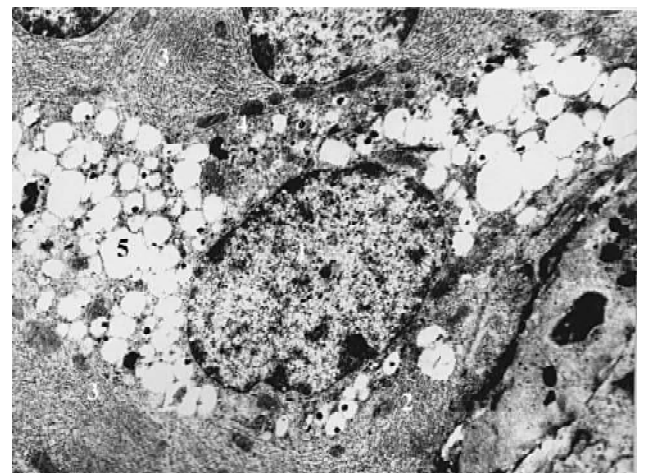


Fig. 3. Ultrastructure of goblet exocrinocytes in the composition of rabbit ileum villi. Electronogram. x10000.

impression that the above cells perforate the latter and due to such interaction is a close connection through the micro-folding cells of the lymph nodes of the lining of the lamina.

Histological preparations between adjacent villi in the depth of the mucous membrane closer to the submucosal layer were determined by the ingrowth into the own plate of the epithelial layer in the form of tubes. By analogy with such structures in the human mucosa, we identified them as crypts whose average diameter was $20.48 \pm 1.63 \mu\text{m}$. These structures were located with respect to the epithelial layer at different and different depths, and their mean depth was $78.66 \pm 16.11 \mu\text{m}$. The average number of crypts was 7.641 ± 0.162 in 10 fields of view.

Among the cellular elements of the crypts were determined: columnar enterocytes with a border whose average number was 22.67 ± 2.18 in 10 fields of view; unbranched columnar enterocytes whose mean number was 30.17 ± 3.62 in 10 fields of view; goblet-shaped exocrinocytes whose mean number was determined at 31.02 ± 3.62 in 10 fields of view; Paneth cells had an average number 11.67 ± 1.84 in 10 fields of view; endocrinocytes of the diffuse endocrine system associated with the mucosa, the average number of which was determined at 7.821 ± 2.362 in 10 fields of view; intraepithelial lymphocytes the average number of which was 1.242 ± 0.061 in 10 fields of view.

Among the elements of the hemomicrocirculatory bed were identified arterioles, capillaries and venules. They were located in both the mucous and submucosal membranes. At the optical level, the arterioles were visualized as structures that clearly contained three membranes and were formed by a layer of endothelial cells located on an elastic membrane; layer of smooth myocytes; and externally they were covered with a non-continuous layer of adventitial fibroblasts. In the mucosa, the mean outer diameter of the arterioles was $11.08 \pm 0.84 \mu\text{m}$; their average lumen diameter was determined at $7.222 \pm 0.911 \mu\text{m}$; the mean wall thickness was $3.863 \pm 0.091 \mu\text{m}$. The capacity (Wogenworth index) of the arterioles of the mucous membrane of the ileum of rabbits was 135.5 ± 4.4 . The submucosal arterioles had an average outer diameter at $10.43 \pm 0.81 \mu\text{m}$. Their average lumen diameter was determined at $9.732 \pm 0.412 \mu\text{m}$, the mean wall thickness was $0.712 \pm 0.061 \mu\text{m}$, and the Wogenworth index was 14.91 ± 0.86 .

Capillaries on histological specimens were defined as vessels of small caliber whose wall was formed by a layer of endothelium located on the basement membrane and a discontinuous layer of serocytes, and unlike the arterioles, the elastic membrane was absent. In the mucosa, the capillaries had an average total diameter $6.153 \pm 0.092 \text{ mm}$. Their average lumen diameter was $5.283 \pm 0.084 \text{ mm}$, the mean wall thickness was $0.872 \pm 0.093 \text{ mm}$, and the Wogenworth index was 35.69 ± 1.18 . In the submucosal layer, the average outer diameter of the capillaries was $6.913 \pm 0.042 \text{ mm}$, the average lumen diameter was $6.132 \pm 0.022 \text{ mm}$, the average wall thickness was

determined at $0.781 \pm 0.023 \text{ mm}$, and the Wogenworth index was determined at 27.09 ± 1.02 .

Venules on histological specimens were defined as irregularly shaped structures and endothelial cells on the basement membrane were visualized as part of their walls, which were covered externally by a continuous layer of fibroblasts. In the mucosa, the outer diameter of the venules was $12.06 \pm 0.81 \text{ mm}$, the average lumen diameter was determined at $8.192 \pm 0.873 \text{ mm}$, the average wall thickness was $3.873 \pm 0.841 \text{ mm}$, and the Wogenworth index was 116.8 ± 3.24 . In the submucosal layer, the mean outer diameter of the venules was $12.96 \pm 0.77 \text{ mm}$, the average lumen diameter was $10.19 \pm 0.85 \text{ mm}$, and the mean wall thickness was $2.772 \pm 0.032 \text{ mm}$, and the Wogenworth index was determined at 61.74 ± 1.91 .

Discussion

Summarizing and analyzing the results obtained, it should be noted that the overall organization of the intestinal wall corresponds to the basic laws of the structure of the ileum of the person, which is confirmed by the data [1]. However, due to the type of nutrition, body placement in space, body weight and linear size of rabbits, they have non-human morphometric measures of medium size, both the wall itself and its layers.

Structural and functional unit of the ileum in humans and rabbits should be considered the crypt villus system. Among the cellular composition of villi in rabbits, as in humans, were columnar cells with a border, goblet exocrinocytes, cells of the diffuse endocrine system associated with the mucosa and intraepithelial lymphocytes. In contrast to the cellular composition of the human ileum, according to data [10], microfold cells that were located in their basal compartments were found in the composition of the villi of the rabbits ileum.

Among the cellular elements of the villi of the mucous membrane of the ileum of the rabbits were columnar enterocytes with a border of their percentage of the total number of cellular elements of the villi was 88.34 %, which is related to their main function. Goblet-like exocrinocytes accounted for 10.51 %, endocrinocytes - 0.71 %, intraepithelial lymphocytes - 0.36 % and poorly differentiated epitheliocytes in the villus composition accounted for 0.11 % of the total cell pool. Thus, the system of the cellular pool of the villi of the ileum of the rabbits provides the processes of absorption of substances, the production and excretion of mucous secretions in the cavity of the villi, and also participates in endocrine regulation and maintenance of immune surveillance. The poorly differentiated cells that are found in the basal departments of the villi belong, in our opinion, to the cambial elements.

Among the cellular elements of crypts, as well as in the crypts of the ileum of the human are defined structural components, namely: columnar enterocytes with a border, columnar enterocytes without a border, goblet

exocrinocytes, Paneth cells, endocrinocytes, intraepithelial cells. Analyzing the distribution of cellular elements in crypts as a percentage, another tendency for the cryptocurrency to function as part of a morpho-functional unit is determined. Thus, among the whole cell pool crypts, columnar enterocytes with a border were 21.49 %, columnar enterocytes without a border were 28.85 %, goblet-like exocrinocytes - 29.66 %, Paneth cells - 11.16 %, endocrinocytes diffuse endocrine system - 7.48 %, intraepithelial lymphocytes - 1.24 %, low-differentiated cells - 0.17 %. Thus, remodeling of the structural components of crypts relative to similar components of the villi indicates a redistribution of functional load toward mucous secretion and secretion, local enhancement of secretion of digestive enzymes and enhancement of local immune protection.

The original data obtained from the study are promising in the future work. They will serve as controls for further experimental development in surgery on the ileum to select the optimal suture material for stitching its wound defect.

References

- [1] Antonyuk, O. P. (2016). Features of organogenesis digestive system of the human. *Bulletin of problems in biology and medicine*, 4(133), 279-284.
- [2] Bilash, S. M. (2013). [Influence of Cryopreserved Placenta on the Morphofunctional State of Stomach Pyloric Glands' Exocrinocytes at Acute Inflammation Processes. *Bulletin of problems in biology and medicine*, 2(99), 224-227.
- [3] Cardamone, C., Parente, R., De Feo, G., & Triggiani, M. (2016). Mast cells as effector cells of innate immunity and regulators of adaptive immunity. *Immunology letters*, 178, 10-14. doi: 10.1016/j.imlet.2016.07.003
- [4] Gomes, J. R., Ayub, L. C., dos Reis, C. A., Machado, M. J., da Silva, J., Omar, N. F., & de Miranda Soares, M. A. (2017). Goblet cells and intestinal alkaline phosphatase expression (IAP) during the development of the rat small intestine. *Acta histochemica*, 119(1), 71-77. doi: 10.1016/j.acthis.2016.11.010
- [5] Hryn, V. H., Kostylenko, Y. P., Yushchenko, Y. P., Ryabushko, M. M., & Lavrenko, D. O. (2018). Comparative histological structure of the gastrointestinal mucosa in human and white rat: a bibliographic analysis. *Wiadomosci lekarskie* (Warsaw, Poland: 1960), 7(71), 1398-1403. PMID: 30448817
- [6] Hryn, V. H., Kostylenko, Y. P., Yushchenko, Y. P., Lavrenko, A. V., & Ryabushko, O. B. (2018). General comparative anatomy of human and white rat digestive systems: a bibliographic analysis. *Wiadomosci lekarskie* (Warsaw, Poland: 1960), 71(8), 1599-1602. PMID: 30684346
- [7] Hryn, V. H., Kostylenko, Y. P., & Yachmin' A. I. (2019). Features of white rats stomach anatomical structure. *World of medicine and biology*, 1(67), 133-137. doi: 10.26724/2079-8334-2019-1-67-133
- [8] Hryn, V. H., Kostylenko, Y. P., Bilash, V. P., & Tarasenko, Y. A. (2019). Features of angioarchitecture of the albino rats stomach and small intestine. *Wiadomosci lekarskie* (Warsaw, Poland: 1960), 3(72), 311-317. PMID: 31050973
- [9] Hryn, V. H., Kostylenko, Y. P., Bilash, V. P., & Ryabushko, O. B. (2019). Microscopic structure of albino rats' small intestine. *Wiadomosci lekarskie* (Warsaw, Poland: 1960), 5(72), 733-738. PMID: 31175762
- [10] Hryn V. Kostylenko Y., Korchan, N., & Lavrenko, D. (2019). Structural form of the follicle-associated epithelium of Peyer's patches of the albino rats' small intestine. *Georgian medical news*, 9(294), 118-123. PMID: 31687962
- [11] Kolesnik, O. O. (2006). Treatment of patients with stromal tumors of the colon (GIST). *Oncology*, 3(8), 272-277.
- [12] Nawaz, M., Shah, N., Zanetti, B. R., Maugeri, M., Silvestre, R. N., Fatima, F., ... & Valadi, H. (2018). Extracellular vesicles and matrix remodeling enzymes: the emerging roles in extracellular matrix remodeling, progression of diseases and tissue repair. *Cells*, 7(10), 167. doi: 10.3390/cells7100167
- [13] Lutsyk, O. D., Chaykovskyy, Yu. B. [Ed.] (2018). *Histology. Cytology. Embryology: a textbook*. Vinnytsia: Nova knyha.
- [14] Omar, N. F., Gomes, J. R., Neves, J. D. S., & Novaes, P. D. (2018). Effects of loss of occlusal contact on the expression of matrix metalloproteinase-2, membrane type 1-MMP, tissue inhibitor of the mmP-2, eruption rate, organization and resistance of collagen fibers of the rat incisor periodontal ligament. *Journal of periodontal research*, 53(1), 40-46. doi: 10.1111/jre.12484
- [15] Phillips, T. M., Fadia, M., Lea-Henry, T. N., Smiles, J., Walters, G. D., & Jiang, S. H. (2017). mmP2 and mmP9 associate with crescentic glomerulonephritis. *Clinical kidney journal*, 10(2), 215-220. doi: 10.1093/ckj/sfw111
- [16] Pronina, O. M., Koptev, M. M., Bilash, S. M., & Yeroshenko, G. A. (2018). Response of hemomicrocirculatory bed of internal organs on various external factors exposure based on the morphological research data. *World of medicine and biology*, 1(63), 153-157. doi: 10.26724/2079-8334-2018-1-63-153-157
- [17] Ryngach, N. O., & Keretsman, A. O. (2015). Diseases of the digestive system: historical parallels changes in classification and epidemiological situation. *Family medicine*, 4, 137-141.
- [18] Xu, H., Bin, N. R., & Sugita, S. (2018). Diverse exocytic pathways for mast cell mediators. *Biochemical Society Transactions*, 46(2), 235-247. doi: 10.1042/BST20170450

Conclusions

1. The ileum of rabbits conforms to the general principles of organization of the intestinal tube of a person, which provides an opportunity for experimental development and implementation of the results.

2. Structural-functional unit of the ileum of rabbits should be considered the villus-crypt system. There is no significant difference between the cellular content of the villus and the crypt in comparison with the similar structure of the villus-crypt system in humans.

3. The peculiarities of the structure of the mucous membrane of the ileum of rabbits in comparison with similar structures in humans is the difference in the cytographic principle of the location of cellular components.

4. The basic organization of the hemomicrocirculatory bed in the mucous and submucous membranes does not differ from the similar system of the ileum of the person.

5. New, original data obtained may further serve as benchmarks for various types of experimental studies.

СТРУКТУРНА ОРГАНІЗАЦІЯ КЛУБОВОЇ КИШКИ ЛАБОРАТОРНИХ ТВАРИН В НОРМІ ТА У ПОРІВНЯЛЬНО-ВИДОВОМУ АСПЕКТІ
Сидоренко М.І.

В останні десятиріччя широкого розповсюдження набули захворювання травної системи, які потребують негайного, як

терапевтичного, так і хірургічного лікування і тому постає закономірне завдання оптимізації існуючих технологій та пошуку нових способів корекції вищезгаданих нозологій. Доклінічні дослідження таких розробок проводять виключно на лабораторних тваринах і знання морфологічних особливостей їх будови для подальшого порівняння з морфологією аналогічних органів людини є актуальним завданням сучасної медико-біологічної науки. Метою роботи було вивчення структурної організації клубової кишки кролів у порівняльно-видовому аспекті та для отримання контрольних даних щодо її морфологічних особливостей. В роботі використані адекватні методи досліджень відповідно до поставленої мети, а саме: гістологічний, гістохімічний, електронно-мікроскопічний, морфометричний і статистичний та були вивчені біоптати клубової кишки 10 кролів. Оцінили правильність розподілу ознак за кожним із отриманих варіаційних рядів, середні значення за кожною вивченою ознакою, стандартні помилки та стандартні відхилення. Достовірність різниці значень між незалежними мікрометричними величинами при нормальному розподілі ознак визначали за критерієм Ст'юдента. В роботі охарактеризовані основні структурні компоненти клубової кишки кролів і порівняні з аналогічними структурами клубової кишки людини. Визначено, що клубова кишка кролів, як і у людини складається з чотирьох оболонок: слизової, підслизової, м'язової і серозної. Слизова оболонка побудована з епітеліального пласту, який розташовується на базальній мембрані і м'язовій пластинці і містить у своєму складі клітинні елементи (екзокриноцити, ентероцити різних видів, елементи дифузної ендокринної системи, асоційованої зі слизовою оболонкою, інтраепітеліальні лімфоцити), кровоносні і лімфатичні судини та нервові закінчення. Підслизова оболонка складається з пухкої волокнистої сполучної тканини, котра у своєму складі містить колагенові і ретикулярні волокна, елементи дифузної лімфоїдної тканини, кровоносні судини і нервові закінчення. М'язова і серозна оболонки побудовані аналогічно клубовій кишці людини. Таким чином, після проведеного дослідження визначено, що морфологічна організація клубової кишки кролів на світлооптичному та електронно-мікроскопічному рівнях має загальні закономірності будови аналогічні клубовій кишці людини.

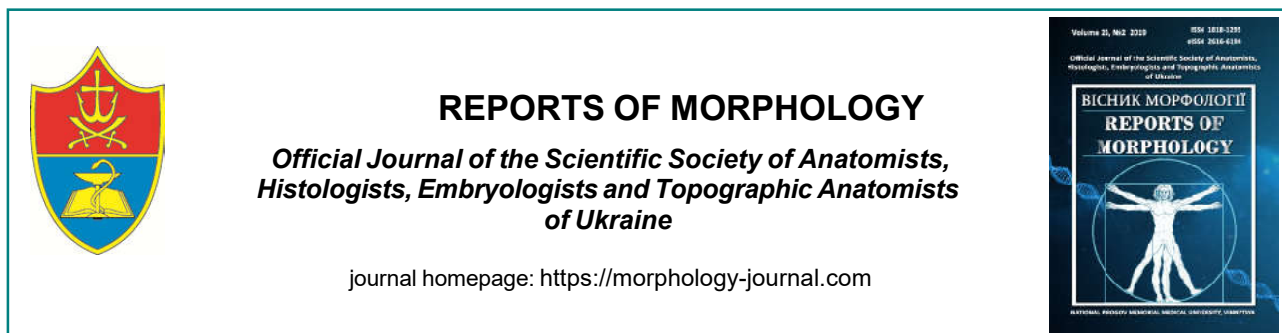
Ключові слова: клубова кишка, оболонки клубової кишки, екзокриноцити, ендокриноцити, лімфоцити, артеріоли, капіляри, венули.

СТРУКТУРНАЯ ОРГАНИЗАЦИЯ ПОДВЗДОШНОЙ КИШКИ ЛАБОРАТОРНЫХ ЖИВОТНЫХ В НОРМЕ И В СРАВНИТЕЛЬНО-ВИДОВОМ АСПЕКТЕ

Сидоренко М. И.

В последние десятилетия широкое распространение получили заболевания пищеварительной системы, требующие немедленного, как терапевтического, так и хирургического лечения и поэтому возникает закономерная задача поиска новых и оптимизация существующих технологий и способов коррекции вышеуказанных нозологий. Доклинические исследования таких разработок проводятся исключительно на лабораторных животных и знания морфологических особенностей их строения для последующего сравнения с морфологией аналогичных органов человека является актуальной задачей современной медико-биологической науки. Целью работы было изучение структурной организации подвздошной кишки кроликов в сравнительно-видовом аспекте и для получения контрольных данных относительно её морфологических особенностей. В работе использованы адекватные методы исследований в соответствии с поставленной целью, а именно: гистологический, гистохимический, электронно-микроскопический, морфометрический и статистический и были изучены биоптаты подвздошной кишки 10 кроликов. Оценили правильность распределения признаков по каждому из полученных вариационных рядов, средние значения по каждому изученному признаку, стандартные ошибки и стандартные отклонения. Достоверность различий значений между независимыми микрометрическими величинами при нормальном распределении признаков определяли по критерию Ст'юдента. В работе охарактеризованы основные структурные компоненты подвздошной кишки кроликов и сравнению с аналогичными структурами подвздошной кишки человека. Определено, что подвздошная кишка кроликов, как и у человека состоит из четырех оболочек: слизистой, подслизистой, мышечной и серозной. Слизистая оболочка построена из эпителиального пласта, который располагается на базальной мембране и мышечной пластинке и содержит в своем составе клеточные элементы (экзокриноциты, энтероциты различных видов, элементы диффузной эндокринной системы, ассоциированной со слизистой оболочкой, интраэпителиальные лимфоциты), кровеносные и лимфатические сосуды и нервные окончания. Подслизистая оболочка состоит из рыхлой волокнистой соединительной ткани, которая в своем составе содержит коллагеновые и ретикулярные волокна, элементы диффузной лимфоидной ткани, кровеносные сосуды и нервные окончания. Мышечная и серозная оболочки построены аналогично подвздошной кишке человека. Таким образом, после проведенного исследования установлено, что морфологическая организация подвздошной кишки кроликов на светоптическом и электронно-микроскопическом уровнях имеет общие закономерности строения аналогичные подвздошной кишке человека.

Ключевые слова: подвздошная кишка, оболочки подвздошной кишки, экзокриноциты, ендокриноциты, лимфоциты, артериолы, капилляры, венулы.



REPORTS OF MORPHOLOGY

Official Journal of the Scientific Society of Anatomists,
Histologists, Embryologists and Topographic Anatomists
of Ukraine

journal homepage: <https://morphology-journal.com>

Modeling of viral-bacterial infections against antibiotic-induced intestinal dysbiosis

Bobyry V.V.¹, Stechenko L.O.¹, Shyrobokov V.P.¹, Cryvosheyeva O.I.¹, Nazarchuk O.A.², Ponyatovskyi V.A.¹, Chuhrai S.M.¹

¹Bogomolets National Medical University, Kyiv, Ukraine

²National Pirogov Memorial Medical University, Vinnytsya, Ukraine

ARTICLE INFO

Received: 25 February, 2019

Accepted: 27 March, 2019

UDC: 616-022.7:578/

.579]:001.57:616.34-008.87-

008.6:615.33

CORRESPONDING AUTHOR

e-mail: nazarchukoa@gmail.com

Nazarchuk O.A.

The study of the role of viral-bacterial associations in the etiology of acute intestinal infections is considered new to medical microbiology. The purpose of the study was to determine the effect of viral-bacterial associations on the manifestation of virulence of pathogens and the degree of development of structural-morphological disorders of the internal organs in animals with antibiotic-induced dysbiosis. In a study of 210 white laboratory mice, BALB/c lines formed dysbiosis using antibacterial agents (ampicillin, gentamicin, metronidazole) followed by simulation of the experimental infection. To simulate salmonella infection, mice were infected with a clinical strain of Salmonella typhimurium intraperitoneally. Similarly, the animals were infected with Coxsackie B3 test culture virus (dose 10^6 TCD₅₀). The sensitivity of mice to Coxsackie B and salmonella viruses was examined for mortality and disease characteristics. The animals were removed from the experiment 24 h after infection, electronically microscopically studied structural and morphological changes of the internal organs were performed. There was no statistically significant difference in morbidity (23.33-26.66 %) and mortality (16.66-20.0 %) of mice infected with Coxsackie virus with dysbiotic disorders and preserved microflora. Dysbiotic conditions have been shown to lead to associated viral-bacterial infections in animals and, accordingly, an increase in the incidence of disease and death in experimental animals. Against the background of disturbance of the composition of the normal intestine microbiota in viral bacterial infections, pronounced degenerative changes in the internal organs of animals were established, with signs of generalization. Electrogram data showed the appearance of activation of immunocompetent cells of the body in viral-bacterial infection in animals with impaired intestine microbiocenosis.

Keywords: antimicrobials, bacteria, viruses, dysbiosis, intestinal microbiocenosis, intestinal infections.

Introduction

Acute intestinal infections (All) remain one of the world's most pressing health care issues [19]. According to WHO, about 1.7 billion cases of acute diarrhea are reported annually alone in children [1]. Among microorganisms of bacterial nature, the main agents of All are representatives of the family *Enterobacteriaceae* [14, 15]. Viruses are also important etiologic factors of All in children, especially in early childhood. Viruses are the cause of acute gastroenteritis due to noroviruses, which account for almost a fifth of All; rotaviruses, especially in young children, cause more than 200,000 deaths annually worldwide [1, 6, 8]. Enteroviruses also occupy a significant niche in this respect [9, 13].

An important part of the All problem is associated infections due to the impact of microorganisms of different species. In recent years, there has been evidence of an increase in the number of such infections, including virus-bacterial infections, especially in the young group. According to scientific literature, it is known that in the conditions of the present virus-associated intestinal infection is recorded in 80-90 % of cases [10].

The issue of viral-bacterial associations is not new to medical microbiology. Back in the middle of the last century, Academician G. Burgwitz proved the ability of yeast cells under the influence of the virus to change their morphological and physiological properties [16]. Interesting

and valuable, especially for practical medicine, is the degree of manifestation of virulent properties of pathogens in conditions of mixed infection. The enhancement of the pathogenic effect of one microorganism by another has been repeatedly shown in experiments aimed at determining virulence [18]. It should be noted that some virulent bacterial strains, in contrast to avirulent, on the contrary, can have an inhibitory effect on the reproduction of viruses, although in general, viral-bacterial associations are more often characterized by mutual enhancement of pathogens of both microorganisms [5].

However, if the issue of viral-bacterial associations is generally studied extensively, the idea of modeling the pathogenic impact of such associations on animals with dysbiosis is new. This is extremely important today also because the problem of impaired composition of the intestinal microflora is of particular importance in connection with the growth of chronic diseases of the digestive system, as well as the widespread use of antibiotics. Undoubtedly, the gastrointestinal tract is an environment for one of the most complex microbial ecosystems and further research in this area will open up new opportunities for the treatment of infectious diseases.

The purpose of this work is to investigate the effect of viral-bacterial associations on the manifestation of virulence of pathogens and the degree of development of structural-morphological disorders of the internal organs in animals with antibiotic-induced dysbiosis.

Materials and methods

The research subjects were white laboratory mice of the *BALB/c* line. In total, 210 mice were used in the experiment, which were bred in the vivarium of Bogomolets National Medical University.

Antibacterial drugs were used to form dysbiotic conditions, the daily dose of which for animals was 10 mg for ampicillin and metronidazole, and 2.9 mg for gentamicin [3]. The simulation of experimental infections was started 48 hours after discontinuation of antibacterial agents for dysbiosis formation. Experimental salmonellosis was modeled by infecting mice with a pathogenic strain of *Salmonella typhimurium* isolated and identified at the Kyiv City Clinical Hospital No. 4 (Clinical Isolate No. 7683). The infection of the animals with bacteria was performed intraperitoneally (i/p) in a volume of 0.5 ml (1 billion microbial bodies) per person. Coxsackie B3 viruses were used as test viruses. Infection of animals by viruses was also performed intraperitoneally at a dose of 10^6 TCD₅₀ per animal.

All experimental animals were divided into 7 groups (30 animals in each group). Group 1 - animals with no dysbiotic disorders infected with Coxsackie B3; group 2 - animals with no dysbiotic disorders, infected with salmonella; group 3 - animals with no dysbiotic disorders, infected with Salmonella and Coxsackie B3; group 4 - animals with dysbiosis infected with Coxsackie B3; group

5 - animals with dysbiosis infected with salmonella; group 6 - animals with dysbiosis infected with Coxsackie B3 and salmonella; group 7 - intact, control. The observation period for animals was 21 days. The comparative susceptibility of mice to Coxsackie B virus and salmonella was studied in terms of mortality and disease (decreased activity, lethargy, trembling, furiousness, diarrhea). The death of animals when infected with Coxsackie B3 virus was observed for 3-6 days, and for Salmonella infection for 3-4 days. Removal of some animals from the experiment and study of structural and morphological changes of internal organs were carried out 24 hours after infection.

For electron microscopic examination, small intestine, spleen, and liver pieces of 1 mm³ size were selected. They were first fixed with a buffer solution of glutaraldehyde retainer for 1 h, then, after washing with buffer, was fixed for 1 h with a buffer solution of 1% osmium tetroxide. The sections were obtained using glass knives on an ultramicrotome "LKB III" (Sweden) and examined using an electron microscope "PEM-125" (Ukraine). Before microscopy, sections were counterstained with uranyl acetate and lead citrate according to the standard procedure.

According to the results of the study, statistical processing was carried out using the software for statistical data processing Microsoft Excel 2016 and "Statistica 5.5" (owned by the Pirogov National Technical University, licensed number AXXR910A374605FA). Probability analysis was performed by Student's t-test. The difference between the indicators was considered statistically significant when the probability of the null hypothesis was less than 5 % ($p < 0.05$).

Results

The study found that there was no statistically significant difference in the incidence and mortality of animals in groups of mice with dysbiotic disorders and animals with persistent microflora infected with Coxsackie virus: the mortality of mice in both groups was determined in the range of 16.66-20.0 %, and diseases were observed in 23.33 % of cases in animals with preserved microflora and in 26.66 % of cases in animals with dysbiosis (Table 1).

It was proved that in the group of animals with preserved microflora the mortality was 16.66 %, and in the group of animals with dysbiosis it increased by 6.66 % and was 23.33 %, while the incidence of infection in the group of animals with preserved microflora was 20.0 %, and in animals with dysbiosis - 30.0 %.

In the group of animals in which virus-bacterial infections were modeled against the background of pronounced antibiotic-induced dysbiosis, there was an increase in the death of animals by 20.0 % and an increase in the incidence of disease by 16.66 %, compared with the group of experimental animals with viral-bacterial infections conducted the experiment without the formation of dysbiotic states (see table. 1).

Electron microscopic examination of internal organs

Table 1. Comparative sensitivity of mice with intestinal dysbiosis to Coxsackie B3 viruses, salmonella and their combinations.

Manifestation	Animals with preserved microbiocenosis						Animals with dysbiosis					
	coxsacks B3 (n=30)		salmonella (n=30)		coxsacks B3 + salmonella (n=30)		coxsacks B3 (n=30)		salmonella (n=30)		coxsacks B3 + salmonella (n=30)	
	abs.	%	abs.	%	abs.	%	abs.	%	abs.	%	abs.	%
Death	5	16,66	5	16,66	7	23,33	6	20,0	7	23,33	13	43,33
Signs of illness	7	23,33	6	20,0	9	30,0	8	26,66	9	30,0	14	46,66
No changes	18	60,0	19	63,33	13	43,33	16	53,33	14	46,66	3	10,0

Notes: the figures in the table indicate the average frequency of detection of a feature, abs. and %.

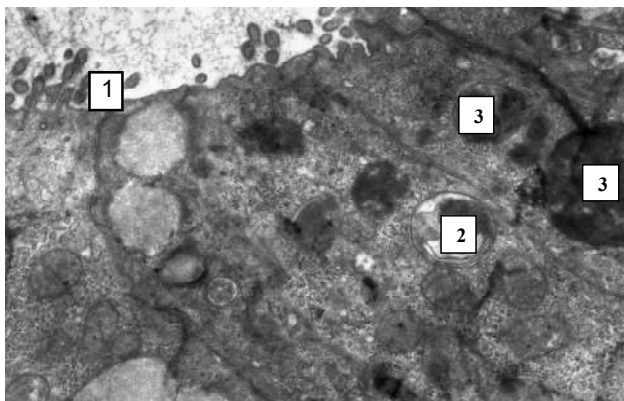


Fig. 1. Electron micrograph. The intestine of mice with dysbiosis after infection with Coxsackie B virus and *Salmonella typhimurium*. Desquamation of microvilli of epitheliocytes (1), cytoplasm filled by autophagosomes (2) and lysosomes (3). Magnification x19200.

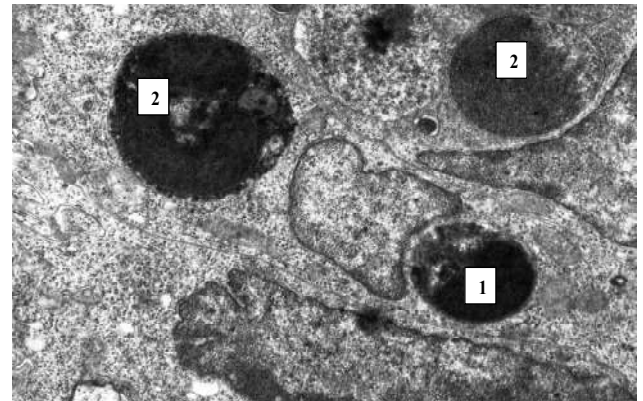


Fig. 2. Electron micrograph. The intestine of mice with dysbiosis after infection with Coxsackie B and *Salmonella typhimurium*: lymphocyte (1), reticular cells with apoptotic bodies (2). Magnification x12000.

(liver, spleen and small intestine) of animals with preserved microflora infected with Coxsackie B virus (experimental group 1) revealed no pathological changes.

As a result of the study of samples of internal organs (liver,

spleen and small intestine) in the intestines of laboratory animals with dysbiosis after viral-bacterial infection, marked structural changes were recorded, which were manifested by total desquamation of microvilli, plasma membrane smoothness, mitochondrial swelling and autophagosome formation (Fig. 1).

In some enterocytes, signs of development of pronounced apoptotic changes were observed, which were accompanied by compaction of cytoplasm, organelles, and formation of apoptotic bodies, which shifted to the apical membrane and were removed from a number of epithelial cells (Fig. 2).

Microbial cells were detected both in the epithelial lining of the mucous membrane and in the lumen of the intestine surrounded by mucus and cellular detritus (Fig. 3A). Signs of minor disorders in the hemomicrocirculatory bed and dystrophic changes in the mucous membrane and submucosal basis of the intestine were noted. The migration of neutrophils, monocytes

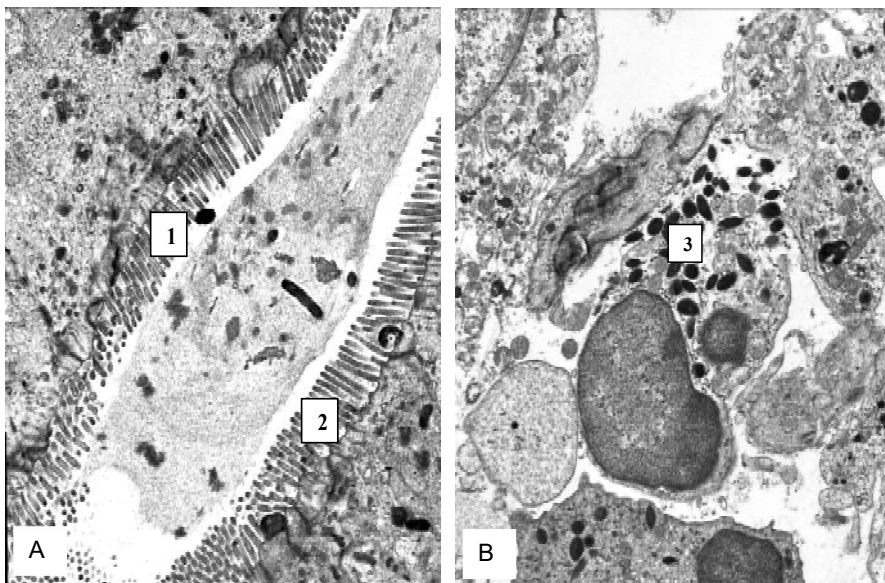


Fig. 3. Electron micrograph. The intestine of mice with dysbiosis after infection with Coxsackie B and *Salmonella typhimurium*: intestinal lumen (1), epitheliocytes microvilli (2) (A), eosinocytes in the inflammatory zone (3) (B). Magnification x12000 (A), x9600 (B).

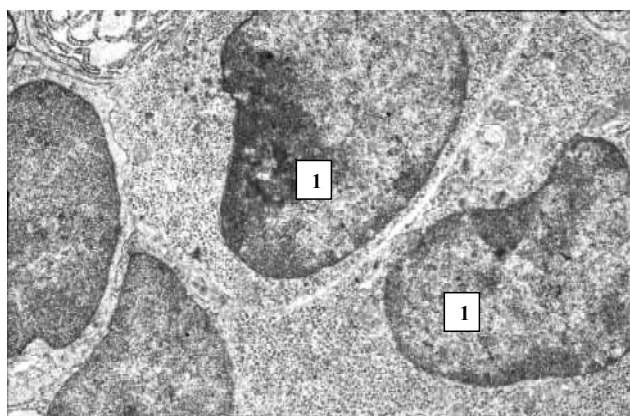


Fig. 4. Electron micrograph. The spleen of mice with dysbiosis after infection with Coxsackie B and *Salmonella typhimurium*: accumulation of white pulp lymphoblasts (1). Magnification x11200.

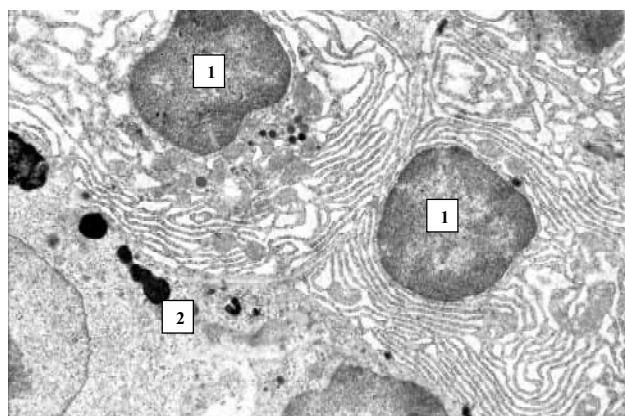


Fig. 5. Electron micrograph. The spleen of mice with dysbiosis after infection with Coxsackie B virus and *Salmonella typhimurium*. Plasmacytes (1), macrophage fragment (2). Magnification x11200.

and lymphocytes into the intestine interstitium, expansion and swelling of the interstitial space, in which free microbial cells were found (see Fig. 3A, B). Activated macrophages were detected in these sites, in the cytoplasm of which microbial bodies were present with no signs of destruction, which should be considered a phenomenon of endocytobiosis. Dystrophy of superficial epitheliocytes and an increase in the number of neutrophils were also noted. The accumulation of microorganisms in the cytoplasm of epitheliocytes with predominant localization around the nucleus has been determined. In addition, increased infiltration of the mucosa by macrophages was noted.

In animals with dysbiosis, changes in the morphofunctional state of the organs of the immune system were also observed in virus-bacterial infection, in particular in the spleen a decrease in the volume fraction

of periarterial lymphoid clutches and an increase in the proportion of light centers of lymph nodes (Fig. 4) were detected.

The introduction of salmonella to animals in the spleen tissue revealed ultrastructural signs of an increase in the number of lymphoblasts, plasma cells with enlarged tubules of the granular endoplasmic reticulum (Fig. 5).

Studies of the morphological structure of the spleen under these conditions allowed us to establish the signs of epithelioid cell granuloma formation. The latter were formed by giant, centrally located granuloma hypertrophic and atrophic epithelial cells located along its periphery. Specific inclusions were recorded in the cytoplasm of such cells. It was found that giant cells were usually surrounded by immunocompetent cells (lymphocytes, macrophages, etc.; Fig. 6A, B).

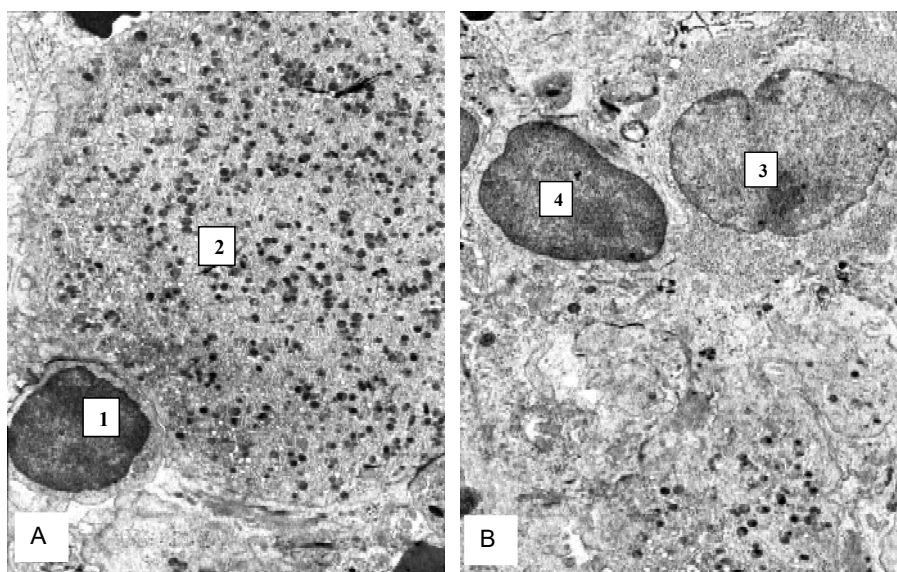


Fig. 6. Electron micrograph. The spleen of mice with dysbiosis after infection with Coxsackie B virus and *Salmonella typhimurium*. T-lymphocyte (1), giant cell with inclusions in the cytoplasm (2) (A), atrophy of epithelial cells at the periphery of the granuloma surrounded by lymphoblast (3) and macrophage (4) (B). Magnification x7000.

As a result of the introduction of experimental mice Coxsackie virus and salmonella in the liver, necrotic changes in the enlightenment of the nuclei due to the violation of the ratio of eu- and heterochromatin were recorded. The cytoplasm of such cells was characterized by complete or partial cytolysis, dissolution in the main cytosol (Fig. 7A-D).

The death of most organelles was noted. Mitochondria were condensed and partially or completely subject to lysis. The tubules of the granular and agranular endoplasmic reticulum were flattened and destructively changed, and the granular mesh lost ribosomes. These changes were indicative of generalization. Destructive changes of sinusoidal capillaries were also recorded.

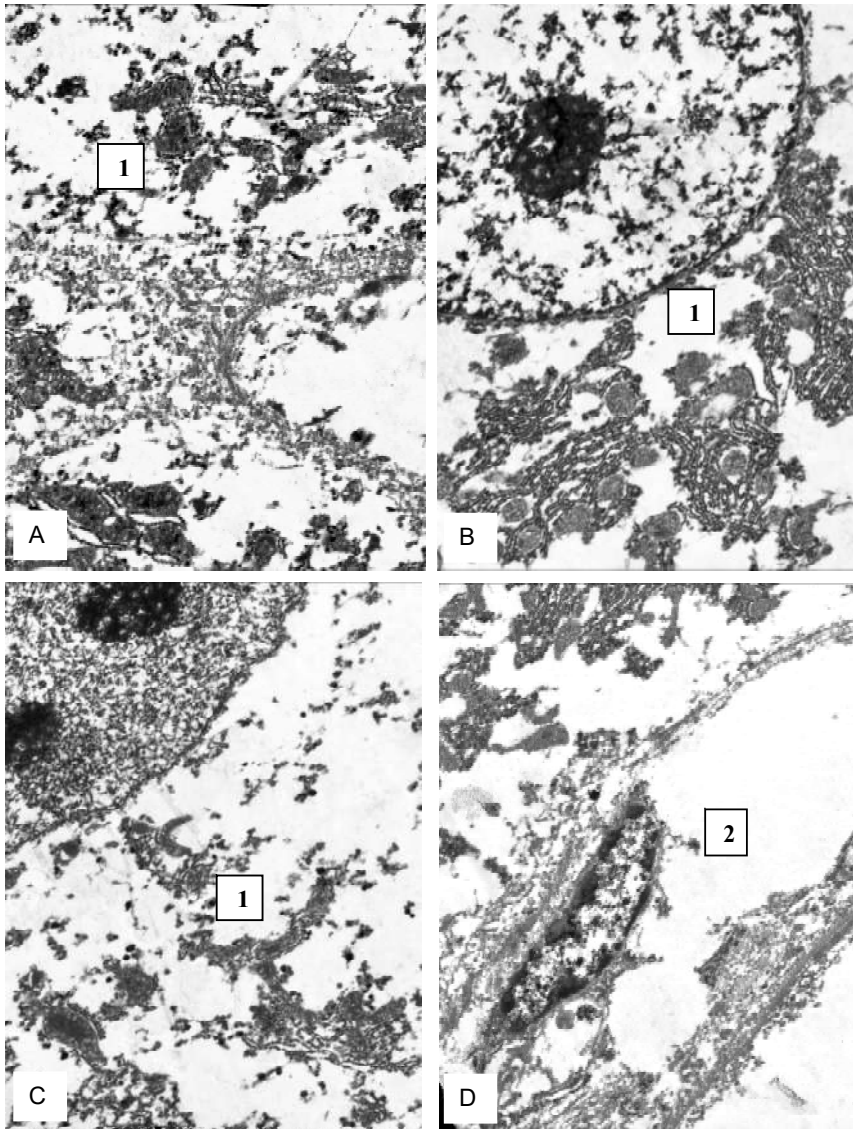


Fig. 7. Electron micrograph. Liver of mice with dysbiosis after infection with Coxsackie B virus and *Salmonella typhimurium*. Necrotic changes in hepatocytes (1) and sinusoidal capillaries (2). Magnification x12000.

Discussion

The use of laboratory animals gives the opportunity to obtain information as close as possible to the human body regarding the features of the pathogenesis of infection, clinical symptoms, immune response or other components of the complex response of the organism to infection. However, modeling of enterovirus infections in animals has certain features that are primarily due to their selective sensitivity to particular types of enteroviruses. Thus, for Coxsackie B viruses effective models are laboratory mice of 1-3 days of age, among polioviruses only 2 serotypes cause clinical symptoms in adult mice, and only with parenteral administration, and to mouse ECOS viruses are not at all sensitive [2, 7, 11, 12]. In general, it should be noted that despite the presence of a certain amount of scientific work on modeling of enterovirus infection in animals,

detailed information on the features of the course and factors affecting the infection process is not enough [17].

The choice of the Coxsackie B3 serotype to model infectious processes is due to its proven virulence for mice and clear multiorgan tropism, which allows one to investigate the effect of viral infection on different organs and systems within one block of experiments. In the simulation of experimental salmonellosis, the mortality of animals in the experiments was slightly lower compared to the data of other scientists who noted the animal's death at about 50 % [4].

However, on the basis of a comparative analysis of the ultrastructure of the liver, spleen and small intestine, the appearance of pronounced changes in the internal organs under conditions of viral-bacterial infection was established, which gave reason to believe that the dysbiotic disorders significantly exacerbate this process. In particular, they cause disorders of the morphofunctional state of the organs of the immune system, in particular the spleen.

Apparently, the introduction of salmonella to mice leads to activation of immunocompetent cells of the spleen, which is manifested by an increase in the number of detected lymphoblasts, plasma cells with enlarged tubules of the granular endoplasmic reticulum, where gammaglobes are known to be produced.

Our findings indicate that viral bacterial infection often leads to the formation of epithelioid cell granuloma in the spleen. As is known, such granulomas are giant cells, consisting of hypertrophic, located in the center of the granuloma, and atrophic at its periphery epithelial cells. In the cytoplasm of such cells there are specific inclusions, as a rule, giant cells are surrounded by lymphocytes, macrophages or other immunocompetent cells.

According to the data obtained in the study, it was proved that the infection of the body with the Coxsackie virus and Salmonella is accompanied by the appearance of significant morphological changes both in the sinusoidal capillaries of the liver and in hepatocytes. The morphological picture is characterized by necrotic changes, which are ultrastructurally accompanied by damage to cell nuclei, cytolysis and death of most organelles. It is common

knowledge that such changes in the liver may have a focal character, but when modeling these viral-bacterial infections against the background of dysbiotic disorders, we observe their generalization.

Conclusions

1. Dysbiotic conditions contribute to the development of associated, in particular virus-bacterial infections in animals, which is primarily manifested by an increase in the incidence and increase in the frequency of

manifestations of the disease. Modeling of viral-bacterial infections against the background of disturbance of the composition of the normal intestinal microflora allows to record the expressed degenerative changes in the internal organs of animals, which are especially pronounced in the liver, often having a generalized character.

2. Based on the analysis of the electronograms, it was also suggested that viral bacterial infections that develop in animals with impaired intestinal microbiocenosis are accompanied by activation of immunocompetent cells.

References

- [1] Ahmed, S. M., Hall, A. J., Robinson, A. E., Verhoef, L., Premkumar, P., Parashar, U. D., ... Lopman, B. A. (2014). Global prevalence of norovirus in cases of gastroenteritis: a systematic review and meta-analysis. *The Lancet infectious diseases*, 14(8), 725-730. doi: 10.1016/S1473-3099(14)70767-4
- [2] Andes, D. R., & Lepak, A. J. (2017). In vivo infection models in the pre-clinical pharmacokinetic/pharmacodynamic evaluation of antimicrobial agents. *Current opinion in pharmacology*, 36, 94-99. doi: 10.1016/j.coph.2017.09.004
- [3] Bobyr, V. V., Ponyatovskiy, V. A., Djugikowa, E. M., & Shyrobokov, V. P. (2015). Modeling of dysbiotic disorders with laboratory animals. *Biomedical and Biosocial Anthropology*, 24, 230-233.
- [4] Chkhenkeli, V. A., Anisimova, A. V., Romanova, E. D., Kalinovich, A. Ye., & Promtov, M. V. (2014). Experimental assessment of the efficiency of the "Trametin" at experimental salmonellosis of laboratory and agricultural animals. *Bulletin of the Eastern Siberian scientific center of the siberian branch of the Russian academy of medical sciences*, 6(100), 80-83.
- [5] E'ssel', A. E., Panteleeva, L. G., & Myasnenko, A. M. (1978). *Viral bacterial associations*. Publishing House Rostovsk. University.
- [6] Gorelov, A. V., & Usenko, D. V. (2008). Rotavirus infection in children. *Current Pediatrics*, 7(6), 78-84.
- [7] Gyssens, I. C. (2019). Animal models for research in human infectious diseases. CMI editorial policy. *Clinical microbiology and infection: the official publication of the European Society of Clinical Microbiology and Infectious Diseases*, 25(6), 649. <https://doi.org/10.1016/j.cmi.2019.04.010>
- [8] Kim, B. H., Kim, T. H., & Lee, M. K. (2016). A Clinico-Epidemiological Comparison Study of Pediatric Acute Viral Gastroenteritis at a Tertiary Care Hospital. *Annals of Clinical Microbiology*, 19(2), 33-38. <https://doi.org/10.5145/ACM.2016.19.2.33>
- [9] Kotloff, K. L. (2017). The burden and etiology of diarrheal illness in developing countries. *Pediatric Clinics*, 64(4), 799-814.
- [10] Kulieva, Z. M. (2015). Characteristics of mixed intestinal infections of early age with emergency conditions. *Russian Medical Journal*, 21(4), 21-23.
- [11] Marsh, E. K., & May, R. C. (2012). *Caenorhabditis elegans*, a model organism for investigating immunity. *Appl. Environ. Microbiol.*, 78(7), 2075-2081. doi: 10.1128/AEM.07486-11
- [12] Osborne, N., Avey, M. T., Anestidou, L., Ritskes-Hoitinga, M., & Griffin, G. (2018). Improving animal research reporting standards. *EMBO reports*, 19(5), e46069. doi: 10.15252/embr.201846069
- [13] Park, J. O., Jeon, J. S., & Kim, J. K. (2019). Epidemiologic Trends of Diarrhea-causing Virus Infection Analyzed by Multiplex Reverse Transcription PCR in Cheonan, Korea, 2010-2018. *Microbiology and Biotechnology Letters*, 47(2), 317-322. <https://doi.org/10.4014/mbl.1811.11007>
- [14] Pollok-Waksmalska, W., Snowiaczek, K., & Wijas, D. (2019). Salmonellosis among children hospitalized in Pediatric Hospital in Bielsko-Biala, Poland, in the years 2014-2015. *Medycyna doswiadczalna i mikrobiologia*, 71, 5-12. doi: 10.32394/mdm.71.01
- [15] Rhoades, N., Barr, T., Hendrickson, S., Prongay, K., Haertel, A., Gill, L., ... & Messaoudi, I. (2019). Maturation of the infant rhesus macaque gut microbiome and its role in the development of diarrheal disease. *Genome biology*, 20(1), 1-16. <https://doi.org/10.1186/s13059-019-1789-x>
- [16] Study of mixed infections in vivo. Retrieved from <http://techpharm.ru/epidemiology1-120>
- [17] Swaenengen, J. R. (2018). Choosing the right animal model for infectious disease research. *Animal models and experimental medicine*, 1(2), 100-108. <https://doi.org/10.1002/ame2.12020>
- [18] Tokar, R. G., Zakstel'skaya, L. Ya., Shendorovich, S. F. (1971). The results of co-infection of tissue culture with influenza virus A2 and Staphylococcus. *Journal of microbiology epidemiology immunobiology*, 6, 100-103.
- [19] World Health Organization (WHO) (2017). Diarrhea [Electronic source]. WHO Bulletin. Retrieved from <http://www.who.int/ru/news-room/fact-sheets/detail/diarrhoeal-disease>

МОДЕЛЮВАННЯ ВІРУСНО-БАКТЕРІАЛЬНИХ ІНФЕКЦІЙ НА ТЛІ АНТИБІОТИКОІНДУКОВАНОГО ДИСБІОЗУ КИШКІВНИКА

Бобир В.В., Стеченко Л.О., Широбоків В.П., Кривошеєва О.І., Назарчук О.А., Понятівський В.А., Чухрай С.М.

Вивчення ролі вірусно-бактеріальних асоціацій в етіології гострих кишкових інфекцій вважають новим для медичної мікробіології. Метою дослідження було визначення впливу вірусно-бактеріальних асоціацій на прояв вірулентності збудників та ступінь розвитку структурно-морфологічних порушень внутрішніх органів у тварин з антибіотикоіндукованим дисбіозом. У дослідженні на 210 білих лабораторних мишах лінії BALB/c формували дисбіоз з використанням антибактеріальних препаратів (ампіцилін, гентаміцин, метронідазол) з подальшим (через 48 год) моделюванням експериментальної інфекції. Для моделювання інфекції сальмонельозу мишей інфікували клінічним штамом *Salmonella typhimurium* внутрішньоочередово. Аналогічно виконували інфікування тварин тест-культурою вірусу Коксакі В3 (доза 10⁶ ТЦД₅₀). Вивчали чутливість мишей до вірусів Коксакі В та сальмонел за показниками смертності та наявністю ознак захворювання. Виводили тварин із досліду через 24 год після інфікування, електронно-мікроскопічно вивчали структурно-морфологічні зміни внутрішніх органів. Встановлено відсутність статистично значущої різниці захворюваності (23,33-26,66 %) та смертності (16,66-20,0 %) мишей, інфікованих вірусом Коксакі, з дисбіотичними розладами та зі збереженою мікрофлорою. Доведено, що дисбіотичні

стани призводили до асоційованих вірусно-бактеріальних інфекцій у тварин, та, відповідно, зростання частоти проявів хвороби та загибелі експериментальних тварин. На фоні порушення складу нормальної мікрофлори кишківника при вірусно-бактеріальних інфекціях встановили виражені дегенеративні зміни у внутрішніх органах тварин з ознаками генералізації. Дані електронограм засвідчили появу ознак активації імунокomпетентних клітин в організмі при вірусно-бактеріальній інфекції у тварин з порушеним мікробіоценозом кишківника.

Ключові слова: антимікробні препарати, бактерії, віруси, дисбіоз, мікробіоценоз кишківника, кишкові інфекції.

МОДЕЛИРОВАНИЕ ВИРУСНО-БАКТЕРИАЛЬНЫХ ИНФЕКЦИЙ НА ФОНЕ АНТИБИОТИКОИНДУЦИРОВАННОГО ДИСБИОЗА КИШЕЧНИКА

Бобыр В.В., Стеченко Л.А., Широбоков В.П., Кривошеева О.И., Назарчук А.А., Понятовский В.А., Чухрай С.М.

Изучение роли вирусно-бактериальных ассоциаций в этиологии острых кишечных инфекций считают новым для медицинской микробиологии. Целью исследования было определение влияния вирусно-бактериальных ассоциаций на проявление вирулентности возбудителей и степень развития структурно-морфологических нарушений внутренних органов у животных с антибиотикоиндуцированным дисбиозом. В исследовании на 210 белых лабораторных мышах линии BALB/c формировали дисбиоз с использованием антибактериальных препаратов (ампициллин, гентамицин, метронидазол) с последующим (через 48 ч) моделированием экспериментальной инфекции. Для моделирования инфекции сальмонеллеза мышей инфицировали клиническим штаммом *Salmonella typhimurium* внутрибрюшинно. Аналогично выполняли инфицирование животных тест-культурой вируса Коксаки В3 (доза составила 10^6 ТЦД₅₀). Изучали чувствительность мышей к вирусам Коксаки В и сальмонелл по показателям смертности и наличию признаков заболевания. Выводили животных из опыта через 24 ч после инфицирования, электронно-микроскопически изучали структурно-морфологические изменения внутренних органов. Установлено отсутствие статистически значимой разницы заболеваемости (23,33-26,66 %) и смертности (16,66-20,0 %) мышей, инфицированных вирусом Коксаки, с дисбиотическими расстройствами и с сохраненной микрофлорой. Доказано, что дисбиотические состояния приводили к ассоциированным вирусно-бактериальным инфекциям у животных, и, соответственно, росту частоты проявлений болезни и гибели экспериментальных животных. На фоне нарушения состава нормальной микрофлоры кишечника при вирусно-бактериальных инфекциях установлены выраженные дегенеративные изменения во внутренних органах животных с признаками генерализации. Данные электронограмм показали появление признаков активации иммунокомпетентных клеток в организме при вирусно-бактериальной инфекции у животных с нарушенным микробиоценозом кишечника.

Ключевые слова: антимикробные препараты, бактерии, вирусы, дисбиоз, микробиоценоз кишечника, кишечные инфекции.

REQUIREMENTS FOR ARTICLES

For publication, scientific articles are accepted only in English only with translation on Ukrainian or Russian, which contain the following necessary elements: UDC code; title of the article (in English, Ukrainian and Russian); surname, name and patronymic of the authors (in English, Ukrainian and Russian); the official name of the organization (institution) (in English, Ukrainian and Russian); city, country (in English, Ukrainian and Russian); structured annotations (in English, Ukrainian and Russian); keywords (in English, Ukrainian and Russian); introduction; purpose; materials and methods of research; research results; discussion; conclusions; bibliographic references.

The title of the article briefly reflects its contents and contains no more than 15 words.

Abstract. The volume of the annotation is 1800-2500 characters without spaces. The text of an annotation in one paragraph should not contain general phrases, display the main content of the article and be structured. The abstract should contain an introductory sentence reflecting the relevance of the study, the purpose of the study, a brief description of the methods of conducting research (2-3 sentences with the mandatory provision of the applied statistical methods), a description of the main results (50-70% of the volume of the abstract) and a concise conclusion (1 sentence). The abstract should be clear without familiarizing the main content of the article. Use the following expressions: "Detected ...", "Installed ...", "Fixed ...", "Impact assessed ...", "Characterized by regularities ...", etc. In an annotation, use an active rather than passive state.

Keywords: 4-6 words (or phrases).

"Introduction"

The introduction reflects the state of research and the relevance of the problem according to the world scientific literature (at least 15 references to English articles in international journals over the past 5 years). At the end of the entry, the purpose of the article is formulated (contains no more than 2-3 sentences, in which the problem or hypothesis is addressed, which is solved by the author).

"Materials and methods"

The section should allow other researchers to perform similar studies and check the results obtained by the author. If necessary, this section may be divided into subdivisions. Depending on the research objects, the ethical principles of the European Convention for the protection of vertebrate animals must be observed; Helsinki Declaration; informed consent of the surveyed, etc. (for more details, see "Public Ethics and its Conflict"). At the end of this section, a "statistical processing of results" section is required, which specifies the program and methods for processing the results obtained by the automobile.

"Results"

Requirements for writing this section are general, as well as for all international scientific publications. The data is presented clearly, in the form of short descriptions, and must be illustrated by color graphics (no more than 4) or drawings (no more than 8) and tables (no more than 4), the information is not duplicated.

"Discussion"

In the discussion, it is necessary to summarize and analyze the results, as possible, compare them with the data of other researchers. It is necessary to highlight the novelty and possible theoretical or practical significance of the results of the research. You should not repeat the information already listed in the "Introduction" section. At the end of the discussion, a separate paragraph should reflect the prospects for using the results obtained by the author.

"Conclusion"

5-10 sentences that summarize the work done (in the form of paragraphs or solid text).

"Acknowledgements"

Submitted after conclusion before bibliographic references.

"References"

References in the text are indicated by Arabic numerals in square brackets according to the numerology in the list of references. The list of references (made without abbreviations) sorted by alphabet, in accordance with the requirements of APA Style (American Psychological Association Style): with the obligatory referencing of all authors, work titles, journal names, or books (with obligatory publication by the publishing house, and editors when they are available), therefore, numbers or releases and pages. In the Cyrillic alphabets references, give the author's surnames and initials in English (Cyrillic alphabet in brackets), the title of the article or book, and the name of the magazine or the publisher first to be submitted in the original language of the article, and then in square brackets in English. If available, doi indexes must be provided on www.crossref.org (at least 80% of the bibliographic references must have their own doi indexes). Links to online publications, abstracts and dissertations are not welcome.

After the list of references, it is necessary to provide information about all authors (in English, Ukrainian and Russian): last name, first name and patronymic of the author, degree, place of work and position, **ORCID number** (each of the authors of the ORCID personal number if absence - free creation on the official website <http://www.orcid.org>) to facilitate the readers of this article to refer to your publications in other scientific publications.

The last page of the text should include the surname, name and patronymic of the author, degree, postal address, telephone number and e-mail of the author, with which the editors will maintain contact.

Concluding remarks

The manuscript should be executed in such a way that the number of refinements and revisions during the editorial of the article was minimal.

When submitting the article, please observe the following requirements. The volume of the article - not less than 15 and not more than 25 pages, Times New Roman, 14 pt, line spacing - one and a half, fields - 2 cm, sheet A4. Text materials should be prepared in the MS Word editor (*.docx), without indentations. Math formulas and equations to prepare in the embedded editor; graphics - in MS Excel. Use the units of the International Measurement System. Tables and drawings must contain the name, be numbered, and references to them in the text should be presented as follows: (fig. 1), or (table 1). The drawings should be in the format "jpg" or "tif"; when scanned, the resolution should be at least 800 dpi; when scanning half-tone and color images, the resolution should be at least 300 dpi. All figures must be represented in the CMYK palette. The statistical and other details are given below the table in the notes. Table materials and drawings place at the end of the text of the manuscript. All elements of the text in images (charts, diagrams, diagrams) must have the Times New Roman headset.

Articles are sent to the editorial board only in electronic form (one file) at the e-mail address nila@vnm.edu.ua

Responsible editor - Gunas Igor Valeryovich (phone number: + 38-067-121-00-05; e-mail: gunas.red@gmail.com).

Signed for print 02.07.2019

Format 60x84/8. Printing offset. Order № 1212. Circulation 100.

Vinnytsia. Printing house "Tvory", Keleckaya St., 51a

PO Box 8825, 600-Richchya Str., 21, Vinnytsya, 21007

Phone: +38 (0432) 603 000

+38 (096) 97-30-934, +38 (093) 89-13-852

e-mail: tvory2009@gmail.com

<http://www.tvoru.com.ua>